Gravitinos and hidden Supersymmetry at the LHC

Dissertation

zur Erlangung des Doktorgrades

des Departments Physik

der Universität Hamburg

vorgelegt von

Sergei Bobrovskyi

aus Kiew

Hamburg

2012

Gutachter der Dissertation:	Prof. Dr. Wilfried Buchmüller Prof. Dr. Peter Schleper Prof. Dr. Daniel Wyler
Gutachter der Disputation:	Prof. Dr. Wilfried Buchmüller Prof. Dr. Jan Louis
Datum der Disputation:	20. Juni 2012
Vorsitzender des Prüfungsausschusses:	Dr. Georg Steinbrück
Vorsitzender des Promotionsausschusses:	Prof. Dr. Peter H. Hauschildt
Dekan der Fakultät für Mathematik, Informatik und Naturwissenschaften:	Prof. Dr. Heinrich Graener

Abstract

We investigate phenomenological consequences of locally supersymmetric extensions of the Standard Model consistent with primordial nucleosynthesis, leptogenesis and dark matter constraints. An unequivocal prediction of local supersymmetry is the existence of the gravitino, the spin-3/2 superpartner of the graviton. Due to its extremely weak couplings, decays involving the gravitino in the initial or the final state may cause problems in the early universe. One class of models solving the gravitino problem makes the gravitino either the heaviest or the lightest supersymmetric particle (LSP), while predicting a higgsino-like neutralino as the LSP or the next-to-lightest superparticle (NLSP), respectively. In both cases the LHC phenomenology is determined by the higgsino states. The mass degeneracy between the charged and neutral states, together with very heavy colored states, prevent an early discovery at the LHC, especially if one demands a lightest Higgs mass compatible with the recent LHC signal excess.

Another class of models, in which the gravitino is also a dark matter candidate, introduces a small violation of R-parity to render the cosmology consistent. In this case, the phenomenology at the LHC is determined by the R-parity violating decays of the NLSP which can be a bino-like or a higgsino-like neutralino or a stau. Using a novel approach to describing bilinear R-parity violation, we compute decay rates of the gravitino and the possible NLSP. Due to a connection between the gravitino and neutralino decay widths, we can predict the neutralino NLSP decay length at the LHC directly from the recent Fermi-LAT results for decaying dark matter searches. The decays of the NLSP in the detectors distort the missing transverse energy (MET) signature, which complicates the searches relying on it, while creating a new secondary vertex signature. We conclude that for gluino and squark masses accessible at the LHC, searches based on secondary vertices can probe values of the R-parity breaking parameter which are far below the present upper bounds obtained from astrophysics and cosmology.

Zusammenfassung

Wir präsentieren eine Untersuchung der phänomenologischen Konsequenzen von lokalen supersymmetrischen Erweiterungen des Standardmodells, welche eine korrekte Menge von dunkler Materie vorhersagen und sich durch eine Vereinbarkeit mit primordialer Nukleosynthese und Leptogenese auszeichnen. Die Existenz vom Gravitino, einem Spin-3/2 Superpartner vom Graviton, ist eine eindeutige Vorhersage der lokalen Supersymmetrie. Die Zerfälle, die das Gravitino im Anfang- oder Endzustand beinhalten, sind Ursache für Probleme im frühen Universum, da das Gravitino nur sehr schwach wechselwirkt.
Eine Klasse von Modellen, in denen das Gravitino-Problem gelöst ist, sagt vorher, dass Gravitino das leichteste oder das schwerste supersymmetrische Teilchen ist, begleitet vom nächstleichtesten oder dem leichtesten Higgsino-artigen Neutralino. In beiden Fällen wird die LHC Phänomenologie von den Higgsino Zuständen beherrscht. Die Massenentartung zwischen den geladenen und den neutralen Zuständen, und die sehr schweren Farb-geladenen Zustände, verhindern eine frühe Entdeckung am LHC, insbesondere wenn man verlangt, dass die Masse des leichtesten Higgs Teilchens nahe dem letzten experimentellen Hinweis vom LHC liegt.
Eine andere Klasse von Modellen, die das Gravitino als Kandidaten für die dunke Materie ansieht, führt eine geringe Verletzung der R-Parität ein, um die Kosmologie konsistent zu machen. Die Phänomenlogie am LHC ist in diesem Fall durch die R-Parität-verletzenden Zerfälle des nächst-leichtesten supersymmetrischen Teilchens bestimmt, welches ein Bino- oder Higgsino-artiges Neutralino oder ein Stau sein kann.
Wir verwenden eine neuartige Beschreibung bilinearer R-Paritäts Verletzung, um die Zerfallsbreiten des Gravitinos und des möglichen nächst-leichtesten supersymmetrischen Teilchens zu berechnen. Da es einen Zusammenhang zwischen den Zerfällen des Gravitinos und denen des Neutralinos gibt, können wir die Zerfallslänge des Neutralinos am LHC direkt aus den Fermi-LAT Ergebnissen der Suche nach kosmischer Gammastrahlung aus den Zerfällen der dunklen Materie vorhersagen. Die Zerfälle des nächst-leichtesten supersymmetrischen Teilchens in den Detektoren am LHC deformieren die Verteilung der fehlenden transversalen Energie so, dass die Suchen nach dieser Signatur erheblich erschwert sind. Gleichzeitig erzeugen sie aber eine neue Signatur, basierend auf den sekundären Vertices. Es stellt sich heraus, dass für die vom LHC erreichbaren Gluino- und Squarkmassen, die Suchen nach den sekundären Vertices solche Werte der R-Paritäts brechenden Parameter untersuchen können, die weit unter den bestehenden oberen Schranken aus der Astrophysik und Kosmologie liegen.

In memory of my father,
Feliks Bobrovskyi

Contents

List of Figures

List of Tables

Chapter 1

Introduction

Quod est superius est sicut quod est inferius - "As above so below" are the words of central meaning in the teaching of the western Hermetic tradition, as they encode the presumed relation between the different layers of reality. Through the millennia the adepts of the occult believed that changes in the constellation of stars and planets are mirrored by the fateful events in the human life. The scientific method has come a long way since that times, explaining the universe around us with unprecedented precision and making attempts to explain even ourselves, our consciousness, through combination of different fields, including neuroscience and psychology, without any recourses to immaterial elements. The progress in physics during the last decades allows us to reinterpret the Hermetic statement and to cast it into a precise, empirically testable form. The laws of the microcosm determine the history of the macrocosm, and the gravitational interaction seen through macroscopic effects presumably play a key role at the smallest scales. Thus, the ultimate quest for the understanding of the cosmogony is the understanding of all of the laws and entities of the microworld combined with an universal treatment of gravity by means of quantum theory. Even leaving the problem of quantum gravity aside, we know that we are just in the beginning of this road, since a number of questions connecting elementary particle physics and cosmology is unanswered or only partially answered so far.

The current paradigm of the elementary particle physics is embodied in the Standard Model (SM), an incredible well tested theory of fundamental interactions built within the framework of quantum field theory upon the principle of local gauge invariance. The Standard Model was established in the seventies and saw its greatest success in the eighties with the discovery of the W and Z boson - the force carriers of the weak interactions. We refer the reader to reference [1] for more details and a historical account. The electroweak part of the Standard Model was tested to high precision at the Large Electron Positron Collider, which confirmed all of SM predictions, except for the spin-zero Higgs particle, connected to the field responsible for the so called "spontaneous breaking" of the electroweak symmetry, which was not found [2–4]. It appears certain that the Higgs particle, or a messenger of an other mechanism for the creation of gauge boson masses, should be seen at the Large Hadron Collider [5–9]. At the time of writing, there are first hints for the Higgs boson with a mass around 125 GeV at the LHC [10–12].

Besides theoretical questions concerning the infrared properties of unbroken gauge theories[1], the SM is also challenged by experimental results from the neutrino experiments. They

[1]The Clay mathematics institute offers a million dollar prize for the solution of the mass gap problem in

have observed flavor changing processes which were then interpreted as neutrino flavor oscillations as a result of non-zero neutrino masses [14–16]. Neutrinos are usually taken to be massless in the Standard Model, but it is easily possible to introduce neutrino masses via two different ways: i) a Dirac mass term can be added to the Lagrangian leading to an extreme small Yukawa coupling, which then has to be explained, or ii) neutrino can be a Majorana particle and acquire its mass via the seesaw-mechanism, which involves introduction of new heavy neutrino states [17–19]. In both cases the Standard Model can be retained with small modifications.

This situation changes if one follows the principle from the beginning of the chapter, i.e. tries to explain the history of the universe with the help of the Standard Model. First of all, one hits the fundamental problem of quantum gravity, as mentioned above, since the gravitational interaction is described by the general theory of relativity, a classical field theory. The fundamental problem can be set aside stating that it becomes important only in extreme situations arising near the singularities of the space-time continuum. Away from these regions, which means sufficiently late in time after the initial singularity, if one considers cosmography, the behavior of matter at small scales will be governed solely by the quantum mechanical laws of particle physics, because of the (super) weak interaction strength of the gravitation. At large scales, the behavior of the universe will be governed only by gravitation sourced by the expectation value of the energy-momentum tensor, due to the short range of the weak and strong interactions and an on average zero charge of matter.

Such approach to gravitation lies at the heart of the current concordance model of cosmology, the Lambda CDM model. We refer the reader to [20, 21] and references therein for an introduction to this topic. It describes an expanding, on average homogeneous and isotropic universe by means of the Friedmann-Lemaître-Robertson-Walker metric within general relativity. The expansion of the universe is confirmed by a wide range of astronomical observations. Projecting this expansion back in time taking into account the matter content of the universe, one comes to the conclusion that the universe should be in a hotter, denser state in the past. The observation of the cosmic microwave background (CMB), a relic from the time of last scattering when photons decoupled from the thermal plasma of electrons and light elements, is the most compelling evidence for such hot thermal phase in the early universe and an example for successful application of the laws of particle physics to cosmology. Another successful application of nuclear physics to cosmology is the process of big bang nucleosynthesis (BBN), i.e. the production of light elements, which took place even earlier in the history of the universe. The abundances of light elements predicted by BBN are in good agreement with astrophysical observations.

Being homogeneous and isotropic at largest scales, the universe exhibits a variety of structure at smaller scales varying from the cosmic web of galaxy superclusters to the planetary systems within galaxies. These inhomogeneities, responsible for our existence, are generated by gravitational instability from some seeds which should be present at earlier times and which are clearly seen as temperature anisotropies in the CMB. The best explanation for these seeds provides inflation - a part of the concordance model proposing a phase of exponential expansion after the initial singularity and before the hot state. This phase can be created by the dynamics of a scalar field, the inflaton. This field is not part of the Standard Model[2] and has to be added to our description of the microcosm. The thermal phase starts after the end of

Yang-Mills theory [13].

[2]Proposals to associate this field with the Higgs field seem to be flawed so far [22–25].

inflation in a process called reheating, which is also not understood so far. Another process which cannot be described by the Standard Model is the generation of the matter-antimatter asymmetry - baryogenesis. Any initial baryon asymmetry (being itself a peculiar initial condition) would be diluted by inflation, making a dynamical creation process necessary. The conditions for successful baryogenesis, which are called Sakharov conditions [26], cannot be satisfied by the particle content and the interactions of the SM[3]. However, it is important to note that baryogenesis can be linked to seemingly unrelated problem of neutrino masses, in particular to the see-saw extension of the Standard Model, a fact vindicating the motto of this chapter.

So far we haven't considered the meaning of the name given to the concordance model, albeit this name itself characterizes quantities lying beyond the Standard Model of particle physics. The greek letter lambda is reserved in cosmology for the constant term proportional to the metric in Einstein's equation of motion. One view is that the cosmological constant is an additional freedom in the definition of the theory arising from the renormalization of the energy momentum tensor [30]. However, the general belief is that the constant is determined by the matter content of the theory as the energy density of the vacuum [31]. The observed positive value of the cosmological constant, while being responsible for seventy percent of the current total energy content of the universe, is an extremely small number which cannot be explained within the scope of the Standard Model or even any quantum field theory to date.

The CDM part in the model name abbreviates cold dark matter - another unresolved problem in cosmology and particle physics. The term dark matter refers to non-luminous source of gravitation which was proposed already in the thirties by Fritz Zwicky to explain radial velocities of the galaxies in the Coma cluster [32]. While the existence of dark matter is firmly established on the basis of astrophysical and cosmological observations, its nature is unknown [33, 34]. It has been proposed, that the observed gravitational effects might be explained by a modification of the theory of gravity [35] or that they might be caused by non-luminous astrophysical objects in the halo of galaxies [36,37]. However, these explanations are strongly disfavored by current experimental data. Again, the best explanation seem to come from the layer of microphysics, dark matter being a new kind of elementary particle obeying all observational constraints, since the Standard Model has no viable candidates [38, 39].

Summing up, one clearly sees that, even not taking into account various purely internal theoretical reasons and quantum gravity, our current description of the elementary particle physics is by far incomplete. However, there is a tension between this certainty originating from astrophysical observations and the lack of direct evidence from the high-energy experiments. This situation has lead to a multitude of theoretical models trying to accommodate the observations and to become a successor of the Standard Model. A definite further progress can only be achieved if we gain new insights into the nature of the phenomena, preferably, from high-energy experiments where new processes happen in the laboratory, and one is able to measure repeatedly a high number of observables. A lot of hope is associated with the Large Hadron Collier, a proton-proton accelerator with a design center-of-mass energy of 14 TeV. It seems probable that the LHC not only allows us to pose further questions concerning the nature of the Higgs mechanism, but also gives us the possibility to shed light on the nature of dark matter. Having summarized the current situation in particle physics and cosmology, we now turn our attention to promising dark matter candidates.

[3]The phase transition occurring in the early universe during electroweak symmetry breaking is not strong enough for a successful electroweak baryogenesis [27–29].

The theoretically best studied dark matter candidates are stable weakly interacting massive particles (WIMPS). Due to the weak interaction strength they would be produced in the right abundance in the early universe. Their stability is usually associated with some discrete symmetry which forbids decays into the lighter stable particles of the Standard Model. The prototype dark matter candidate of this class is the lightest neutralino in the Minimal Supersymmetric Standard Model (MSSM) with conserved R-parity [40]. Depending on the spectrum of new particles, neutralinos could be produced at the LHC and would then be detected by the large experiments. Besides being produced at the LHC, WIMPs should also annihilate in the halo of the milky way and contribute to the spectra of cosmic rays. Furthermore, they would scatter off nuclei in the dedicated direct detection experiments while traversing the Earth.

Only a combination of evidence from all these experiments will allow to perform the connection between particles and the cosmos identifying the nature of dark matter. However, the simplest supersymmetric models with easily accessible spectra seem already to be excluded in direct searches, as well as in indirect searches at colliders [41–43]. It is expected that neutralino dark matter will be detected or completely excluded within the next decade.

Being very popular, weakly interacting massive particles, and in particular neutralino, are not the only viable dark matter candidates. A very interesting particle is the gravitino, the gauge fermion of supergravity, which is present in all locally supersymmetric theories [44,45]. The discovery of the gravitino would be as important as the discovery of the W and Z bosons of the Standard Model. Since the mass of the gravitino is tightly linked to the unknown mechanism of supersymmetry breaking, the gravitino can have a wide range of masses and be the lightest superparticle and therefore a natural dark matter candidate [46, 47].

Further hints for gravitino dark matter originate from the interplay between cosmologically successful predictions of the Standard Model, its seesaw-extension, and the preferable mechanism for baryogenesis linked to it. Leptogenesis creates the baryon asymmetry via C and CP violating out of equilibrium decays of heavy right-handed neutrinos. These decays violate also a lepton number and create lepton asymmetry. The sphaleron processes which are in thermal equilibrium at high temperature transform the lepton asymmetry into baryon asymmetry [48–50]. The right-handed neutrinos must have a mass of the order of 10^{10} GeV in order to create the mass scale of the light neutrinos, which is below 1 eV, via the see-saw mechanism. Therefore, leptogenesis requires the universe to be very hot so that the heavy neutrino states can be produced from the thermal bath.

At such high temperature the gravitinos will be also copiously produced in thermal scatterings [51]. If gravitinos can decay into lighter particles, their decays will in general spoil the predictions of primordial nucleosynthesis for the abundance of light elements [52].

One possible solution to this gravitino problem involves a super-heavy gravitino of several tenth of TeV, which can be realized in models with anomaly-mediated SUSY breaking [53–55]. A recent study [56] showed that an AMSB model with very heavy spectrum but light higgsinos can lead to a consistent cosmology including WIMP dark matter. Another solution makes gravitino the lightest supersymmetric particle and hence a dark matter candidate, as stated above. Gravitino is an elusive dark matter candidate, due to its super-weak interactions suppressed by the Planck scale, and will be probably never seen in direct detection experiments, without some technology far beyond the current state of the art. Stable gravitinos in the halo would also produce no measurable signal.

The prospects for indirect detection at colliders depend strongly on the gravitino mass and the full superparticle spectrum. If the mass difference between the gravitino and the

next to lightest supersymmetric particle is not large enough, the lifetime of the (NLSP) is very long and it does not decay inside of the detector leading to the usual missing transverse energy signature. If the mass of the NLSP is too large it cannot be produced in the decay-chains or in extreme case it cannot be even directly produced at the LHC. Only if the full spectrum and the NLSP-LSP mass difference allows it, the gravitino can manifest itself as missing transverse energy accompanied by gauge bosons.

Moreover, the late decays of the NLSP into the gravitino will in general also lead to conflicts with big bang nucleosynthesis. However, it is possible to reconcile gravitino dark matter, leptogenesis and the primordial nucleosynthesis if one allows for small R-parity violation. Such small R-parity breaking couplings can be naturally induced if the breaking of R-parity is associated with the breaking of the difference between the baryon and the lepton number [57]. If R-parity is broken, NLSP will decay before big bang nucleosynthesis directly into particles of the Standard Model. Gravitino becomes also unstable but its lifetime exceeds by far the age of the universe, since its coupling is suppressed not only by the Planck scale but also by the small amount of R-parity breaking [58]. Therefore, gravitino remains a perfect dark matter candidate.

The breaking of R-parity endows gravitino with a rich phenomenology. The decays of the gravitino may be seen in the late universe as signals in the diffuse gamma ray flux [57–62], in the fluxes of cosmic-ray antimatter [61–64], or in the flux of neutrinos [63, 65]. This is possible, in spite of the extremely long gravitino lifetime, due to the high density of dark matter in the galactic halo. Additionally, the experiments at the LHC may see the NLSP decays into Standard Model particles. The signatures depend on the nature of the NLSP and range from long maximally ionizing tracks in the case of heavy charged particles to secondary vertices in the inner or outer detector components for neutral NLSP [57, 66–71]. However, a direct detection of gravitinos seems still not viable [72].

Most studies so far were focused on the indirect detection prospects of the decaying gravitino dark matter. The present work, on the other hand, emphasizes the consequences of gravitino cosmology for new physics searches at colliders. Thus, it is complementary to the recent work [72] investigating in detail the direct and indirect detection prospects for decaying gravitino dark matter. Furthermore, we also consider the consequences of models with R-parity conservation and super heavy gravitinos.

The main motivation of the present work is the aforementioned tension between the astrophysical observations and the negative results from the LHC. Taking local supersymmetry seriously we consider two possible solutions for the gravitino problem: i) gravitino as the heaviest supersymmetric particle ii) gravitino as the lightest supersymmetric particle. In the first case, we consider the AMSB model [73] with higgsino-like neutralino LSP leading to consistent cosmology [56]. In the second case, one also can obtain consistent cosmology if one allows additional entropy production in case of higgsino-like neutralino NLSP predicted in models with hybrid gauge-gravity mediated SUSY breaking [74, 75]. The popular mSUGRA model of SUSY breaking predicts however a bino-like neutralino or a stau NLSP, and additional entropy production cannot solve the NLSP decay problem [76]. However, a small violation of R-parity can render the cosmology consistent and leads to a multitude of signatures in the sky from decaying gravitino and at the LHC from decaying NLSP, as stated above. The R-parity can also be broken in models with higgsino NLSP and gravitino dark matter and lead to slightly different signatures at the LHC.

The LHC phenomenology of models with conserved R-parity and higgsino-like neutralino NLSP or LSP turns out to be very similar. Both models predict very heavy colored particles,

such that they cannot be produced at the LHC. The only accessible SUSY production channel is then direct electroweak production of higgsino states leading to negligible transverse momentum of the event. This fact, combined with the mass degeneracy between charged and neutral higgsino states, leads to the absence of visible signatures at the LHC, which we have confirmed in our study including the effects of detector simulation. The only hope for a LHC discovery is the search for monojet or monophoton signatures arising from initial state radiation giving rise to a transverse momentum kick and a jet or a photon.

Taking into consideration only the results for the lower bound on the Higgs mass, the hybrid gauge-gravity mediation model allows for light stop states leading to a spectrum similar to the one obtained in natural SUSY proposals, see [77] and references therein. Stops decaying into higgsinos consequently play the most important role in one of our studies. Because of the usually large mass difference, this decay will give rise to very high-energetic jets, which provides a handle to distinguish signal events from Standard Model backgrounds. On the other hand, we can also discriminate between our light higgsino scenario and a generic MSSM with comparable squark and gluino masses. This is because in the latter one would expect to see also events with high-energetic isolated leptons from chargino and neutralino decays. Such events are absent in our scenario, since the higgsino-like chargino and neutralinos are nearly degenerate in mass; consequently, leptons in the final state are too soft to be detected.

If R-parity is violated gravitino LSP and the NLSP will decay. Using a novel description of bilinear R-parity violation, which yields a trilinear coupling previously not discussed in the literature, we derive in a simple way all decay modes of the gravitino, the neutralino, for both bino and higgsino-like cases, and the stau. Then, we compute the gravitino decay into photon and neutrino as well as all neutralino and stau decays using the two-component spinor technique for fermions. Especially the computation of the gravitino decay is simplified compared to the usual four-component approach. Having the decay widths, we discuss cosmological constraints on the size of R-parity violation and compare them with the bounds obtained in direct searches and with indirect bounds from low-energy processes. Additionally, we review the bounds on the size of R-parity violation from the gravitino decays. An important observation of this work is the connection between the gravitino decays into photon and neutrino and the neutralino decays. Using the bounds on R-parity violating couplings from the Fermi-LAT data, we are able to make rather model independent predictions for the neutralino decay length at the LHC. If the NLSP is a stau, we obtain a lower bound on the stau decay length from the requirement that the baryon asymmetry is not washed out.

Focusing on the results for neutralino NLSP, we observe that the predicted decay lengths are macroscopic. The neutralinos decay, therefore, throughout the detector volume and distort the missing transverse energy signature. We have evaluated this distortion on the generator level, since there is no disposable realistic detector simulation taking into account the final radial size of the detector. Nevertheless, we show that the distribution of missing transverse momentum is sufficiently different from the R-parity conserving case and SUSY can be hidden from searches relying on the usual signatures. In order to find the signal, we derive all signatures of decaying neutralinos. While a detailed study of a higgsino-like neutralino at the LHC is work in progress, we present a search for bino-like neutralino decays at the LHC using muons coming from secondary vertices. This study is based on our implementation of muon reconstruction process in cases where they are coming not from the primary interaction point. As a result, we find that for gluino and squark masses accessible at the LHC, values of the R-parity breaking parameter can be probed which are one to two orders of magnitude smaller than the present upper bound obtained from astrophysics and cosmology. Finally, we

also estimate the discovery reach of the LHC if all NLSP decays are taken into account.

This thesis is organized as follows. In Chapter 2 we introduce the concepts of supersymmetry and supergravity and provide the main arguments why this theory is considered to be the best motivated extension of the Standard Model. The discussion of the supergravity Lagrangian uses modern two-component notation for fermions introduced in Appendix A, and the Lagrangian was rewritten from the notation of Wess and Bagger [78]. Having discussed the breaking of supersymmetry, we present a number of models leading to consistent cosmology. The supersymmetric particle spectra predicted by these models are used for the discussion of the LHC signatures. Finally, we provide a short review of the field-theoretical description of the gravitino in the two-component formalism and summarize its implications for cosmology. Chapter 3 motivates the breaking of R-parity and provides an introduction to this topic. After the presentation of consistent patterns of R-parity breaking, we focus on the bilinear R-parity breaking scenario. The phenomenological consequences of R-parity breaking are derived in Chapter 4. We also review the bounds on R-parity breaking couplings from various sources. The connection between consistent cosmology and hidden supersymmetry at the LHC is explored in Chapter 5. Finally, we will present our conclusions and a short outlook.

The appendices contain supporting material on the calculations in this work: Appendix A introduces the two-component spinor technique extending the usual discussion to the case of gravitino decays. Appendix B presents the diagonalization of neutralino and chargino matrices, as well as the derivation of neutral and charged currents.

The discussion of the bilinear R-parity violation as well as the presentation of the model for spontaneous R-parity breaking in Chapter 3 are based on the work published in [69]. Compared to the published results, the discussion is vastly expanded and includes the full supercurrent. The phenomenological discussion of neutralino and stau decays in Chapter 4 is also based on the publication [69]. However, the whole discussion of the neutralino decays was updated taking into account the recent LHC results as well as the results from [72]. Additionally, we have included the decay channel into the lightest Higgs boson and neutrino neglected in [69]. Furthermore, the discussion of the higgsino-like neutralino case is completely new, as well as the discussion of gravitino decays. The discussion of the Higgsino world scenario in Chapter 5 is based on the publication [79]. The search for bino-like neutralino NLSP decays via muons from secondary vertices has been published in [70]. Compared to the published result, we have updated the discussion in view of the recent LHC results. We have also analyzed a larger amount of Monte Carlo data for the backgrounds. The discussion of searches for higgsino-like neutralino is work in progress.

Chapter 2

Supersymmetry and Supergravity

Supersymmetry (SUSY) [80–84] is a hypothetical symmetry between fermionic and bosonic degrees of freedom of a quantum field theory. It introduces fermionic charges transforming fermions into bosons and vice-versa:

$$Q\,|\text{boson}\rangle \simeq |\text{fermion}\rangle\,, \qquad Q\,|\text{fermion}\rangle \simeq |\text{boson}\rangle\,. \tag{2.1}$$

At first sight, these transformations seem to be similar to internal global symmetry transformations, for example to isospin, which relates protons and neutrons. Global internal symmetries lead to conserved charges and superselection sectors within the Hilbert space of states, cf. [85] and references therein. In this sense they are *physical* opposed to local gauge transformations which represent redundancies in the description of the system. Internal global symmetries have a *unifying role*, since the states have to be arranged in definite representations of the considered symmetry group, and these representations can be seen as the basic ontological objects, as long as the symmetry is unbroken. In the case of isospin, this view would imply that the true existing objects are nucleon doublets. Proton and neutron appear as individual objects due to the breaking of isospin by electromagnetic interactions.

The most prominent physical symmetries are the external symmetries of space-time. Therefore, it would be natural to obliterate the distinction between internal and external symmetries by combining the global symmetry group with the Lorentz group into some simple (non-compact) symmetry group. However, it is impossible to accomplish this project as it was shown by Coleman and Mandula [86].

Here the interesting nature of supersymmetry comes into play, as it turns out that supersymmetry is the only possible extension of the Poincaré algebra [87], and hence unifies the boson-fermion relation with the symmetries of space-time. This distinctive nature of supersymmetry makes it theoretically attractive, irrespective of the possible phenomenological implications [88]. Unbroken SUSY would imply the existence of mass-degenerate bosons for each fermion of the Standard Model and vice versa, since it is impossible to combine known fermions and bosons into supermultiplets, see [89] for a historical overview and references. Since no such particles were discovered so far, SUSY must be broken.

Nevertheless, SUSY is the most studied extension of the Standard Model and it is expected to find at least parts of the new particle spectrum of the SM superpartners at the LHC. A possible attempt for the classification of arguments in favor of the existence of supersymmetry in nature and for the connection between SUSY and the Fermi-scale can proceed as follows:

Metaphysical arguments

- Supersymmetry is an extension of the Poincaré algebra. The true symmetry of space-time should be the largest possible (mathematically-consistent) symmetry.
- Supersymmetry is intrinsically elegant. The more elegant a theory is, the more probable it is that this is a true theory.
- Unification I : Supersymmetry blurs the distinction between matter-particles and force-carriers.

Inner-theoretical arguments

- Supersymmetry improves the renormalization properties of theories. Some quantities even acquire no radiative corrections for the case of unbroken SUSY.
- Energy is represented by a positive operator, no extra assumption is needed to ensure the positivity of energy (in global SUSY only).
- Supersymmetry presents solution to the *hierarchy problem*: The scale of the electroweak symmetry breaking is stabilized via cancellation of the quadratic divergences in the radiative corrections to the mass-square of the Higgs-boson. This argument works if the sparticles weigh less than about 1 TeV (at least the superpartners of the third generation). [**FS**]
- Unification II : The running gauge couplings of the Standard Model come close to each other at some high scale, suggesting that they are descendants of a fundamental coupling connected to a simple gauge group broken to the SM at the high scale. However, the couplings do not actually meet in the SM. The inclusion of superpartners in the renormalization-group equations (RGEs) for the gauge couplings permit them to unify at the scale $M_{GUT} \approx 10^{16}$ GeV. The unification happens if the supersymmetric mass scale is at most around 10 TeV. [FS]
- Unification III : Local supersymmetry, or supergravity, incorporates Einstein's theory and improves the renormalization properties of the usual gravity. However, the theory still remains non-renormalizable.
- Supersymmetry is essential for string theory and string theory is believed to be the best candidate for a fundamental theory at the Planck scale.

Experimental hints

- The lightest supersymmetric particle in models with conserved R-parity is a natural candidate for dark matter. The observed dark matter density can be explained if the lightest supersymmetric particle weighs less than 1 TeV. A similar argument can be made for the gravitino dark matter. [**FS**]
- Direct searches, as well as electroweak fits, suggest that Higgs boson is lighter than 127 GeV, in agreement with predictions of simplest supersymmetric theories.

- The mass of the Higgs boson is connected with the stability of the electroweak vacuum. If the Higgs is very light, the vacuum would be destabilized by radiative corrections due to the top quark, unless the Standard Model is supplemented by additional scalar particles. This happens automatically in SUSY. One can even argue, that any mechanism to stabilize the electroweak vacuum must resemble SUSY [90].

- The measured value of the anomalous magnetic moment of the muon disagrees with the Standard Model prediction. Light supersymmetric spectrum can explain the measured value, but such spectrum is in tension with the recent LHC results [91].

The arguments are extracted from [88, 90, 92, 93]; a bold FS in brackets indicates a strong hint for super-partners of the SM particles (superparticles) withing the LHC reach, whereas FS in a regular font indicates a possibility for discovery.

Examining these points it becomes clear that supersymmetry is intertwined with the program of unification. The metaphysical underpinning of this school of thought is the idea that nature is as simple and as economical as possible. A minimal number of interactions and minimal number of fundamental objects seem desirable. However, the perceived nature possesses a multitude of structures and rich dynamics making symmetry breaking as important as the symmetries themselves, since a perfectly symmetric world would be static and structureless. Therefore, it is natural that almost all symmetries are broken and we observe only their remnants. In the case of supersymmetry it is not known at which point in the history of the universe this breaking happened and whether SUSY was an exact symmetry at all, since it is broken by thermal effects and at zero temperature if the vacuum has non vanishing energy density.

Being very attractive, the idea of unification between fermion and bosons does not automatically follow from the SUSY algebra, as it was pointed out by Fayet [94], since it does not require the existence of fundamental bosons. Using non-linear realization of SUSY a fermionic field can be transformed into composite bosonic field made of fermionic ones. Additionally, even in usual supersymmetric theories the unification program is incomplete, since the Yukawa-type interactions are not unified with the gauge-interactions. This feature is connected with the problem of flavor, since the symmetry, if there is any, behind flavor is not understood. As the author of [95] points out: "In fact, it [Flavor symmetry] poses some embarrassment for SUSY when considering flavor: if SUSY is broken, why do we not have FCNCs all over the place ?".

One of the main arguments for Fermi-scale SUSY is the hierarchy problem sketched above. It is important to note that the hierarchy problem depends on one's view on renormalization. It is an inner-theoretical problem, often connected with the question of unification, within the framework of effective field theory. Assuming that there is a physics beyond the Standard Model (usually the particles and interactions associated with the unification force), the cut-off arising in the regularization procedure is interpreted as physical validity border for the original theory. The hierarchy problem does not arise in different interpretations of the renormalization procedure, e.g. if one performs renormalization directly in the position space with methods of causal perturbation theory build upon the renormalization scheme of Epstein and Glaser, see [96, 97] and references therein. In this case one will not even encounter divergent integral. On the other hand one could argue that this method simply hides the problem.

It is interesting to note that a possible discovery of the Higgs-boson with a mass around 125 GeV can point to a stable or at least meta-stable electroweak vacuum [98, 99] all the way

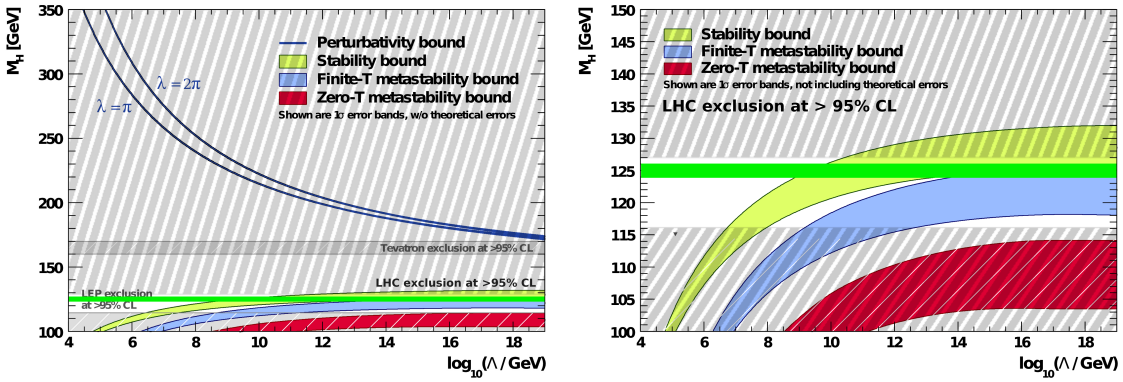

Figure 2.1: The left figure shows the scale Λ at which the two-loop RGEs drive the quartic SM Higgs coupling to become non-perturbative, and the scale Λ at which the RGEs create an instability in the electroweak vacuum. The width of the bands indicates the errors induced by the uncertainties in m_t and α_s (added quadratically). The perturbativity upper bound is given for $\lambda = \pi$ (lower bold line [blue]) and $\lambda = 2\pi$ (upper bold line [blue]). Their difference indicates the size of the theoretical uncertainty in this bound. The absolute vacuum stability bound is displayed by the light shaded [green] band, while the less restrictive finite-temperature and zero-temperature metastability bounds are medium [blue] and dark shaded [red], respectively. The dark [green] line indicates a Higgs-boson with a mass of 125 ± 1 GeV. Shaded regions indicate various exclusion bounds from direct searches. The lower bound from the LHC searches is not shown. The right picture is identical to the left-one, but has a zoomed ordinate, and exclusion bounds (upper and lower) only from the LHC Higgs searches (combination of the results from ATLAS and CMS) [10,101]. Both figures are adapted versions from [99].

to the Planck scale making the supersymmetric extension unnecessary. Figure 2.1 shows on the left the stability and perturbativity bounds on the Higgs mass as a function of the scale where the Higgs quartic coupling becomes either negative, signaling that the electroweak vacuum is only a local minimum, or develops a Landau pole. The right picture shows a zoom to the low-mass region. Both figures are adapted from [99]; a green line indicates the presumed Higgs boson mass of 125 ± 1 GeV.

Another interesting argument for no physics beyond the Standard Model is the prediction of the Higgs mass around 126 GeV by Shaposhnikov and Wetterich [100] from the assumption, that the Standard Model supplemented by asymptotically safe gravity is valid up to the Planck scale.

Finally, even the metaphysical claim of the elegance can be challenged, since Haag found the resulting scheme of their work not very beautiful, because the fermionic charges generated the space-time translations but not the Lorentz transformations [93].

Summing up, we conclude that supersymmetry remains the best-motivated theory for physics beyond the Standard Model. If it is realized in nature near the Fermi scale, it will be found by the LHC. An absence of SUSY signals does not imply that it is falsified, since the mechanism of SUSY breaking is not understood and the breaking scale cannot be predicted so far. However, in this case, supersymmetry loses some of its explanatory power, e.g. its connection to dark matter and especially the hierarchy problem, and the focus of the

research will probably shift to another scenarios. Therefore, it is important to look beyond standard scenarios and investigate different realizations of supersymmetric models, which can be hidden from the LHC. This is the main topic of the present work. In the following we will introduce our notations, some aspects of the formalism, and the phenomenological implications of supersymmetry which will be needed in the following chapters. The discussion follows references [78,89,102,103] which contain a comprehensive introduction to these topics.

2.1 Global Supersymmetry

We investigate the properties of $N = 1$ supersymmetry, which is the only phenomenologically interesting realization of supersymmetry in four dimensions. The supersymmetric extension of the Poincaré algebra reads:

$$\left\{Q_\alpha,\, Q^\dagger_{\dot\alpha}\right\} = 2\sigma^\mu_{\alpha\dot\alpha}P_\mu, \quad \{Q_\alpha,\, Q_\beta\} = \left\{Q^\dagger_{\dot\alpha},\, Q^\dagger_{\dot\beta}\right\} = 0, \quad [P^\mu, Q_\alpha] = \left[P^\mu, Q^\dagger_{\dot\alpha}\right] = 0. \tag{2.2}$$

Representations Irreducible representations of the supersymmetry algebra are called supermultiplets, they unify fermionic and bosonic degrees of freedom. There are two such (massless) supermultiplets in our case, the *chiral* and the *vector* supermultiplet.

The chiral multiplet contains one complex scalar ϕ and one two-component fermion ψ transforming in the defining representation of $SL(2,\mathbb{C})$, see Appendix A for details on the two-component notation. In order for the SUSY algebra to close off-shell, the chiral multiplet is augmented with an auxiliary complex scalar F, which has no kinetic term in the full theory.

The vector supermultiplet contains one massless vector field A^μ, one two-component fermion λ_α transforming also as $(\frac{1}{2}, 0)$, and off-shell a real auxiliary scalar D. Since the supersymmetry generators commute with the generators of the gauge transformations, the whole supermultiplet transforms in the same representation of the gauge group, in particular the fermion λ transforms in the adjoint representation.

Superfields We have seen that supersymmetry has a peculiar feature being on the one hand an internal symmetry, and on the other hand an extension of the external Poincaré group. Both notions can be conciliated if one introduces *superspace* as natural stage for supersymmetry. Superspace is obtained by adding four *fermionic* coordinates to the usual bosonic space-time coordinates. Points in superspace are labeled by coordinates:

$$x^\mu, \quad \theta^\alpha, \quad \theta^\dagger_{\dot\alpha}. \tag{2.3}$$

Here θ^α and $\theta^\dagger_{\dot\alpha}$ are constant complex anticommuting two-component spinors with dimension $[\text{mass}]^{-1/2}$. The components of θ are anticommuting Grassmann numbers. The objects living in superspace are superfields, functions of the superspace coordinates, containing the component fields of the supermultiplets. They embody linear representation of the SUSY transformations, since global supersymmetry transformations are represented as infinitesimal translations in the superspace. Consequently, the dichotomy between the internal and external nature of the SUSY transformations is resolved: they are external physical transformations in superspace perceived as internal symmetries from the viewpoint of ordinary space. This discussion suggests that superspace should be taken as real and not as a pure heuristic instrument, a view surely open for debate.

Superfields can be easily defined by a power series expansion in the anticommuting variables, with components that are functions of x^μ. Such expansion always terminates, with each term containing at most two θ's and two $\theta^\dagger$'s, due to the anticommuting nature of the variables. The general superfield reads:

$$S(x,\theta,\theta^\dagger) = a + \theta\xi + \theta^\dagger\chi^\dagger + \theta\theta b + \theta^\dagger\theta^\dagger c + \theta^\dagger\bar{\sigma}^\mu\theta\nu_\mu + \theta^\dagger\theta^\dagger\theta\eta + \theta\theta\theta^\dagger\zeta^\dagger + \theta\theta\theta^\dagger\theta^\dagger d. \quad (2.4)$$

The components of the general superfield S are eight complex bosonic fields a, b, c, d and ν_μ, and four two-component fermionic fields $\xi, \chi^\dagger, \eta, \zeta^\dagger$. The spinorial products are discussed in Appendix A. The number of degrees of freedom match, although there are more degrees of freedom than in the chiral or vector supermultiplet. Therefore, the general superfield is a reducible representation of the SUSY algebra. In order to find the irreducible representations, one must impose constraints on the general superfield. Important constraints arise from chiral covariant derivatives, which are also supersymmetric covariant: acting on superfields, they return superfields. Two of the derivatives read:

$$D_\alpha = \frac{\partial}{\partial\theta^\alpha} - i(\sigma^\mu\theta^\dagger)_\alpha\partial_\mu, \qquad D^{\dagger\dot{\alpha}} = \frac{\partial}{\partial\theta^\dagger_{\dot{\alpha}}} - i(\bar{\sigma}^\mu\theta)^{\dot{\alpha}}\partial_\mu \quad (2.5)$$

The chiral supermultiplet is contained in the (left-)*chiral superfield* $\Phi(x,\theta,\theta^\dagger)$, which is defined via the constraint:

$$D^\dagger_{\dot{\alpha}}\Phi = 0. \quad (2.6)$$

The complex conjugate field Φ^* is called *antichiral* (or right-chiral) superfield and satisfies

$$D_\alpha\Phi^* = 0. \quad (2.7)$$

A chiral superfield has a dimension [mass], and its expansion reads:

$$\Phi = \phi(x) - i\theta\sigma^\mu\theta^\dagger\partial_\mu\phi(x) - \frac{1}{4}\theta\theta\theta^\dagger\theta^\dagger\partial_\mu\partial^\mu\phi(x) + \sqrt{2}\theta\psi(x) - \frac{i}{\sqrt{2}}\theta\theta\theta^\dagger\bar{\sigma}^\mu\partial_\mu\psi(x) + \theta\theta F(x),$$

where we clearly identify the components of the chiral supermultiplet. Any holomorphic function $W(\Phi_i)$ of chiral superfields is again a chiral superfield.

A vector (or real) superfield V is obtained by imposing the constraint $V = V^*$ on a general superfield. It is dimensionless and has the expansion:

$$\begin{aligned} V(x,\theta,\theta^\dagger) = a + \theta\xi + \theta^\dagger\xi^\dagger + \theta\theta b + \theta^\dagger\theta^\dagger b^* + \theta\sigma^\mu\theta^\dagger A_\mu + \theta^\dagger\theta^\dagger\theta(\lambda - \frac{i}{2}\sigma^\mu\partial_\mu\xi^\dagger) \\ + \theta\theta\theta^\dagger(\lambda^\dagger - \frac{i}{2}\bar{\sigma}^\mu\partial_\mu\xi) + \theta\theta\theta^\dagger\theta^\dagger(\frac{1}{2}D - \frac{1}{4}\partial_\mu\partial^\mu a). \end{aligned} \quad (2.8)$$

A superfield cannot be both chiral and real at the same time, unless it is identically constant (i.e., independent of x^μ, θ, and $\theta^\dagger$). However, if Φ is a chiral superfield, then $\Phi + \Phi^*$ and $i(\Phi - \Phi^*)$ and $\Phi\Phi^*$ are all real (vector) superfields.

The vector superfield contains, in general, more fields than the vector supermultiplet, as it can be seen in the expansion above. The additional auxiliary fields are : a real scalar a, a two-component fermion ξ, and a complex scalar b, with mass dimensions respectively 0, 1/2, and 1. These fields can be *supergauged* away by the transformation:

$$V \to V + i(\Omega^* - \Omega), \quad (2.9)$$

where Ω is a chiral superfield gauge transformation parameter, if V was associated with a $U(1)$ gauge symmetry. After making a supergauge transformation to eliminate a, ξ, and b, the vector superfield is said to be in Wess-Zumino gauge, and is simply given by:

$$V_{\text{WZ gauge}} \;=\; \theta\sigma^{\mu}\theta^{\dagger}A_{\mu} + \theta^{\dagger}\theta^{\dagger}\theta\lambda + \theta\theta\theta^{\dagger}\lambda^{\dagger} + \frac{1}{2}\theta\theta\theta^{\dagger}\theta^{\dagger}D. \tag{2.10}$$

Adopting Wess-Zumino gauge is equivalent to partially fixing the supergauge, while still maintaining the full freedom to do ordinary gauge transformations.

Renormalizable Actions in Superspace An action is a scalar (real) quantity invariant under all symmetries of the system. The invariance under external symmetries is obtained by integrating some dynamical quantity over the full manifold under consideration. In the supersymmetric case one therefore has to integrate over the full superspace.

The only surviving quantity after the full integration is the $\theta\theta\theta^{\dagger}\theta^{\dagger}$ (or D-term) component of some (composite) vector superfield, which transforms into a total derivative under the SUSY transformations confirming the initial idea. Additionally, one can add some (composite) chiral superfield and its complex conjugate and integrate only over the $\theta\theta$ subspace, since the F-term transforms also into a total derivative under SUSY transformations. The composite vector superfield is in general a function of (primitive) chiral and antichiral superfields and is called *Kähler potential*, while the general chiral superfield is a function of only (primitive) chiral superfields and is called *superpotential*.

Imposing the *renormalizability* constraint specifies the possible functions. The Kähler potential is at most a quadratic polynomial of chiral and antichiral superfields, whereas the superpotential is at most cubic in chiral superfields.

It turns out, that the Kähler potential contains exactly the kinetic terms for the dynamic fields of the chiral supermultiplet. Therefore, it is natural to incorporate gauge interactions via the minimal coupling into the Kähler potential. If a general gauge symmetry is realized on chiral superfields Φ_i in a representation R with matrix generators T_i^{aj}, one defines matrix-valued vector and gauge parameter superfields in the representation R:

$$V_i{}^j = 2g_a T_i^{aj} V^a, \qquad\qquad \Omega_i{}^j \;=\; 2g_a T_i^{aj}\Omega^a, \tag{2.11}$$

and writes the gauge transformations on chiral superfields as:

$$\Phi_i \to \left(e^{i\Omega}\right)_i{}^j \Phi_j, \qquad\qquad \Phi^{*i} \to \Phi^{*j}\left(e^{-i\Omega^{\dagger}}\right)_j{}^i. \tag{2.12}$$

The Kähler potential then has the form:

$$K\left(\Phi_i^*, \Phi_j\right) = \Phi^{*i}(e^V)_i{}^j\Phi_j \;. \tag{2.13}$$

The kinetic terms and self-interactions of the vector multiplets are obtained from the chiral field-strength superfield:

$$\mathcal{W}_{\alpha} \;=\; -\frac{1}{4}D^{\dagger}D^{\dagger}\left(e^{-V}D_{\alpha}e^{V}\right), \tag{2.14}$$

via the following term:

$$\frac{1}{4k_a g_a^2}\mathrm{Tr}[\mathcal{W}^{\alpha}\mathcal{W}_{\alpha}]_F = [\mathcal{W}^{a\alpha}\mathcal{W}^a_{\alpha}]_F, \tag{2.15}$$

where $|_F$ indicates integration over half of the superspace, as discussed above and k_a is the normalization factor for generators usually set to $1/2$.

The general renormalizable Lagrangian for a supersymmetric gauge theory (including superpotential interactions for the chiral supermultiplets when allowed by gauge invariance and omitting $U(1)$ D-terms) reads:

$$\mathcal{L} = \left(\frac{1}{4} - i\frac{g_a^2\Theta_a}{32\pi^2}\right)[\mathcal{W}^{a\alpha}\mathcal{W}^a_\alpha]_F + \text{c.c.} + \left[\Phi^{*i}(e^{2g_aT^aV^a})_i{}^j\Phi_j\right]_D + ([W(\Phi_i)]_F + \text{c.c.})\,. \quad (2.16)$$

General Actions in Superspace The extension of supersymmetry to supergravity requires the discussion of general non-renormalizable interactions. Furthermore, as we will be interested in understanding physics at very high energy scales connected with the breaking of supersymmetry, additional gauge symmetries and R-parity, we regard our current theories as low-energy approximations to some fundamental theory and are therefore allowed to introduce non-renormalizable terms.

A non-renormalizable gauge-invariant theory involving chiral and vector superfields can be constructed as:

$$\mathcal{L} = \left[K(\Phi_i,\,\tilde{\Phi}^{*j})\right]_D + \left(\left[\frac{1}{4}f_{ab}(\Phi_i)\widehat{\mathcal{W}}^a\widehat{\mathcal{W}}^b \,+\, W(\Phi_i)\right]_F + \text{c.c.}\right), \quad (2.17)$$

where

$$\tilde{\Phi}^{*j} \equiv \Phi^{*k}\left(e^{2T^a\widehat{V}^a}\right)_k{}^j, \quad \widehat{V}^a = g_aV^a\ , \quad (2.18)$$

and we have omitted higher derivative terms.

The action depends on couplings encoded in three functions of the superfields:

- The superpotential W with dimension [mass]^3, which is an arbitrary gauge-invariant holomorphic function of the chiral superfields.

- The real Kähler potential K with dimension [mass]^2, which is a supergauge invariant function of chiral, antichiral and vector superfields. This function is called Kähler potential, because the action is invariant under the Kähler transformation:

$$K(\Phi_i,\,\tilde{\Phi}^{*j}) \to K(\Phi_i,\,\tilde{\Phi}^{*j}) + F\,(\Phi) + F^*\,(\Phi^*)\,, \quad (2.19)$$

  with a holomorphic function F, since the D-term of a chiral superfield is a total derivative on space-time.

- The dimensionless *gauge kinetic function* $f_{ab}(\Phi_i)$, which is a holomorphic function of the chiral superfields and encodes in general the non-renormalizable couplings of the gauge supermultiplets to the chiral supermultiplets. It is symmetric under interchange of the two indices a, b running over the adjoint representations of the simple and Abelian component gauge groups of the model. In the special case of renormalizable supersymmetric Lagrangians at tree level, it is independent of the chiral superfields, and is equal to $f_{ab} = \delta_{ab}(1/g_a^2 - i\Theta_a/8\pi^2)$.

The whole component field Lagrangian after integrating out the auxiliary fields will be determined in terms of the functions W, K, f_{ab}, and their derivatives.

Supersymmetry breaking As stated already in the introduction to this chapter, supersymmetry must be broken. The only interesting case is spontaneous breaking of supersymmetry, in which case it is still a symmetry of the laws but not the symmetry of the vacuum state. Supersymmetry is spontaneously broken if the variation of some fermionic field operator acquires a vacuum expectation value (VEV). It is often stated that spontaneous SUSY breaking is indicated by the vacuum expectation value of the Hamiltonian, but this is not the case, since the Hamiltonian would be undefined if the Hamiltonian density would acquire a VEV. In fact, the generators of the superalgebra cease to exist after the breaking of supersymmetry. The explicit known models of SUSY breaking give vacuum expectation values either to a D-term or to an F-term in the scalar potential. However, there are severe difficulties if the are renormalizable tree-level couplings between the SUSY-breaking fields and quarks and leptons. Either the obtained spectrum is unrealistic (F-term breaking due to supertrace rules), or there are quantum anomalies (D-term breaking). Therefore, the idea is to decouple the sector of supersymmetry breaking from the observable sector of quarks, leptons, and gauge interactions. One refers to the former as a *hidden sector*. After the breaking, the information must somehow reach the observable sector. Some of the models for this mechanism which are used in the present work will be presented in the Section 2.4.

In phenomenological discussions one usually introduces explicit SUSY-breaking terms, which do not introduce quadratic divergences and are therefore called *soft*. Augmented by these terms supersymmetric models still solve the hierarchy problem. The allowed terms have been classified and are remarkably simple:

- Scalar mass terms m^2 and b:

$$m^2\phi^*\phi + b\phi^2 + b^*\phi^{*2}, \tag{2.20}$$

  where the first term treats the scalar and the pseudoscalar (real and imaginary part) of the supermultiplet equivalently, whereas the other terms introduce a gap between them.

- Gaugino masses M_a for each gauge group:

$$\frac{1}{2}M_a\,\lambda^a\lambda^a. \tag{2.21}$$

- Trilinear scalar couplings a:

$$a\phi^3 + a^*\phi^{*3}. \tag{2.22}$$

- Tadpole coupling t^i, which can occur if one scalar is a singlet under all gauge groups:

$$t^i\phi_i \tag{2.23}$$

The terms presented above clearly break supersymmetry, because they involve only scalars and gauginos but not their superpartners. Having established the techniques and notions of supersymmetry, we summarize the features of the minimal extension of the Standard Model introducing our notation.

Names	Superfield	Spin-0	Spin-1/2	$SU(3)_C, SU(2)_L, U(1)_Y$
Squarks, Quarks	Q	$\tilde{q} = (\tilde{u}\ \tilde{d}\,)$	$q = (u\ d)$	$\left(\mathbf{3},\ \mathbf{2},\quad +\frac{1}{6}\right)$
($\times$ 3 families)	U	$\tilde{\bar{u}}$	$\bar{u}$	$\left(\bar{\mathbf{3}},\quad \mathbf{1},\quad -\frac{2}{3}\right)$
	D	$\tilde{\bar{d}}$	$\bar{d}$	$\left(\bar{\mathbf{3}},\quad \mathbf{1},\quad +\frac{1}{3}\right)$
Sleptons, Leptons	L	$\tilde{l} = (\tilde{\nu}\ \tilde{e})$	$l = (\nu\ e)$	$\left(\mathbf{1},\quad \mathbf{2},\quad -\frac{1}{2}\right)$
($\times$ 3 families)	E	$\tilde{\bar{e}}$	$\bar{e}$	$(\mathbf{1},\quad \mathbf{1},\quad +1)$
Higgs, Higgsinos	H_u	$H_u = (H_u^+\ H_u^0)$	$h_u = (h_u^+\ h_u^0)$	$\left(\mathbf{1},\quad \mathbf{2},\quad +\frac{1}{2}\right)$
	H_d	$H_d = (H_d^0\ H_d^-)$	$h_d = (h_d^0\ h_d^-)$	$\left(\mathbf{1},\quad \mathbf{2},\quad -\frac{1}{2}\right)$

Table 2.1: Chiral supermultiplets, their components and quantum numbers in the Minimal Supersymmetric Standard Model. The spin-0 fields are complex scalars, and the spin -1/2 fields are two-component fermions transforming in the fundamental representation of $SL(2,\mathbb{C})$. Note that the bars over the fields are parts of the name. This notation is introduced in Appendix A.

Names	Superfield	Spin-1/2	Spin-1	$SU(3)_C, SU(2)_L, U(1)_Y$
Gluino, Gluon	G	g	G	$(\mathbf{8},\quad \mathbf{1},\quad 0)$
Winos, W-bosons	W	$w^1,\ w^2,\ w^3$	$W^1,\ W^2,\ W^3$	$(\mathbf{1},\quad \mathbf{3},\quad 0)$
Bino, B-boson	B	b	B	$(\mathbf{1},\quad \mathbf{1},\quad 0)$

Table 2.2: Gauge supermultiplets, their components and quantum numbers in the Minimal Supersymmetric Standard Model.

2.2 The Minimal Supersymmetric Standard Model

The Minimal Supersymmetric Standard Model (MSSM) is a supersymmetrized version of the Standard Model with minimal number of additional particles and without new gauge interactions. The matter content as well as the gauge fields of the SM are incorporated into supersymmetric multiplets and the interactions between them are supersymmetrized. Table 2.1 introduces our notation for the chiral supermultiplets of the MSSM fields and their components as well as their transformation properties under the Standard Model gauge group. In comparison with the Standard Model there are two Higgs multiplets with opposite hypercharge. This is needed since the superpotential is a holomorphic function and therefore one cannot employ conjugate fields. Additionally, this is required for the anomaly freedom of the electroweak theory due to contributions from fermionic partners.

Table 2.2 introduces our notation for the vector superfields of the MSSM and their component fields, as well as their transformation properties under the SM gauge group. The gauge interactions and kinetic terms are defined by the usual renormalizable Kähler potential. The superpotential of the MSSM reads:

$$W_{MSSM} = h^u_{ij} Q_i H_u U_j + h^d_{ij} Q_i H_d D_j + h^e_{ij} L_i H_d E_j + \mu H_u H_d + h.c. \tag{2.24}$$

The dimensionless Yukawa coupling parameters h^u, h^d, h^e are 3×3 matrices in family space;

and the i, j are the corresponding family indices. All of the gauge indices are suppressed. The μ term is the supersymmetric version of the Higgs boson mass and the only dimensionful supersymmetric parameter, which we choose to be real.

Contrary to the case of the Standard Model, the Yukawa couplings presented so far are not the most general couplings compatible with gauge invariance and renormalizability. Additional potentially dangerous terms violating baryon and lepton number can be added. These terms are usually forbidden by discrete symmetry, R-parity, which will be the topic of the next chapter. Therefore, at this stage the MSSM is defined as the model with the minimal field and coupling content.

The description of the MSSM is completed with the specification of the soft supersymmetry breaking terms discussed in the previous section:

$$\begin{aligned} -\mathcal{L}_{soft}^{MSSM} = & \frac{1}{2}\left(M_3\, g\, g + M_2\, w\, w + M_1\, b\, b + h.c.\right) \\ & + \left(a^u\, \tilde{q} H_u\, \tilde{\bar{u}} + a^d\, \tilde{q} H_d\, \tilde{\bar{d}} + a^e\, \tilde{l} H_d\, \tilde{\bar{e}} + h.c.\right) \\ & + \widetilde{m}_q^2\, \tilde{q}^\dagger \tilde{q} + \widetilde{m}_l^2\, \tilde{l}^\dagger \tilde{l} + \widetilde{m}_u^2\, \tilde{\bar{u}}^\dagger \tilde{\bar{u}} + \widetilde{m}_d^2\, \tilde{\bar{d}}^\dagger \tilde{\bar{d}} + \widetilde{m}_e^2\, \tilde{\bar{e}}^\dagger \tilde{\bar{e}} \\ & + m_u^2\, H_u^\dagger H_u + m_d^2 H_d^\dagger H_d + \left(B H_u H_d + h.c.\right). \end{aligned} \tag{2.25}$$

In eq. (2.25), M_3, M_2, and M_1 are the gluino, wino, and bino mass terms. We have suppressed the adjoint representation gauge indices on the wino and gluino fields, and the gauge indices on all of the chiral supermultiplet fields. The second line in eq. (2.25) contains the (scalar)^3 couplings. Each of a^u, a^d, a^e is a complex 3×3 matrix in family space, with dimensions of [mass]. They are in one-to-one correspondence with the Yukawa couplings of the superpotential. The third line of eq. (2.25) consists of squark and slepton mass terms, the mass matrices are in general 3×3 matrices in family space that can have complex entries, but they must be hermitian so that the Lagrangian is real. In the last line of eq. (2.25) one has the supersymmetry-breaking contributions to the Higgs potential; m_u^2 and m_d^2 are squared-mass terms of the m^2 type, while B is the only squared-mass term of the type b in e.q. (2.20) that can occur in the MSSM[1]. The dagger on H_u and H_d indicates the contraction of the doublets in contrast to terms like $H_u H_d$ which should be read as $\varepsilon_{ij} H_{ui} H_{dj}$, $\varepsilon = i\sigma^2$ being the $SU(2)$ metric. The soft breaking terms introduce many new parameters not present in the Standard Model. It turns out that the MSSM Lagrangian has 105 physical masses, phases and mixing angles, which have no counterpart in the Standard Model. This arbitrariness in the Lagrangian is not inherent to supersymmetry but arises from the unknown mechanism of supersymmetry breaking. Most of the new parameters imply flavor mixing or CP-violating processes, which are restricted by experimental data. This is precisely the point attacked by author of [95], as mentioned in the introduction to this chapter. Usually, it is assumed that supersymmetry breaking is *universal*, meaning that the squark and slepton squared-mass matrices are flavor blind. Additionally, one assumes that the scalar trilinear couplings are proportional to Yukawa couplings and that the soft parameters do not introduce new complex phases. These relations should result naturally from the specific model for the origin of SUSY breaking. We will discuss such simplified models in the end of this chapter.

For the later discussion we will need the effects of the electroweak symmetry breaking in the MSSM, which we introduce in the following section.

[1]The parameter called B in this work is often denoted by b or $B\mu$.

2.2.1 Electroweak Symmetry Breaking

Electroweak symmetry breaking in the MSSM occurs dynamically, as the soft Higgs mass m_u receives radiative corrections which drive it negative. The Higgs fields which turn out to be neutral under the unbroken $U(1)_{em}$ already have suggestive names. They acquire vacuum expectation values $\langle H_u^0 \rangle = v_u$ and $\langle H_d^0 \rangle = v_d$. The ratio of the Higgs VEVs is a new parameter of the theory and is denoted by:

$$\tan\beta \equiv \frac{v_u}{v_d}. \tag{2.26}$$

The vacuum expectation values of the Higgs doublets are related to the Fermi scale in the following way:

$$v^2 = v_u^2 + v_d^2 = 174\,\text{GeV}, \quad v_u = v\sin\beta, \quad v_d = v\cos\beta. \tag{2.27}$$

Analogously to electroweak symmetry breaking in the SM, the gauge fields acquire masses except for the photon which stays massless. The masses of the W and Z bosons are given by:

$$m_W = \frac{gv}{\sqrt{2}}, \quad \text{and} \quad m_Z = \frac{gv}{\sqrt{2}\cos\theta_w} = \frac{\sqrt{g^2+g'^2}v}{\sqrt{2}}, \tag{2.28}$$

where θ_w is the weak mixing angle defined by:

$$\sin\theta_w = \frac{g'}{\sqrt{g^2+g'^2}}, \qquad \cos\theta_w = \frac{g}{\sqrt{g^2+g'^2}}. \tag{2.29}$$

The couplings constants g' and g are the couplings of hypercharge and weak isospin respectively. The charged gauge bosons are defined as:

$$W^\pm = \frac{1}{\sqrt{2}}\left(W_\mu^1 \mp iW_\mu^2\right), \tag{2.30}$$

while the Z boson is defined via

$$Z_\mu = -\sin\theta_w B_\mu + \cos\theta_w W_\mu^3. \tag{2.31}$$

The Higgs sector of the MSSM is more complicated than its counterpart in the SM due to two Higgs doublets. There are five physical Higgs mass eigenstates consisting of two CP-even neutral scalars h and H, one CP-odd neutral scalar A^0, and a pair of charge conjugate scalars $H^\pm$. The gauge-eigenstate fields can be expressed in terms of the mass eigenstate fields as:

$$\begin{pmatrix} H_u^0 \\ H_d^0 \end{pmatrix} = \begin{pmatrix} v_u \\ v_d \end{pmatrix} + \frac{1}{\sqrt{2}} R_\alpha \begin{pmatrix} h \\ H \end{pmatrix} + \frac{i}{\sqrt{2}} R_{\beta_0} \begin{pmatrix} G^0 \\ A^0 \end{pmatrix}, \tag{2.32}$$

$$\begin{pmatrix} H_u^+ \\ H_d^{-*} \end{pmatrix} = R_{\beta_\pm} \begin{pmatrix} G^+ \\ H^+ \end{pmatrix}, \tag{2.33}$$

where the orthogonal rotation matrices

$$R_\alpha = \begin{pmatrix} \cos\alpha & \sin\alpha \\ -\sin\alpha & \cos\alpha \end{pmatrix}, \tag{2.34}$$

$$R_{\beta_0} = \begin{pmatrix} \sin\beta_0 & \cos\beta_0 \\ -\cos\beta_0 & \sin\beta_0 \end{pmatrix}, \qquad R_{\beta_\pm} = \begin{pmatrix} \sin\beta_\pm & \cos\beta_\pm \\ -\cos\beta_\pm & \sin\beta_\pm \end{pmatrix}, \tag{2.35}$$

are chosen such that the quadratic part of the potential has diagonal squared-masses. In the tree-level approximation one finds that $\beta_0 = \beta_\pm = \beta$, and that the Nambu-Goldstone bosons G^0, $G^\pm$ have zero mass and can be set to zero in the unitary gauge. The masses of the physical Higgs bosons are given by:

$$m^2_{A^0} = 2B/\sin(2\beta) = 2|\mu|^2 + m_u^2 + m_d^2, \tag{2.36}$$

$$m^2_{h,H} = \frac{1}{2}\Big(m^2_{A^0} + m_Z^2 \mp \sqrt{(m^2_{A^0} - m_Z^2)^2 + 4m_Z^2 m^2_{A^0}\sin^2(2\beta)}\Big), \tag{2.37}$$

$$m^2_{H^\pm} = m^2_{A^0} + m_W^2. \tag{2.38}$$

The mixing angle α is determined, at tree-level, by

$$\frac{\sin 2\alpha}{\sin 2\beta} = -\left(\frac{m_H^2 + m_h^2}{m_H^2 - m_h^2}\right), \qquad \frac{\tan 2\alpha}{\tan 2\beta} = \left(\frac{m^2_{A^0} + m_Z^2}{m^2_{A^0} - m_Z^2}\right), \tag{2.39}$$

and is traditionally chosen to be negative; it follows that $-\pi/2 < \alpha < 0$ (provided $m_{A^0} > m_Z$).

In the *decoupling limit*, i.e. in the case $m_{A^0} \gg m_Z$, the Higgs particles H, A^0 and $H^\pm$ are very heavy and decoupled from the low-energy phenomenology. The lightest Higgs particle h behaves as the Standard Model Higgs boson with the mass near the Fermi scale. The mixing angle α becomes $\beta - \pi/2$, which will be important in the discussion of the R-parity violating coupling of the neutralino to the Higgs boson.

Including all loop corrections, supersymmetry provides an upper bound on the mass of the lightest Higgs boson, which is often used in its support in the light of the recent experimental data and electroweak fits. The bound is:

$$m_h \lesssim 135\,\text{GeV}. \tag{2.40}$$

The μ Problem and Giudice-Masiero Mechanism We have already noted that the μ parameter which couples the Higgs doublets in the superpotential is the only dimensionful parameter allowed by *unbroken* supersymmetry. However, it also plays an important role during electroweak symmetry breaking, since it is obviously connected with the Higgs sector. Writing down the squared Z boson mass in terms of the fundamental parameters:

$$m_Z^2 = \frac{\left|m_d^2 - m_u^2\right|}{\sqrt{1 - \sin^2(2\beta)}} - m_u^2 - m_d^2 - 2\left|\mu\right|^2, \tag{2.41}$$

one discovers that, barring large cancellations, all of the parameters should have values near the Fermi scale. Why a SUSY-preserving parameter should have a value near the SUSY-breaking scale is completely unclear. On the other hand, this problem would be solved if one could connect the μ term with the breaking of supersymmetry. A solution was proposed by Giudice and Masiero [104]. They observed that the μ term is generated in supergravity models from non-renormalizable terms in Kähler potential. One way to analyze the mechanism is to consider the low-energy effective theory below M_P involving a non-renormalizable Kähler potential:

$$K = H_u^* H_u + H_d^* H_d + \left(\frac{\lambda_\mu}{M_P} H_u H_d X^* + h.c.\right), \tag{2.42}$$

where λ_μ is a dimensionless coupling and X is a chiral superfield which breaks SUSY through its auxiliary F field: $X^* \to \theta^\dagger\theta^\dagger \langle F_X^* \rangle$, where $\langle F_X^* \rangle$ is the SUSY breaking vacuum expectation value. The integration of $\theta^\dagger\theta^\dagger \langle F_X^* \rangle H_u H_d$ over the full superspace amounts then to integration of $\langle F_X^* \rangle H_u H_d$ over the half of the superspace, as it should be in case of superpotential contributions, cf. Section 2.1. After the breaking the μ term is given by :

$$\mu = \frac{\lambda_\mu}{M_P} \langle F_X^* \rangle . \tag{2.43}$$

Note that the additional term in eq. (2.42) is the only leading-order contribution to K. We will see in Section 2.4, that $\langle F_X^* \rangle \sim m_{3/2} M_P \sim m_{\text{soft}} M_P$ which gives us a desired μ term. The B-term in the soft SUSY breaking sector can arise similarly from Kähler potential terms. In the later discussion we will see a mechanism of this kind generating R-parity violating terms.

In the next section we look at the effects of the electroweak symmetry breaking in the gaugino-higgsino sector. We are interested in neutralinos because the lightest of them is often either the lightest supersymmetric particle (LSP), or the next-to-lightest supersymmetric particle (NLSP) (if gravitino is the LSP) in the models considered in the present work, see Sections 2.4.1 and 2.4.2. In the following section we introduce our notation and set the ground for the later discussion of the neutralino-chargino sector in models with R-parity violation.

2.2.2 Neutralinos and Charginos

The higgsinos and electroweak gauginos mix with each other because of the effects of electroweak symmetry breaking. The neutral higgsinos (h_u^0 and h_d^0) and the neutral gauginos (b, w^0) combine to form four mass eigenstates called *neutralinos* χ_i^0. The charged higgsinos (h_u^+ and h_d^-) and winos (w^+ and w^-) mix to form two mass eigenstates with charge ± 1 called *charginos* $\chi_i^\pm$. By convention, these are labeled by their masses in ascending order, so that $m_{\chi_i^0} < m_{\chi_{i+1}^0}$ and $m_{\chi_1^\pm} < m_{\chi_2^\pm}$.

In the gauge eigenstates basis $\psi^0 = (b, w^0, h_u^0, h_d^0)^T$, the neutralino mass part of the Lagrangian is given by:

$$-\mathcal{L}_{\text{neutralino mass}} = \frac{1}{2} \psi^{0T} \mathcal{M}^N \psi^0 + h.c. , \tag{2.44}$$

where

$$\mathcal{M}^N = \begin{pmatrix} M_1 & 0 & m_Z s_\beta s_w & -m_Z c_\beta s_w \\ 0 & M_2 & -m_Z s_\beta c_w & m_Z c_\beta c_w \\ m_Z s_\beta s_w & -m_Z s_\beta c_w & 0 & -\mu \\ -m_Z c_\beta s_w & m_Z c_\beta c_w & -\mu & 0 \end{pmatrix} . \tag{2.45}$$

Here we have introduced abbreviations $s_\beta = \sin\beta$, $c_\beta = \cos\beta$, $s_w = \sin\theta_w$, and $c_w = \cos\theta_w$. The entries of the mass matrix follow from the soft breaking terms of the MSSM, the superpotential mass term for the Higgs fields, and the gauge couplings to Higgs and higgsino after electroweak symmetry breaking. The mass matrix $\mathcal{M}$ is symmetric; the mass eigenstates can be found via the Takagi diagonalization, see Appendix B :

$$U^{(n)T} \mathcal{M}^N U^{(n)} = \mathcal{M}^N_{\text{diag}}. \tag{2.46}$$

The unitary matrix $U^{(n)}$ relates the neutral gauge eigenstates to the mass eigenstates χ_i^0. The masses and the mixing matrix can be given in closed form, but the results are in general

not very illuminating. However, in all cases considered in the present work, the electroweak symmetry breaking effects are only small perturbations on the neutralino mass matrix and there is a hierarchy between the gaugino and higgsino mass terms:

$$m_Z < |\mu \pm M_1|\,,\ |\mu \pm M_2|\,. \tag{2.47}$$

In this case it is possible to perturbatively diagonalize the mass matrix and the neutralino mass eigenstates are very nearly "bino-like", "wino-like" and "higgsino-like". The ordering of the masses depends on the ordering of gaugino and higgsino masses. If $m_Z < M_1 < M_2 < \mu$ we diagonalize the mass matrix to the second order in m_Z/μ and find:

$$\begin{aligned}
m_{\chi_1^0} &= M_1 - \frac{m_Z^2 s_w^2 (M_1 + \mu s_{2\beta})}{(\mu^2 - M_1^2)} \left(1 + \mathcal{O}\left(\frac{m_Z^2}{\mu^2}\right)\right)\ , \\
m_{\chi_2^0} &= M_2 - \frac{m_Z^2 c_w^2 (M_2 + \mu s_{2\beta})}{(\mu^2 - M_2^2)} \left(1 + \mathcal{O}\left(\frac{m_Z^2}{\mu^2}\right)\right)\ , \\
m_{\chi_3^0} &= \mu + \frac{m_Z^2 (1 - s_{2\beta})(\mu + M_1 c_w^2 + M_2 s_w^2)}{2(\mu + M_1)(\mu + M_2)} \left(1 + \mathcal{O}\left(\frac{m_Z^2}{\mu^2}\right)\right)\ , \\
m_{\chi_4^0} &= \mu + \frac{m_Z^2 (1 + s_{2\beta})(\mu - M_1 c_w^2 - M_2 s_w^2)}{2(\mu - M_1)(\mu - M_2)} \left(1 + \mathcal{O}\left(\frac{m_Z^2}{\mu^2}\right)\right)\ ,
\end{aligned} \tag{2.48}$$

where we have defined $s_{2\beta} = \sin(2\beta)$, and have assumed that sign $(\mu) = +1$. The lightest neutralino is bino-like, as expected. The perturbative diagonalization technique will be essential in the case of R-parity violation. It is summarized in Appendix B.

The chargino mass term in the gauge eigenstate basis $\psi^- = (w^-, h_d^-)$, $\psi^+ = (w^+, h_u^+)^T$ reads:

$$-\mathcal{L}_{\text{chargino mass}} = \psi^- \mathcal{M}^C \psi^+ + h.c.\,, \tag{2.49}$$

where

$$\mathcal{M}^C = \begin{pmatrix} M_2 & \sqrt{2} m_Z s_\beta c_w \\ \sqrt{2} m_Z c_\beta c_w & \mu \end{pmatrix}. \tag{2.50}$$

The chargino mass matrix is an arbitrary complex matrix, therefore one has to use its singular value decomposition (also described in Appendix B), in order to obtain the physical masses:

$$U^{(c)\dagger} \mathcal{M}^C \tilde{U}^{(c)} = \mathcal{M}^C_{\text{diag}}, \tag{2.51}$$

where $U^{(c)}$ and $\tilde{U}^c$ are unitary. The chargino masses can be easily given in analytical form, but we are again interested in the limit of eq. (2.47), in which case the chargino mass eigenstates consist of a wino-like $\chi_1^\pm$ and a higgsino-like $\chi_2^\pm$, with masses

$$\begin{aligned}
m_{\chi_1^\pm} &= M_2 - \frac{m_Z^2 c_w^2 (M_2 + \mu s_{2\beta})}{(\mu^2 - M_2^2)} \left(1 + \mathcal{O}\left(\frac{m_Z^2}{\mu^2}\right)\right) \\
m_{\chi_2^\pm} &= \mu + \frac{m_Z^2 c_w^2 (\mu + M_2 s_{2\beta})}{(\mu^2 - M_2^2)} \left(1 + \mathcal{O}\left(\frac{m_Z^2}{\mu^2}\right)\right).
\end{aligned} \tag{2.52}$$

The lightest chargino is degenerate with the neutralino χ_2^0 up to the higher orders. The mass degeneracies between the charginos and neutralinos will have important phenomenological

consequences in the case of higgsino-like neutralino NLSP with gravitino LSP and R-parity conservation, discussed in Chapter 5.

Another particle turning out to be the LSP in mSUGRA-type models is the scalar partner of the tau lepton, the stau. Usually, this region is excluded since dark matter is obviously not charged. However, stau is a viable NLSP in models with gravitino dark matter. In the following section we introduce our notation in the stau sector.

2.2.3 Scalar Tau Leptons

The mass pattern of the third generation of squarks and sleptons differs from their counterparts in the first two families due to various effects of large Yukawa-couplings. Besides the diagonal SUSY-breaking mass terms for the $\tilde{\tau}$ and $\tilde{\bar{\tau}}^\dagger$ scalars there are also diagonal mass terms proportional to the tau lepton mass from the quartic F-terms in the scalar potential after the electroweak symmetry breaking. Additionally, there is a substantial mixing between the both stau states, which are usually called left- and right-handed, coming from trilinear F- and a-terms. The quadratic Lagrangian has the form :

$$-\mathcal{L}_{\text{stau mass}} = \psi_{\tilde{\tau}}^\dagger m_{\tilde{\tau}}^2 \psi_{\tilde{\tau}}, \tag{2.53}$$

where $\psi_{\tilde{\tau}}^T = (\tilde{\tau},\ \tilde{\bar{\tau}}^\dagger)$, and the stau mass-matrix $m_{\tilde{\tau}}^2$ reads:

$$m_{\tilde{\tau}}^2 = \begin{pmatrix} \widetilde{m}_{l_3}^2 + m_\tau^2 & v(a_{33}^{e*}\cos\beta - h_{33}^e \mu \sin\beta) \\ v(a_{33}^e \cos\beta - h_{33}^e \mu^* \sin\beta) & \widetilde{m}_{e_3}^2 + m_\tau^2 \end{pmatrix}. \tag{2.54}$$

We have included the quantum corrections into the diagonal masses. The hermitian mass matrix can be diagonalized via a unitary transformation to give mass eigenstates:

$$\begin{pmatrix} \tilde{\tau}_1 \\ \tilde{\tau}_2 \end{pmatrix} = \begin{pmatrix} \sin\theta_\tau & \cos\theta_\tau \\ \cos\theta_\tau & -\sin\theta_\tau \end{pmatrix} \begin{pmatrix} \tilde{\tau} \\ \tilde{\bar{\tau}}^\dagger \end{pmatrix}, \tag{2.55}$$

were we have assumed that the off-diagonal elements of the mass matrix are real. The mixing angle θ_τ can be chosen in the range $0 \leq \theta_\tau < \pi$. The mass eigenstates are ordered, such that $\tilde{\tau}_1$ is always the lightest state and therefore our NLSP.

Having established the important ingredients of the MSSM in the context of global supersymmetry, we now explore the gravitational theory of the superspace: *Supergravity*. Another road to supergravity, without superspace, follows from local supersymmetry transformations which require introduction of a spin-2 field, which couples to the energy-momentum tensor for matter, and whose quanta are identified with gravitons.

2.3 Supergravity

Supergravity is the gravitational theory of the superspace. It includes Einstein's theory of gravitation and is therefore non-renormalizable as the theory of gravitation itself. Supergravity arises as the low-energy limit of superstring theories and is viewed as an effective field theory whose infinities will be cured by the fundamental theory of gravitation. Furthermore, supergravity emerges if one attempts to promote the global supersymmetry transformations to local ones.

The phenomenological importance of supergravity resides in the fact that it is believed that the SM superpartners cannot acquire tree-level masses via spontaneous breaking of global

Name	Spin-2	Spin-3/2	$SU(3)_C$, $SU(2)_L$, $U(1)_Y$
Graviton, Gravitino	$g_{\mu\nu}$	ψ_μ	$(\mathbf{1}, \quad \mathbf{1}, \quad 0)$

Table 2.3: The gravity supermultiplet present in all locally supersymmetric theories. Listed are quantum numbers with respect to the Standard Model gauge group

supersymmetry at the TeV scale, since it would lead to problems with tree-level sum rules which imply that some scalar partners of fermions (sfermions) must be lighter than fermions. The MSSM is, therefore, regarded as a low energy effective theory to be derived from a theory which incorporates supersymmetry breaking. Often, this theory is assumed to be a supergravity theory.

Upon promoting SUSY to a local symmetry, one is forced to add a new supermultiplet to the theory, the *gravity multiplet*, which consists of the spin-2 graviton and the spin-3/2 gravitino (see Table 2.3). Local transformations of the usual SUSY Lagrangian will require the introduction of the spin-3/2 field, whose variation under local SUSY transformations couples to the energy-momentum tensor and is canceled by the variation of the spin-2 field. Supergravity is covered in detail in the Book by Wess and Bagger [78] and in the review by Van Nieuwenhuizen [105], see references therein for the original works. Note that our definition of the metric signature and sigma-matrices differs from the definition of Wess and Bagger. The notational conventions of this chapter follow partly [103] (but also with different signature).

2.3.1 The Supergravity Lagrangian

As stated above, supergravity is a non-renormalizable theory and therefore should in general depend on the three functions defined in section on general actions in superspace. The remarkable feature of the supergravity Lagrangian is that it depends on the gauge kinetic function and just one combination:

$$G = K/M_P^2 + ln\left(|W|^2/M_P^6\right), \tag{2.56}$$

of the Kähler potential and the superpotential. G is called *Kähler function* and is real and dimensionless. We have maintained the dependence on the reduced Planck mass:

$$M_P = \frac{1}{\sqrt{8\pi G_N}} \simeq 2.4 \times 10^{18} \text{ GeV}. \tag{2.57}$$

In what follows, derivatives of the Kähler function with respect to the chiral superfields are denoted by:

$$G^i = \left.\frac{\partial G}{\partial \Phi_i}\right|_{\Phi_i \to \phi_i}, \quad \text{and} \quad G_j = \left.\frac{\partial G}{\partial \Phi^{*j}}\right|_{\Phi_j \to \phi_j}. \tag{2.58}$$

Note that the superfields have been replaced by their scalar components after differentiation. The position of the indices corresponds to the chirality of the superfield with respect to which the quantity is differentiated. Raised (lowered) indices i correspond to derivatives with respect to Φ_i (Φ^{*i}). The Kähler metric

$$G_i^j = \left.\frac{\partial^2 G}{\partial \Phi_j \partial \Phi^{*i}}\right|_{\Phi_i \to \phi_i} = \frac{K_j^i}{M_P^2}, \tag{2.59}$$

does not depend on the superpotential. The inverse of the Kähler metric is denoted $(G^{-1})^j_i$, so that:

$$(G^{-1})^k_i G^j_k = \delta^j_i \ . \tag{2.60}$$

It can be also written as $M_P^2 (K^{-1})^j_i$. Additionally, we define the Kähler "connection" Γ^{kij}, and the "curvature" R^{ik}_{jl}, where we differentiate now directly with respect to the scalars:

$$\Gamma^{ij}_k = \left(G^{-1}\right)^l_k \frac{\partial}{\partial \phi_i} G^j_l \,, \tag{2.61}$$

$$R^{ik}_{jl} = \frac{\partial}{\partial \phi_i}\frac{\partial}{\partial \phi^{*j}} G^k_l - (G^{-1})^n_m \left(\frac{\partial}{\partial \phi^{*j}} G^m_l\right)\left(\frac{\partial}{\partial \phi_i} G^k_n\right). \tag{2.62}$$

The purely bosonic part of the supergravity Lagrangian is of the form

$$\begin{aligned}\frac{\mathcal{L}_B}{\sqrt{-g}} = &-\frac{M_P^2}{2} R + M_P^2 G^i_j \left(\tilde{\mathcal{D}}_\mu \phi_i\right)\left(\tilde{\mathcal{D}}^\mu \phi^{*j}\right) - V(\phi, \phi^*) \\ &- \frac{1}{4}\left(\mathrm{Re} f_{ab}\right) F^a_{\mu\nu} F^{b\mu\nu} + \frac{1}{4}\left(\mathrm{Im} f_{ab}\right) F^a_{\mu\nu} \tilde{F}^{b\mu\nu},\end{aligned} \tag{2.63}$$

where $g = \det g_{\mu\nu}$ is the determinant of the space-time metric. The first part involving the Ricci scalar R is the Einstein-Hilbert term, the second part is the kinetic term of the scalar fields, in general, not in the canonical form, the third term is the scalar potential, while the last two terms correspond to the kinetic term of the gauge bosons and the CP-violating term due to instanton effects. From now on, we write explicitly the dependence on the gauge coupling g_a. The field space of the scalars is a Kähler manifold, with the metric defined in eq. (2.59).

The covariant derivative of the scalars has the form:

$$\tilde{\mathcal{D}}_\mu \phi_i = \partial_\mu \phi_i - g_a A^a_\mu X^a_i = \partial_\mu \phi_i + i g_a A^a_\mu (G^{-1})^j_i \frac{\partial D^a}{\partial \phi^{*j}}, \tag{2.64}$$

where the X^{ia} are holomorphic Killing vector fields corresponding to isometries of the Kähler metric G^i_j and the D^a are the associated Killing potentials. In the case of a renormalizable Kähler potential $K = \Phi_i \tilde{\Phi}^{i*}$, the Killing vectors and the Killing potential take the following form:

$$X^a_i = -i \left(T^a\right)_i{}^j \phi_j \tag{2.65}$$

$$D^a = \phi^{*i} \left(T^a\right)_i{}^j \phi_j \tag{2.66}$$

leading to the usual covariant derivative.

The scalar potential $V(\phi, \phi^*)$ is a sum of two contributions:

$$V = V_F + V_D, \tag{2.67}$$

where V_F is the generalization of the F-term contribution to the scalar potential and is given by

$$V_F = M_P^4 \, e^G \left[G^i \left(G^{-1}\right) G_j - 3\right]. \tag{2.68}$$

Unlike the case of global supersymmetry, the scalar potential in supergravity is not necessarily non-negative, because of the -3 term. This fact spoils the nice feature of global supersymmetry, which was one of the theoretical arguments in its favor. We will reflect on this issue further in the next section. The D-term contribution from gauge interactions reads:

$$V_D = \frac{g_a^2}{2}(\mathrm{Re}f_{ab}^{-1})D^a D^b \tag{2.69}$$

where we have extracted the dependence on g_a from the gauge kinetic function as noted above. Before proceeding with the full supergravity Lagrangian in component form, we will give the covariant derivatives of the fermion χ which constitutes the chiral multiplet together with the scalar ϕ, the fermion λ which belongs to the gauge multiplet and the gravitino ψ. We will use the derivatives of the Kähler potential K when appropriate.

$$\begin{aligned}
\tilde{\mathcal{D}}_\mu\chi_i \equiv{}& \partial_\mu\chi_i - \frac{i}{2}\omega_\mu^{ab}\sigma_{ab}\chi_i + \Gamma_i^{jk}\tilde{\mathcal{D}}_\mu\phi_j\chi_k - g_a\left(\mathrm{Re}f_{ab}\right)A_\mu^a\frac{\partial X^{ib}}{\partial\phi_j}\chi_j \\
&- \frac{1}{4M_P^2}\left(K^j\tilde{\mathcal{D}}_\mu\phi_j - K_j\tilde{\mathcal{D}}_\mu\phi^{*j}\right)\chi_i - \frac{i}{2M_P^2}g_a\left(\mathrm{Re}f_{ab}\right)A_\mu^a\mathrm{Im}F^b\chi_i
\end{aligned} \tag{2.70}$$

$$\begin{aligned}
\tilde{\mathcal{D}}_\mu\lambda^a \equiv{}& \partial_\mu\lambda^a - \frac{i}{2}\omega_\mu^{ab}\sigma_{ab}\lambda^a - g_a f^{abc}A_\mu^b\lambda^c \\
&+ \frac{1}{4M_P^2}\left(K^j\tilde{\mathcal{D}}_\mu\phi_j - K_j\tilde{\mathcal{D}}_\mu\phi^{*j}\right)\lambda^a + \frac{i}{2M_P^2}g_a\left(\mathrm{Re}f_{bc}\right)A_\mu^b\mathrm{Im}F^c\lambda^a
\end{aligned} \tag{2.71}$$

$$\begin{aligned}
\tilde{\mathcal{D}}_\mu\psi_\nu \equiv{}& \partial_\mu\psi_\nu - \frac{i}{2}\omega_\mu^{ab}\sigma_{ab}\psi_\nu \\
&+ \frac{1}{4M_P^2}\left(K^j\tilde{\mathcal{D}}_\mu\phi_j - K_j\tilde{\mathcal{D}}_\mu\phi^{*j}\right)\psi_n u + \frac{i}{2M_P^2}g_a\left(\mathrm{Re}f_{bc}\right)A_\mu^b\mathrm{Im}F^c\psi_\nu\,.
\end{aligned} \tag{2.72}$$

In these expressions ω_μ^{ab} is the spin connection, and

$$F^a \equiv -iG_j^i\frac{\partial D^a}{\partial\phi^{*j}}\frac{\partial K}{\partial\phi^i} + iD^a\,, \tag{2.73}$$

$$\sigma^{\mu\nu} \equiv \frac{i}{4}\left(\sigma^\mu\bar{\sigma}^\nu - \sigma^\nu\bar{\sigma}^\mu\right). \tag{2.74}$$

The most general supergravity Lagrangian [106] is lengthy. It can be found in terms of two- and four-component spinors in the book by Wess and Bagger and also with our metric in the work of Moroi [107]. However, nota bene that some of our signs differ from the ones in [107]. Here we give the Lagrangian for the simplified case $f_{ab} = \delta_{ab}(1 - i\Theta_a/8\pi^2)$ restoring the dependence on the Planck mass and with our metric and sigma matrix conventions:

$$\begin{aligned}
\frac{\mathcal{L}}{\sqrt{-g}} = \frac{\mathcal{L}_B}{\sqrt{-g}} &- \epsilon^{\mu\nu\rho\sigma}\psi_\mu^\dagger\bar{\sigma}_\nu\tilde{\mathcal{D}}_\rho\psi_\sigma \\
&+ M_P^2\left(iG_j^i\chi^{\dagger j}\overline{\sigma}^\mu\tilde{\mathcal{D}}_\mu\chi_i + \sqrt{2}g_a G_j^i X^{*aj}\chi_i\lambda^a + \sqrt{2}g_a G_j^i X_i^a\chi^{\dagger j}\lambda^{\dagger a}\right) \\
&+ \frac{i}{2}(\mathrm{Re}f_{ab})\left[\lambda^a\sigma^\mu\tilde{\mathcal{D}}_\mu\lambda^{\dagger b} + \lambda^{\dagger a}\overline{\sigma}^\mu\tilde{\mathcal{D}}_\mu\lambda^b\right] - \frac{1}{2}(\mathrm{Im}f_{ab})\tilde{\mathcal{D}}_\mu\left[\lambda^a\sigma^\mu\lambda^{\dagger b}\right] \\
&+ \frac{1}{M_P}\left[\frac{g_a}{2}(\mathrm{Re}f_{ab})\left(D^a\psi_\mu\sigma^\mu\lambda^{\dagger b} - D^a\psi_\mu^\dagger\overline{\sigma}^\mu\lambda^b\right)\right. \\
&\qquad\left. - \frac{M_P^2}{\sqrt{2}}G_j^i\left(\tilde{\mathcal{D}}_\nu\phi^{*j}\chi_i\sigma^\mu\bar{\sigma}^\nu\psi_\mu + \tilde{\mathcal{D}}_\nu\phi_i\chi^{\dagger j}\overline{\sigma}^\mu\sigma^\nu\psi_\mu^\dagger\right)\right.
\end{aligned}$$

$$
\begin{aligned}
&\quad - \frac{1}{4}(\mathrm{Re}f_{ab})\left(\psi_\mu\sigma^{\rho\sigma}\sigma^\mu\lambda^{\dagger a} + \psi_\mu^\dagger\bar\sigma^{\rho\sigma}\overline{\sigma}^\mu\lambda^a\right)\left(F^b_{\rho\sigma}+\hat F^b_{\rho\sigma}\right)\Big] \\
&+\frac{1}{M_P^2}\Bigg[-\frac{M_P^2}{4}G^i_j\left(i\epsilon^{\mu\nu\rho\sigma}\psi_\mu\sigma_\nu\psi^\dagger_\rho - \psi_\rho\sigma^\sigma\psi^{\dagger\rho}\right)\chi_i\sigma_\sigma\chi^{\dagger j} \\
&\qquad + \frac{3}{16}(\mathrm{Re}f_{ab})(\mathrm{Re}f_{cd})\lambda^a\sigma^\mu\lambda^{\dagger b}\lambda^c\sigma_\mu\lambda^{\dagger d} \\
&\qquad - \frac{M_P^4}{8}\left(G^i_jG^k_l - 2R^{ik}_{jl}\right)\chi_i\chi_k\chi^{\dagger j}\chi^{\dagger l} - \frac{M_P^2}{8}G^i_j(\mathrm{Re}f_{ab})\chi^{\dagger j}\overline{\sigma}^\mu\chi_i\lambda^{\dagger a}\bar\sigma_\mu\lambda^b\Bigg] \\
&+ ie^{G/2}M_P\left(\psi_\mu\sigma^{\mu\nu}\psi_\nu + \psi_\mu^\dagger\bar\sigma^{\mu\nu}\psi_\nu^\dagger\right) - \frac{i}{\sqrt{2}}e^{G/2}M_P^2\left(G^i\chi_i\sigma^\mu\psi^\dagger_\mu + G_i\chi^{\dagger i}\overline{\sigma}^\mu\psi_\mu\right) \\
&- e^{G/2}M_P^3\left[\frac{1}{2}\left(G^{ij}+G^iG^j\right)\chi_i\chi_j + \frac{1}{2}\left(G_{ij}+G_iG_j\right)\chi^{\dagger i}\chi^{\dagger j}\right], \qquad (2.75)
\end{aligned}
$$

where

$$
\hat F^a_{\mu\nu} \equiv F^a_{\mu\nu} - \frac{i}{2M_P}\left(\psi_\mu\sigma_\nu\lambda^{\dagger a} + \psi_\mu^\dagger\bar\sigma_\nu\lambda^a + \psi_\nu\sigma_\mu\lambda^{\dagger a} + \psi_\nu^\dagger\overline{\sigma}^\mu\lambda^a\right). \qquad (2.76)
$$

Note, that G^i_j has dimension $[\mathrm{mass}]^{-2}$, and G^i has the dimension of $[\mathrm{mass}]^{-1}$. The total Lagrangian contains interactions between the gravitino field ψ_μ and the supercurrent S_μ needed in the later discussion. Therefore, we extract these interactions:

$$
\begin{aligned}
\frac{\mathcal{L}_{\psi S}}{\sqrt{-g}} &= -\frac{1}{\sqrt{2}M_P}K^i_j\left(\tilde{\mathcal{D}}_\nu\phi^{*j}\chi_i\sigma^\mu\bar\sigma^\nu\psi_\mu + \tilde{\mathcal{D}}_\nu\phi_i\chi^{\dagger j}\overline{\sigma}^\mu\sigma^\nu\psi^\dagger_\mu\right) \\
&\quad - \frac{1}{2M_P}(\mathrm{Re}f_{ab})\left(\psi_\mu\sigma^{\rho\sigma}\sigma^\mu\lambda^{\dagger a} + \psi_\mu^\dagger\bar\sigma^{\rho\sigma}\overline{\sigma}^\mu\lambda^a\right)F^b_{\rho\sigma}. \qquad (2.77)
\end{aligned}
$$

2.3.2 The Super-Higgs mechanism

In order for local or global SUSY to be broken, the expectation value of the variation of a spinorial operator under supersymmetric transformations has to be non-zero. The variation of the chiral fermion includes a term

$$
F_i = -M_P^2e^{G/2}\left(G^{-1}\right)^j_i G_j. \qquad (2.78)
$$

The F_i are order parameters for symmetry breaking in supergravity and are generalizations of the auxiliary fields F in global supersymmetry. Therefore, local SUSY is broken if one of the F_i acquires a vacuum expectation value. The breaking of global supersymmetry is accompanied by the appearance of a massless Goldstone fermion in the spectrum - the goldstino. In supergravity, as in ordinary gauge theory, the goldstino gets mixed with the gravitino and provides it with the longitudinal degrees of freedom and hence a mass. This phenomenon is called the super-Higgs mechanism. The converse statement is however not true. Gravitino mass is, in general, not the order parameter of SUSY breaking.

Gravitino acquires a mass if the Kähler function G acquires a vacuum expectation value. The would-be gravitino mass term can be found in the Lagrangian eq. (2.75) and reads

$$
ie^{G/2}M_P\left(\psi_\mu\sigma^{\mu\nu}\psi_\nu + \psi_\mu^\dagger\bar\sigma^{\mu\nu}\psi_\nu^\dagger\right). \qquad (2.79)
$$

The mass of the gravitino is given by

$$
m_{3/2} = e^{G_0/2}M_P, \qquad (2.80)
$$

where G_0 is the expectation value of the Kähler function G. Writing the scalar potential as

$$V_F = K^i_j F_i F^{*j} - 3e^{K/M_P^2} W W^*/M_P^2, \tag{2.81}$$

with F_i defined in eq. (2.78), one sees that SUSY can be unbroken in spaces with negative vacuum energy (AdS) and non-vanishing gravitino mass if G_j vanishes.

If SUSY is broken, the potential (2.81) tells us that the vacuum can have an arbitrary value of the cosmological constant. However, even if astrophysical observations imply a tiny cosmological constant, the value is far too low to be associated with SUSY breaking, since in general at the minimum $V \approx m_{3/2} M_P^2$. Therefore, it is usually assumed that the vacuum energy vanishes. Why this is the case, is not understood. In the case of the vanishing cosmological constant one finds:

$$\left\langle K^i_j F_i F^{*j} \right\rangle = 3 M_P^4 e^{\langle G \rangle}, \tag{2.82}$$

which leads to an equivalent formula for the gravitino mass:

$$m_{3/2}^2 = \frac{\left\langle K^i_j F_i F^{*j} \right\rangle}{3 M_P^2}. \tag{2.83}$$

2.4 Origins of Supersymmetry Breaking

The MSSM, as presented in the previous sections, has a huge number of free parameters associated with the breaking of supersymmetry. Therefore, the general MSSM is not a tractable framework for phenomenological studies. Usually, the general features of the MSSM are associated with the conservation of R-Parity, which leads to signatures involving missing transverse energy from the lightest stable supersymmetric particle. However, even this prediction is not robust, since R-parity might be violated. It is possible to obtain some hints about the structure of the SUSY breaking terms from low energy experiments looking for flavor changing neutral currents and violation of CP symmetry. Effects from arbitrary patterns (including phases) of squark mass matrices would enter via loops into the low energy observables like the mass difference between the long-lived and short-lived Kaons, or the electric dipole moment of the neutron. The tight constraints on such effects suggest a pattern of universality in the scalar mass terms. It is assumed that they are real, proportional to the identity matrix, and degenerate in the first two generations. Usually, one takes the third family also to be degenerate in mass with the first two. Additionally, the renormalization group evolution of the gaugino masses is proportional to the evolution of the corresponding gauge couplings. Since the gauge couplings should unify at the scale of grand unification, it is natural to assume that also the masses of the gauginos unify at the GUT scale.

In order to obtain control over the huge parameter space of the MSSM, one has to make assumptions on the structure of some underlying theory which is approximated by the MSSM in the low energy regime. These assumptions are reflected in different phenomenological models of supersymmetry which reduce the number of free parameters by exploiting the hints presented above. In these models SUSY is broken at some high scale $F \gg M_W^2$ in a hidden sector, whose dynamics is unimportant for phenomenology. The important part is the nature of the agent, which is a superheavy particle of mass m_X transmitting the SUSY breaking to the fields of the observable sector. The coupling of the goldstino to the observable

sector is suppressed by a power of $\sqrt{F}/M_X$, and the soft SUSY breaking masses are of order $m_{\text{soft}} \sim F/M_X$. The soft masses are required to be comparable to the weak scale, even though the fundamental SUSY breaking scale may be much larger.

The different supersymmetric models are distinguished by the nature of the SUSY breaking messenger:

- Going beyond global supersymmetry to the local case includes gravity into the description of nature. Since quantum gravity couples universally to energy mediation of SUSY breaking by gravitationally coupled degrees of freedom is always present. Therefore, the scale M_X is associated with the Planck scale and $\sqrt{F} \sim 10^{10}$ GeV. All soft masses are connected with the gravitino mass which should be thus near the Fermi scale .

- Even if effects of gravity are always present, one may exclude them from the effective description, if one assumes that some other effects give dominant contributions, e. g. the breaking is mediated by SM gauge interactions. In gauge-mediated supersymmetry breaking models (GMSB), new messenger fields M, that couple directly to the hidden sector but which also have SM gauge couplings act as mediators. The supersymmetry breaking masses are created only at the loop level, evading the tree-level sum rules. The SUSY-breaking masses are given by

$$m_i \propto \frac{g_i^2 n_i}{16\pi^2} \frac{\langle F_S \rangle}{M}, \tag{2.84}$$

  where $\langle F_S \rangle$ is the induced SUSY-breaking vacuum expectation value, M is the messenger sector mass, and n_i are group-theoretical factors. Since M can be much smaller than the Planck scale the expectation value F_S can have much smaller value than in gravity mediation models. The gravitino mass, however, is determined by the Planck mass and the fundamental SUSY breaking scale F with typically $F_S < F$ or $F_S \sim F$, leading to a gravitino mass which is much smaller than in the case of gravity mediation and also much smaller than the masses of other superparticles.

In the following we will describe the models which will be used throughout the present work.

2.4.1 Minimal Supergravity (mSUGRA) Model

In supergravity models of SUSY breaking, the superpotential consists of the visible and hidden sector terms which are completely independent. The dynamics of the hidden sector breaks supersymmetry. The goldstino degrees of freedom are absorbed by the gravitino which obtains a mass $m_{3/2}$. The low energy effective theory is obtained by taking the Planck scale to infinity while keeping the gravitino mass fixed. The theory obtained consist of the supersymmetric version of the SM augmented by SUSY breaking masses of order $m_{3/2} \sim m_W$ and higher dimensional operators suppressed by appropriate powers of M_P.

In general, all gaugino masses are different and the trilinear a terms are not proportional to the corresponding superpotential Yukawa couplings. However, the most studied model of gravity mediated supersymmetry breaking, which will be also used in the present work is the minimal supergravity model. The "minimal" in the name refers to the choice of a renormalizable Kähler potential i.e. flat Kähler metric leading to a common mass of all scalars $m_0^2 = m_{3/2}^2 + V_0/M_P^2$, where V_0 is the minimum of the scalar potential. Common

gaugino masses arise either by unification of gauge interactions or from a universal gauge kinetic function for each factor of gauge symmetry. The fundamental parameters of this model are :

$$m_0, \quad m_{1/2}, \quad A_0, \quad \tan\beta, \quad \text{sign}(\mu), \tag{2.85}$$

where m_0 is the common mass of the scalars, $m_{1/2}$ is the common gaugino mass, A_0 is the universal proportionality constant between an a-term and the corresponding Yukawa coupling, $\tan\beta$ is the ratio of the Higgs vacuum expectation ratios, as defined in section 2.2.1 which is treated for the B-term after electroweak symmetry breaking, and $\text{sign}(\mu)$ is the sign of μ term, whose magnitude is fixed by the Z-boson mass after electroweak symmetry breaking. It is assumed that the universality of the parameters holds at the scale of grand unification rather than at M_P. The model is also called the CMSSM for constrained minimal supersymmetric Standard Model rather than mSUGRA, since supergravity does not necessary lead to high scale universality, in contrast to what was originally thought [102].

2.4.2 Hybrid Gauge-Gravity Mediation

The apparent unification of gauge couplings at the scale $M_{GUT} \approx 10^{16}$ GeV is a strong hint for the paradigm of unification presented in the beginning of this chapter. The forces should unify and be described by a simple gauge group. However, since now all particles have to form multiplets of the larger gauge group, which is at least $SU(5)$, one faces the problem of $SU(3)$-triplet Higgs fields which lead to the proton decay via dimension-5 operators. Therefore, it is assumed that Higgs multiplets are incomplete (split). The question why matter appears in complete representations, while the Higgs multiplets are split, is one of the motivations for grand unified theories on orbifolds.

In these models the usual space-time is augmented by compact extra dimensions. The compact manifold $\mathcal{M}$ and the quantum-field theory under discussion are both thought to be symmetric under a discrete group G. If the manifold possesses fixed-points under the non-trivial action of the group, the physical shape of the extra dimensions is a quotient manifold $\mathcal{C} = \mathcal{M}/G$ which turns out to be an orbifold (orbit-manifold). It is not smooth, but has singular points which are precisely the fixed points. The fields living on the orbifold (bulk fields) have to obey special boundary conditions at the fixed points, which can differ from fixed point to fixed point. The physical fields in the effective 4-dimensional theory are the zero modes of the Kaluza-Klein expansion on the orbifold which respect all boundary conditions and the fields living on the branes at the fixed-points. The effects of the orbifold construction can be twofold: The gauge symmetry can be reduced from the full gauge group to a subgroup either in the bulk or at the brane located at some fixed point, if not all gauge fields posses zero modes. The same mechanism can lead to appearance of split multiplets in the case of matter or Higgs fields.

Any incomplete multiplet, besides the Higgs, should have a mass near M_{GUT} in order not to spoil gauge coupling unification. They can obtain masses from SM singlet fields acquiring vacuum expectation values of the order of M_{GUT}. Since the incomplete multiplets are charged under the SM gauge group, the singlets couple always to conjugate pairs i.e. to a "vector-like" representation of the SM gauge group. Therefore, vector-like pairs of exotics obtain masses. The number of such exotics in orbifold models can be large. If the singlets also obtain F-term expectation values (break SUSY) from some dynamics, the vector-like fields will act as messengers for gauge-mediated SUSY breaking. The resulting patter of SUSY-breaking terms will be different from the usual low-scale gauge mediation scenarios sketched above,

where the messengers need to form complete GUT multiplets in order to allow for gauge coupling unification. Since the messenger scale is M_{GUT}, the gauge-mediated contribution to soft SUSY breaking terms is comparable with the gravity-mediated contribution:

$$m_{\text{soft}} = \frac{\langle F_S \rangle}{16\pi^2 M_{GUT}} \approx \frac{\langle F_S \rangle}{M_P} \sim \frac{\langle F \rangle}{M_P} \sim m_{3/2}. \tag{2.86}$$

This is the reason why this possible pattern of breaking is called hybrid gauge-gravity mediation, see [74, 75] and referenced therein. In cases where the number of messengers is large the gauge mediated terms will dominate. However, gauge mediation cannot give rise to the μ term which is still generated by the Giudice-Masiero mechanism, see section 2.2.1. The μ term as well as the B and the trilinear a terms can therefore be smaller than the soft-masses. The GUT-scale MSSM parameters are then characterized by the hierarchy:

$$\left\{\mu, m_{3/2}, A, \sqrt{B}\right\} \ll \left\{m_{1/2}, m_0, m_{u/d}\right\}. \tag{2.87}$$

This hierarchy allows for peculiar low-energy spectra: The only light states can be the lightest Higgs state and higgsinos with masses around 100 GeV. The gravitino is the natural lightest supersymmetric particle, with a higgsino-like neutralino NLSP. The second neutralino and a higgsino-like chargino are slightly heavier. The mass of the lightest Higgs scalar can be lifted to around $120 - 125$ GeV by large squark loop effects. All the remaining states are very heavy and may be even non accessible at the LHC. We will investigate, in detail, the phenomenological consequences of this model in Chapter 5.

2.4.3 Anomaly Mediation

Another breaking mechanism involving extra spatial dimensions is the anomaly-mediated supersymmetry breaking (AMSB) [108, 109]. Assuming one additional hidden dimension all fields of the MSSM can be localized at the 4-dimensional hypersurface - the MSSM brane, while the SUSY-breaking sector is confined to another parallel hypersurface - the hidden brane. The transmission of supersymmetry breaking takes then place entirely due to (super)gravity effects.

The Planck-scale can enter the supergravity formulation [106] as the vacuum expectation value of the scalar component of a non-dynamical chiral supermultiplet $\langle \phi \rangle = 1$, usually called *conformal compensator*. Without this VEV the theory exhibits enlarged symmetry - the local superconformal invariance which must be broken since the real-world gravitational interactions set a preferred scale given by the Newton's constant. The SUSY breaking at the hidden brane given by $\langle F \rangle \neq 0$ causes the F-term of the conformal compensator which has a dimension of mass also to obtain a VEV:

$$\langle F_\phi \rangle \sim \frac{\langle F \rangle}{M_P} \sim m_{3/2}. \tag{2.88}$$

However, the supersymmetry is still unbroken at the MSSM brane at the classical level, since the effects of SUSY breaking are exponentially suppressed by the extra-dimensions. In the quantum description, on the other hand, the scale-invariance is anomalously violated, see for example dimensional transmutation in QCD, and since SUSY is also broken by the conformal compensator field the effects of SUSY breaking appear at loop level at the MSSM brane. The gaugino masses arise at one-loop order while the scalar-squared masses arise at two loop order, see also [103] for details.

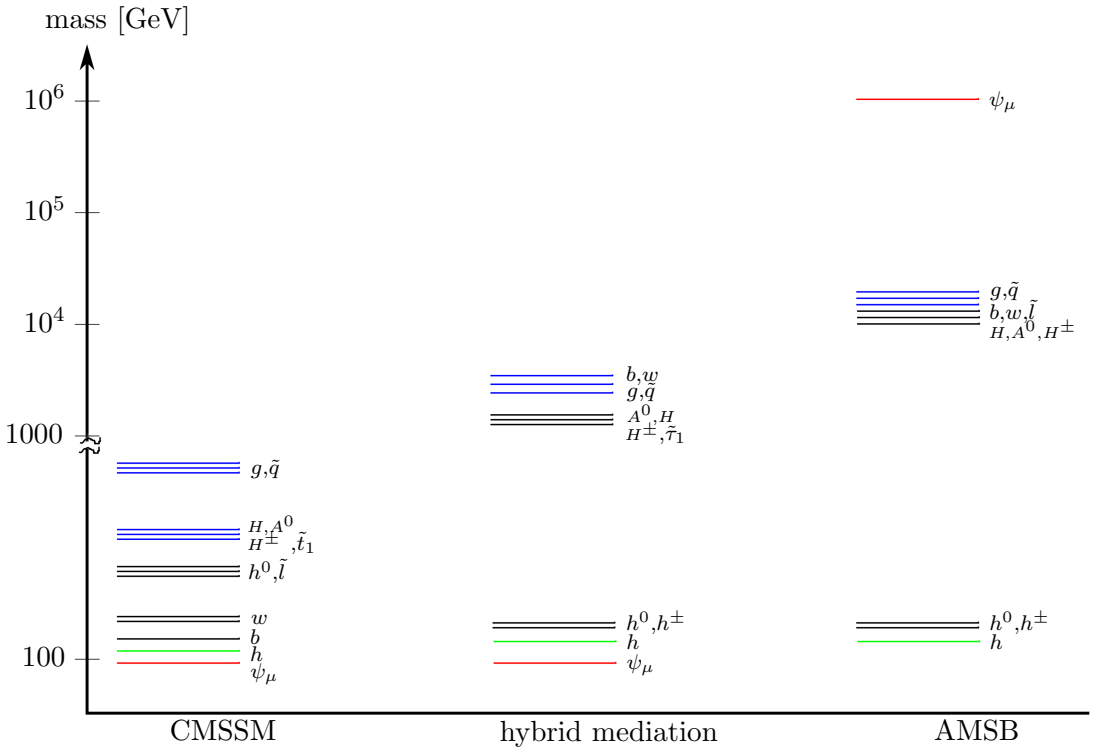

Figure 2.2: Possible mass spectra of supersymmetric particles in different scenarios of SUSY breaking. The blue lines indicate colored particles, while the green [red] line indicates the lightest neutral Higgs [gravitino]. Neutralinos and charginos are written in terms of the dominant gauge-eigenstate contribution. In case of the CMSSM the NLSP is a bino-like neutralino, while it is a higgsino-like neutralino in the case of hybrid gauge-gravity mediation. In the heavy gravitino scenario the LSP is also the higgsino-like neutralino. The CMSSM spectrum was obtained by means of `SOFTSUSY` [110] with $m_0 = m_{1/2} = 350$ GeV, $A_0 = 0$, $\tan\beta = 10$, $\text{sign}(\mu) = 1$. The hybrid spectrum is taken from [75], while the AMSB spectrum is taken from [73].

The discussion above does not constrain the supersymmetric higgsino mass parameter and allows for following hierarchical mass spectra:

$$\mu \ll m_{soft} \ll m_{3/2}\,, \tag{2.89}$$

for example with $\mu \sim \mathcal{O}(100)$ GeV, $m_{soft} \sim \mathcal{O}(10^4)$ GeV, and $m_{3/2} \sim \mathcal{O}(10^6)$ GeV. Such extreme hierarchy could for example solve the μ problem [73] and give rise to a Higgs mass compatible with the current experimental bounds and close to the current hints at the LHC. In general, such scenarios involve superheavy gravitino, heavy scalars and gauginos, the only light SUSY particles being the higgsinos.

Figure 2.2 summarizes the possible supersymmetric mass spectra in different SUSY breaking scenarios. Although the CMSSM is the most studied case it is obvious that SUSY breaking can be realized in nature in many different ways which can lead to a dramatically different LHC phenomenology. We will investigate in the following chapters why such unusual spectra might be well motivated by cosmology and estimate their impact on the results of SUSY searches at the LHC. As we have seen in this chapter the gravitino obtains a mass after the breaking of supersymmetry and appears somewhere in the supersymmetric spectrum. In the

next section we discuss the massive gravitino and review the implications of the presence of the gravitino in the early universe.

2.5 The massive Gravitino

The massive gravitino in the flat limit is described by the following Lagrangian which can be inferred from eq. (2.75):

$$\mathcal{L}_{3/2} = -\epsilon^{\mu\nu\rho\sigma}\psi_\mu^\dagger\bar{\sigma}_\nu\partial_\rho\psi_\sigma + im_{3/2}(\psi_\mu\sigma^{\mu\nu}\psi_\nu + \psi_\mu^\dagger\bar{\sigma}^{\mu\nu}\psi_\nu^\dagger) + \mathcal{L}_{int}. \tag{2.90}$$

Translated into the four-component notation with $\Psi_\mu = (\psi_\mu, \psi_\mu^\dagger)^T$ using the notation from reference [111], we obtain the Lagrangian [51]:

$$\mathcal{L}_{3/2} = -\frac{1}{2}\epsilon^{\mu\nu\rho\sigma}\bar{\Psi}_\mu\gamma^5\gamma_\nu\partial_\rho\Psi_\sigma - \frac{1}{4}m_{3/2}(\bar{\Psi}_\mu[\gamma^\mu,\gamma^\nu]\Psi_\nu) + \mathcal{L}_{int}. \tag{2.91}$$

In this section we will make a number of comparisons with the four-component notation used in other works for calculations involving gravitinos in order to check our results. However, we will perform all calculations directly in the two-component notation as in the rest of this work.

From eq. (2.90) we obtain following equation of motion for the free gravitino:

$$-\epsilon^{\mu\nu\rho\sigma}\bar{\sigma}_\nu\partial_\rho\psi_\sigma + 2im_{3/2}(\bar{\sigma}^{\mu\nu}\psi_\nu^\dagger) = 0. \tag{2.92}$$

Differentiating both sides of the equation with ∂_μ we obtain

$$-\frac{1}{2}m_{3/2}\left[(\partial\sigma)\bar{\sigma}^\nu\psi_\nu^\dagger - \sigma^\nu(\partial\bar{\sigma})\psi_\nu^\dagger\right] = 0. \tag{2.93}$$

Equation (2.92) can be further modified using the relations

$$\epsilon^{\mu\rho\sigma\nu}\bar{\sigma}_\nu = i\left(\bar{\sigma}^\mu\sigma^\rho\bar{\sigma}^\sigma - g^{\mu\rho}\bar{\sigma}^\sigma + g^{\mu\sigma}\bar{\sigma}^\rho - g^{\rho\sigma}\bar{\sigma}^\mu\right), \tag{2.94}$$

and

$$2i(\bar{\sigma}^{\mu\nu})^{\dot{\alpha}}{}_{\dot{\beta}} = g^{\mu\nu}\delta^{\dot{\alpha}}{}_{\dot{\beta}} - (\bar{\sigma}^\mu\sigma^\nu)^{\dot{\alpha}}{}_{\dot{\beta}}, \tag{2.95}$$

leading to

$$-i\bar{\sigma}^\nu\partial_\nu\psi_\mu - i\bar{\sigma}^\mu\sigma^\rho\bar{\sigma}^\sigma\psi_\sigma + i\partial_\mu\bar{\sigma}^\sigma\psi_\sigma + i\bar{\sigma}^\mu\partial^\nu\psi_\nu = -m\psi_\nu^\dagger + m\bar{\sigma}^\mu\sigma^\nu\psi_\nu^\dagger. \tag{2.96}$$

Equations (2.93) and (2.96) lead to the Rarita-Schwinger equations [112]:

$$\bar{\sigma}^\mu\psi_\mu(x) = 0, \tag{2.97}$$
$$\sigma^\nu\psi_\nu^\dagger(x) = 0, \tag{2.98}$$
$$\partial^\mu\psi_\mu(x) = 0, \tag{2.99}$$
$$i\bar{\sigma}^\nu\partial_\nu\psi_\mu(x) = m\psi_\mu^\dagger(x), \tag{2.100}$$

which read in the four-component notation:

$$\gamma^\mu\Psi_\mu(x) = 0 \quad \text{and} \quad (i\partial\!\!\!/ - m_{3/2})\Psi_\mu(x) = 0. \tag{2.101}$$

The Rarita-Schwinger equations can be solved, as usual, in the momentum space and one obtains the positive and negative frequency solutions

$$\psi_\mu^+(p,s), \quad \text{and} \quad \psi_\mu^-(p,s), \quad \text{with} \quad s = \pm\frac{3}{2}, \pm\frac{1}{2}, \tag{2.102}$$

which in turn obey similar constraints as the position space wave-functions. A detailed field-theoretical treatment of massive gravitino in the four-component notation can be found in [107,113,114]. For the calculation of unpolarized matrix elements we will need the gravitino polarization tensors

$$P_{\mu\nu}^{\pm}(p) = \sum_s \psi_\mu^{\pm}(p,s)\psi_\nu^{\dagger\pm}(p,s), \tag{2.103}$$

$$\overline{P}_{\mu\nu}^{\pm}(p) = \sum_s \psi_\mu^{\pm\dagger}(p,s)\psi_\nu^{\pm}(p,s), \tag{2.104}$$

where the sum is performed over the four helicity states. The polarization tensors for a gravitino with four-momentum p are given by

$$P_{\mu\nu}^{\pm}(p) = -(\sigma p)\Phi_{\mu\nu}(p) \tag{2.105}$$

for both the positive and negative frequency mode functions. For the conjugate tensor we obtain

$$\overline{P}_{\mu\nu}^{\pm}(p) = -(\bar{\sigma} p)\widetilde{\Phi}_{\mu\nu}(p). \tag{2.106}$$

In the above expressions we use

$$\Pi_{\mu\nu}(p) = \left(g_{\mu\nu} - \frac{p_\mu p_\nu}{m_{3/2}^2}\right), \tag{2.107}$$

and

$$\Phi_{\mu\nu}(p) = \Pi_{\mu\nu}(p) - \frac{1}{3}\Pi_{\mu\sigma}(p)\Pi_{\nu\lambda}(p)\bar{\sigma}^\sigma\sigma^\lambda, \tag{2.108}$$

$$\widetilde{\Phi}_{\mu\nu}(p) = \Pi_{\mu\nu}(p) - \frac{1}{3}\Pi_{\mu\sigma}(p)\Pi_{\nu\lambda}(p)\sigma^\sigma\bar{\sigma}^\lambda. \tag{2.109}$$

These expressions are derived in Section A.5. The interaction part of the gravitino Lagrangian will be considered in Chapter 4.

2.5.1 Gravitino Cosmology

If local supersymmetry is realized in nature, violent conditions in the early universe will create gravitinos. The presence of gravitinos, in general, poses a number of intertwined constraints on several mechanisms operating during different epochs in the history of the universe. Many of these are not welcomed and therefore the network of constraints is usually summarized by the term *the cosmological gravitino problem.*

In the universe without inflation, the gravitino would reach thermal equilibrium and have very high abundance, which would lead to an energy density larger than the critical density, for stable gravitinos not lighter than $\mathcal{O}(\text{eV})$ [46]. If the gravitino is very light, its energy density is simply negligible for the energy budget of the universe, however, the theory possesses then no dark matter candidates, since all other supersymmetric particles are unstable.

Inflation solves these problems by diluting any initial abundance of gravitinos during the exponential expansion of the universe [115]. It is assumed that the gravitino does not enter thermal equilibrium after inflationary phase. Nevertheless, gravitinos are produced from the thermal bath via supersymmetric QCD reactions of the form $G + G \to g + \psi_\mu$. The gravitino relic density is then proportional to the reheating temperature T_R [116, 117] and is given by [51, 118–120]

$$\Omega_{3/2}h^2 \simeq 0.5 \left(\frac{T_R}{10^{10}\,\mathrm{GeV}}\right)\left(\frac{100\,\mathrm{GeV}}{m_{3/2}}\right)\left(\frac{m_g}{1\,\mathrm{TeV}}\right)^2, \tag{2.110}$$

where m_g is the gluino mass. Depending on the reheating temperature of the universe the gravitinos can have again significant impact on cosmology. Thus, the gravitino problem is recreated after inflation.

We have seen in the previous sections, that the gravitino mass depends on the unknown nature of supersymmetry breaking. Gravitino can, therefore, be either an unstable particle somewhere in the supersymmetric spectrum or the lightest supersymmetric particle and hence stable if one assumes R-parity conservation.

If gravitino is not the LSP, it will decay via interactions suppressed by the Planck scale with a lifetime [53]

$$\tau_{3/2} \sim \frac{M_P^2}{m_{3/2}^3} \approx 3 \text{ years } \left(\frac{100\,\mathrm{GeV}}{m_{3/2}}\right)^3. \tag{2.111}$$

Clearly, in general the lifetime is longer than couple of seconds and therefore gravitino decays take also place during BBN. The electromagnetic and/or hadronic cascades from gravitino decays can significantly alter the predictions of light element abundances and spoil the successful predictions of big bang nucleosynthesis. If one requires that the density of gravitinos is small enough to let the predictions of nucleosynthesis unchanged, one has to assume that the reheating temperature of the universe was at most 10^6 GeV [121–126]. Unfortunately, leptogenesis cannot happen for such low temperatures and one has to look for other explanations for matter-antimatter asymmetry in the universe.

However, the gravitino decays early enough if its mass is larger than $\mathcal{O}(10)$ TeV, cf. eq. (2.111). As we have seen in Section 2.4 , such heavy gravitinos can appear in scenarios where anomaly mediated contributions to the soft masses are significant. If there is significant amount of gravitino decays after the freeze-out of the LSP, they will give rise to a non-thermal component of the LSP energy-density, assuming R-parity conservation. It turns out, that such non-thermal production of pure wino- or higgsino-like neutralino LSP in heavy gravitino decays can account for the observed amount of dark matter and simultaneously fulfill the constraints from BBN, while allowing for reheating temperatures needed for leptogenesis [56]. In the case of higgsino LSP, the usual SUSY searches at the LHC may be insufficient for the discovery. We will investigate the consequences of higgsino LSP (NLSP) for the LHC phenomenology in Section 5.1. An alternative solution to the unstable gravitino case, is a supersymmetric particle spectrum that allows only for decays into particle species decoupled from the thermal bath [127].

If the gravitino is the LSP, and R-parity is conserved, it is stable and there are no dangerous gravitino decays. In this case the gravitino relic density eq.(2.110) can explain the observed dark matter density for reasonable values of gluino mass, the gravitino mass in the $\mathcal{O}(100)$ GeV range and $T_R \approx \mathcal{O}(10^{10})$ GeV allowing for leptogenesis. If the gravitino is too light, the gravitino relic density, however, may exceed the critical density of the universe for high reheating temperatures needed for leptogenesis. A very light gravitino with a mass of $\mathcal{O}(1)$

keV which can enter thermal equilibrium and allow for arbitrary reheating temperature is excluded by warm dark matter constraints [128].

In case of gravitino LSP, one has also to take care of the NLSP[2] decays, since the coupling of the NLSP to the gravitino is also suppressed by the Planck scale. The NLSP lifetime is given by

$$\tau_{\rm NLSP} \leq 2 \text{ months } \left(\frac{m_{3/2}}{100 \text{ GeV}}\right)^2 \left(\frac{200 \text{ GeV}}{m_{\rm NLSP}}\right)^5 \ll 1 \text{ s} \sim t_{\rm BBN}, \tag{2.112}$$

and one once again recovers potential tension with the predictions of the BBN [129]. Whether the NLSP decay problem truly occurs or not, depends on the nature of the NLSP. The hadronic decays of a neutralino NLSP typically dissociate the primordial light elements [130–132] and also the stop NLSP is strongly constrained [133, 134]. A long lived stau NLSP can form a bound state with ^{4}He and catalyze the production of ^{6}Li [135–138] but it is possible to obtain a consistent cosmology with leptogenesis in some corners of its parameter space [139–141]. Also a sneutrino NLSP can allow for consistent cosmological scenarios due to its invisible decays [142–144].

Although there are some regions in the parameter space of the theories allowing for consistent cosmology, as presented above, there are also other mechanisms which can circumvent the NLSP problem and lead to interesting consequences. The gravitino may be degenerate in mass with the NLSP, so that its decay products are low-energetic and do not change the predictions of BBN [141]. The gravitino could also have additional decay channels to hidden sector particles and decay before the BBN [145, 146]. Also a light gravitino with a super-light neutralino is a possible spectrum solving all problems [147]. Furthermore, the number density of the NLSPs can be diluted by late-time entropy production before the BBN [76, 137, 148]. A recent work exploring some of this ideas is [149].

In the present work we will mainly pursue another line of thought: Small violation of R-parity is sufficient to cause the NLSP to decay into the SM particles before the onset of BBN. In the next chapter we will extensively review R-parity violation and introduce the R-parity violating couplings. In general, a gravitino coupling to the SM particles of the order of 10^{-13} is sufficient to solve the NLSP decay problem [57]. We will review the upper bounds on R-parity violating couplings from cosmology in Chapter 4, but we can state already here that there is a several orders of magnitude wide range for the couplings allowed by all constraints. The gravitino will also decay into SM particles but its decay is double suppressed due to the Planck scale and the tiny R-parity violating couplings, and it therefore remains a viable (decaying) dark matter candidate with a life-time exceeding the age of the universe [58]. The gravitino abundance in such scenario is determined only by the thermal production rate and can explain the abundance of dark matter. Thus, small amount of R-parity breaking renders supersymmetric cosmology consistent and allows additionally for interesting LHC phenomenology involving long lived particles. In some cases the presence of R-parity violation can significantly change supersymmetric signatures and hide SUSY from LHC searches. This will be investigated in Section 5.2. Additionally, small violation of R-parity may also relax cosmological constraints on the axion multiplet and therefore be connected with the solution to the strong CP problem [150].

Summing up, we note that the presence of gravitino in the supersymmetric spectrum can significantly change the course of the history of the universe. In order to achieve consistent

[2]In the context of gravitino LSP, the NLSP is sometimes called LOSP - lightest ordinary supersymmetric particle.

cosmology involving generation of light elements via big bang nucleosynthesis and generation of the matter-antimatter asymmetry via leptogenesis, one has to change the usual supersymmetric scenarios. These changes can in turn have an impact on the signatures at the LHC, along the lines of our motto - as above so below. In this work we will focus on consistent cosmological scenarios involving i) a higgsino LSP, NLSP in models with super-heavy gravitino, gravitino dark matter and late time entropy production, respectively, ii) a higgsino, bino, or stau NLSP in models with gravitino dark matter and R-parity violation. In both cases supersymmetry can escape searches at the LHC largely relying on missing transverse energy signature.

In the next chapter we will review the ideas behind R-parity and investigate in detail bilinear pattern of R-parity breaking. In the following chapters we will then explore the connection between gravitinos and the LHC phenomenology.

Chapter 3

R-parity Breaking

R-parity [151–156] is a discrete remnant of a group of continuous $U(1)_R$ transformations acting on the supersymmetry generators. It is closely connected with the baryon and lepton numbers and its conservation naturally allows for conserved baryon and lepton numbers in supersymmetric theories. The inverse statement is also true and the violation of R-parity requires violation of B or L conservation laws. We have seen in the previous chapter that the MSSM is defined as the theory with minimal number of interactions without possible terms violating L or B, which are otherwise allowed by renormalizability and gauge invariance. Since these terms would lead to possible rapid proton decay, it seems rational to impose conservation of R-parity. Furthermore, as it will be shown, conservation of R-parity ensures the stability of the lightest supersymmetric particle, making it a natural dark matter candidate. On the other hand, we know that at some stage in the history of the universe the baryon number conservation law had to be violated, in order to allow for the creation of the matter anti-matter asymmetry. This observation follows the general pattern, introduced in the last chapter, stating that most symmetries are either approximative, slightly broken or do not hold at all scales, in order to allow for the diverse phenomenology of the observed world. Therefore, it is possible that a slight violation of R-parity can be present in nature, leading to new phenomena. As stated in the previous chapter, small amount of R-parity breaking not only preserves the successful predictions of the MSSM, but leads to a consistent cosmological picture including neutrino masses, leptogenesis, and gravitino dark matter. From the experimental point of view, it on the one hand can shed light on the ethereal gravitino dark matter, and on the other hand possibly hide the next-to-lightest supersymmetric particle from a fast discovery at the LHC. We will discuss these topics in the following chapters.

This chapter introduces the continuous R-symmetry and its descendant R-parity, as well as possible patterns of R-parity breaking. Since the breaking of R-parity can be connected with the breaking of the lepton number leading to a model with bilinear R-parity breaking, we investigate, in detail, the general Lagrangian for this breaking pattern. We choose a particular basis of scalar $SU(2)$ doublets where all bilinear mixing terms vanish. This leads to new Yukawa and gaugino couplings, one of which was previously not discussed in the literature. Some parts of the presentation follow [89, 103] and the extensive review [157], which includes also historical introduction.

3.1 R-symmetry

It turns out that the super Poincaré algebra presented in the previous chapter can be enlarged by the introduction of a global internal $U(1)$ symmetry group acting on the supersymmetry charges. This group is unique and is called R-symmetry. Its generators satisfy the following relations:

$$[Q_\alpha, R] = Q_\alpha, \tag{3.1}$$
$$[Q^\dagger_{\dot\alpha}, R] = -Q^\dagger_{\dot\alpha}. \tag{3.2}$$

In the linear realization of supersymmetry the action of the group can be understood geometrically as a phase rotation of the complex coordinates θ and $\theta^\dagger$:

$$R\,\theta = e^{i\alpha}\theta, \qquad R\,\theta^\dagger = e^{-i\alpha}\theta^\dagger. \tag{3.3}$$

where α parametrizes R-transformations. The different charges of the coordinates give rise to the different transformation properties of the component fields, which can be anticipated since R-symmetry does not commute with supersymmetry. The action of R-symmetry on the chiral superfield reads:

$$R\,\Phi(y,\theta) = e^{ir\alpha}\Phi(y, e^{-i\alpha}\theta), \tag{3.4}$$
$$R\,\Phi^*(y^*,\theta^\dagger) = e^{-ir\alpha}\Phi^*(y^*, e^{i\alpha}\theta^\dagger), \tag{3.5}$$

where $y^\mu = x^\mu - i\theta\sigma^\mu\theta^\dagger$ and r is by definition the R-charge of the supermultiplet. In terms of the component fields this reads:

$$R\,\phi(x) = e^{ir\alpha}\phi(x), \tag{3.6}$$
$$R\,\psi(x) = e^{i(r-1)\alpha}\psi(x), \tag{3.7}$$
$$R\,F(x) = e^{i(r-2)\alpha}F(x). \tag{3.8}$$

Vector superfields are real and therefore have charge 0. It follows that their components transform as:

$$R\,A^\mu(x) = A^\mu(x), \tag{3.9}$$
$$R\,\lambda(x) = e^{i\alpha}\lambda(x), \tag{3.10}$$
$$R\,D(x) = D(x), \tag{3.11}$$

while the chiral field-strength superfield $\mathcal{W}_\alpha$ has R-charge +1. The full superspace integration measure is invariant under the R-symmetry, while the integration measure $d^2\theta$ becomes $e^{2i\alpha}d^2\theta$ if θ goes to $e^{-i\alpha\theta}$. As a consequence, all terms in the SUSY Lagrangian coming from vector superfields are R-symmetric, as well as all terms coming from renormalizable Kähler potential. However, the full Lagrangian exhibits this symmetry only if the superpotential has the charge +2, which is not always the case.

The historical introduction of R-symmetry is connected with the question of how to define conserved fermionic quantum numbers, like B or L in supersymmetric theories [94, 157]. The original idea was to unify the known fermions with gauge bosons inside the vector supermultiplet. Fermionic Majorana components could be then combined into Dirac fermions, cf.

Superfield	Q	U	D	L	E	H_u	H_d	G	W	B
R-charge	1	1	1	1	1	0	0	0	0	0

Table 3.1: R-charges of the superfields in the Minimal Supersymmetric Standard Model. The scalar components have the charges r of the superfields, while the fermionic components have charges $r - 1$.

Section A.3, and the R-symmetry might be tentatively identified as lepton number. However it turned out that such models are untenable for various reasons. The modern solution to the problem of fermionic quantum numbers is the attribution of the latter to the scalar partners of the fermions inside of chiral superfields, an approach which had earlier been viewed as a rather heretic idea.

R-symmetry reappears in modern approaches to SUSY, since the Nelson-Seiberg theorem [158] enforces exact $U(1)_R$ symmetry upon a theory with generic superpotential which breaks SUSY by a non-zero F-term. This conclusion can be avoided if the SUSY-breaking vacuum is only metastable, which seems to be the case in our universe, since exact R-symmetry is associated with phenomenological problems, see [103] and the following discussion.

3.2 From R-symmetry to R-parity

As we have seen in the previous section, most terms in the Lagrangian of a supersymmetric theory are naturally also R-symmetric. The only care has to be taken in the superpotential, in order to ensure that it has the charge 2. Considering the minimal extension of the standard model, it is desirable to have the trilinear terms of the MSSM, in order to give masses to the fermions via the Higgs mechanism. Furthermore, it is possible to attribute charge 0 to all SM particles, including the Higgs boson, while giving the superpartners charges ± 1. These requirements fix the charges of the squark and lepton superfields to 1 and the charges of the Higgs superfields to 0 as shown in table 3.1. It turns out, that some terms of the MSSM cannot be recovered in the theory with R-invariance. First, the supersymmetric mass term for the Higgs bosons has charge 0 and is therefore forbidden. This is not a big drawback, since it is possible to replace the μ term by a trilinear coupling involving an extra chiral singlet field with R-charge 2, as in the Next-to Minimal Supersymmetric Standard Model (NMSSM) which then spontaneously breaks R-symmetry. However, R-symmetry also forbids the Majorana mass terms of the gauginos which correspond to a change in R of $\Delta R = \pm 2$ after a R-transformation, and it is very difficult to create a model generating this terms by spontaneous R-symmetry breaking. Massless Majorana fermions are phenomenologically untenable, since massless gluinos would lead to the existence of R-hadrons, while massless winos and higgsinos would lead to a chargino lighter than the W-boson, all phenomena which have not been observed, see [157] and references therein. Additionally, unbroken $U(1)_R$ prevents supersymmetry from being spontaneously broken in context of supergravity theories, because it forces also the gravitino to stay massless.

Consequently, one has to abandon the continuous R-invariance. However, having excluded the R-symmetry from the constraints on a supersymmetric theory, one is faced with potentially dangerous interaction mediated not by gauge bosons, but by new scalars carrying B or L. A natural solution to this problem, which is also compatible with the experimental constraints, is

the introduction of a discrete *R-parity*. The gravitino mass term appearing after the breaking of supersymmetry breaks itself the $U(1)_R$ into a discrete $\mathbb{Z}_2$ subgroup, since it is invariant under a $U(1)_R$ transformation with angle $\alpha = \pi$:

$$e^{i2\pi}\psi_\mu\sigma^{\mu\nu}\psi_\nu = \psi_\mu\sigma^{\mu\nu}\psi_\nu = (-1)^2\,\psi_\mu\sigma^{\mu\nu}\psi_\nu. \tag{3.12}$$

As a result, one no longer distinguishes between the value $+1$ and -1 of the additive quantum number R, but only between R-odd particles having $R_P = -1$ and R-even ones having $R_P = 1$. In the superspace picture the R-parity symmetry operator is a reflection of the anticommuting fermionic Grassmann coordinate $\theta \to -\theta$. R-parity allows the gaugino mass terms as well as the μ term in the superpotential. The size of the μ term appears now to be connected with the scale of the $U(1)_R$ breaking which is also the scale of SUSY breaking - the gravitino mass $m_{3/2}$. Thus, the solution of the μ problem is connected with the breaking of $U(1)_R$ into R-parity. We will see this in more detail in the Section 3.5.

Imposing R-parity (allowing only terms having $R_P = +1$) one forbids dangerous B- and L-violating terms in the Lagrangian. In order to see this, one first notes that R-even particles are precisely the particles of the SM, while R-odd particles are their superpartners:

$$R_P = (-1)^R = \begin{cases} +1 & \text{SM particles,} \\ -1 & \text{superpartners,} \end{cases} \tag{3.13}$$

where we write now the $U(1)_R$ charge r as R. In the next step R-parity can be re-expressed in terms of the spin S and matter-parity $(-1)^{3(B-L)}$ [156] as

$$R_P = (-1)^{2S}(-1)^{3(B-L)}. \tag{3.14}$$

Both definitions coincide because, as we noted in the previous section, B and L are purely fermionic quantum numbers in the SM. Matter parity is a remainder of the continuous $U(1)_{B-L}$ [159–161], the difference between the baryon and lepton number. Global $B - L$ is an accidental symmetry of the SM without neutrino masses conserved classically and at the quantum level. This is not the case for B or L symmetries alone because they are violated by non-perturbative effects [162]. The $U(1)_{B-L}$ is often gauged and broken in models beyond SM in order to allow for Majorana neutrino masses needed for the see-saw mechanism. We will connect the breaking of $B-L$ to the breaking of R-parity in Section 3.5. Note that some authors define the R-parity directly as descendant of matter parity [103].

Summing up, the consequences of exact R-parity are:

- Conservation of B and L at each vertex.
- Stability of the lightest supersymmetric particle.
- Each supersymmetric particle other than the LSP will decay in a cascade into an odd number of LSPs.
- In collider experiments, supersymmetric particles can only be produced in even numbers.

MSSM is defined to conserve R-parity, see section 2.2, because of the desirable phenomenological consequences. Nevertheless, there is no a priori reason for R-parity conservation. Its breaking is possible as long as it is not in conflict with experimental results. As stated in the introduction to this chapter, R-parity breaking can even render gravitino dark matter compatible with leptogenesis. Therefore, we will investigate R-parity breaking in the following sections.

3.3 Patterns of R-parity Breaking

In the absence of R-parity, R-parity odd terms allowed by renormalizability and gauge invariance have to be included in the superpotential of the MSSM :

$$W = W_{MSSM} + \mu_i H_u L_i + \frac{1}{2}\lambda_{ijk} L_i L_j E_k + \lambda'_{ijk} L_i Q_j D_k + \frac{1}{2}\lambda''_{ijk} U_i D_j D_k, \tag{3.15}$$

where we have suppressed the summation over the gauge indices. Gauge invariance enforces the antisymmetry of the λ_{ijk} couplings with respect to their first two indices, and antisymmetry of λ''_{ijk} couplings with respect to their last two indices. As expected, first three additional terms of the superpotential break lepton number conservation, while the last term breaks baryon number. Altogether eq. 3.15 involves 48 complex parameters: 3 dimensionful parameters μ_i mixing the lepton and down-type Higgs superfields, and 45 dimensionless Yukawa-type couplings.

After the breaking of supersymmetry one must also allow for R-parity violating soft terms which have to be added to the soft-terms of the MSSM:

$$\begin{aligned} -\mathcal{L}_{soft} = -\mathcal{L}^{MSSM}_{soft} &+ \frac{1}{2} a_{ijk} \tilde{l}_i \tilde{l}_j \tilde{\bar{e}}_k + a'_{ijk} \tilde{l}_i \tilde{q}_j \tilde{\bar{d}}_k + \frac{1}{2} a''_{ijk} \tilde{\bar{u}}_i \tilde{\bar{d}}_j \tilde{\bar{d}}_k \\ &+ B_i H_u \tilde{l}_i + m^2_{id} \tilde{l}^{\dagger}_i H_d + h.c. \end{aligned} \tag{3.16}$$

The new soft terms in eq. 3.16 introduce 51 new complex parameters: 45 a-terms with the same antisymmetry properties as the corresponding trilinear superpotential couplings, 3 B_i associated with the bilinear superpotential terms, and 3 R-parity violating soft mass parameters m^2_{id} mixing the down-type Higgs boson with the slepton fields.

Depending on the model of R-parity breaking not all of these terms will be present in the theory. A priori, one can try to investigate the effects of some particular R-parity breaking terms added to the MSSM. However, in order to be consistent at the quantum level, one has to include all terms at the tree-level, which could otherwise be created by radiative corrections. The consistent patterns of R-parity breaking can be classified in the following way:

- **General R-parity breaking**. This is the most general possibility involving all terms defined in this section. It corresponds to the introduction of dimension 2, 3, and 4 operators breaking R_P. This pattern introduces 96 physically meaningful R_P breaking parameters.

- **R-parity breaking through d = 2 and d = 3 operators**. This pattern consist of the bilinear breaking terms from the superpotential augmented by all R_P-breaking soft terms. It introduces 54 new parameters.

- **R-parity breaking through d = 2 operators**. This pattern contains only bilinear soft terms and can be parametrized by 6 parameters.

- **Bilinear R-parity breaking**. In this scenario the R-parity is broken only by bilinear terms coming both from the superpotential and the soft Lagrangian. Although, it leaves out $d = 3$ a-terms, the scenario is consistent, since these terms are not generated from quantum corrections. This pattern introduces 9 new parameters.

Note, that the popular scenario of explicit trilinear R-parity breaking is not included in this list, since bilinear R_P violating couplings in this scenario cannot be completely absent.

They are generated through one-loop diagrams involving lepton-number violating trilinear R_P-breaking interactions. The only consistent possibility is then R-parity breaking solely by the UDD operator. As an example, the $d = 4$ operators, which are the fermion-fermion-scalar terms from the superpotential would induce the $d = 3$ higgsino-lepton mixing terms $\mu_i h_u l_i$ and $d = 2$ Higgs-slepton mixing mass terms $B_i H_u \tilde{l}_i$ and $m^2_{id} \tilde{l}^\dagger_i H_d$ [163–165]. In the following we will investigate in detail bilinear R-parity breaking. We are interested in this pattern, because it does not lead to proton decay (due to the absence of B-violating terms), is described by only 9 parameters, and can lead to consistent gravitino dark matter cosmology.

3.4 Bilinear R-parity Breaking

The minimal supersymmetric standard model including bilinear R-parity breaking [166] is described by the following superpotential:

$$W = \mu_i H_u L_i + \mu H_u H_d + h^u_{ij} Q_i H_u U_j + h^d_{ij} Q_i H_d D_j + h^e_{ij} L_i H_d E_j. \tag{3.17}$$

After supersymmetry breaking, soft SUSY breaking terms have to be added to the Lagrangian:

$$\begin{aligned} -\mathcal{L} = {} & \widetilde{m}^2_{q_i}\, \tilde{q}^\dagger \tilde{q} + \widetilde{m}^2_{l_i}\, \tilde{l}^\dagger \tilde{l} + \widetilde{m}^2_{u_i}\, \tilde{u}^\dagger \tilde{u} + \widetilde{m}^2_{d_i}\, \tilde{d}^\dagger \tilde{d} + \widetilde{m}^2_{e_i}\, \tilde{e}^\dagger \tilde{e} \\ & + m^2_u\, H^\dagger_u H_u + m^2_d H^\dagger_d H_d + \Big(B H_u H_d + B_i H_u \tilde{l}_i + m^2_{id} \tilde{l}^\dagger_i H_d + h.c. \Big), \end{aligned} \tag{3.18}$$

where we show only the scalar mass terms from the usual $\mathcal{L}^{MSSM}_{soft}$. For simplicity, we have assumed flavor diagonal mass matrices.

Electroweak symmetry breaking Contrary to the case of pure MSSM, cf. Section 2.2.1, the electroweak symmetry is broken by vacuum expectation values of all scalar $SU(2)$ doublets (for a generic choice of parameters):

$$\langle H^0_u \rangle = v_u \ , \quad \langle H^0_d \rangle = v_d \ , \quad \langle \tilde{\nu}_i \rangle = v_i. \tag{3.19}$$

In order to find the value of the sneutrino VEV, one has to minimize the full scalar potential. Having replaced the neutral components of the scalar $SU(2)$ doublets with their VEVs, we obtain the following expression for the minimum of the potential:

$$\begin{aligned} V_{\min} = {} & \sum_i |\mu|^2 (v^2_d + v^2_u) + (\mu \mu^*_i + \mu \mu_i) v_d v_i + |\mu_i|^2 (v^2_u + v^2_i) + m^2_d v^2_d + m^2_u v^2_u \\ & - (B + B^*) v_u v_d + \tilde{m}^2_{l_i} v^2_i - (B_i + B^*_i) v_u v_i + (m^2_{id} + m^2_{id}) v_d v_i \\ & + \frac{1}{8} \left(g^2 + g'^2 \right) (v^2_u - v^2_d - v^2_i)^2 \end{aligned} \tag{3.20}$$

The parameters B and B_i can always be chosen real by a suitable choice of the phases of the slepton and Higgs fields, see [167] and references therein. We will assume that the parameters governing the R-parity violation are small. In the next section we will present a model which gives us such parameters. In this case, the vacuum expectation values of the Higgs fields are not changed by the effects or R-parity violation. The VEVs of the sneutrino fields can then be found by investigation of the minimum of the scalar potential in the sneutrino directions:

$$\begin{aligned} 0 \stackrel{!}{=} \left. \frac{\partial V}{\partial \tilde{\nu}^*_i} \right|_{\min} = {} & \mu (\mathrm{Re}\, \mu_i) v_d + |\mu_i|^2 v_i + \tilde{m}^2_{l_i} v_i - B_i v_u + m^2_{id} v_d \\ & + \frac{1}{4} \left(g^2 + g'^2 \right) (v^2_u - v^2_d + v^2_i) v_i. \end{aligned} \tag{3.21}$$

Neglecting all terms which are cubic or higher in the small parameters μ_i and/or v_i, one obtains the following expression for the VEVs of the sneutrino fields:

$$\widehat{\epsilon}_i \equiv \frac{v_i}{v_d} = \frac{B_i \tan\beta - m_{id}^2 - \mu(\mathrm{Re}\,\mu_i)}{\widetilde{m}_{li}^2 + \frac{1}{2}m_Z^2 \cos 2\beta}. \tag{3.22}$$

Choice of the Weak Interaction Basis In the absence of R-parity and, therefore, in the absence of lepton number conservation there is no distinction between the H_d and L_i superfields, which have the same gauge quantum numbers, cf. Table 2.1. Appealing to the Leibnizean principle of the identity of indiscernibles we conclude that all these objects are different degrees of freedom of the same entity, and one can therefore freely rotate the weak eigenstate basis by a unitary transformation:

$$\begin{pmatrix} H_d \\ L_i \end{pmatrix} \to \begin{pmatrix} H'_d \\ L'_i \end{pmatrix} = U \begin{pmatrix} H_d \\ L_i \end{pmatrix}, \tag{3.23}$$

where U is an $SU(4)$ matrix.

The μ and the R_P violating μ_i terms can now be written in compact form in the superpotential

$$W \supset \mu_\alpha H_u H_\alpha, \tag{3.24}$$

where $\mu_\alpha = (\mu, \mu_i)$, and $H_\alpha = (H_d,\, L_i)^T$. The same expression can be rewritten in another basis:

$$\mu_\alpha H_u H_\alpha = \mu_\alpha H_u \left(U^{-1}\right)_{\alpha\beta} H'_\beta. \tag{3.25}$$

We are interested in a infinitesimal transformation $U = \mathbb{1} + T$, with $T^\dagger = -T$ and neglecting $\mathcal{O}(T^2)$ terms. Using it, we can find the expressions for the μ and μ_i terms in the Lagrangian in the new (primed) basis.

$$\mu' = \mu + T_{0i}^* \mu_i, \tag{3.26}$$

$$\mu'_i = -T_{0i}\mu + \mu_i + T_{ij}^* \mu_j. \tag{3.27}$$

Similar expressions can be found for the other parameters. The equations above make it clear that the values of lepton number violating couplings are basis dependent. Therefore, it is crucial for the discussion of the effects of R_P breaking to specify the basis one is using. Another option, pursued by some authors, is to define a complete set of basis-independent quantities parameterizing the effects of R-parity breaking, see [157] and references therein.

We will discuss the predictions of the model in a basis of $SU(2)$ doublets where the mass mixings μ_i, B_i and m_{id}^2 in eqs. (3.17) and (3.18) are traded for R-parity breaking Yukawa couplings. This basis simplifies the discussion of the phenomenological consequences. First, we go into a basis in which the μ_i term vanishes. Looking at eq. (3.27), we find the following transformation:

$$T_{ij}^* = 0, \quad T_{0i} = \epsilon_i = \frac{\mu_i}{\mu}. \tag{3.28}$$

The full transformation matrix then has the following form:

$$U^{-1} = \begin{pmatrix} 1 & -\epsilon_i \\ \epsilon_i^* & \mathbb{1}_{3\times 3} \end{pmatrix}, \tag{3.29}$$

and the transformations of the superfields read:

$$H_d = H'_d - \epsilon_i L'_i \ , \quad L_i = L'_i + \epsilon_i H'_d \ , \tag{3.30}$$

where we have assumed that the μ_i are real. Note that the assumption $\mu_i \ll \mu$ makes the whole procedure consistent. As wanted, the bilinear term (3.17) vanishes for the new fields, i.e., $\mu'_i = 0$, and one obtains instead the cubic R-parity violating terms

$$\Delta W' = \frac{1}{2}\lambda_{ijk} L'_i E_j L'_k + \lambda'_{ijk} D_i Q_j L'_k \ , \tag{3.31}$$

where

$$\lambda_{ijk} = -h^e_{ij}\epsilon_k + h^e_{kj}\epsilon_i \ , \quad \lambda'_{ijk} = -h^d_{ij}\epsilon_k \ . \tag{3.32}$$

The new R-parity breaking mass mixings are given by:

$$B'_i = B_i - B\epsilon_i \ , \quad m^{2\prime}_{id} = m^2_{id} + \epsilon_i(\widetilde{m}^2_{li} - m^2_d) \ . \tag{3.33}$$

The corrections for R-parity conserving mass terms are negligible. In this basis the sneutrino VEVs are given by:

$$\widehat{\epsilon}_i{}' = \frac{B'_i \tan\beta - m^{2\prime}_{id}}{\widetilde{m}^2_{li} + \frac{1}{2}m^2_Z \cos 2\beta}. \tag{3.34}$$

For the second step, we note that after the breaking of supersymmetry we are not forced to perform basis changes or field redefinitions simultaneously in bosonic and fermionic sectors. The up-type Higgs field εH^*_u has the same quantum numbers as the down-type Higgs field H_d and the scalar lepton field $\tilde{l}_i$, with $\varepsilon = i\sigma^2$ cf. eq. (A.40). Therefore, it is possible to arrange them in a vector and write all quadratic terms as a multiplication with a matrix:

$$-\mathcal{L}_{\text{quadratic}} = \left(H^T_u\varepsilon \ , H^{\dagger\prime}_d \ , l^{\dagger\prime}_i\right) \begin{pmatrix} -m^2_u & B & B'_i \\ B & m^2_d & m^{2\prime}_{id} \\ B'_i & m^{2\prime}_{id} & \widetilde{m}^2_{l_i} \end{pmatrix} \begin{pmatrix} \varepsilon H^*_u \\ H'_d \\ \tilde{l}'_i \end{pmatrix} . \tag{3.35}$$

Then one can perform a non-supersymmetric infinitesimal $SU(5)$ rotation among all scalar $SU(2)$ doublets:

$$H'_d = H''_d - \epsilon'_i \tilde{l}''_i \ , \quad \varepsilon H^*_u = \varepsilon H'^*_u - \epsilon''_i \tilde{l}''_i \ , \quad \tilde{l}'_i = \tilde{l}''_i + \epsilon'_i H''_d + \epsilon''_i \varepsilon H'^*_u \ , \tag{3.36}$$

$$H^{\dagger\prime}_d = H^{\dagger\prime\prime}_d - \epsilon'_i \tilde{l}^{\dagger\prime\prime}_i \ , \quad H^T_u\varepsilon = H'^T_u\varepsilon + \epsilon''_i \tilde{l}^{\dagger\prime\prime}_i \ , \quad \tilde{l}^{\dagger\prime}_i = \tilde{l}^{\dagger\prime\prime}_i + \epsilon'_i H^{\dagger\prime\prime}_d - \epsilon''_i H^T_u\varepsilon \ . \tag{3.37}$$

The R-parity conserving parameters change by a negligible amount, while the bilinear R-parity breaking terms become:

$$B''_i = B'_i - \epsilon'_i B + (m^2_u - \widetilde{m}^2_{l_i})\epsilon''_i \tag{3.38}$$

$$m^{2\prime\prime}_{id} = m^{2\prime}_{id} + \epsilon''_i B + (\widetilde{m}^2_{l_i} - m^2_d)\epsilon'_i \tag{3.39}$$

Choosing

$$\epsilon'_i = -\frac{B'_i B + m^{2\prime}_{id}\left(\widetilde{m}^2_{l_i} - m^2_u\right)}{\left(\widetilde{m}^2_{l_i} - m^2_u\right)\left(\widetilde{m}^2_{l_i} - m^2_d\right) - B^2} \ , \tag{3.40}$$

$$\epsilon''_i = \frac{B'_i\left(\widetilde{m}^2_{l_i} - m^2_d\right) + B m^{2\prime}_{id}}{\left(\widetilde{m}^2_{l_i} - m^2_u\right)\left(\widetilde{m}^2_{l_i} - m^2_d\right) - B^2} \ , \tag{3.41}$$

the $H_u\tilde{l}_i$ and $\tilde{l}^\dagger H_d$ mixing terms vanish in the new basis of doublets:

$$B_i'' = 0 \ , \quad m_{id}^{2\prime\prime} = 0 \ . \tag{3.42}$$

According to (3.34) also the scalar lepton VEVs $\langle\tilde{\nu}_i\rangle$ vanish in this basis. In the discussion above, the Higgs mass terms m_u^2 and m_d^2 already contain the contributions $|\mu|^2$ from the superpotential (3.17), which are invariant under the redefinitions in the scalar sector.

R_P violating Couplings and Mixings It is straightforward to work out the R-parity violating Yukawa couplings which are induced by the rotation (3.36). We are particularly interested in the terms containing one light superparticle, i.e, a scalar lepton, bino, wino or higgsino. The corresponding couplings read, after dropping prime and double-prime superscripts on all fields:

$$\begin{aligned} -\Delta\mathcal{L} \supset\ & \frac{1}{2}\lambda_{ijk} l_i \tilde{\bar{e}}_j l_k + \lambda'_{ijk}\bar{d}_i q_j \tilde{l}_k + \hat{\lambda}_{ijk} l_i \bar{e}_j \tilde{l}_k + \hat{\lambda}'_{ijk} q_i \bar{u}_j \varepsilon \tilde{l}_k^* \\ & + h^e_{ij}(\epsilon'_i H_d + \epsilon''_i \varepsilon H_u^*)\bar{e}_j h_d \\ & - \frac{g'}{\sqrt{2}}(\epsilon'_i H_d^\dagger - \epsilon''_i H_u^T \varepsilon) l_i b + \frac{g}{\sqrt{2}}(\epsilon'_i H_d^\dagger - \epsilon''_i H_u^T \varepsilon)\sigma^a l_i w^a + h.c. \ , \end{aligned} \tag{3.43}$$

where the Yukawa couplings are given by

$$\lambda_{ijk} = -h^e_{ij}\epsilon_k + h^e_{kj}\epsilon_i \ , \quad \lambda'_{ijk} = -h^d_{ij}(\epsilon_k + \epsilon'_k) \ , \tag{3.44}$$

$$\hat{\lambda}_{ijk} = -h^e_{ij}(\epsilon_k + \epsilon'_k) + h^e_{kj}\epsilon_i \ , \quad \hat{\lambda}'_{ijk} = h^u_{ij}\epsilon''_k \ . \tag{3.45}$$

Since the field transformations are non-supersymmetric, the couplings λ_{ijk} and $\hat{\lambda}_{ijk}$ are no longer equal as in eq. (3.32). Furthermore, a new coupling of right-handed up-quarks, $\hat{\lambda}'_{ijk}$, has been generated.

After electroweak symmetry breaking one obtains new mass mixings between higgsinos, gauginos and leptons,

$$-\Delta\mathcal{L}_M \supset\ m^e_{ij}\frac{\zeta_i}{c_\beta}\bar{e}_j h_d^- - m_Z s_w \zeta_i^* \nu_i b + m_Z c_w \zeta_i^* \nu_i w^3 + \sqrt{2} m_Z c_w \zeta_i^* e_i w^+ + h.c. \ , \tag{3.46}$$

where we have defined

$$\zeta_i = \frac{\epsilon'_i v_d + \epsilon''_i v_u}{v} \ , \tag{3.47}$$

$$m^e_{ij} = h^e_{ij} v_d \ , \tag{3.48}$$

and used the definition of the Z-boson mass eq. (2.28).

Additionally, one also obtains couplings of the bino and wino to lepton doublets and Higgs:

$$-\Delta\mathcal{L} = -\frac{g'}{\sqrt{2}}\left(\epsilon'_i H_d^{0*}\nu_i + \epsilon''_i H_u^0 \nu_i\right) b + \frac{g}{\sqrt{2}}\left(\epsilon'_i H_d^{0*}\nu_i + \epsilon''_i H_u^0 \nu_i\right) w^3 + h.c. \ , \tag{3.49}$$

where we have shown only the couplings to the neutral Higgs states. The neutral higgsino, on the other hand, only couples to charged Higgs. Introducing the physical Higgs fields in the

unitary gauge, see eq. (2.32), and taking only the coupling to the lightest Higgs into account one obtains:

$$-\Delta\mathcal{L} = -\frac{1}{2}g'\kappa_i h\nu_i b + \frac{1}{2}g\kappa_i h\nu_i w^3 + h.c. \tag{3.50}$$

where

$$\kappa_i = \epsilon'_i \sin(-\alpha) + \epsilon''_i \cos(\alpha). \tag{3.51}$$

In the Higgs decoupling limit, cf. Section 2.2.1, $\alpha \simeq \beta - \pi/2$ and therefore $\kappa_i \simeq \zeta_i$. We will show that all models considered in the present work satisfy the decoupling limit.

Given the Yukawa couplings h^u_{ij}, h^d_{ij} and h^e_{ij}, the Lagrangian (3.43) predicts 108 R-parity breaking Yukawa couplings in terms of 9 independent parameters which may be chosen as

$$\mu_i \ , \ B_i \ , \ m^2_{id} \quad \text{or} \quad \epsilon_i \ , \ \epsilon'_i \ , \ \epsilon''_i \ . \tag{3.52}$$

These parameters determine the lepton-gaugino mass mixings, lepton-slepton, and quark-slepton Yukawa couplings as well as couplings of the Higgs fields to gauginos and leptons, and therefore the low-energy phenomenology. The values of these parameters depend on the pattern of supersymmetry breaking and the flavor structure of the supersymmetric standard model.

3.4.1 Neutralinos and Charginos

The R-parity breaking described in the previous section leads to mass mixings between the neutralinos b, w^3, h^0_u, h^0_d with the neutrinos ν_i, and the charginos w^+, h^+_u, w^-, h^-_d with the charged leptons $\bar{e}_i$, e_i, respectively.

The 7×7 neutralino mass matrix reads in the gauge eigenbasis

$$\mathcal{M}^N = \begin{pmatrix} M_1 & 0 & m_Z s_\beta s_w & -m_Z c_\beta s_w & -\zeta_i m_Z s_w \\ 0 & M_2 & -m_Z s_\beta c_w & m_Z c_\beta c_w & \zeta_i m_Z c_w \\ m_Z s_\beta s_w & -m_Z s_\beta c_w & 0 & -\mu & 0 \\ -m_Z c_\beta s_w & m_Z c_\beta c_w & -\mu & 0 & 0 \\ -\zeta_i m_Z s_w & \zeta_i m_Z c_w & 0 & 0 & 0 \end{pmatrix} , \tag{3.53}$$

where we have neglected neutrino masses. All effects of R-parity violation in the neutralino sector are parametrized by the three parameters ζ_i. As is in the case of the MSSM, cf. Section 2.2.2, the neutralino mass matrix can be perturbatively diagonalized, which we will do explicitly in Chapter 4 for the case of bino- and higgsino-like neutralino LOSP (LSP).

The 5×5 chargino mass matrix which connects the states (w^-, h^-_d, e_i) and (w^+, h^+_u, e^c_i) is given by

$$\mathcal{M}^C = \begin{pmatrix} M_2 & \sqrt{2} m_Z s_\beta c_w & 0 & 0 & 0 \\ \sqrt{2} m_Z c_\beta c_w & \mu & \zeta_1 h^e_{11}\mu & \zeta_2 h^e_{22}\mu & \zeta_3 h^e_{33}\mu \\ \sqrt{2}\zeta_1 m_Z c_w & 0 & h^e_{11} v c_\beta & 0 & 0 \\ \sqrt{2}\zeta_2 m_Z c_w & 0 & 0 & h^e_{22} v c_\beta & 0 \\ \sqrt{2}\zeta_3 m_Z c_w & 0 & 0 & 0 & h^e_{33} v c_\beta \end{pmatrix} , \tag{3.54}$$

and will also be diagonalized in Chapter 4.

3.4.2 Gravitino Interactions

In addition to the effects in the slepton and gaugino sectors, bilinear R-parity breaking will also affect the gravitino interactions eq. (2.77). On the one hand, the basis transformations discussed in the previous section cause various mixings between gauginos and leptons, which are discussed in Chapter 4. On the other hand, the non-supersymmetric rotation will directly change the interactions of the gravitino with scalars fermions and gauge-bosons:

$$\begin{aligned}\mathcal{L}_{\not{R}_P\psi} = -\frac{1}{\sqrt{2}M_P}\Big\{&\left(\epsilon_i'(D_\nu H_d) + \epsilon_i''(D_\nu \varepsilon H_u^*)\right) l_i^\dagger \overline{\sigma}^\mu\sigma^\nu\psi_\mu^\dagger \\ &- \left(\epsilon_i'(D_\nu \tilde{l}_i)h_d^\dagger + \epsilon_i''(D_\nu \tilde{l}_i^\dagger)\varepsilon h_u^\dagger\right)\overline{\sigma}^\mu\sigma^\nu\psi_\mu^\dagger + h.c.\Big\}\ ,\end{aligned} \tag{3.55}$$

where we have assumed flat spacetime. Having evaluated the covariant derivative in terms of mass eigenstate fields (cf. Appendix B) we obtain following interaction terms:

$$\begin{aligned}\mathcal{L}_{\not{R}_P\psi} = -\frac{1}{\sqrt{2}M_P}\Big\{\Big[&(\epsilon_i'(\partial_\nu H_d^0) + \epsilon_i''(\partial_\nu H_u^{0*}))\nu_i^\dagger + (\epsilon_i'(\partial_\nu H_d^-) - \epsilon_i''(\partial_\nu H_u^{+*}))e_i^\dagger \\ &- (\epsilon_i'(\partial_\nu\tilde{\nu})h_d^{0\dagger} + \epsilon_i''(\partial_\nu\tilde{\nu}_i^\dagger)h_u^{0\dagger}) - (\epsilon_i'(\partial_\nu\tilde{e}_i)h_d^{-\dagger} - \epsilon_i''(\partial_\nu\tilde{l}_i^\dagger)h_u^{+\dagger}) \\ &+ \frac{ig}{\sqrt{2}}\left((\epsilon_i'H_d^- - \epsilon_i''H_u^{+*})\nu_i^\dagger - (\epsilon_i'\tilde{e}_i h_d^{0\dagger} + \epsilon_i''h_u^{+\dagger}\tilde{\nu}_i^\dagger)\right)W_\nu^+ \\ &+ \frac{ig}{\sqrt{2}}\left((\epsilon_i'H_d^0 + \epsilon_i''H_u^{0*})e_i^\dagger - (\epsilon_i'\tilde{\nu}_i h_d^{-\dagger} - \epsilon_i''\tilde{e}^\dagger h_u^{0\dagger})\right)W_\nu^- \\ &+ \frac{ig}{2c_w}\Big((\epsilon_i'H_d^0 + \epsilon_i''H_u^{0*})\nu_i^\dagger - (\epsilon_i'H_d^- - \epsilon_i''H_u^{+*})e_i^\dagger \\ &-(\epsilon_i\tilde{\nu}_i h_d^{0\dagger} - \epsilon_i''\tilde{\nu}_i^\dagger h_u^{0\dagger}) + (\epsilon_i'\tilde{e}_i h_d^{-\dagger} + \epsilon_i''\tilde{e}_i^\dagger h_u^{+\dagger})\Big)Z_\nu \\ &+ \frac{ig}{c_w}s_w^2\left((\epsilon_i'H_d^- - \epsilon_i''H_u^{+*})e_i^\dagger - (\epsilon_i'\tilde{e}_i h_d^{-\dagger} + \epsilon_i''\tilde{e}_i^\dagger h_u^{+\dagger})\right)Z_\nu \\ &+ ie\left(-(\epsilon_i'H_d^- - \epsilon_i''h_u^{+*})e_i^\dagger + (\epsilon_i'\tilde{e}_i h_d^{-\dagger} + \epsilon_i''\tilde{e}_i^\dagger h_u^{+\dagger})\right)A_\nu\ \Big]\overline{\sigma}^\mu\sigma^\nu\psi_\mu^\dagger + h.c.\Big\}\end{aligned} \tag{3.56}$$

After electroweak symmetry breaking we obtain inter alia the following trilinear interactions:

$$\mathcal{L}_{\not{R}_P\psi} \supset -\frac{1}{2M_P}\left(i\left(m_Z\zeta_i\nu_i^\dagger Z_\nu + \sqrt{2}m_Z c_w\zeta_i e_i^\dagger W_\nu^-\right) + \kappa_i(\partial_\nu h)\nu_i^\dagger\right)\overline{\sigma}^\mu\sigma^\nu\psi_\mu^\dagger + h.c.\ . \tag{3.57}$$

The interactions in the equations above, together with the R_P violating interactions mediated via the mixing terms, cover all R-parity violating interactions of the gravitino found in the literature, see [72] and references therein. Nota bene that we also find new R-parity violating four-vertex interactions, for example of the form $\psi_\mu \to h\, l_i^- W^+\, (h\,\nu_i\, Z)$, which have to be taken into account for the computation of the three body decays of heavy gravitinos. Note also that our approach allows for a transparent identification of all relevant terms without the need to use sneutrino VEVs or mass-insertion techniques.

3.5 Spontaneous R-parity Breaking

In this section we compute the parameters ϵ_i, ϵ_i' and ϵ_i'' in a specific example where the spontaneous breaking of R-parity is related to the spontaneous breaking of $B-L$, the difference

Superfield	Ψ	H_u	H_d	S	$\bar{S}$	Φ	X	Z
R_P-charge	1	0	0	0	-2	-1	4	0

Table 3.2: R_P-charges of matter superfields $\Psi = Q, U, D, E, L, \bar{N}$, Higgs superfields and gauge singlet superfields.

of baryon and lepton number [57][1].

We consider a supersymmetric extension of the standard model with the symmetry group

$$G = SU(3) \times SU(2) \times U(1)_Y \times U(1)_{B-L} \times U(1)_R \ . \tag{3.58}$$

In addition to three quark-lepton generations and the Higgs fields H_u and H_d the model contains three right-handed neutrinos $\bar{N}_i$, two non-Abelian singlets $\bar{S}$ and S, which transform as $\bar{N}$ and its complex conjugate, respectively, and three gauge singlets X, Φ and Z. The part of the superpotential responsible for neutrino masses has the usual form:

$$W_\nu = h^\nu_{ij} L_i \bar{N}_j H_u + \frac{1}{M_P} h^n_{ij} \bar{N}_i \bar{N}_j S^2 \ . \tag{3.59}$$

The expectation value of H_u generates Dirac neutrino masses, whereas the expectation value of the singlet Higgs field S generates the Majorana mass matrix of the right-handed neutrinos $\bar{N}_i$. The superpotential responsible for $B - L$ breaking is chosen as:

$$W_{B-L} = X(S\bar{S} - \Phi^2) \ , \tag{3.60}$$

where unknown Yukawa couplings have been set equal to one. Φ plays the role of a spectator field, which will finally be replaced by its expectation value, $\langle \Phi \rangle = v_{B-L}$. Similarly, Z is a spectator field which breaks supersymmetry $\langle Z \rangle = F_Z \theta\theta$ and the continuous $U(1)_R$ down to R_P, since its F-term causes change in R of $\Delta R = -2$, cf. Section 3.2. The superpotential in eqs. (3.59) and (3.60) is the most general one consistent with the R-charges listed in Table 3.2, up to nonrenormalizable terms which are irrelevant for our discussion.

The expectation value of Φ leads to the breaking of $B - L$. The scalar potential reads :

$$V_{B-L} = \left|\tilde{s}\tilde{\bar{s}} - v^2_{B-L}\right|^2 + |\tilde{x}|^2|\tilde{\bar{s}}|^2 + |\tilde{x}|^2|\tilde{s}|^2 + \frac{1}{2} g''^2 \left(|\tilde{s}|^2 - |\tilde{\bar{s}}|^2\right)^2 , \tag{3.61}$$

where g'' is the coupling of $U(1)_{B-L}$, and $\tilde{f}$ denotes the scalar component of the superfield F. Minimizing the potential, we find:

$$\langle S \rangle = \langle \bar{S} \rangle = \langle \Phi \rangle = v_{B-L} \ , \tag{3.62}$$

where the first equality is a consequence of the $U(1)_{B-L}$ D-term. The VEV of the S field generates a Majorana mass matrix M for the right-handed neutrinos with three large eigenvalues $M_3 > M_2 > M_1$. If the largest eigenvalue of h^n is $\mathcal{O}(1)$, one has $M_3 \simeq v^2_{B-L}/M_P$, c.f eq. (3.59). Integrating out the heavy Majorana neutrinos one obtains the familiar dimension-5

[1]The connection between $B - L$ breaking and R-parity breaking in the context of string compactifications is discussed in [168, 169].

seesaw operator which yields the light neutrino masses. Note that we will treat neutrinos as massless in phenomenological discussions.

Since the field Φ carries R-charge -1, the VEV $\langle\Phi\rangle$ breaks R-parity, which is conserved by the VEV $\langle Z\rangle$. Thus, the breaking of $B-L$ is tied to the breaking of R-parity, which is then transmitted to the low-energy degrees of freedom via higher-dimensional operators in the superpotential and the Kähler potential. Bilinear R-parity breaking, as discussed in the previous section, is obtained from a correction to the Kähler potential,

$$\begin{aligned}\Delta K = &\frac{1}{M_P^3}\left(a_i Z^*\Phi^*\bar{S}H_u L_i + a_i' Z^*\Phi S^* H_u L_i\right)\\ &+\frac{1}{M_P^4}\left(b_i Z^* Z\Phi^*\bar{S}H_u L_i + b_i' Z^* Z\Phi S^* H_u L_i\right.\\ &\left.+c_i Z^* Z\Phi^*\bar{S}L_i^* H_d + c_i' Z^* Z\Phi S^* L_i^* H_d\right) + h.c.\ . \end{aligned} \tag{3.63}$$

Note that the products Z^*Z of the SUSY breaking fields are proportional to $\theta^\dagger\theta^\dagger\theta\theta$ after the breaking and the operators involving these products therefore solely give rise to products of scalars in the Lagrangian. Replacing the spectator fields Z and Φ, as well as $\bar{S}$ and S by their expectation values, one obtains the correction to the superpotential

$$\Delta W = \mu_i H_u L_i\ ,$$

with

$$\mu_i = \sqrt{3}(a_i + a_i')m_{3/2}\Theta\ , \quad \Theta = \frac{v_{B-L}^2}{M_P^2} \simeq \frac{M_3}{M_P}\ , \tag{3.64}$$

where $m_{3/2} = F_Z/(\sqrt{3}M_P)$ is the gravitino mass. Note that Θ can be increased or decreased by including appropriate Yukawa couplings in eqs. (3.59) and (3.60). The corresponding corrections to the scalar potential are given by

$$-\Delta\mathcal{L} = B_i H_u\tilde{l}_i + m_{id}^2\tilde{l}_i^\dagger H_d + h.c.\ ,$$

where

$$B_i = 3(b_i + b_i')m_{3/2}^2\Theta\ , \quad m_{id}^2 = 3(c_i + c_i')m_{3/2}^2\Theta\ . \tag{3.65}$$

The neutrino mass scale $m_\nu \simeq 0.01$ eV implies for the heaviest right-handed neutrinos $M_2 \sim M_3 \sim 10^{12}$ GeV. The corresponding scales for $B-L$ breaking and R-parity breaking are

$$v_{B-L} \simeq 10^{15}\ \text{GeV}\ , \quad \Theta = \frac{v_{B-L}^2}{M_P^2} \simeq 10^{-6}\ . \tag{3.66}$$

As desired, the model produces tiny R-parity violation. The estimation of parameters is self-consistent, since the neutrino masses generated by R-parity violation are quadratic in R-parity breaking couplings (cf. eq. (4.21)) and are therefore negligible compared to the seesaw contribution, for the size of the R-parity violating couplings predicted by our model, cf. eq. (3.73).

The R-parity conserving terms are generated by the Giudice Masiero mechanism, cf. Section 2.2:

$$K \supset \frac{a_0}{M_P}H_u H_d Z^* + \frac{b_0}{M_P^2}H_u H_d Z^* Z + h.c.\ , \tag{3.67}$$

Superfield	$\mathbf{10}_3$	$\mathbf{10}_2$	$\mathbf{10}_1$	$\mathbf{5}^*_3$	$\mathbf{5}^*_2$	$\mathbf{5}^*_1$	$\bar{N}_3$	$\bar{N}_2$	$\bar{N}_1$	H_u	H_d	Φ	X	Z
Charge	0	1	2	1	1	2	0	0	1	0	0	0	0	0

Table 3.3: Froggatt-Nielsen charges of the superfields of our model. The MSSM fields are combined in representations of $SU(5)$: $\mathbf{10}_i = (Q_i, U_i, E_i)$, $\mathbf{5}^*_i = (D_i, L_i)$, $i = 1 \dots 3$.

which yields

$$W \supset \mu H_u H_d \ , \qquad \mu = \sqrt{3} a_0 m_{3/2} \ , \tag{3.68}$$

$$-\mathcal{L} \supset B H_u H_d + h.c. \ , \qquad B = 3 b_0 m^2_{3/2} \ . \tag{3.69}$$

Higher dimensional operators yield further R-parity violating couplings between scalars and fermions. However, the cubic couplings allowed by the symmetries of our model are suppressed by one power of M_P compared to ordinary Yukawa couplings and cubic soft supersymmetry breaking terms. Note that the coefficients of the nonrenormalizable operators are free parameters, which are only fixed in specific models of supersymmetry breaking. In particular, one may have $\mu^2, \widetilde{m}^2_i > m^2_{3/2}$ and hence a gravitino LSP. All parameters are defined at the GUT scale and have to be evolved to the electroweak scale by the renormalization group equations.

The phenomenological viability of the model depends on the size of R-parity breaking mass mixings and therefore on the scale v_{B-L} as well as the parameters $a_i \dots c'_i$ in eq. (3.63). Any model of flavor physics, which predicts Yukawa couplings, will generically also predict the parameters $a_i \dots c'_i$.

3.5.1 Hierarchy of R-parity violating Couplings

As a typical example, we use a model [170] for quark and lepton mass hierarchies based on a Froggatt-Nielsen $U(1)$ flavor symmetry, which is consistent with thermal leptogenesis and all constraints from flavor changing processes [171].

Froggatt-Nielsen Mechanism The Froggatt-Nielsen mechanism [172] explains the emergence of flavor from an underlying symmetry. In general, flavor assignment means that some particles having the same transformation properties under all symmetry groups have different masses. This situation needs an explanation because the appearance of three identical families contradicts the idea that differences in masses should follow from other different properties. In other words the hierarchy in Yukawa matrices is unexplained in the MSSM or SM. The idea of Froggatt and Nielsen follows the pattern seen in various discussions of this and the previous chapter: The families are considered not to be identical but to differ by a charge under a new $U(1)$ symmetry. This symmetry gets broken above the GUT scale by an expectation value of some field ϕ called flavon which is otherwise a gauge singlet. The charge of ϕ is -1 while other particles have positive or zero charges. Besides the particles of the MSSM the theory possesses a number of heavy states which appear in "spaghetti"-like diagrams [173] between the MSSM fields, see figure 3.1. All the heavy states have the same mass of the order of the flavor scale Λ. The Yukawa couplings as well as other family-dependent couplings arise from this non-renormalizable interactions ("spaghetti-diagrams") after the flavon acquires

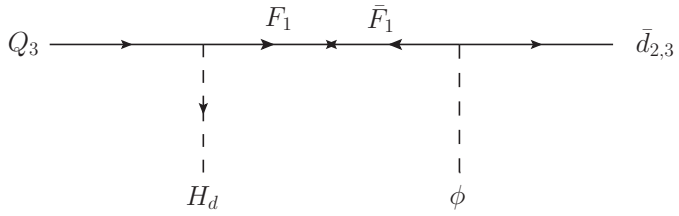

Figure 3.1: An example interaction between the Froggatt-Nielsen fields F_i, the flavon ϕ and the MSSM fields which will give rise to a Yukawa coupling $h^d_{3(2,3)}$. The diagram follows the rules presented in Section A.4.

vacuum expectation value. The entries of the Yukawa couplings depend on the number of flavon-tadpoles needed to cancel the charges of MSSM fields in the interactions, each tadpole contributing $\eta \simeq \langle\phi\rangle/\Lambda$.

In the models we consider the scale Λ is given by $\Lambda = \langle\phi\rangle/\eta > \Lambda_{GUT}$, $\eta \simeq 0.06$. The η-dependence of Yukawa couplings and bilinear mixing terms for multiplets ψ_i with charges Q_i is given by

$$h_{ij} \propto \eta^{Q_i+Q_j}, \quad \mu_i \propto \eta^{Q_i}, \quad B_i \propto \eta^{Q_i}, \quad m^2_{id} \propto \eta^{Q_i} \ . \tag{3.70}$$

The charges Q_i for quarks, leptons, Higgs fields and singlets are listed in table 3.3.

The R-parity breaking parameters μ_i, B_i and m^2_{id} strongly depend on the mechanism of supersymmetry breaking. In the example considered in this section all mass parameters are $\mathcal{O}(m_{3/2})$, which corresponds to gravity or gaugino mediation. From eqs. (3.64),(3.65) and (3.70) one reads off

$$\mu_i = \hat{a}\eta^{Q_i} m_{3/2}\Theta \ , \quad B_i = \hat{b}\eta^{Q_i} m^2_{3/2}\Theta \ , \quad m^2_{id} = \hat{c}\eta^{Q_i} m^2_{3/2}\Theta \ , \tag{3.71}$$

with $\hat{a}, \hat{b}, \hat{c} = \mathcal{O}(1)$. Correspondingly, one obtains for ϵ-parameters (cf. (3.40),(3.41))

$$\epsilon_i = a\eta^{Q_i}\Theta \ , \quad \epsilon'_i = b\eta^{Q_i}\Theta \ , \quad \epsilon''_{id} = c\eta^{Q_i}\Theta \ , \tag{3.72}$$

with $a, b, c = \mathcal{O}(1)$. Thus, the predicted size of R-parity breaking coupling is

$$\epsilon'_i \simeq \epsilon''_i \simeq \zeta \simeq \eta\Theta \simeq 6 \times 10^{-8}. \tag{3.73}$$

Our phenomenological analysis of stau decays in Chapter 4 will be based on this parametrization of bilinear R-parity breaking.

Depending on the mechanism of supersymmetry breaking, the R-parity breaking soft terms may vanish at the GUT scale [157, 174, 175],

$$B_i(\Lambda_{\rm GUT}) = m^2_{id}(\Lambda_{\rm GUT}) = 0 \ . \tag{3.74}$$

Non-zero values of these parameters at the electroweak scale are then induced by radiative corrections. The renormalization group equations for the bilinear R-parity breaking mass

terms read (cf. [157, 174, 175], $t = \ln \Lambda$):

$$16\pi^2 \frac{d\mu_i}{dt} = 3\mu_i \left(h^u_{jk} h^{u*}_{jk} - \frac{1}{5} g_1^2 - g_2^2 \right) + \mu_k h^e_{ij} h^{e*}_{kj} - \mu \left(\lambda_{ijk} h^{e*}_{kj} + 3\lambda'_{kji} h^{d*}_{kj} \right) \ , \tag{3.75}$$

$$\begin{aligned} 16\pi^2 \frac{dB_i}{dt} &= 3B_i \left(h^u_{jk} h^{u*}_{jk} - \frac{1}{5} g_1^2 - g_2^2 \right) + 6\mu_i \left(\frac{1}{5} g_1^2 M_1 + g_2^2 M_2 \right) \\ &\quad + B_k h^e_{ij} h^{e*}_{kj} - B \left(\lambda_{ijk} h^{e*}_{kj} + 3\lambda'_{kji} h^{d*}_{kj} \right) \ , \end{aligned} \tag{3.76}$$

$$\begin{aligned} 16\pi^2 \frac{dm^2_{id}}{dt} &= \lambda^*_{kji} h^e_{kj} m^2_d - m^2_{jd} h^e_{jk} h^{e*}_{ik} - 3\lambda'_{kji} h^d_{kj} m^2_d + h^e_{jk} h^{e*}_{jk} m^2_{id} \\ &\quad + 3h^{d*}_{kj} h^d_{kj} m^2_{id} + \widetilde{m}^2_{li} \lambda^*_{nki} h^e_{nk} - 3\widetilde{m}^2_{li} \lambda'^*_{nki} h^e_{nk} \\ &\quad + 2\lambda^*_{kji} \widetilde{m}^2_{lk} \lambda_{kj} + 2\lambda^*_{kji} h^e_{kj} \widetilde{m}^2_{ej} - 6\lambda'^*_{kji} h^d_{kj} \widetilde{m}^2_{dk} - 6\lambda'^*_{kji} \widetilde{m}^2_{qj} h^d_{kj} \ . \end{aligned} \tag{3.77}$$

In bilinear R-parity breaking, the R-parity violating Yukawa couplings vanish at the GUT scale. One-loop radiative corrections then yield the following soft terms at the electroweak scale (cf. eqs. (3.75),(3.76); $\epsilon_i = \mu_i/\mu$):

$$B_i(\Lambda_{\rm EW}) = \frac{\mu_i}{16\pi^2} \left(\frac{6}{5} g'^2 M_1 + 6g^2 M_2 \right) \ln \frac{\Lambda_{\rm GUT}}{\Lambda_{\rm EW}} \ , \quad m^2_{id}(\Lambda_{\rm EW}) = 0 \ . \tag{3.78}$$

This illustrates that the bilinear R-parity breaking terms μ_i^2, B_i and m^2_{id} are not necessarily of the same order of magnitude at the electroweak scale.

Chapter 4

Broken R-parity: From the Sky to the LHC

Supersymmetric extensions of the Standard Model with broken R-parity have a rich phenomenology [166, 174, 176, 177]. In most models rather large R-parity violating couplings are considered, which lead to prompt decays of the lightest superparticle in the detector. In models where small R-parity violating interactions generate neutrino masses, macroscopic decay lengths up to 1 mm are obtained [175]. In the case of gauge mediated supersymmetry breaking, R-parity violating decays then compete with R-parity conserving decays where the final state contains a gravitino [178].

In the present work we are interested in the case of very small R-parity breaking couplings, as they occur if R-parity is spontaneously broken at the grand unification scale, since they lead to a consistent cosmology including primordial nucleosynthesis, thermal leptogenesis and gravitino dark matter, cf. Section 2.5.

The introduction of such small couplings, leads to decays of the gravitino LSP and the NLSP into particles of the Standard Model, while all other particles of the supersymmetric spectrum decay via the usual R-parity conserving interactions. In the following sections we first obtain R-parity breaking matrix elements of neutral current, charged current, and supercurrent assuming bilinear R-parity violation as presented in the previous chapter. Then, using these matrix elements and the trilinear R-parity breaking couplings, we compute gravitino, neutralino, and stau decays. Having the analytical formulas for the decay lengths, we review the constraints on the strength of R-parity violation from cosmology and verify our initial assumptions. In the next step we summarize the constraints on the R-parity breaking couplings from direct and indirect searches, and finally establish a direct connection between the expected gamma-ray flux from gravitino decays and the decay length of the neutralino NLSP at the LHC. This connection will lead to a lower bound on the neutralino NLSP decay length from the results of the indirect searches for decaying gravitino dark matter. If the NLSP is a stau, we obtain a lower bound on the stau decay length from the requirement that the baryon asymmetry is not washed out.

4.1 Neutral, Charged and Supercurrents

In Section 3.4 we have discussed R-parity violating Yukawa couplings as well as R-parity violating couplings of the Higgs field in our model. For a phenomenological analysis we also

need the couplings of the gauge fields, i.e., photon, W-bosons and gravitino, to charged and neutral matter,

$$\mathcal{L} = -eJ_{e\mu}A^{\mu} - \frac{g}{c_w}J_{Z\mu}Z^{\mu} - \frac{g}{\sqrt{2}}J_{\mu}^{-}W^{+\mu} - \frac{g}{\sqrt{2}}J_{\mu}^{+}W^{-\mu} - \frac{1}{2M_P}\left(\psi_{\mu}S^{\mu} + h.c.\right) \ . \tag{4.1}$$

The corresponding currents are derived in Appendix B and read

$$\begin{aligned}
J_{e\mu} =& J^3_{e\mu} + J^{2,1}_{e\mu} \\
=& \ w^{+\dagger}\bar{\sigma}_{\mu}w^{+} - w^{-\dagger}\bar{\sigma}_{\mu}w^{-} - e_i^{\dagger}\bar{\sigma}_{\mu}e_i + \bar{e}_i^{\dagger}\bar{\sigma}_{\mu}\bar{e}_i - h_d^{-\dagger}\bar{\sigma}_{\mu}h_d^{-} + h_u^{+\dagger}\bar{\sigma}_{\mu}h_u^{+} \ , \\
J_{Z\mu} =& -\frac{1}{2}h_u^{0\dagger}\bar{\sigma}_{\mu}h_u^{0} + \frac{1}{2}h_d^{0\dagger}\bar{\sigma}_{\mu}h_d^{0} + \frac{1}{2}\nu_i^{\dagger}\bar{\sigma}_{\mu}\nu_i \\
& + w^{+\dagger}\bar{\sigma}_{\mu}w^{+} - w^{-\dagger}\bar{\sigma}_{\mu}w^{-} - \frac{1}{2}e_i^{\dagger}\bar{\sigma}_{\mu}e_i - \frac{1}{2}h_d^{-\dagger}\bar{\sigma}_{\mu}h_d^{-} + \frac{1}{2}h_u^{+\dagger}\bar{\sigma}_{\mu}h_u^{+} - s_w^2 J^{2,1}_{e\mu} \ , \\
J_{\mu}^{-} =& \sqrt{2}\left(w^{3\dagger}\bar{\sigma}_{\mu}w^{-} - w^{+\dagger}\bar{\sigma}_{\mu}w^{3}\right) + \nu_i^{\dagger}\bar{\sigma}_{\mu}e_i + h_d^{0\dagger}\bar{\sigma}_{\mu}h_d^{-} + h_u^{+\dagger}\bar{\sigma}_{\mu}h_u^{0} \ , \\
J_{\mu}^{+} =& \sqrt{2}\left(w^{-\dagger}\bar{\sigma}_{\mu}w^{3} - w^{3\dagger}\bar{\sigma}_{\mu}w^{+}\right) - e_i^{\dagger}\bar{\sigma}_{\mu}\nu_i - h_d^{-\dagger}\bar{\sigma}_{\mu}h_d^{0} - h_u^{0\dagger}\bar{\sigma}_{\mu}h_u^{+} \ , \\
S^{\mu} =& \ \sigma^{\rho\sigma}\sigma^{\mu}\left(b^{\dagger}B_{\rho\sigma} + w^{\dagger a}W^{a}_{\rho\sigma}\right) \\
& + \sigma^{\nu}\bar{\sigma}^{\mu}\Big((\cos\alpha\, h_u^0 - \sin\alpha\, h_d^0)(\partial_{\nu}h) - i\sqrt{2}m_Z c_w\left(\cos\beta\, W_{\nu}^{+}h_d^{-} + \sin\beta\, W_{\nu}^{-}h_u^{+}\right) \\
& \qquad - \frac{ig}{\sqrt{2}}\left(\cos\alpha\, W_{\nu}^{-}h_u^{+} - \sin\alpha\, W_{\nu}^{+}h_d^{-}\right)h - im_Z\left(\cos\beta\, h_d^0 - \sin\beta\, h_u^0\right)Z_{\mu} \\
& \qquad + \frac{ig}{2c_w}\left(\sin\alpha\, h_d^0 + \cos\alpha\, h_u^0\right)hZ_{\mu} \\
& \qquad - im_Z\zeta_i\nu_i Z_{\nu} - i\sqrt{2}m_Z c_w\zeta_i e_i W_{\nu}^{+} + \kappa_i\nu_i(\partial_{\nu}h)\Big) \ .
\end{aligned} \tag{4.2}$$

The upper indices of the electromagnetic currents indicate the transformation properties of the fields in the current under $SU(2)_L$.

In eq. (4.2) we have only listed contributions to the currents which will be relevant in our phenomenological analysis.

As stated in the previous chapter, the R-parity breaking leads to mass mixings between the neutralinos b, w^3, h_u^0, h_d^0 with the neutrinos ν_i, and the charginos w^+, h_u^+, w^-, h_d^- with the charged leptons $\bar{e}_i$, e_i, respectively. The 7×7 neutralino mass matrix reads in the gauge eigenbasis

$$\mathcal{M}^N = \begin{pmatrix}
M_1 & 0 & m_Z s_\beta s_w & -m_Z c_\beta s_w & -\zeta_i m_Z s_w \\
0 & M_2 & -m_Z s_\beta c_w & m_Z c_\beta c_w & \zeta_i m_Z c_w \\
m_Z s_\beta s_w & -m_Z s_\beta c_w & 0 & -\mu & 0 \\
-m_Z c_\beta s_w & m_Z c_\beta c_w & -\mu & 0 & 0 \\
-\zeta_i m_Z s_w & \zeta_i m_Z c_w & 0 & 0 & 0
\end{pmatrix} , \tag{4.3}$$

where we have neglected neutrino masses induced by the see-saw mechanism. Correspondingly, the 5×5 chargino mass matrix which connects the states (w^-, h_d^-, e_i) and (w^+, h_u^+, e_i^c)

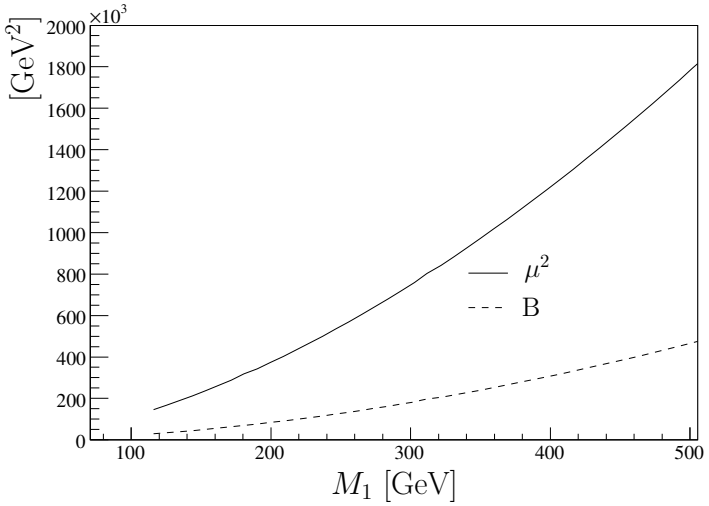

Figure 4.1: The parameters μ and B of eqs. (3.17) and (3.18), respectively, as functions of the bino mass M_1 in mSUGRA models. The plot has been obtained by means of `SOFTSUSY` [110].

is given by

$$\mathcal{M}^C = \begin{pmatrix} M_2 & \sqrt{2}\, m_Z s_\beta c_w & 0 & 0 & 0 \\ \sqrt{2}\, m_Z c_\beta c_w & \mu & \zeta_1 h^e_{11}\mu & \zeta_2 h^e_{22}\mu & \zeta_3 h^e_{33}\mu \\ \sqrt{2}\, \zeta_1 m_Z c_w & 0 & h^e_{11} v c_\beta & 0 & 0 \\ \sqrt{2}\, \zeta_2 m_Z c_w & 0 & 0 & h^e_{22} v c_\beta & 0 \\ \sqrt{2}\, \zeta_3 m_Z c_w & 0 & 0 & 0 & h^e_{33} v c_\beta \end{pmatrix} . \tag{4.4}$$

Note that all gaugino and higgsino mixings with neutrinos and charged leptons are governed by the three parameters ζ_i.

In the following sections we shall need the couplings of gravitino, W and Z bosons to neutralino and chargino mass eigenstates. Since $\zeta_i \ll 1$, diagonalization of the mass matrices to first order in ζ_i is obviously sufficient. Moreover, similar to the MSSM case, we consider only models where the effects of electroweak symmetry breaking are small perturbations on the mass matrix. In the case of mSUGRA models (cf. Section 2.4.1) the supersymmetry breaking parameters satisfy the inequalities (cf. Figure 4.1):

$$m_Z < M_{1,2} < \mu \ , \tag{4.5}$$

while in the case of hybrid gauge-gravity mediation or AMSB (cf. Sections 2.4.2 and 2.4.3) the inequalities are:

$$m_Z < \mu < M_{1,2}. \tag{4.6}$$

The gaugino-higgsino mixings are $\mathcal{O}(m_Z/\mu)$ or $\mathcal{O}(m_Z/M_{1,2})$, and therefore suppressed, and χ^0_1, the lightest neutralino, is either bino or higgsino-like.

The mass matrices $\mathcal{M}^N$ and $\mathcal{M}^C$ are diagonalized by Takagi diagonalization and singular value decomposition, respectively,

$$U^{(n)T}\mathcal{M}^N U^{(n)} = \mathcal{M}^N_{\rm diag} \ , \quad U^{(c)\dagger}\mathcal{M}^C \widetilde{U}^{(c)} = \mathcal{M}^C_{\rm diag} \ , \tag{4.7}$$

where $U^{(n)\dagger}U^{(n)} = U^{(c)\dagger}U^{(c)} = \widetilde{U}^{(c)\dagger}\widetilde{U}^{(c)} = \mathbf{1}$. These unitary transformations relate the neutral and charged gauge eigenstates to the mass eigenstates (χ_a^0, ν_i') $(a = 1, \ldots, 4)$ and (χ_α^-, e_i'), $(\chi_\alpha^+, \bar{e}_i)$ $(\alpha = 1, 2)$, respectively. Inserting these transformations in eqs. (4.2) and dropping prime superscripts, one obtains electromagnetic current , neutral current , charged current and supercurrent in the mass eigenstate basis:

$$\begin{aligned}
J_{e\mu} &= \chi_\alpha^{-\dagger}\bar{\sigma}_\mu V_{\alpha\beta}^{(\chi^-)}\chi_\beta^- + \chi_\alpha^{+\dagger}\bar{\sigma}_\mu V_{\alpha\beta}^{(\chi^+)}\chi_\beta^+ + e_i^\dagger\bar{\sigma}_\mu V_{ij}^{(e)}e_j + \bar{e}_i^\dagger\bar{\sigma}_\mu V_{ij}^{(\bar{e})}\bar{e}_j \qquad (4.8)\\
&\quad + \left(\chi_\alpha^{-\dagger}\bar{\sigma}_\mu V_{\alpha j}^{(\chi^-,e)}e_j + \chi_\alpha^{+\dagger}\bar{\sigma}_\mu V_{\alpha j}^{(\chi^+,\bar{e})}\bar{e}_j + h.c.\right) ,\\
J_{Z\mu} &= \chi_a^{0\dagger}\bar{\sigma}_\mu V_{ab}^{(\chi^0)}\chi_b^0 + \chi_\alpha^{-\dagger}\bar{\sigma}_\mu V_{\alpha\beta}^{(\chi^-)}\chi_\beta^- + \chi_\alpha^{+\dagger}\bar{\sigma}_\mu V_{\alpha\beta}^{(\chi^+)}\chi_\beta^+ + \nu_i^\dagger\bar{\sigma}_\mu V_{ij}^{(\nu)}\nu_j + e_i^\dagger\bar{\sigma}_\mu V_{ij}^{(e)}e_j \qquad (4.9)\\
&\quad + \bar{e}_i^\dagger\bar{\sigma}_\mu V_{ij}^{(\bar{e})}\bar{e}_j + \left(\chi_a^{0\dagger}\bar{\sigma}_\mu V_{aj}^{(\chi,\nu)}\nu_j + \chi_\alpha^{-\dagger}\bar{\sigma}_\mu V_{\alpha j}^{(\chi^-,e)}e_j + \chi_\alpha^{+\dagger}\bar{\sigma}_\mu V_{\alpha j}^{(\chi^+,\bar{e})}\bar{e}_j + h.c.\right) - s_w^2 J_{e\mu} ,\\
J_\mu^- &= \chi_a^{0\dagger}\bar{\sigma}_\mu V_{a\beta}^{(\chi)}\chi_\beta^- + \chi_\alpha^{+\dagger}\bar{\sigma}_\mu V_{\alpha b}^{(\chi)}\chi_b^0 + \chi_a^{0\dagger}\bar{\sigma}_\mu V_{aj}^{(\chi,e)}e_j + \bar{e}_i^\dagger\bar{\sigma}_\mu V_{ib}^{(\chi,e)}\chi_b^0 \qquad (4.10)\\
&\quad + \nu_i^\dagger\bar{\sigma}_\mu V_{i\beta}^{(\nu,\chi)}\chi_\beta^- + \chi_\alpha^{+\dagger}\bar{\sigma}_\mu V_{\alpha j}^{(\nu,\chi)}\nu_j + \nu_i^\dagger\bar{\sigma}_\mu V_{ij}^{(\nu,e)}e_j + \bar{e}_i^\dagger\bar{\sigma}_\mu V_{ij}^{(\nu,e)}\nu_j ,\\
S^\mu &= \sigma^{\rho\sigma}\sigma^\mu\left(\left(\chi_a^{0\dagger}U_a^{(\widetilde{\gamma},\chi)} + \nu_i^\dagger U_i^{(\widetilde{\gamma},\nu)}\right)F_{\rho\sigma} - \left(\chi_a^{0\dagger}U_a^{(\widetilde{Z},\chi)} + \nu_i^\dagger U_i^{(\widetilde{Z},\nu)}\right)Z_{\rho\sigma}\right. \qquad (4.11)\\
&\qquad \left. + \left(\chi_\alpha^{+\dagger}\widetilde{U}_{1\alpha}^{(\chi^+)} + \bar{e}_i^\dagger\widetilde{U}_{1i}^{(\chi^+,\bar{e})}\right)W_{\rho\sigma}^+ + \left(\chi_\alpha^{-\dagger}U_{1\alpha}^{(\chi^-)} + e_i^\dagger U_{1i}^{(\chi^-,e)}\right)W_{\rho\sigma}^-\right)\\
&\quad + \sigma^\nu\overline{\sigma}^\mu\left(\left(U_a^{(\chi^0,h)}\chi_a^0 + U_i^{(\nu,h)}\nu_i\right)(\partial_\nu h)\right.\\
&\qquad - i\sqrt{2}m_Z c_w\left(c_\beta W_\nu^+\left(U_{2\alpha}^{(\chi^-)}\chi_\alpha^- + U_{2i}^{(\chi^-,e)}e_i\right) + s_\beta W_\nu^-\left(\widetilde{U}_{2\alpha}^{(\chi^+)}\chi_\alpha^+ + \widetilde{U}_{2i}^{(\chi^+,\bar{e})}\bar{e}_i\right)\right)\\
&\qquad - \frac{ig}{\sqrt{2}}\left(c_\alpha W_\nu^-\left(\widetilde{U}_{2\alpha}^{(\chi^+)}\chi_\alpha^+ + \widetilde{U}_{2i}^{(\chi^+,\bar{e})}\bar{e}_i\right) - s_\alpha W_\nu^+\left(U_{2\alpha}^{(\chi^-)}\chi_\alpha^- + U_{2i}^{(\chi^-,e)}e_i\right)\right)h\\
&\qquad - im_Z\left(U_a^{(\chi^0,Z)}\chi_a^0 + U_i^{(\nu,Z)}\nu_i\right)Z_\nu + \frac{ig}{\sqrt{2}}\left(U_a^{(\chi^0,h,Z)}\chi_a^0 + U_i^{(\nu,h,Z)}\nu_i\right)hZ_\nu\\
&\qquad \left. - im_Z\zeta_i\nu_i Z_\nu - i\sqrt{2}m_Z c_w\zeta_i e_i W_\nu^+ + \kappa_i\nu_i(\partial_\nu h)\right) ,
\end{aligned}$$

where we have defined the following matrix elements:

$$U_a^{(\widetilde{\gamma},\chi)} = c_w U_{1a}^{(\chi^0)} + s_w U_{2a}^{(\chi^0)} , \qquad U_i^{(\widetilde{\gamma},\nu)} = c_w U_{1i}^{(\chi_0,\nu)} + s_w U_{2i}^{(\chi^0,\nu)} , \qquad (4.12)$$

$$U_a^{(\widetilde{Z},\chi)} = s_w U_{1a}^{(\chi^0)} + c_w U_{2a}^{(\chi^0)} , \qquad U_i^{(\widetilde{Z},\nu)} = s_w U_{1i}^{(\chi_0,\nu)} + c_w U_{2i}^{(\chi^0,\nu)} , \qquad (4.13)$$

$$U_a^{(\chi^0,h)} = c_\alpha U_{3a}^{(\chi^0)} - s_\alpha U_{4a}^{(\chi^0)} , \qquad U_i^{(\nu,h)} = c_\alpha U_{3i}^{(\chi^0,\nu)} - s_\alpha U_{4i}^{(\chi^0,\nu)} , \qquad (4.14)$$

$$U_a^{(\chi^0,Z)} = c_\beta U_{4a}^{(\chi^0)} - s_\beta U_{3a}^{(\chi^0)} , \qquad U_i^{(\nu,Z)} = c_\beta U_{4i}^{(\chi^0,\nu)} - s_\beta U_{3i}^{(\chi^0,\nu)} , \qquad (4.15)$$

$$U_a^{(\chi^0,h,Z)} = s_\alpha U_{4a}^{(\chi^0)} + c_\alpha U_{3a}^{(\chi^0)} , \qquad U_i^{(\nu,h,Z)} = s_\alpha U_{4i}^{(\chi^0,\nu)} + c_\alpha U_{3i}^{(\chi^0,\nu)} , \qquad (4.16)$$

and abbreviations for the mixing angles:

$$s_\alpha = \sin\alpha , \qquad c_\alpha = \cos\alpha , \qquad (4.17)$$

$$s_\beta = \sin\beta , \qquad c_\beta = \cos\beta . \qquad (4.18)$$

The unitary transformations between gauge and mass eigenstates and the resulting matrix elements of neutral and charged currents are given to next-to-leading order in m_Z/μ ($m_Z/M_{1,2}$) in Appendix B. As we shall see, that expansion converges remarkably well.

The explicit expressions for the couplings as well as for the mass eigenvalues depend on the nature of the neutralino wave function. In this work we will consider only bino- and higgsino-like neutralinos. We will give the couplings for these cases in the later discussion, but provide here the masses of the neutralino states for both cases. Additionally, we discuss the generation of neutrino masses induced by R-parity breaking.

Bino-like Neutralino As shown above, we can treat the breaking of electroweak symmetry as a small perturbation of the neutralino and chargino mass matrices, and perturbatively diagonalize them to first order in ζ_i and to second order in m_Z/μ. The neutralino mass eigenstates read:

$$\begin{aligned}
m_{\chi_1^0} &= M_1 - \frac{m_Z^2 s_w^2 (M_1 + \mu s_{2\beta})}{(\mu^2 - M_1^2)} \left(1 + \mathcal{O}\left(\frac{m_Z^2}{\mu^2}\right)\right), \\
m_{\chi_2^0} &= M_2 - \frac{m_Z^2 c_w^2 (M_2 + \mu s_{2\beta})}{(\mu^2 - M_2^2)} \left(1 + \mathcal{O}\left(\frac{m_Z^2}{\mu^2}\right)\right), \\
m_{\chi_3^0} &= \mu + \frac{m_Z^2 (1 - s_{2\beta})(\mu + M_1 c_w^2 + M_2 s_w^2)}{2(\mu + M_1)(\mu + M_2)} \left(1 + \mathcal{O}\left(\frac{m_Z^2}{\mu^2}\right)\right), \\
m_{\chi_4^0} &= \mu + \frac{m_Z^2 (1 + s_{2\beta})(\mu - M_1 c_w^2 - M_2 s_w^2)}{2(\mu - M_1)(\mu - M_2)} \left(1 + \mathcal{O}\left(\frac{m_Z^2}{\mu^2}\right)\right), \\
m_\nu &= 0.
\end{aligned} \tag{4.19}$$

Obviously, the mass eigenstates at this order in ζ_i are precisely the same as in R-parity conserving SUSY, cf. eq. (2.48). The effects of R-parity violation first appear at the order ζ^2, in particularly R-parity violation generates one neutrino mass at tree-level which will be considered in the following. We have numerically checked that varying M_1 between 120 and 500 GeV, the relative correction to the lightest neutralino mass is less than 10%.

Higgsino-like Neutralino The diagonalization of the mass matrices in the case of a higgsino-like neutralino is very similar to the bino-like case. We expand to first order in ζ and to second order in m_Z/M_1 and obtain the following neutralino masses:

$$\begin{aligned}
m_{\chi_1^0} &= \mu - \frac{m_Z^2 (1 + s_{2\beta})(M_1 c_w^2 + M_2 s_w^2 - \mu)}{2(M_1 - \mu)(M_2 - \mu)} \left(1 + \mathcal{O}\left(\frac{m_Z^2}{M_1^2}\right)\right), \\
m_{\chi_2^0} &= \mu + \frac{m_Z^2 (1 - s_{2\beta})(\mu + M_1 c_w^2 + M_2 s_w^2)}{2(\mu + M_1)(\mu + M_2)} \left(1 + \mathcal{O}\left(\frac{m_Z^2}{M_1^2}\right)\right), \\
m_{\chi_3^0}\,, m_{\chi_4^0} &= M_1 + \frac{m_Z^2 s_w^2 (M_1 + \mu s_{2\beta})}{(M_1^2 - \mu^2)} \left(1 + \mathcal{O}\left(\frac{m_Z^2}{M_1^2}\right)\right), \\
&= M_2 + \frac{m_Z^2 c_w^2 (M_2 + \mu s_{2\beta})}{(M_2^2 - \mu^2)} \left(1 + \mathcal{O}\left(\frac{m_Z^2}{M_1^2}\right)\right), \\
m_\nu &= 0,
\end{aligned} \tag{4.20}$$

where we have not specified the hierarchy between M_1 and M_2. We have numerically checked that at the points of interest, the relative correction to the masses is less than 5%.

Neutrino Masses Irrespectively of the neutralino wave function, the neutralino-neutrino mixing generates tree-level neutrino mass at the order ζ^2:

$$m_\nu = \zeta^2 m_Z^2 \left(\frac{s_w^2}{M_1} + \frac{c_w^2}{M_2}\right)\left(1 + \mathcal{O}\left(\frac{m_Z^2}{\mu^2}\right)\right), \tag{4.21}$$

where

$$\zeta^2 = \sum_i \zeta_i^2 \,, \tag{4.22}$$

and we have assumed a bino-like neutralino for the calculation. The appearance of the neutrino mass can be understood as a kind of seesaw mechanism due to the strong hierarchy between the gaugino-higgsino 4×4 block M_χ and the off-diagonal 3×4 block m in the neutralino mass matrix:

$$\mathcal{M}^N = \begin{pmatrix} M_\chi & m^T \\ m & \mathbf{0}_{3\times 3} \end{pmatrix}. \tag{4.23}$$

The effective mass matrix is obtained by integrating out the neutralinos and is given by:

$$M^\nu_{\text{tree}} \simeq -m\, M_\chi^{-1} m^T. \tag{4.24}$$

Using our parametrization of $\mathcal{M}^N$ we can exactly diagonalize the neutrino mass matrix. As expected, we obtain two zero eigenvalues and one neutrino mass :

$$m_\nu = \zeta^2 m_Z^2 \frac{M_1 c_w^2 + M_2 s_w^2}{M_1 M_2 - m_Z^2/\mu\, s_{2\beta}(M_1 c_w^2 + M_2 s_w^2)}. \tag{4.25}$$

Note that our expression is equal to the result obtained in [179] up to the effect of the second basis transformation, see Section 3.4. Without the non-supersymmetric rotation the coupling between gauginos and neutrinos is given by:

$$\zeta_i = \frac{\mu_i}{\mu}\frac{v_d}{v} = \frac{\mu_i}{\mu}\cos\beta \,. \tag{4.26}$$

Neutrino masses also receive loop contributions from R-parity violating couplings, see [157] and references therein, and, therefore, are lifted from zero. For our choice of the parameters $\zeta_i \sim 10^{-8}$, the tree-level mass, and consequently the loop induced masses are much smaller than the contributions from the usual see-saw mechanism, assuming a neutrino mass scale of 0.01 eV, cf. eq. (3.66). Thus, they can be safely neglected, as stated in Section 3.5. On the other hand, if one takes our parametrization of bilinear R-parity violation and disregards cosmological implications, one can fix the size of R-parity violation demanding that $m_\nu < 1$ eV for some supersymmetric model. For example, choosing $M_1 = 100$ GeV and $M_2 = 200$ GeV one obtains $\zeta \lesssim 4.5 \times 10^{-6}$. However, it would be also necessary to fix the other parameters of the model, in order to explain all neutrino oscillation data.

Chargino Masses Although we will not use them in the following work, we also show the chargino mass eigenvalues:

$$\begin{aligned} m_{\chi_1^\pm} &= M_2 - \frac{m_Z^2 c_w^2 (M_2 + \mu s_{2\beta})}{(\mu^2 - M_2^2)}\left(1 + \mathcal{O}\left(\zeta_2\zeta_3\right)\right), \\ m_{\chi_2^\pm} &= \mu + \frac{m_Z^2 c_w^2 (\mu + M_2 s_{2\beta})}{(\mu^2 - M_2^2)}\left(1 + \mathcal{O}\left(\zeta_2\zeta_3\right)\right), \\ m_{e_i} &= h^e_{ii} v c_\beta \left(1 + \mathcal{O}\left(\zeta_2\zeta_3\right)\right). \end{aligned} \tag{4.27}$$

The masses of the charginos at this order in ζ_i coincide with the results in the R-parity conserving SUSY, cf. eq. (2.52).

4.2 R-parity violating Decays

Various mass mixings induced by R-parity violation as well as direct trilinear R-parity violating couplings lead to decays of the supersymmetric particles into the particles of the Standard Model. We are interested in the decays of the gravitino LSP, stau NLSP, and neutralino NLSP.

4.2.1 Gravitino Decays

The gravitino decay channels can be found from the supercurrent in the mass eigenstate basis, cf. eq (4.11). The two-body decays are

$$\psi_\mu \to \nu\,\gamma\ , \qquad \psi_\mu \to \nu\,Z\ , \qquad \psi_\mu \to \nu\,h\ , \qquad \psi_\mu \to e^+\,W^-\ , \tag{4.28}$$

whereas the three-body decays are

$$\psi_\mu \to e^+\,W^-\,h\ , \qquad \psi_\mu \to \nu\,Z\,h\ . \tag{4.29}$$

To the best of our knowledge the three body decays presented above have not been considered in the literature. However, they are suppressed and can only play a role for a sufficient heavy gravitino. If the gravitino is lighter than the gauge bosons, it will decay into photon and neutrino and also into trilepton final states via virtual gauge bosons. Above the threshold for the production of W and Z bosons the gravitino will predominantly decay into W boson and charged lepton and Z boson and neutrino. These decays were first discussed in [60], however, a part of the contribution was omitted. Two additionally diagrams were taken into account in [61], and finally two more diagrams were discussed in [72]. We refer the reader to the work [72] for the calculations and results. Note that in our approach we recover all contributions in a transparent way. The interaction Lagrangian responsible for the decay into Z boson and neutrino is given by

$$\mathcal{L}_{\psi Z\nu} = \frac{1}{2M_P}\psi_\mu \left(\sigma^{\rho\sigma}\sigma^\mu \nu_i^\dagger U_i^{(\widetilde{Z},\nu)} Z_{\rho\sigma} + i\sigma^\nu\overline{\sigma}^\mu m_Z \left(U_i^{(\nu,Z)} + \zeta_i\right)\nu_i Z_\nu\right) + h.c.\ , \tag{4.30}$$

and the interaction Lagrangian responsible for the decay into W boson and charged lepton is given by:

$$\begin{aligned}\mathcal{L}_{\psi Wl} = &-\frac{1}{2M_P}\psi_\mu \left(\sigma^{\rho\sigma}\sigma^\mu \bar{e}_i^\dagger \widetilde{U}_{1i}^{(\chi^+,\bar{e})} W^+_{\rho\sigma} - i\sqrt{2}\sigma^\nu\overline{\sigma}^\mu m_Z c_w \left(c_\beta U_{2i}^{(\chi^-,e)} + \zeta_i\right) e_i W^+_\nu\right)\\ &-\frac{1}{2M_P}\psi_\mu^\dagger \left(\bar{\sigma}^{\rho\sigma}\overline{\sigma}^\mu e_i U_{1i}^{(\chi^-,e)} W^+_{\rho\sigma} + i\sqrt{2}\bar{\sigma}^\nu\sigma^\mu m_Z c_w s_\beta \widetilde{U}_{2i}^{(\chi^+,\bar{e})} \bar{e}_i^\dagger W^+\nu\right) + h.c.\ .\end{aligned} \tag{4.31}$$

If the gravitino is heavy enough to decay into the Higgs bosons, the branching ration into photon and neutrino is even more suppressed. This leads to the reduction of the strength of a monoenergetic signal of gamma rays from gravitino decays in indirect detection experiments. Neglecting threshold effects, the decay into the Higgs boson has the same strength as the decay into the Z boson and neutrino. The reader is referred to [72, 114] for a detailed discussion.

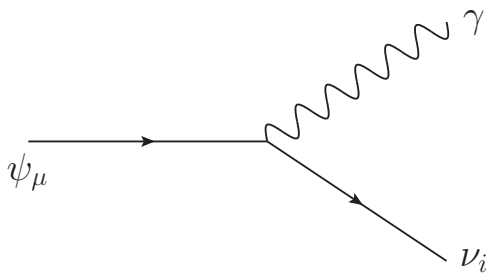

Figure 4.2: Gravitino decay into photon and neutrino.

The interaction Lagrangian which gives rise to the decay into the Higgs boson and neutrino reads

$$\mathcal{L}_{\psi h\nu} = -\frac{1}{2M_P}\psi_\mu \left(\sigma^\nu \overline{\sigma}^\mu \left(U^{(\nu,h)} + \kappa_i\right) \nu_i (\partial_\nu h)\right) + h.c. \ . \tag{4.32}$$

In the present work we are primarily interested in the decay of the gravitino into photon and neutrino, which we shall compute in the two component spinor formalism in the next section.

Gravitino Decay $\psi_\mu \to \gamma\nu$

The interaction Lagrangian responsible for this decay is given by

$$\mathcal{L}_{\psi\gamma\nu} = -\frac{1}{2M_P}\psi_\mu \sigma^{\rho\sigma}\sigma^\mu \nu_i^\dagger U_i^{(\widetilde{\gamma},\nu)} F_{\rho\sigma} \ . \tag{4.33}$$

The decay is shown in Figure 4.2 and was computed first in [58]. Here we will compute this decay using the two component formalism in order to show the assets of this method. The Feynman rules can be directly read off from the Lagrangian following the general rules presented in Appendix A. If the photon has the momentum k, the gravitino the momentum q, and neutrino the momentum p, the gravitino-photon-neutrino coupling reads

$$\frac{1}{2M_P} U_i^{(\widetilde{\gamma},\nu)} (\sigma k)\bar{\sigma}^\sigma \sigma^\mu \ , \tag{4.34}$$

for the appropriate choice of the spinor index structure. The matrix elements are then given by

$$\begin{aligned} i\mathcal{M} &= \frac{1}{2M_P} U_i^{(\widetilde{\gamma},\nu)} \psi_\mu^+(q)(\sigma k)\bar{\sigma}^\sigma \sigma^\mu x_i^\dagger(p)\epsilon_\sigma^*(k) \ , \\ -i\mathcal{M}^* &= \frac{1}{2M_P} U_i^{(\widetilde{\gamma},\nu)*} \psi_\nu^{+\dagger}(q)(\bar{\sigma} k)\sigma^\gamma \bar{\sigma}^\nu x_i(p)\epsilon_\gamma(k) \ . \end{aligned} \tag{4.35}$$

The matrix element squared reads

$$|\mathcal{M}|^2 = \frac{1}{4M_P^2}|U_i^{(\widetilde{\gamma},\nu)}|^2 \left(\epsilon_\sigma^* \epsilon_\gamma\right) \left(x^\dagger \overline{\sigma}^\mu \sigma^\sigma (\bar{\sigma} k)\psi_\mu^+\right) \left(\psi_\nu^{+\dagger}(\bar{\sigma} k)\sigma^\gamma \bar{\sigma}^\nu x\right) \ , \tag{4.36}$$

where we have dropped the momentum dependence of the wave functions. We have rewritten the matrix elements in the form appropriate for the computation using the spinor algebra

rules from Appendix A. Summing over the spins of the final states and averaging over the gravitino spin states ,we obtain

$$\frac{1}{4}\sum_{(\lambda_\psi,\lambda_\nu,\lambda_\gamma)}|\mathcal{M}|^2 = -\frac{1}{16M_P^2}|U_i^{(\widetilde{\gamma},\nu)}|^2\mathrm{Tr}\left[\overline{\sigma}^\mu\sigma^\sigma(\bar{\sigma}k)P^+_{\mu\nu}(\bar{\sigma}k)\sigma_\sigma\bar{\sigma}^\nu(\sigma p)\right] \ , \tag{4.37}$$

where $P^+_{\mu\nu}$ is the gravitino polarization tensor given in eq. (2.108). Using the explicit expression for $P^+_{\mu\nu}$ we finally obtain

$$\begin{aligned}\frac{1}{4}\sum_{(\lambda_\psi,\lambda_\nu,\lambda_\gamma)}|\mathcal{M}|^2 &= \frac{1}{16M_P^2}|U_i^{(\widetilde{\gamma},\nu)}|^2 \qquad (4.38)\\ \times\,\mathrm{Tr}&\left[\overline{\sigma}^\mu\sigma^\sigma(\bar{\sigma}k)(\sigma q)\left\{g_{\mu\nu}-\frac{4}{3}\frac{q_\mu q_\nu}{m_{3/2}^2}-\frac{1}{3}\bar{\sigma}_\mu\sigma_\nu+\frac{1}{2}\bar{\sigma}_\mu\frac{q_\nu(\sigma q)}{m_{3/2}^2}+\frac{1}{3}\frac{q_\mu(\bar{\sigma}q)\sigma_\nu}{m_{3/2}^2}\right\}(\bar{\sigma}k)\sigma_\sigma\bar{\sigma}^\nu(\sigma p)\right].\end{aligned}$$

Each summand in the trace can be computed separately using eqs. (A.52), (A.53) and eqs. (A.56) - (A.58), as well as the relation $(\bar{\sigma}l)(\sigma l) = l^2$ for some momentum l. Note that $(\bar{\sigma}k)(\sigma k)$ is equal to zero for the photon momentum k. The results of the traces are

$$\mathrm{Tr}\left[\overline{\sigma}^\mu\sigma^\sigma(\bar{\sigma}k)(\sigma q)g_{\mu\nu}(\bar{\sigma}k)\sigma_\sigma\bar{\sigma}^\nu(\sigma p)\right] = 16(k\cdot q)(k\cdot p) \ , \tag{4.39}$$

$$\mathrm{Tr}\left[\overline{\sigma}^\mu\sigma^\sigma(\bar{\sigma}k)(\sigma q)q_\mu q_\nu(\bar{\sigma}k)\sigma_\sigma\bar{\sigma}^\nu(\sigma p)\right] = -8(k\cdot q)\left[2(k\cdot q)(q\cdot p)-m_{3/2}^2(k\cdot p)\right] \ , \tag{4.40}$$

$$\mathrm{Tr}\left[\overline{\sigma}^\mu\sigma^\sigma(\bar{\sigma}k)(\sigma q)\bar{\sigma}_\mu\sigma_\nu(\bar{\sigma}k)\sigma_\sigma\bar{\sigma}^\nu(\sigma p)\right] = 0 \ , \tag{4.41}$$

$$\mathrm{Tr}\left[\overline{\sigma}^\mu\sigma^\sigma(\bar{\sigma}k)(\sigma q)\bar{\sigma}_\mu q_\nu(\sigma q)(\bar{\sigma}k)\sigma_\sigma\bar{\sigma}^\nu(\sigma p)\right] = -16(k\cdot q)\left[2(k\cdot q)(q\cdot p)-m_{3/2}^2(k\cdot p)\right] \ , \tag{4.42}$$

$$\mathrm{Tr}\left[\overline{\sigma}^\mu\sigma^\sigma(\bar{\sigma}k)(\sigma q)q_\mu(\bar{\sigma}q)\sigma_\nu(\bar{\sigma}k)\sigma_\sigma\bar{\sigma}^\nu(\sigma p)\right] = 0 \ . \tag{4.43}$$

Therefore, we obtain the following result for the unpolarized matrix element squared:

$$\begin{aligned}\frac{1}{4}\sum_{(\lambda_\psi,\lambda_\nu,\lambda_\gamma)}|\mathcal{M}|^2 &= \frac{1}{16M_P^2}|U_i^{(\widetilde{\gamma},\nu)}|^2\\ &\quad\times\left(16(k\cdot q)(k\cdot p)+\frac{16}{3m_{3/2}^2}(k\cdot q)\left[2(k\cdot q)(q\cdot p)-m_{3/2}^2(k\cdot p)\right]\right)\\ &= \frac{2}{3M_P^2m_{3/2}^2}|U_i^{(\widetilde{\gamma},\nu)}|^2\left((k\cdot q)^2(q\cdot p)+m_{3/2}^2(k\cdot q)(k\cdot p)\right) \ . \qquad (4.44)\end{aligned}$$

The products of the momenta can be evaluated in the center-of-mass system of the reaction:

$$(k\cdot p) = \frac{m_{3/2}^2-m_\nu^2}{2} \ , \tag{4.45}$$

$$(k\cdot q) = \frac{m_{3/2}^2-m_\nu^2}{2} \ , \tag{4.46}$$

$$(q\cdot p) = \frac{m_{3/2}^2+m_\nu^2}{2} \ . \tag{4.47}$$

Using them, we obtain the following result:

$$\frac{1}{4}\sum_{(\lambda_\psi,\lambda_\nu,\lambda_\gamma)}|\mathcal{M}|^2 = \frac{1}{12}\frac{1}{M_P^2m_{3/2}^2}|U_i^{(\widetilde{\gamma},\nu)}|^2\left(m_{3/2}^2-m_\nu^2\right)^2\left(m_\nu^2+3m_{3/2}^2\right) \ . \tag{4.48}$$

We will neglect the neutrino mass hereafter.

The total decay width of a two body decay process is given by [4]

$$\Gamma = \frac{\left|\overline{\mathcal{M}}\right|^2}{8\pi}\frac{|\vec{p}_1|}{M^2} \ , \tag{4.49}$$

where M is the mass of the decaying particle, $\overline{\mathcal{M}}$ is the unpolarized matrix element squared and $|\vec{p}_1|$ is the final state momentum given in the center of mass frame by

$$|\vec{p}_1| = \frac{1}{2M}\sqrt{\left(M^2-(m_1+m_2)^2\right)\left(M^2-(m_1-m_2)^2\right)} \ , \tag{4.50}$$

where m_1, m_2 are masses of the final-state particles.

It follows that the total rate for gravitino decay into photon and neutrino is given by

$$\Gamma_{3/2}(\gamma\nu) = \frac{1}{32\pi}\sum_i |U_i^{(\tilde{\gamma},\nu)}|^2 \frac{m_{3/2}^3}{M_P^2} \ , \tag{4.51}$$

where we also took into account the decay rate into photon and antineutrino.

So far, we have obtained the gravitino decay rate as a function of an unspecified photino-neutrino matrix element. In general, such matrices depend on the nature of the NLSP. However, it turns out that the photino-neutrino mixing needed for the gravitino decay is independent of the neutralino wave function as long as the parameters of the mass matrix are hierarchical. In both bino and higgsino-like neutralino case the matrix element is given by[1]:

$$U_i^{(\tilde{\gamma},\nu)} = \zeta_i \frac{m_Z s_w c_w \left(M_2 - M_1\right)}{M_1 M_2}\left(1+\mathcal{O}\left(s_{2\beta}\frac{m_Z^2}{\mu^2}\right)\right) \ . \tag{4.52}$$

Inserting the matrix element (4.52) into the gravitino decay width (4.51) one obtains the gravitino lifetime

$$\tau_{3/2}(\gamma\nu) = \frac{32\sqrt{2}}{\alpha\zeta^2}\frac{G_F M_P^2}{m_{3/2}^3}\frac{M_1^2 M_2^2}{\left(M_2-M_1\right)^2}\left(1+\mathcal{O}\left(s_{2\beta}\frac{m_Z^2}{\mu^2}\right)\right) \ , \tag{4.53}$$

where α is the electromagnetic fine-structure constant evaluated at the Fermi scale. The corrections to the leading order expression in (4.53) are less than 10%.

4.2.2 Neutralino Decays

The neutralino decay channels follow from the neutral and charge currents, cf. eqs. (4.9), and (4.10), and also directly from the R-parity violating coupling of the gauginos to the Higgs boson, cf. eq. (3.50), after both have been evaluated in the mass eigenstate basis.

Thus, we obtain following decay channels, c.f Fig. 4.3.

$$\chi_1^0 \to \nu\, Z \ , \qquad \chi_1^0 \to \nu\, h \ , \qquad \chi_1^0 \to e^-\, W^+ \ . \tag{4.54}$$

The interaction Lagrangian responsible for the neutralino decay into neutrino and Z boson

[1]The matrix element $U_i^{(\tilde{\gamma},\nu)}$ agrees with the one used in [60, 114] for $M_2 - M_1 \ll M_1$. Note that this assumption is unjustified in models assuming grand unification.

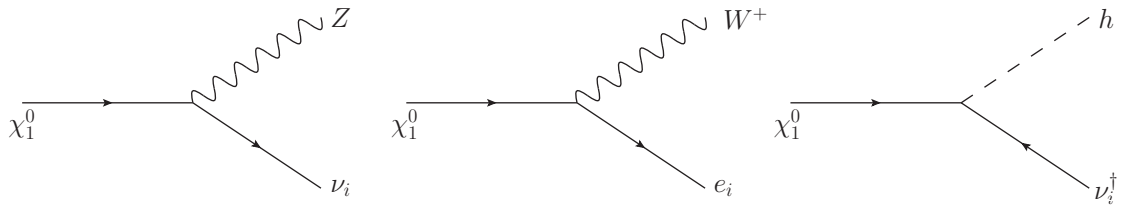

Figure 4.3: Neutralino decays into neutrino and Z boson, charged lepton and W boson, and neutrino and the lightest Higgs boson.

is given by

$$\mathcal{L}_{\chi_1^0 \nu Z} = -\frac{g}{c_w} \chi_1^0 \sigma_\mu V_{1i}^{(\chi,\nu)*} \nu_i^\dagger Z^\mu + h.c. \ , \tag{4.55}$$

while the interaction Lagrangian responsible for the neutralino decay into charged lepton and W boson reads

$$\mathcal{L}_{\chi_1^0 e_i W} = -\frac{g}{\sqrt{2}} \chi_1^0 \sigma_\mu V_{1i}^{(\chi,e)*} e_i^\dagger W^{-\mu} + h.c. \ . \tag{4.56}$$

The interaction Lagrangian responsible for the neutralino decay into neutrino and the lightest Higgs boson is given by

$$\mathcal{L}_{\chi_1^0 \nu h} = \frac{1}{2} g \nu_i \widetilde{V}_{i1}^{(\nu,\chi)} \chi_1^0 h + h.c. \ , \tag{4.57}$$

where we have defined the matrix element

$$\widetilde{V}_{i1}^{(\nu,\chi)} = \sum_j \kappa_j \left(\tan\theta_w (U_{1j}^{(\chi^0,\nu)} U_{i1}^{(\nu,\chi^0)} + U_{ij}^{(\nu)} U_{11}^{\chi^0}) - (U_{2j}^{(\chi^0,\nu)} U_{i2}^{(\nu,\chi^0)} + U_{ij}^{(\nu)} U_{21}^{\chi^0}) \right) \ . \tag{4.58}$$

The transformation matrices appearing in $\widetilde{V}_{i1}^{(\nu,\chi)}$ are defined in Appendix B, and will be evaluated in the following sections.

Let us first compute the decay into charged lepton and W boson. The matrix element reads

$$i\mathcal{M} = -\frac{i}{\sqrt{2}} g V \varepsilon_\mu^* x_i^\dagger \sigma^\mu x_j \ , \tag{4.59}$$

where the neutralino has momentum p_j, the lepton has momentum k_i, the W boson has momentum k_W and the external wave functions are $x_j \equiv y(p_j, \lambda_j)$, $x_i^\dagger \equiv y^\dagger(k_i, \lambda_i)$, and $\varepsilon_\mu^* \equiv \varepsilon_\mu^*(k_W, \lambda_k)$. The mixing matrix $V_{1i}^{(\chi,e)}$ is represented in the calculation by V. The square of the matrix element gives:

$$|\mathcal{M}|^2 = |V|^2 \frac{g^2}{2} \varepsilon_\mu^* \varepsilon_\nu \left(x_i^\dagger \bar{\sigma}^\mu x_j \right) \left(x_j^\dagger \bar{\sigma}^\nu x_i \right) \ . \tag{4.60}$$

Performing the sum over the polarizations of the W boson and the lepton and averaging over the neutralino polarizations we obtain

$$\begin{aligned} \frac{1}{2} \sum_{\text{spins}} |\mathcal{M}|^2 &= |V|^2 \frac{g^2}{2} \left(-g_{\mu\nu} + \frac{k_{W\mu} k_{W\nu}}{m_W^2} \right) \left(k_j^\mu p_i^\nu + k_j^\nu p_i^\mu - g^{\mu\nu} k_j p_i \right) \\ &= |V|^2 \frac{g^2}{2} \left(k_j p_i + \frac{2(k_W k_j)(k_W p_i)}{m_W^2} \right) \ , \end{aligned} \tag{4.61}$$

The momentum contractions are completely similar to the gravitino case, and we are led to the following result:

$$\frac{1}{2}\sum_{(\lambda_\chi,\lambda_e,\lambda_W)}|\mathcal{M}|^2 = |V|^2\,\frac{g^2}{4m_W^2}(m_{\chi_1^0}^2 - m_W^2)(2m_W^2 + m_{\chi_1^0}^2)\ . \tag{4.62}$$

Now we introduce Fermi's constant using the relation:

$$\frac{8G_F}{\sqrt{2}} = \frac{g^2}{m_W^2}\ , \tag{4.63}$$

and obtain

$$\frac{1}{2}\sum_{(\lambda_\chi,\lambda_e,\lambda_W)}|\mathcal{M}|^2 = |V|^2\,\sqrt{2}G_F(m_{\chi_1^0}^2 - m_W^2)(2m_W^2 + m_{\chi_1^0}^2)\ . \tag{4.64}$$

The total decay rate follows the general two body decay formula introduced in the previous section and reads

$$\Gamma\left(\chi_1^0 \to W^+ e_i^-\right) = \frac{G_F}{8\pi\sqrt{2}}\left|V_{1i}^{(\chi,e)}\right|^2 m_{\chi_1^0}^3\left(1-\frac{m_W^2}{m_{\chi_1^0}^2}\right)^2\left(1+2\frac{m_W^2}{m_{\chi_1^0}^2}\right)\ . \tag{4.65}$$

The computation of the neutralino decay into Z boson and neutrino is completely similar, the only change being the mixing matrix $V_{1i}^{(\chi,\nu)}$ and the coupling g/c_w. The result reads

$$\Gamma\left(\chi_1^0 \to Z\nu_i\right) = \frac{G_F}{4\pi\sqrt{2}}\left|V_{1i}^{(\chi,\nu)}\right|^2 m_{\chi_1^0}^3\left(1-\frac{m_Z^2}{m_{\chi_1^0}^2}\right)^2\left(1+2\frac{m_Z^2}{m_{\chi_1^0}^2}\right)\ . \tag{4.66}$$

Finally, we have to compute the decay of the neutralino into neutrino and the lightest Higgs boson. The matrix element for this decay is given by

$$i\mathcal{M}_1 = \frac{i}{2}g\widetilde{V}_{i1}^{(\nu,\chi^0)}x_i y_j\ , \tag{4.67}$$

where the neutralino has momentum p_i, the antineutrino has momentum k_i and the external wave functions are $x_i \equiv x(p_i,\lambda_i)$, $y_j \equiv y(k_j,\lambda_j)$. The square of the matrix element reads

$$|\mathcal{M}|^2 = \frac{1}{4}g^2\left|\widetilde{V}_{i1}^{(\nu,\chi^0)}\right|^2\left(x_i y_j y_j^\dagger x_i^\dagger\right)\ , \tag{4.68}$$

and the unpolarized matrix element squared is given by

$$\begin{aligned}\frac{1}{2}\sum_{(\lambda_\chi,\lambda_\nu)}|\mathcal{M}|^2 &= \frac{1}{8}g^2\left|\widetilde{V}_{i1}^{(\nu,\chi^0)}\right|^2(\mathrm{Tr}(k_j\sigma p_i\overline{\sigma}))\\ &= \frac{1}{4}g^2\left|\widetilde{V}_{i1}^{(\nu,\chi^0)}\right|^2(p_i\cdot k_j)\\ &= \frac{1}{8}g^2\left|\widetilde{V}_{i1}^{(\nu,\chi^0)}\right|^2\left(m_{\chi_1^0}^2 - m_h^2\right)\ .\end{aligned} \tag{4.69}$$

Thus, the decay rate is given by

$$\Gamma\left(\chi_1^0 \to h\nu_i\right) = \frac{1}{32}\frac{\alpha}{s_w^2}\left|\widetilde{V}_{i1}^{(\nu,\chi^0)}\right|^2 m_{\chi_1^0}\left(1-\frac{m_h^2}{m_{\chi_1^0}^2}\right)^2 , \tag{4.70}$$

where we have used the following relation:

$$\frac{g^2}{4\pi} = \frac{\alpha}{s_w^2} . \tag{4.71}$$

Neutralino-Higgs Coupling

So far, the coupling of the neutralino to the neutrino and the lightest Higgs boson is governed by the R-parity breaking parameter κ_i and not by ζ_i which governs the other channels. As stated before, $\kappa_i \simeq \zeta_i$ in the Higgs decoupling limit. In this section we show that the Higgs decoupling limit is satisfied in all models considered in the present work.

The R-parity violating coupling of the lightest Higgs boson

$$\kappa_i = \epsilon_i' \sin(-\alpha) + \epsilon_i'' \cos(\alpha) , \tag{4.72}$$

depends on the Higgs mixing angle α, which is connected with the mass of the CP-odd Higgs scalar A^0 and $\tan\beta$:

$$\frac{\tan 2\alpha}{\tan 2\beta} = \frac{m_{A^0}^2 + m_Z^2}{m_{A^0}^2 - m_Z^2} . \tag{4.73}$$

The so-called decoupling limit occurs when $m_{A^0} \gg m_Z$. Then, the lightest CP-even Higgs h saturates the upper bound on the Higgs mass with $m_h^2 \simeq m_Z^2 \cos^2(2\beta) + \text{loop corrections}$. In this case the angle α is very nearly $\beta - \pi/2$ and h has the same couplings to the particles of the Standard Model as would the ordinary Higgs boson without supersymmetry. The bino-like neutralino is the NLSP if we choose the following boundary conditions for the supersymmetry breaking parameters of the MSSM at the grand unification scale:

$$m_0 = m_{1/2} , \qquad A_0 = 0 , \qquad \tan\beta = 10 . \tag{4.74}$$

Now we can evaluate the mass of the CP-odd Higgs for different values of $m_{1/2}$. Since the neutralino mass also depends on the gaugino mass parameter, we can evaluate the A^0 mass for every value of the neutralino mass. Figure 4.4a shows the mass of the CP-odd Higgs A^0 as a function of the neutralino mass $m_{\chi_1^0}$. It is obvious that the condition for the decoupling limit is satisfied even for small neutralino masses. In order to further quantify this relation, we show the difference between α and $\beta - \pi/2$ as a function of the neutralino mass in Fig. 4.4b, where we have defined

$$\Delta\alpha = \left|\alpha - \beta + \frac{\pi}{2}\right| . \tag{4.75}$$

For neutralino masses around 100 GeV, $\Delta\alpha \lesssim 0.01$ and the decoupling limit is satisfied.

In the case of a higgsino-like neutralino NLSP we are in the extreme decoupling limit [74], since we start with very large parameters $m_{u,d}^2$ and small parameter μ at the GUT scale. The mass of the Z boson at the electroweak scale can be approximated by

$$-\frac{m_Z^2}{2} \simeq |\mu|^2 + m_u^2 , \tag{4.76}$$

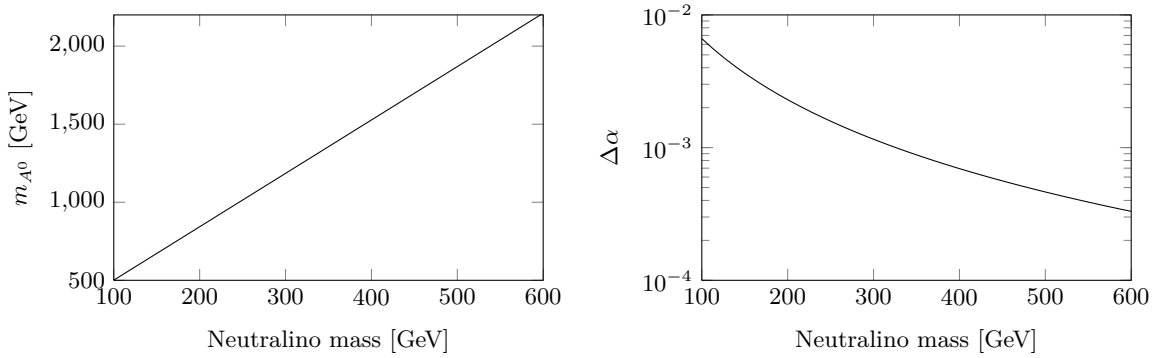

(a) The mass of the CP-odd Higgs A^0.

(b) The difference between the Higgs mixing angle α and Higgs VEV angle $\beta - \pi/2$.

Figure 4.4: Two functions of the neutralino mass $m_{\chi_1^0}$ which demonstrate that the decoupling limit is satisfied for the boundary conditions giving bino-like neutralino NLSP.

for $\tan\beta \geq 5$, while the mass of the CP-odd Higgs, cf. eq. (2.36) is then given by

$$m_{A^0}^2 \simeq m_Z^2 + m_d^2 \,. \tag{4.77}$$

The parameter m_d^2 stays large after the evolution from the GUT scale to the electroweak scale and therefore $m_Z \ll m_{A^0}$.

Since the decoupling limit is satisfied in all cases considered in the present work, we will replace κ_i by ζ_i in all relevant expressions. In particular, the coupling of the neutralino to neutrino and the lightest Higgs boson is given by

$$\widetilde{V}_{i1}^{(\nu,\chi)} = \sum_j \zeta_j \left(\tan\theta_w (U_{1j}^{(\chi^0,\nu)} U_{i1}^{(\nu,\chi^0)} + U_{ij}^{(\nu)} U_{11}^{\chi^0}) - (U_{2j}^{(\chi^0,\nu)} U_{i2}^{(\nu,\chi^0)} + U_{ij}^{(\nu)} U_{21}^{\chi^0}) \right). \tag{4.78}$$

Total Neutralino Decay Width

Let us first inspect the phase space factors of the various decay channels:

$$\begin{aligned} f_{W,Z}(m_{\chi_1^0}) &= \left(1 - \frac{m_{W,Z}^2}{m_{\chi_1^0}^2}\right)^2 \left(1 + 2\frac{m_{W,Z}^2}{m_{\chi_1^0}^2}\right) \,, \\ f_h(m_{\chi_1^0}) &= \left(1 - \frac{m_h^2}{m_{\chi_1^0}^2}\right)^2 \,. \end{aligned} \tag{4.79}$$

One sees immediately that the decay into the Higgs is suppressed compared to the decay into the gauge bosons which have three degrees of freedom instead of one. Additionally, the longitudinal mode of the gauge boson has a larger contribution than each transversal mode. This fact is called the Nambu-Goldstone enhancement [180].

The total neutralino decay width including decays into the antiparticles is given by:

$$\begin{aligned} \Gamma_{\chi_1^0} = \frac{G_F}{2\pi\sqrt{2}} m_{\chi_1^0}^3 \sum_i \left(\frac{1}{2} \left| V_{1i}^{(\chi,e)} \right|^2 f_W(m_{\chi_1^0}) + \left| V_{1i}^{(\chi,\nu)} \right|^2 f_Z(m_{\chi_1^0}) \right) \\ + \frac{1}{16} \frac{\alpha}{s_w^2} m_{\chi_1^0} \sum_i \left| \widetilde{V}_{i1}^{(\nu,\chi)} \right|^2 f_h(m_{\chi_1^0}) \end{aligned} \tag{4.80}$$

For further evaluation of the decay width we need the various matrix elements appearing in the expression above . Since they depend on the neutralino wave function, they have to be given separately for both cases considered in the present work.

Bino-like Neutralino After the diagonalization of the mass matrices the charged and neutral current couplings are given by

$$V_{1i}^{(\chi,\nu)} = -\zeta_i \frac{m_Z s_w}{2M_1}\left(1+\mathcal{O}\left(s_{2\beta}\frac{m_Z^2}{\mu^2}\right)\right) , \tag{4.81}$$

$$V_{1i}^{(\chi,e)} = -\zeta_i \frac{m_Z s_w}{M_1}\left(1+\mathcal{O}\left(s_{2\beta}\frac{m_Z^2}{\mu^2}\right)\right) . \tag{4.82}$$

Note that they agree up to the isospin factor at leading order in m_Z^2/μ^2, i.e., $V_{1i}^{(\chi,\nu)} = V_{1i}^{(\chi,e)}/2$. The coupling of the neutralino to the lightest Higgs boson and the neutrino is given at the leading order by

$$\widetilde{V}_{i1}^{(\nu,\chi)} = \zeta_i \tan\theta_w + \mathcal{O}\left(\frac{m_Z^2}{\mu^2}\right). \tag{4.83}$$

The neutralino decay width reads

$$\Gamma_{\chi_1^0} = \frac{1}{4}\frac{\alpha}{c_w^2}\zeta^2 m_{\chi_1^0}\left(\frac{1}{2}f_W(m_{\chi_1^0}) + \frac{1}{4}f_Z(m_{\chi_1^0}) + \frac{1}{4}f_h(m_{\chi_1^0})\right) , \tag{4.84}$$

where we have used $M_1 \simeq m_{\chi_1^0}$.

Higgsino-like Neutralino The charged and neutral current couplings in the higgsino-like neutralino case have a more complicated form:

$$V_{1i}^{(\chi,\nu)} = \frac{\zeta m_Z^2}{2\sqrt{2}\mu}\left(\left(\frac{s_w^2}{M_1}+\frac{c_w^2}{M_2}\right)(s_\beta - c_\beta) - \frac{M_1 c_w^2 + M_2 s_w^2 - \mu}{(M_1-\mu)(M_2-\mu)}(s_\beta + c_\beta)\right)\left(1+\mathcal{O}\left(\frac{m_Z^2}{M_2^2}\right)\right) , \tag{4.85}$$

$$V_{1i}^{(\chi,e)} = \frac{\zeta m_Z^2}{\sqrt{2}\mu}\left(2\frac{\mu c_w^2}{M_2(M_2-\mu)}(s_\beta + c_\beta) - \frac{M_1 c_w^2 + M_2 s_w^2 - \mu}{(M_1-\mu)(M_2-\mu)}(s_\beta + c_\beta) - 2\frac{c_w^2}{M_2}s_\beta\right) \times\left(1+\mathcal{O}\left(\frac{m_Z^2}{M_2^2}\right)\right) . \tag{4.86}$$

The neutralino-neutrino-Higgs coupling reads

$$\widetilde{V}_{i1}^{(\nu,\chi^0)} = \frac{\zeta_i m_Z}{\sqrt{2}}\left(\frac{c_w}{M_2-\mu}+\frac{s_w t_w}{M_1-\mu}\right)(s_\beta + c_\beta)\left(1+\mathcal{O}\left(\frac{m_Z^2}{M_2^2}\right)\right). \tag{4.87}$$

The calculation of the total decay width of the neutralino gives a lengthy expression:

$$\begin{aligned}\Gamma_{\chi_1^0} \simeq \frac{1}{32}\zeta^2\alpha m_Z^2 m_{\chi_1^0}\Bigg[& f_{h^0}(m_{\chi_1^0})\left(\frac{t_w}{M_1-\mu}+\frac{t_w^{-1}}{M_2-\mu}\right)^2(s_\beta+c_\beta)^2 \\ & + \frac{2}{s_w^2 c_w^2}f_W(m_{\chi_1^0})\left(2\frac{\mu c_w^2}{M_2(M_2-\mu)}(s_\beta+c_\beta) - \frac{M_1 c_w^2 + M_2 s_w^2 - \mu}{(M_1-\mu)(M_2-\mu)}(s_\beta+c_\beta) - 2\frac{c_w^2}{M_2}s_\beta\right)^2 \\ & + \frac{1}{s_w^2 c_w^2}f_Z(m_{\chi_1^0})\left(\left(\frac{s_w^2}{M_1}+\frac{c_w^2}{M_2}\right)(s_\beta - c_\beta) - \frac{M_1 c_w^2 + M_2 s_w^2 - \mu}{(M_1-\mu)(M_2-\mu)}(s_\beta+c_\beta)\right)^2\Bigg] ,\end{aligned} \tag{4.88}$$

where we have used $m_{\chi_1^0} \simeq \mu$.

4.2.3 Stau Decays

Contrary to the neutralino NLSP decay, which will be connected to the gravitino decay in the last section, the R-parity violating decays of a $\tilde{\tau}_1$-NLSP strongly depend on the flavor structure and the supersymmetry breaking parameters, because they arise due to the direct R-parity violating trilinear couplings, cf. eqs. (3.44), (3.45). Since the R-parity breaking Yukawa couplings are proportional to the ordinary Yukawa couplings, decays into fermions of the second and third generation dominate. The leading partial decay widths of left- and right-handed $\tilde{\tau}$-leptons, ignoring the masses of the final state particles, are (cf. eq. (3.43))

$$\Gamma_{\tilde{\tau}}(\bar{\tau}^\dagger \nu^\dagger) = \frac{1}{16\pi} \sum_i |\hat{\lambda}_{i33}|^2 m_{\tilde{\tau}} \ , \tag{4.89}$$

$$\Gamma_{\tilde{\tau}}(t^\dagger \bar{b}^\dagger) = \Gamma_{\tilde{\tau}}(t^\dagger \bar{s}^\dagger) = \frac{3}{16\pi} |\lambda'_{333}|^2 m_{\tilde{\tau}} \ , \tag{4.90}$$

$$\Gamma_{\tilde{\tau}}(\bar{t}\ b) = \frac{3}{16\pi} |\hat{\lambda}'_{333}|^2 m_{\tilde{\tau}} \ , \tag{4.91}$$

$$\Gamma_{\tilde{\bar{\tau}}^\dagger}(\tau\nu) = \Gamma_{\tilde{\bar{\tau}}^\dagger}(\mu\nu) = \frac{1}{16\pi} \sum_i |\lambda_{i33}|^2 m_{\tilde{\bar{\tau}}} \ . \tag{4.92}$$

Note that in the usual notation $\tilde{\bar{\tau}}^\dagger \equiv \tilde{\tau}_R$. In the flavor model discussed in section 3.5.1, the order of magnitude of the various decay widths is determined by the power of the hierarchy parameter η ($\eta^2 \simeq 1/300$),

$$\begin{aligned} \Gamma_{\tilde{\tau}}(\bar{\tau}^\dagger \nu^\dagger) &\sim \Gamma_{\tilde{\bar{\tau}}^\dagger}(\tau\nu) = \Gamma_{\tilde{\bar{\tau}}^\dagger}(\mu\nu) \\ &\sim \Gamma_{\tilde{\tau}}(t^\dagger \bar{b}^\dagger) \sim \Gamma_{\tilde{\tau}}(t^\dagger \bar{s}^\dagger) \sim \eta^4 \Theta^2 m_{\tilde{\tau}} \ , \end{aligned} \tag{4.93}$$

$$\Gamma_{\tilde{\tau}}(\bar{t}\ b) \sim \eta^2 \Theta^2 m_{\tilde{\tau}} \ . \tag{4.94}$$

The lightest mass eigenstate $\tilde{\tau}_1$ is a linear combination of $\tilde{\tau}$ and $\tilde{\bar{\tau}}^\dagger$, cf. Section 2.2.3,

$$\tilde{\tau}_1 = \sin\theta_\tau \tilde{\tau} + \cos\theta_\tau \tilde{\bar{\tau}}^\dagger \ . \tag{4.95}$$

From the above equations we obtain the $\tilde{\tau}_1$-decay width

$$\Gamma_{\tilde{\tau}_1} = \sin^2\theta_\tau \left(\Gamma_{\tilde{\tau}}(\bar{\tau}^\dagger \nu^\dagger) + 2\Gamma_{\tilde{\tau}}(t^\dagger \bar{b}^\dagger) + \Gamma_{\tilde{\tau}}(\bar{t}\ b) \right) + 2\cos^2\theta_\tau \Gamma_{\tilde{\bar{\tau}}^\dagger}(\tau\nu) \ . \tag{4.96}$$

The total width is dominated by the contributions $\tilde{\bar{\tau}}^\dagger \to \tau\nu, \mu\nu$ and $\tilde{\tau} \to \bar{t}\ b$, respectively,

$$\Gamma_{\tilde{\tau}_1} = \sin^2\theta_\tau \Gamma_{\tilde{\tau}}(\bar{t}\ b) + 2\cos^2\theta_\tau \Gamma_{\tilde{\bar{\tau}}^\dagger}(\tau\nu) \ , \tag{4.97}$$

and it can be directly expressed in terms of the τ-lepton and top-quark masses,

$$\Gamma_{\tilde{\tau}_1} = 3\frac{\epsilon^2}{16\pi v^2}\frac{m_t^2}{m_{\tilde{\tau}_1}^3} \sin^2\theta_\tau \left(m_{\tilde{\tau}_1}^2 - m_t^2\right)^2 + 2\frac{\epsilon^2}{16\pi v^2}\frac{m_\tau^2}{m_{\tilde{\tau}_1}^3} \tan^2\beta \cos^2\theta_\tau \left(m_{\tilde{\tau}_1}^2 - m_\tau^2\right)^2 \ , \tag{4.98}$$

where we have restored the dependence on the final state masses, used

$$h_{33}^e = m_\tau/(v\cos\beta) \approx m_\tau \tan\beta/v \tag{4.99}$$

for $\tan\beta = 10$, and assumed

$$\epsilon_{2,3} = \epsilon'_{2,3} = \epsilon''_{2,3} \equiv \epsilon \ . \tag{4.100}$$

This corresponds to the parameter choice $a = b = c = 1$ in Eq. (3.72). Note that the $\tilde{\tau}_1$-decay width and branching ratios are affected with a considerable uncertainty since these parameters depend on the unspecified mechanism of supersymmetry breaking.

4.3 Bounds on R-parity violating Couplings

The assumption of broken R-parity in general introduces a number of new interactions between ordinary and supersymmetric particles, which can contribute to a variety of low-, intermediate- and high-energy processes. The range of R-parity violating couplings considered in the present work is set by the requirement of obtaining a consistent cosmology. It turns out that in order to satisfy the cosmological bounds, the R-parity violating couplings must be small, a fact which was assumed throughout the present work. Such couplings could for example arise via a model presented in Section 3.5. Assuming such small couplings, the only relevant phenomenological effects should be the decays of the gravitino LSP and the NLSP, as stressed in the introduction to this chapter. Nevertheless, we shall briefly summarize general indirect bounds on the R-parity odd interactions, and present direct searches for R-parity violation at colliders. Finally, we obtain limits on the gravitino lifetime from the analysis of cosmic rays. Using these limits we are able to reduce the allowed range of the R-parity violating couplings, and make predictions for LHC phenomenology.

4.3.1 Bounds from Cosmology

The desire for a consistent cosmology is the main motivation for the present work. As pointed out in Section 2.5.1, the presence of the gravitino in the spectrum can cause a number of problems for the presumed mechanisms operating in the early universe, for example for BBN. It was stated that these problems can be solved by the introduction of a small amount of R-parity violation. In this section we shall determine the range of the R-parity breaking couplings which leads to a consistent cosmological picture.

Assuming gravitino dark matter, we first obtain a lower bound on the R-parity violating couplings by demanding that the NLSP decays take place before the BBN. In the case of a charged NLSP, like a scalar tau lepton, its lifetime has to be $\tau_{\tilde{\tau}} \leq (10^3 - 10^4)$ s [135, 136]. In case of a neutralino, BBN excludes lifetimes longer than 10^2 s due to the strong constraints from hadronic showers [130, 181, 182]. The NLSP lifetime becomes sufficiently short for $\zeta > 4 \times 10^{-13}, \lambda > 2 \times 10^{-14}$ in case of a neutralino and stau NLSP

$$\begin{aligned} \tau_{\chi_1^0} &\simeq 10^2 \text{ s } \left(\frac{\zeta}{4 \times 10^{-13}}\right)^{-2} \left(\frac{m_{\chi_1^0}}{100 \text{ GeV}}\right)^{-1} , \\ \tau_{\text{NLSP}} &\simeq 10^3 \text{ s } \left(\frac{\lambda}{10^{-14}}\right)^{-2} \left(\frac{\widetilde{m}}{100 \text{ GeV}}\right)^{-1} , \end{aligned} \tag{4.101}$$

where in the second equation we have assumed a generic charged NLSP decaying via a trilinear R-parity breaking coupling.

The upper bound on the size of the R-parity breaking can be obtained from the requirement that the baryon asymmetry of the universe survives in the presence of R-parity violating interactions, which also violate $B - L$. Above the critical temperature of $T_C \sim 100$ GeV and up to very high temperatures of $\mathcal{O}(10^{12})$ GeV, sphaleron processes are in thermal equilibrium [162,183]. These processes correspond to level crossing [184,185] of all $SU(2)$ doublets in the bosonic background of a topologically non-trivial gauge field configuration (the sphaleron) leading to the simultaneous creation or disappearance of 9 quarks and 3 leptons, one lepton and three quarks from each generation. Thus, each combination

$$\frac{B}{3} - L_\alpha \tag{4.102}$$

is conserved in sphaleron processes although the baryon number B and the individual lepton numbers L_α, $\alpha = 1, 2, 3$ are violated. The baryon asymmetry of the universe can, therefore, be generated above the Fermi scale only in the form of $B - L$. The presence of additional baryon or lepton number violating interactions (which obviously break $B - L$) in thermal equilibrium would wash out any generated $B - L$ asymmetry and hence spoil the predictions of otherwise successful theories of baryogenesis like leptogenesis [186–190]. This problem can be circumvented if the R-parity breaking interactions are out of equilibrium. This means that their rate is smaller than the Hubble parameter, i.e. their characteristic timescale is longer than the age of the universe at a given epoch.

The best bounds on trilinear couplings are obtained from the decays of squarks and sleptons in two fermions, and the corresponding rate is given by [187, 191]:

$$\Gamma_\lambda \simeq 1.4 \times 10^{-2} \, |\lambda|^2 \, \frac{\widetilde{m}}{T} \ , \tag{4.103}$$

where $\widetilde{m}$ is the mass of the decaying sfermion, and λ stands for any trilinear R-parity violating coupling. Since

$$H \simeq 1.66 \sqrt{g^*} \frac{T^2}{M_P} \ , \tag{4.104}$$

where g^* is the number of the effectively massless degrees of freedom at the temperature T, and we demand $\Gamma_\lambda < H$, the best bound is obtained at the critical (the lowest) temperature. Assuming $\widetilde{m} \sim T \sim 100$ GeV, one obtains [191] the rather generic prediction

$$|\lambda_{ijk}| \, , \ \left|\lambda'_{ijk}\right| \ , \left|\lambda''_{ijk}\right| \lesssim 10^{-7}. \tag{4.105}$$

However, its often argued [190] that the above cosmological constraints can be circumvented if the baryon number and *one* of the lepton flavor numbers are sufficiently conserved. That means it should be sufficient that only the processes violating one particular combination in eq. (4.102) are out of equilibrium, even if the other two combinations are violated by processes in thermal equilibrium. For example, if $\lambda'_{1ijk} \lesssim 10^{-7}$ is satisfied, then it is often assumed that λ'_{2jk}an λ'_{3jk} can be much larger.

In a recent study Endo, Hamaguchi and Iwamoto [192] have shown that the conclusion above becomes unjustified in all models with tiny lepton flavor violation (LVF). They stated that LVF is a rather generic prediction of SUSY models, and appears, for example, in see-saw models with gravity mediated SUSY breaking with a typical size which is large enough to erase the flavor dependence of $B/3 - L_\alpha$. Under the assumption of small LVF they obtained the following bounds:

$$\sqrt{\sum_{ijk} \left|\lambda''_{ijk}\right|^2} \lesssim (4 - 5) \times 10^{-7} \ , \tag{4.106}$$

$$\sqrt{\sum_{ijk} \left|\lambda'_{ijk}\right|^2} \lesssim (3 - 6) \times 10^{-7} \ , \tag{4.107}$$

$$\sqrt{\sum_{ijk} |\lambda_{ijk}|^2} \lesssim (0.6 - 1) \times 10^{-6} \ , \tag{4.108}$$

$$\sqrt{\sum_{i} \left|\frac{\mu_i}{\mu}\right|^2} \lesssim (1 - 2) \times 10^{-6} \ , \tag{4.109}$$

for $\widetilde{m}_{\tilde{q}} \simeq 200 - 1200$ GeV, and $\widetilde{m}_{\tilde{l}} \simeq 100 - 400$ GeV. We use these bounds in the present work.

Let us finally check that the gravitino is still a viable dark matter candidate. The gravitino lifetime is given by

$$\tau_{3/2}(\gamma\nu) = 1 \times 10^{25}\ s\ \left(\frac{\zeta}{10^{-6}}\right)^{-2} \left(\frac{M_1}{100\ \text{GeV}}\right)^{2} \left(\frac{m_{3/2}}{10\ \text{GeV}}\right)^{-3} , \tag{4.110}$$

assuming a SUSY breaking scenario where $M_2 \simeq 2M_1$ at the electroweak scale. Thus, we are led to the conclusion that for the allowed values of R-parity breaking parameters, the gravitino is still a viable dark matter candidate and, therefore, all cosmological constraints can be satisfied at once. Nevertheless, the gravitino will decay, and its decays taking place in the galactic halo or extragalactic structures will produce additional contributions to the spectra of cosmic rays which might be observable on top of the astrophysical background. The limits on the gravitino lifetime from searches for decaying dark matter will be the topic of the last part of this section.

Having established the parameter range of R-parity violation of interest to us

$$10^{-13} \lesssim \zeta \lesssim 10^{-6}\ ,\ 10^{-14} \lesssim \lambda \lesssim 10^{-7}\ , \tag{4.111}$$

(where we have assumed $\epsilon \simeq \zeta$, which follows from our model of R-parity breaking, and λ is a generic R-parity violating trilinear coupling) we note that the amount of R-parity violation produced in the model of Section 3.5 falls exactly within this range. In the next step we can check whether some parts of this parameter space have already been excluded by various direct and indirect searches for new physics.

It is not possible to summarize all of the present direct and indirect bounds within the scope of this work, and we will, therefore, present an assortment of results and refer the reader to the review [157] for a detailed account. Note that since the authors of [157] are interested in bilinear R-parity violation as source of the neutrino masses, their conclusion concerning the use of R-parity violation for consistent gravitino cosmology is diametrically opposed to the one put forward in the present work.

4.3.2 Indirect Bounds

The requirement that R-parity violating contributions do not spoil the successful predictions of the Standard Model for various observables, or do not exceed experimental upper limits on rare processes, allows us to put constraints on the size of the R-parity violation. Additionally, it is possible to provide some weak constraints by requiring that the R-parity violating couplings stay perturbative up to the scale of the unification, i.e.

$$\frac{\lambda_{ijk}^2(M_{GUT})}{(4\pi)^2} < 1\ , \tag{4.112}$$

where λ_{ijk} is a generic trilinear coupling.

It is interesting to note that all indirect bounds are obtained directly for the trilinear R-parity violating couplings (often assuming the trilinear breaking scenario). If the trilinear couplings are generated from bilinear R-parity violation, their properties, however, can be different compared to the pure trilinear case, cf. eqs.(3.44), (3.45). Furthermore, most of the established indirect bounds have been derived under the hypothesis that one particular

Coupling	Bound	Origin
λ_{12k}	$0.05\ \tilde{\tilde{e}}_k^\dagger$	V_{ud}
λ_{23k}	$0.07\ \tilde{\tilde{e}}_k^\dagger$	R_τ
λ_{233}	0.9	RGE
λ'_{111}	$3.3 \times 10^{-4}\ \tilde{q}^2 g^{1/2}$	$\beta\beta0\nu$
λ'_{333}	$0.32\ \tilde{\tilde{b}}^\dagger$	$B \to \tau\nu X$
λ'_{i33}	$4 \times 10^{-4}\ b\widetilde{m}^{-1/2}$	$m_\nu < 1$ eV
ζ	$4.4 \times 10^{-6}\ \chi_0^{1-1}$	$m_\nu < 1$ eV

Table 4.1: Single (indirect) bounds on the R-parity violating couplings at the 2σ level. The abbreviations in the last column refer to the processes explained in the text. The indices i, j, k run over the three generations. The dependence on the (super)particle mass is noted as p^q, which stands for $\left(\frac{m_p}{100\,\mathrm{GeV}}\right)^q$, where m_p is the mass of the particle p; $\widetilde{m}$ is an average mass scale of superparticles. Parts of the table are extracted from [157].

coupling dominates over all other contributions. This assumption is called the *single coupling dominance hypothesis*. The bounds derived under this hypothesis are in general moderately strong and involve a linear dependence on the superparticle mass [157]:

$$\lambda, \lambda', \lambda'' < (10^{-2} - 10^{-1}) \frac{\widetilde{m}}{100\ \mathrm{GeV}}\ , \tag{4.113}$$

where $\lambda, \lambda', \lambda''$ denote the trilinear couplings and $\widetilde{m}$ is the superparticle mass scale. Some of the indirect bound chosen to demonstrate different sources of constraints are summarized in Table 4.1. We omit the bounds on the baryon number violating coupling, since this coupling is not generated by bilinear R-parity violation. The absence of this coupling ensures the stability of the proton. In the last column of the table we indicate via which process the bound in question was obtained. There the abbreviation RGE stands for bounds obtained from the perturbativity requirement, cf. eq (4.112). The abbreviation V_{ud} indicates that the bound was obtained from the measurement of the CKM matrix elements. The experimental value of V_{ud} is determined from comparison between the nuclear β decay and the muon decay, and is changed if R-parity violating interactions are present. R_τ stands for the ration of the leptonic τ-lepton decay widths

$$R_\tau = \frac{\Gamma(\tau \to \nu_e^\dagger \nu_\tau)}{\Gamma(\tau \to \mu \nu_\mu^\dagger)\nu_\tau}\ , \tag{4.114}$$

which is affected by the decays mediated by the scalars. The abbreviation $\beta\beta0\nu$ refers to the bounds obtained from the neutrinoless double beta decay. The bound quoted here is obtained in the minimal supergravity framework from the lower limit on the half-life of ^{76}Ge measured by the Heidelberg-Moscow experiment [193]. $B \to \tau\nu X$ indicates that the corresponding limit was derived from the inclusive semileptonic B meson decay process $B^- \to X_q \tau^- \nu^\dagger$ which can be expressed solely in terms of the single coupling constant λ'_{333} assuming the single coupling constant dominance hypothesis. The limit on λ'_{i33} can be, furthermore, derived from the loop-induced neutrino masses, since, as we have seen in this chapter, R-parity violation generates one neutrino mass at tree-level, while other masses are generated via loops. This limit is indicated by $m_\nu < 1$ eV . The trilinear couplings λ, λ' contribute to each entry of the neutrino mass matrix M^ν_{ij} through the lepton-slepton and quark-squark loops. Assuming

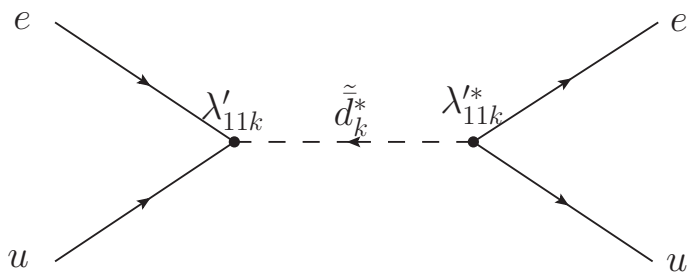

Figure 4.5: Sample Feynman diagram for the single resonant s-channel production of the $\tilde{\bar{d}}$ squark in $e-p$ collisions with subsequent decay into SM particles via the λ'_{11k} Yukawa coupling.

degenerate scalar masses, A-terms proportional to the Yukawa couplings of the MSSM, and a flavor hierarchy of the trilinear R-parity violating couplings linked to the one found in the Yukawa couplings of the MSSM, which is natural if both are generated by the Froggatt-Nielsen mechanism (cf. Section 3.5.1), one obtains

$$M^{\nu}_{ij}\big|_{\lambda'} \sim \lambda'_{i33}\lambda'_{i33}(7.7\times 10^6\,\mathrm{eV})\left(\frac{m_b}{4.5\,\mathrm{GeV}}\right)^2\left(\frac{100\,\mathrm{GeV}}{\widetilde{m}}\right)\,, \tag{4.115}$$

where $\widetilde{m}$ is the average scalar mass. Demanding that the neutrino mass scale stays below 1 eV one can set limits on the couplings. Note that no bounds have been derived so far on the coupling of right-handed up-quarks, $\hat{\lambda}'_{ijk}$ introduced in Section 3.4.

We can also obtain a bound on ζ from the requirement that the tree-level neutrino mass, eq. (4.21), generated by bilinear R-parity violation is smaller than the experimental bound of 1 eV:

$$\zeta < 4.5\times 10^{-6}\,M_1 = 100\,\mathrm{GeV}\;,\;\; M_2 = 200\,\mathrm{GeV}\;, \tag{4.116}$$

$$\zeta < 2\times 10^{-5}\,M_1 = 2000\,\mathrm{GeV}\;,\;\; M_2 = 4000\,\mathrm{GeV}\;. \tag{4.117}$$

We assumed in both cases hierarchical spectra a with bino-like neutralino and large μ in the first case and a higgsino-like neutralino in the second case. Note that in this case the model for the spontaneous R-parity breaking, cf. Section 3.5, is not consistent, since it uses a neutrino mass scale of 0.01 eV which is dominated by the see-saw contribution. Demanding its validity, i.e. $m_\nu \lesssim 0.01$ eV, lowers both limits exactly by one order of magnitude.

Let us now look at some of the recent results from the direct searches for R-parity violation at colliders.

4.3.3 Bounds from direct Searches

First, we quote part of the results from the search for squarks in supersymmetric models with R-parity violation at the HERA accelerator in Hamburg [194]. Being a hadron-electron storage ring, HERA allows for resonant single squark production via the LQD operator, cf. eq. (3.15). A non-zero coupling λ'_{1jk} leads to the production of squarks which then decay into SM particles, via cascades of neutralinos, charginos, gluinos and possibly lighter squarks and sleptons. Figure 4.5 shows one possible Feynman diagram for such process.

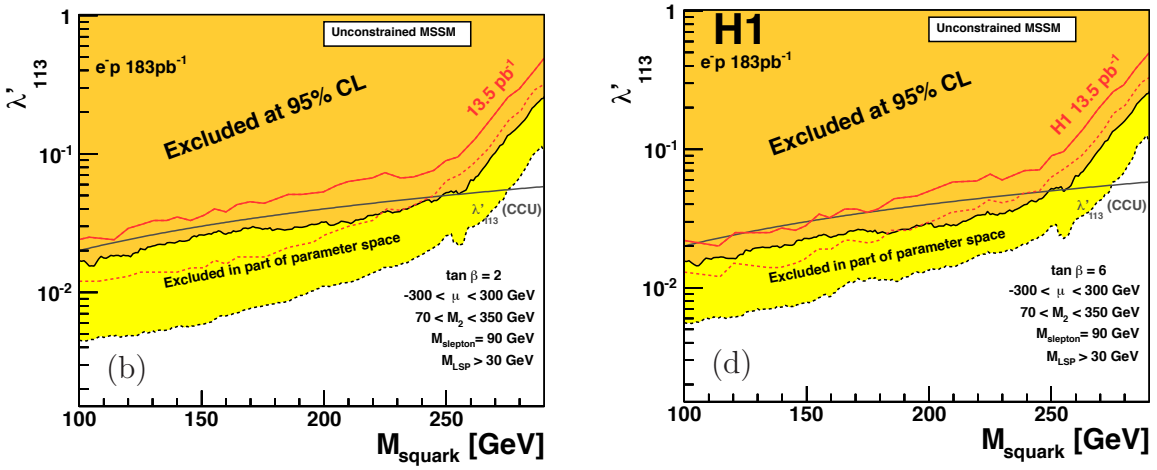

(a) (b)

Figure 4.6: 95% C.L. exclusion limits on λ'_{113} for (a) $\tan\beta = 2$ and (b) $\tan\beta = 6$ as a function of the squark mass derived from a scan of the MSSM parameter space, as indicated in the figures using $183\,\mathrm{pb}^{-1}$ of $e-p$ collision data. The dark shaded region indicates values of the coupling λ'_{113} excluded in all investigated scenarios, whereas the light shaded region is excluded only in part of the scenarios. Indirect limits from neutrinoless double beta decay experiments ($\beta\beta0\nu$) and tests of charged current universality (CCU) are also shown, as well as previous results of the H1 collaboration. Both figures are taken from [194].

No significant deviation from the SM predictions could be observed in the analysis of the data sets of the H1 experiment corresponding to integrated luminosities of 183 pb^{-1} of electron-proton, and 255 pb^{-1} of positron-proton collision data collected at a center-of-mass energy of $\sqrt{s} = 319$ GeV. The non-observation of a signal was interpreted in a phenomenological version of the MSSM. The masses of squarks and sleptons were set to fixed values and the gaugino masses were determined via the set of parameters μ, M_2, and $\tan\beta$. The gluino mass was set to a large value $M_g \sim M_3 \ll M_2$. Mixing effects in the sfermion sector were neglected for the first two squark generations, and sleptons were considered to be degenerate in mass. Their masses were set to 90 GeV. Furthermore, as in the case of indirect limits, the single coupling dominance hypothesis was assumed.

Figure 4.6 shows exclusion limits on the strength of the R-parity violating coupling λ'_{113} depending on the squark mass hypothesis. The limits were derived in the MSSM by a scan of the supersymmetric parameters $70\,\mathrm{GeV} < M_2 < 350\,\mathrm{GeV}$ and $-300\,\mathrm{GeV} < \mu < 300\,\mathrm{GeV}$ at $\tan\beta = 2$ and 6. The limits exclude the coupling λ'_{11k} at the level

$$\lambda'_{11k} < 0.5 \times 10^{-2}\ ,\ \text{at}\ M_{\tilde{q}} = 100\,\mathrm{GeV}\ , \tag{4.118}$$

$$\lambda'_{11k} < 0.5\ ,\ \text{at}\ M_{\tilde{q}} = 290\,\mathrm{GeV}\ , \tag{4.119}$$

for all three squark generations $k = 1, 2, 3$. A similar result was also obtained for the coupling λ'_{1j1}.

After the shutdown of HERA and Tevatron, LHC is the only running particle physics experiment which could possibly look for direct R-parity violating production and decays of supersymmetric particles. The LHC collaborations now put great effort into the analysis

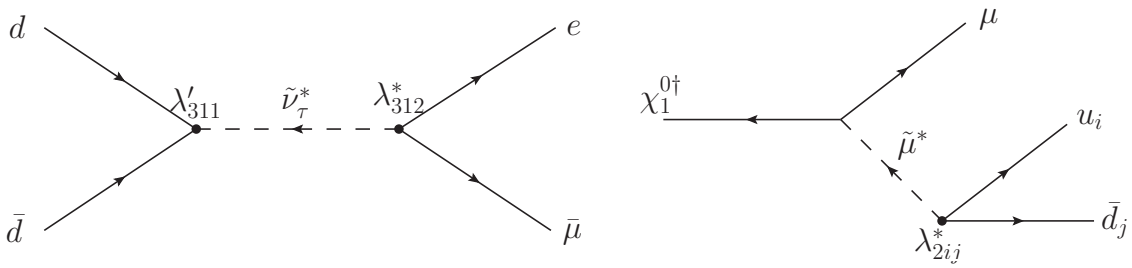

Figure 4.7: Feynman diagrams for the two R-parity violating processes under consideration by the ATLAS collaboration. LH: Production of a single tau sneutrino at the LHC with subsequent decay into oppositely charged electron and muon pairs. RH: Neutralino decaying into a muon and two jets, via a virtual smuon possibly leading to a displaced vertex.

of the LHC data searching primarily for R-parity conserving supersymmetry. However, also some results concerning the R-parity violating SUSY have been published. The ATLAS collaboration has searched for resonant single slepton production with a subsequent R-parity violating decay into oppositely charged electron and muon pairs and also for displaced vertices from neutralino decays, see [195] and references therein. Figure 4.7 shows the processes under consideration.

In the search for the electron-muon resonance the collaboration assumed that all R-parity violating couplings except λ'_{311} and λ_{312} are zero. Furthermore, it was assumed that the tau sneutrino is the LSP, because in this case the only contribution to the $e\ \mu$ final state originates from $\tilde{\nu}_\tau$. The collaboration analyzed $1.07 \pm 0.04\text{fb}^{-1}$ of data collected in 2011 and observed 4053 $e\,\mu$ candidates, while 4150 ± 250 events were expected from Standard Model processes. Since no evidence for a signal was observed, the collaboration set an upper limit on $\sigma(pp \to \tilde{\nu}\tau) \times \text{BR}(\tilde{\nu}\tau \to e\mu)$ using a Bayesian method with a uniform prior for the signal cross section. Figure 4.8a shows the 95% C.L. upper limits on the λ'_{311} coupling as a function of the tau sneutrino mass for four values of λ_{312}. The regions above the curves are excluded in each case.

The ATLAS collaboration also searched for a heavy particle decaying into multiple charged particles at distances between 4 mm and 180 mm from the primary vertex in events containing a muon with high transverse momentum. It was assumed that the neutralino decays into this final state due to a non-zero λ'_{2ij} coupling, cf. right hand side of Fig. 4.7. Note that the ATLAS collaboration assumed an explicit trilinear R-parity breaking scenario with a dominant LQD operator, a scenario which is not consistent at the quantum level since bilinear R-parity violating couplings would be generated via loops. In the case of bilinear R-parity violation, the neutralino would predominantly decay via two body decays presented in this work, cf. Section 4.2.2. Events were selected from a data sample of 33 pb^{-1} collected in 2010 and had to pass the $p_T > 40$ GeV single-muon trigger requirement. A primary vertex (PV) originating from the pp collision was required to contain a minimum of five tracks and a z position within 200 mm. A displaced vertex was reconstructed by selecting only tracks with $p_T > 1$ GeV. A large impact parameter (> 2 mm), with respect to the transverse position of the PV was required, rejecting 98% of all tracks originating from the primary pp interaction. The discriminating variables for the search were the mass of the reconstructed vertex (m_{DV}) and the number of reconstructed charged tracks (N^{trk}_{DV}). A vertex satisfied the selection criteria if $m_{\text{DV}} > 10$ GeV and $N^{trk}_{\text{DV}} > 4$. No vertices were found in the signal region. The collaboration

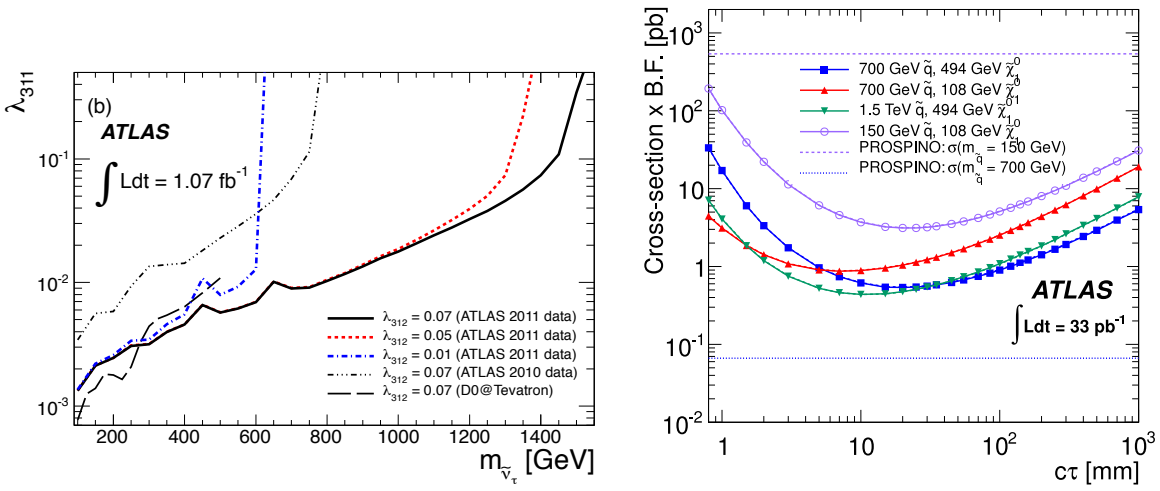

(a) (b)

Figure 4.8: Exclusion limits on R-parity violating couplings from the ATLAS experiment at LHC. (a) 95% C.L. upper limits on the λ'_{311} coupling as a function of the tau sneutrino mass. (b) 95% C.L. upper limits on the production cross section times branching fraction vs. the neutralino lifetime times the speed of light for different combinations of squark and neutralino masses, based on the observation of zero events in a 33 pb^{-1} data sample. The horizontal lines show the cross sections for squark masses of 700 GeV and 150 GeV. Note that the model under consideration in the present work is beyond the scope of the presented search for displaced vertices. Both figures are taken from [195].

set upper limits on the supersymmetry production cross section times the branching fraction of the simulated signal decays for different combinations of squark and neutralino masses, and for different values of the theoretical decay length $c\tau$, where c is the speed of light and τ the neutralino lifetime. The observed limit is shown in Fig. 4.8b.

Using their result, we can set limits on the models presented in this work. Assuming a bino-like neutralino with a mass of 100 GeV, which as we will see is the lower mass limit, a ζ of 6.9×10^{-8} is required in oder to have a decay length of one meter, which is the upper bound in the plot. Then, we can exclude models with such value of ζ if they have a production cross section of approximately 12 pb, since the neutralino will decay into W boson and muon with a branching ratio of 1/3, cf. Section 4.4.1. Note that the models which will be intensively studied in the present work are beyond the scope of this search, due to small cross sections and small R-parity violating couplings. However, the situation could change in the future if this search was performed with new data.

Finally, the ATLAS collaboration has interpreted a generic search in terms of bounds on SUSY with bilinear R-parity violation [196]. They assumed an mSUGRA/CMSSM SUSY production model, with bilinear R-parity breaking parameters fitted to the neutrino oscillations data as described in [197] under the assumption that the tree-level contribution dominates [198]. The neutralino LSP is unstable and decays through modes including neutrinos, cf. Section 4.2.2. It was assumed that such decays, along with the presence of neutrinos in SUSY decay chains such as $\chi^{\pm} \to \nu\chi^0_1$, would lead to a significant missing transverse momentum signature. The observed number of events in the data was consistent with the Standard

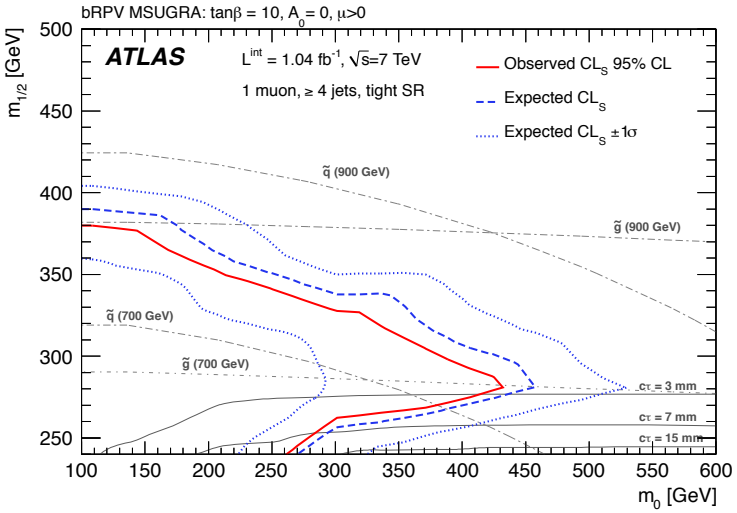

Figure 4.9: Observed and expected 95% CL exclusion limits, as well as the $\pm 1\sigma$ variation on the expected limit, from ATLAS experiment for the bilinear R-parity violation model fitted to neutrino mass parameters in mSUGRA parameter space using the tight four-jet selection in the muon channel. The region with LSP lifetimes $c\tau > 15$ mm is not shown. The figure is taken from [196].

Model expectation, and the collaboration set 95% C.L. exclusion limits in the mSUGRA parameter space using tight four-jet selection in events with exactly one muon. The tight selection demanded four jets with at least 40 GeV transverse momentum. The leading jet was required to have $p_T > 60$ GeV. Additionally, the missing transverse energy E_T^{miss} was required to be larger than 200 GeV, $E_T^{\text{miss}}/m_{\text{eff}} > 0.15$, $m_{\text{eff}} > 500$ GeV, where

$$m_{\text{eff}} = p_T^l + \sum_i p_T^{\text{jet}_i} + E_T^{\text{miss}} \ , \tag{4.120}$$

the sum is taken over the four leading jets, and p_T^l is the muon transverse momentum. The exclusion limits are shown in Figure 4.9. The ATLAS collaboration states that the model was not tested for regions of parameter space where $c\tau$ of the LSP exceeds about 15 mm. Within the context of the model considered by ATLAS , and for equal squark and gluino masses, masses below 760 GeV are excluded.

We note that the authors of [196] do not describe how exactly the neutralino lifetime affects the limits. If the lifetime becomes larger, more of the neutralinos should decay outside of the detector, leading to more missing transverse energy creating signatures similar to R-parity conserving SUSY. The difficulties probably arise in the intermediate regime where most of the decays happen inside of the detector volume but outside of the inner tracking system. It would be very helpful if the collaborations would shed more light on the difficulties and prospects for discovery in such cases, since this is the prediction of the model put forward in the present work.

Furthermore, the assumption that significant amount of missing energy is created if neutralinos decay in the inner parts of the detector is not model independent. We will show in the later discussion that, assuming that all R-parity violating parameters ζ_i are equal, the

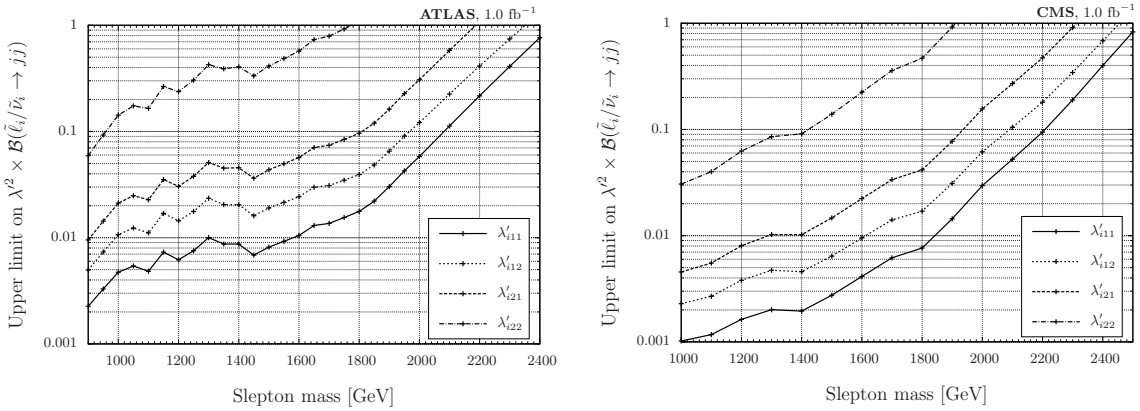

(a) (b)

Figure 4.10: Upper bounds on $\lambda'^2 \times BR(\tilde{e}_i, /\tilde{\nu}_i \to jj)$ derived from the (a) ATLAS and (b) CMS dijet resonance searches with 1 fb^{-1} of data. Both figures are taken from [199].

cut on $E_T^{\text{miss}} > 200$ GeV is too severe even for $\zeta = 3 \times 10^{-8}$. The requirement to explain neutrino masses with R-parity violation sets in our model $\zeta = 4.5 \times 10^{-6}$, and therefore most of the neutralinos would decay inside of the inner part of the detector, leading to a much smaller amount of missing transverse energy compared to the R-parity conserving case or to the scenario with $\zeta = 3 \times 10^{-8}$. However, in order to explain all of the measured properties of neutrino oscillations, more parameters of the model have to be fitted to the data and, therefore, more neutrinos could be in principle produced.

For values of the R-parity violating parameter considered in the present work, the neutralino decay length is much larger than 15 mm and thus all models are not affected by the presented constraints. Even if one does note take the restriction on the lifetime into account, the distribution of E_T^{miss} in our models is sufficiently different and we assume that even the lightest supersymmetric spectrum in the present work is not excluded. This topic will be central to our discussion in Section 5.2.

Recently, Dreiner and Stefaniak [199] reinterpreted the ATLAS and CMS searches for dijet resonances, as well as the ATLAS search for like-sign dimuon pairs in terms of bounds on the λ' coupling. They investigated resonant slepton production at the LHC via the LQD operator followed by decays either via the same operator resulting in resonant dijet production, or via a neutralino leading to a signature with same-sign dileptons due to the Majorana nature of neutralinos.

Figure 4.10 shows upper limits on the R-parity violating couplings (λ'_{i11}, λ'_{i12}, λ'_{i21} , λ'_{i22}, $i = 1, 2, 3$) squared times the branching ratio to dijets of the resonant slepton, for a given resonant slepton mass $\widetilde{m}$. The limits were derived (a) from the ATLAS and (b) from the CMS searches for dijet resonances. In the case of an intermediate third generation slepton ($i = 3$), the limit has to be multiplied by $\cos^2\theta_\tau$ to account for possible mixing in the stau sector. The strictest limits were obtained from the CMS searches. Assuming $BR(\tilde{e}_i, /\tilde{\nu}_i \to jj) \approx 100\%$ the upper bounds obtained are

$$\lambda'_{i11} \leq 0.03 \ (0.05) \ , \tag{4.121}$$

$$\lambda'_{i22} \leq 0.18 \ (0.37) \ , \tag{4.122}$$

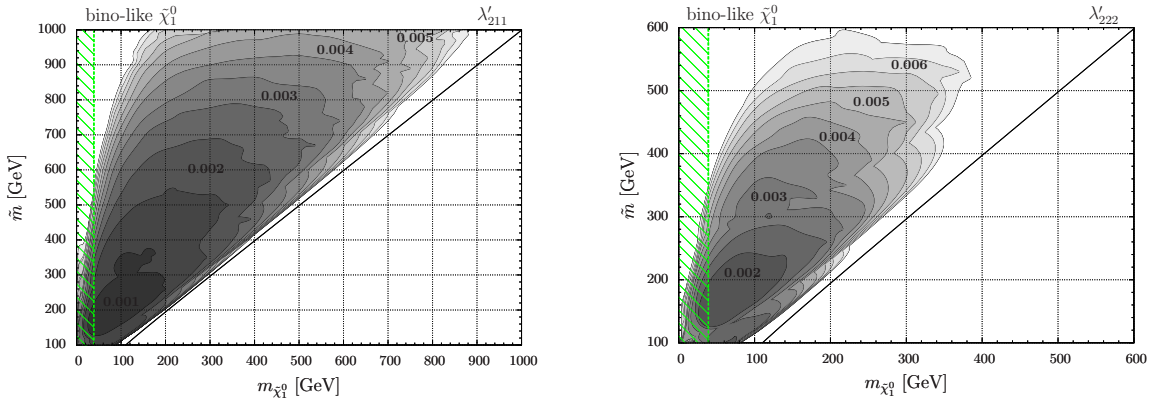

(a) (b)

Figure 4.11: Upper limits on the couplings (a) λ'_{211} and (b) λ'_{222} derived from the ATLAS search for anomalous production of prompt like-sign muon pairs assuming a bino-like neutralino. Both figures are taken from [199].

for a slepton mass $\widetilde{m} = 1000$ (1500) GeV.

Figure 4.11 shows the upper limits on the couplings (a) λ'_{211} and (b) λ'_{222} derived from the ATLAS search for anomalous production of prompt like-sign muon pairs in models with a bino-like neutralino. The authors of [199] assumed resonant production of a smuon $\tilde{\mu}$ with a following decay into the lightest neutralino and muon. The neutralino can then decay to a muon with the same charge. The bounds are presented as contours in the $(m_{\chi_1^0}, \widetilde{m})$ mass plane, where $\widetilde{m}$ is the smuon mass. The green striped region indicates the LEP lower mass limit on the lightest neutralino $m_{\chi_1^0} \geq 39$ GeV. The derived upper bounds on λ' range from 0.001 (dark) to 0.0065 (bright) and are displayed in steps of 0.0005 in grayscale. Since the single slepton production cross section decreases with the slepton mass, the bounds become weaker for heavier smuons. Also due to the insensitivity of the like-sign dimuon search in the regions of low neutralino mass and low mass difference between the smuon and neutralino, upper bounds on λ' could not be obtained in these regions.

We have chosen to show the upper limits on λ'_{211} and λ'_{222} since these couplings were the two extreme cases in the study under consideration. The most stringent limits were obtained on λ'_{211} due to the large cross section. For a roughly elliptic region with $m_{\chi_1^0} \sim \widetilde{m} - 100$ GeV and $\widetilde{m} \sim (150 - 300)$ GeV they obtained

$$\lambda'_{211} \leq 0.001. \tag{4.123}$$

The weakest bounds were set on λ'_{222}, ranging from 0.002 for $(m_{\chi_1^0}, \widetilde{m}) \sim (100, 200)$ GeV to 0.0065 for smuon masses $\widetilde{m} \leq 550$ GeV.

It is important to note that the presented analysis has improved the existing bounds. For instance, the bound on λ'_{211} for a slepton mass of 300 (400) GeV and neutralino mass of 150 (200) GeV was improved from the D0 result at the Tevatron $\lambda'_{211} \leq 0.04$ (0.08) to $\lambda'_{211} \leq 0.001$ (0.0015). Figure 4.2 summarizes the recent bounds on R-parity violating couplings from direct searches.

Coupling	Bound	Condition	Origin
λ'_{11k}	5×10^{-3}	$\tilde{q}$	HERA resonant single squark
λ'_{211}	1×10^{-3}	χ_1^0 $m_{\tilde{\mu}} = 200$ GeV	ATLAS like-sign muon (D.S.)
λ'_{222}	2×10^{-3}	χ_1^0 $m_{\tilde{\mu}} = 200$ GeV	ATLAS like-sign muon (D.S.)
λ'_{311}	2.5×10^{-3}	$\lambda_{312} = 0.07$	ATLAS resonant single slepton
λ'_{i11}	0.03	$m_{\tilde{l}} = 1$ TeV	CMS dijet resonance (D.S.)
λ'_{i22}	0.18	$m_{\tilde{l}} = 1$ TeV	CMS dijet resonance (D.S.)
ζ	6.9×10^{-8}	χ_1^{0-1} $\sigma \geq 12$ pb	ATLAS secondary vertex

Table 4.2: Bounds on the R-parity violating couplings from direct searches. The abbreviations in the last column refer to the collaboration and search strategy mentioned in the text. The indices i, j, k run over the three generations. The dependence on the (super)particle mass is noted as p^q, which stands for $\left(\frac{m_p}{100\,\mathrm{GeV}}\right)^q$, where m_p is the mass of the particle p if not stated otherwise. (D.S.) refers to the independent interpretation of the LHC results in [199].

4.3.4 Searches for decaying Dark Matter

The indirect detection of dark matter is an active research topic and we refer the reader to the recent work by Grefe [72] for an extensive discussion of prospects of indirect detection of gravitino dark matter. In this section we shortly summarize the results needed for the present work. The obtained limits are given as bounds on the gravitino lifetime vs. the gravitino mass. The interpretation of these limits in terms of the R-parity breaking parameters is model dependent, since the gravitino lifetime depends on the gaugino mass parameters M_1 and M_2. We will present such interpretations in the following section. The R-parity violating gravitino decays will lead to the production of intermediate SM particles that eventually hadronize or decay further into a set of stable particles: electrons, protons, deuterons, neutrinos and photons. These secondary particles propagate through the intergalactic medium and can be observed in the fluxes of cosmic rays by ground-based and spaceborne experiments. While charged cosmic rays are affected by magnetic fields, photons and neutrinos propagate on straight paths.

Let us begin with the lower limits on the gravitino lifetime derived from charged cosmic rays. They are obtained from the requirement that the contribution of the gravitino signal to the flux stays below the error bars of the measurements. We refer the reader to Ref. [72] and references therein for a detailed discussion. Figure 4.12 shows the bounds obtained from the PAMELA measurement of the positron fraction [200], the measurements of the total electron + positron flux by Fermi LAT [201] and H.E.S.S. [202, 203], and the PAMELA measurement of the antiproton flux [204].The best bounds are obtained from antimatter particles, since it is usually assumed that the only astrophysical process contributing to the creation of antimatter is spallation involving high energetic cosmic rays impinging on the interstellar medium. The best limits are obtained from antiprotons, due to the famous excess above the astrophysical background in the PAMELA measurement of the positron fraction. A gravitino lifetime of the order of 10^{26} seconds could explain the rise of the positron fraction in the data. However, this possibility is ruled out by the constraints from the antiproton channel. Figure 4.12 shows, additionally, an estimate of the sensitivity of the forthcoming antideuteron experiments to the gravitino parameter space. The experiments which were taken into account are: The Gaseous Antiparticle Spectrometer (GAPS) [205], and the recently launched AMS-02 experiment on

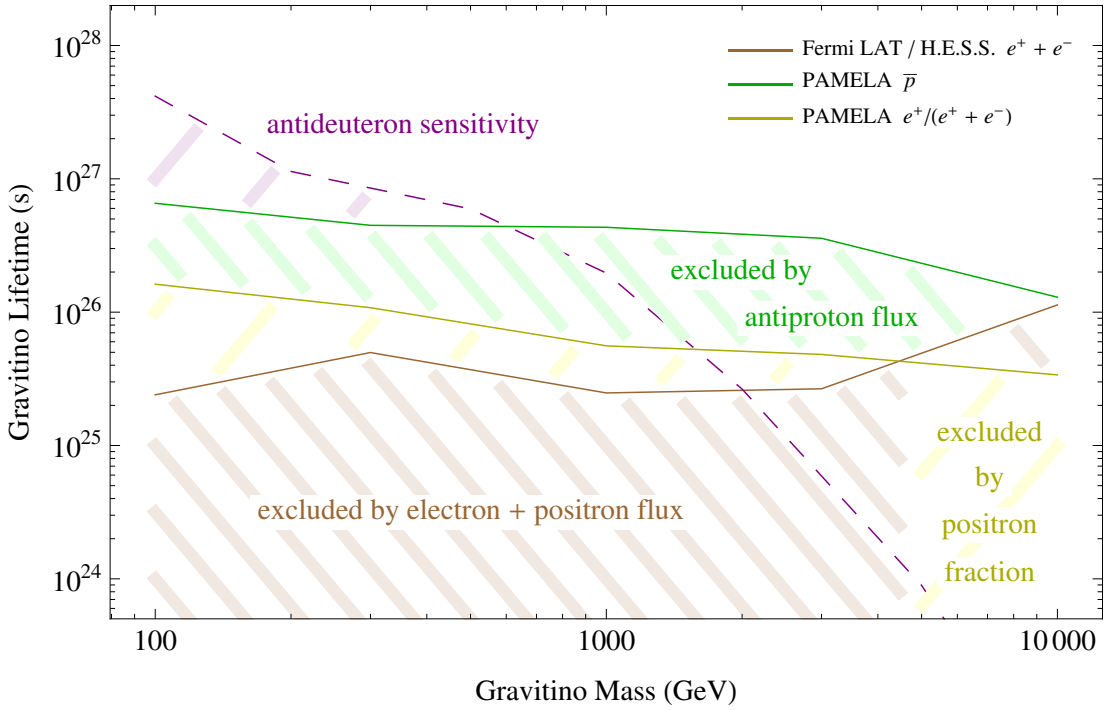

Figure 4.12: Bounds on the gravitino lifetime from observations of charged cosmic rays and sensitivity of forthcoming experiments. The figure is taken from [72].

the International Space Station [206].

The most important limits on the gravitino lifetime can be obtained from the photon (gamma-ray) signal which contains spectral and directional information [72]. Decaying gravitinos will produce a diffuse flux from all directions with only mild angular dependence contributing to the isotropic diffuse gamma-ray background This background is a diffuse flux of high-energetic photons that is thought to have its origin in unresolved astrophysical sources. Demanding that the gravitino decays do not produce an excess of photons incompatible with the observations one can constrain the gravitino lifetime. Additionally, it is possible to search for a monochromatic signal in the photon spectrum. Such signal is an unambiguous signature for non-astrophysical processes creating photons, since gamma rays of astrophysical origin are expected to have a power-law spectrum. The observation of such a gamma-ray line would, thus, be of paramount interest for the understanding of dark matter in the Universe. So far no gamma-ray lines have been observed[2] and limits on the partial lifetime of gravitino dark matter decaying via a two-body decay into at least one photon have been derived.

Figure 4.13 shows the results of the conservative lifetime estimate from the diffuse flux and the photon line searches. The data on isotropic diffuse gamma-ray flux was taken from the observations of Fermi-LAT [208], the bounds from photon-lines were obtained also by the Fermi-LAT collaboration [209] shown in black, and independently in a larger energy range by Vertongen and Weniger [210] from the available Fermi-LAT data. The sharp fall-off of the bound in the region where the gravitino mass becomes compatible with the W boson mass

[2] A recent independent analysis of the Fermi-LAT data [207] claims to have found an evidence for a gamma ray line at 130 GeV with a significance of 3.3σ.

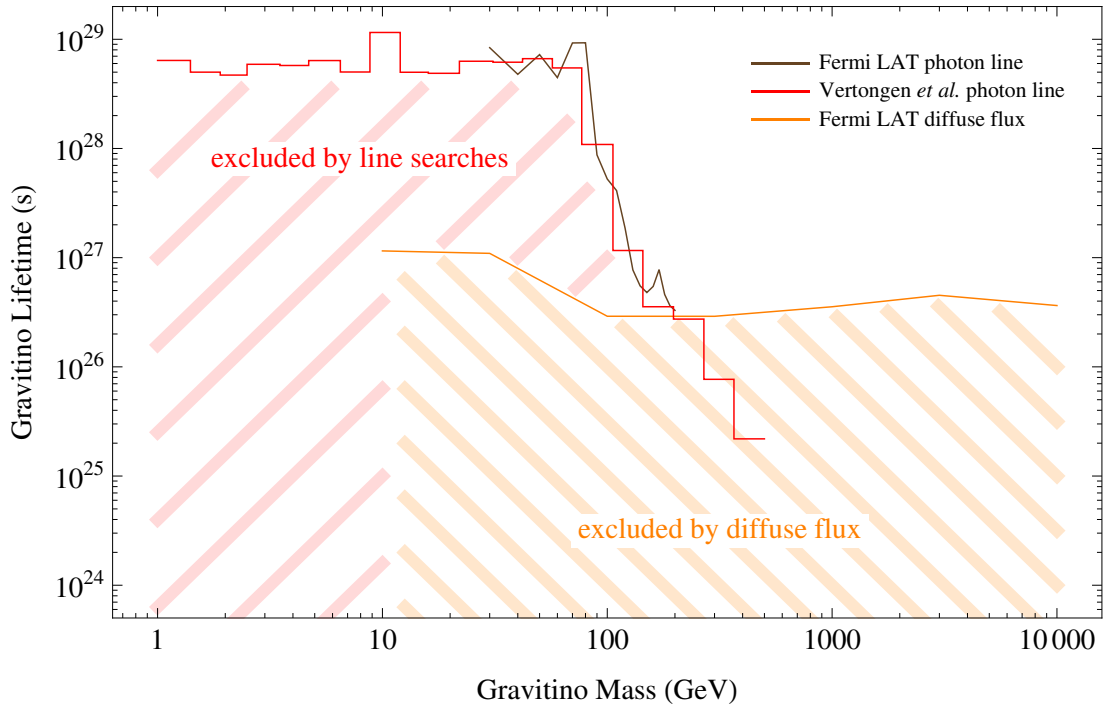

Figure 4.13: Bounds on the gravitino lifetime from observations of the diffuse extragalactic gamma-ray background and from photon line searches. The figure is taken from [72].

is caused by the drop of the branching ration of gravitino into photon and neutrino after the decay into the W boson becomes available, cf. Section 4.2.1. Thus, we obtain the following limits on the gravitino lifetime:

$$\tau_{3/2} \gtrsim 5 \times 10^{28}\ s\ ,\ m_{3/2} \leq 80\ \text{GeV}\ , \tag{4.124}$$

$$\tau_{3/2} \gtrsim 3 \times 10^{26}\ s\ ,\ m_{3/2} > 100\ \text{GeV}\ . \tag{4.125}$$

We refer the reader to the reference [72] for more details on the calculation.

Summing up, we conclude that searches for gamma-ray lines provide the best limit on the gravitino lifetime for light gravitinos, while bounds from charged cosmic rays become more important for gravitino masses above 100 GeV. In that region the lifetime should be larger than 6×10^{26} seconds.

Assuming a bino-like neutralino NLSP $M_2 \simeq 2M_1 \simeq 2m_{\chi_1^0}$, we can translate the limit on the gravitino lifetime into limit on the R-parity breaking parameter ζ,

$$\zeta \leq 2 \times 10^{-9}\ ,\ m_{3/2} = 60\ \text{GeV}\ ,\ m_{\chi_1^0} = 203\ \text{GeV}\ , \tag{4.126}$$

$$\zeta \leq 1.4 \times 10^{-8}\ ,\ m_{3/2} = 10\ \text{GeV}\ ,\ m_{\chi_1^0} = 100\ \text{GeV}\ , \tag{4.127}$$

where the parameters where chosen such as to obtain a conservative limit, see next section for details and limits on other parameter regions.

4.3.5 Summary

We have to conclude that the region of the R-parity violating parameters set by cosmology and considered in the present work has been tested so far only by searches for decaying dark matter. The best indirect bound was obtained on the coupling ζ, $\zeta \leq 10^{-6}$, from the requirement that the tree-level neutrino mass generated by R-parity violation does not exceed the experimental limits. However, this bound coincides with the cosmological constraints. The most promising study for the detection of R-parity violation at the LHC seems to us the search for secondary vertices [211]. It is desirable to repeat the search with more data looking for secondary vertices farther away from the primary interaction point. So far this study could only set limit on ζ, $\zeta \lesssim 6.9 \times 10^{-8}$ for very light squarks and gluino. Furthermore, it is essential to see the reinterpretation of the usual searches for R-parity conserving SUSY in bilinear R-parity breaking scenarios without fitting the scenario to the neutrino data, since is unclear how the bounds on gluino and squark masses would change. Additionally, it is important to understand the limitation on the obtained bounds coming from the neutralino decay length. In the next section we will explore the implications of the searches for decaying gravitino dark matter for LHC phenomenology.

4.4 NLSP Decays at the LHC

We are now ready to evaluate the implications of the Fermi-LAT data and cosmological constraints for signatures of decaying dark matter at the LHC. We shall first discuss the parameter ranges for gravitino and neutralino masses which are consistent with electroweak precision tests, gravitino dark matter as well as leptogenesis, and then analyze the implications for a neutralino and a $\tilde{\tau}$-NLSP, respectively.

We will consider two SUSY scenarios with gravitino dark matter:

- Hybrid gauge-gravity mediation, cf. Section 2.4.2, leading to a higgsino-like neutralino NLSP, and
- The CMSSM (mSUGRA), cf. Section 2.4.1.

In case of the CMSSM we will, furthermore, consider two typical boundary conditions for the supersymmetry breaking parameters at the grand unification scale,

$$\text{(A)} \quad m_0 = m_{1/2}, \quad A_0 = 0, \quad \tan\beta = 10 \ , \tag{4.128}$$

with equal universal scalar and gaugino masses, m_0 and $m_{1/2}$, respectively; in this case a bino-like neutralino is the NLSP. The second boundary condition corresponds to no-scale models or gaugino mediation,

$$\text{(B)} \quad m_0 = 0, \quad m_{1/2}, \quad A_0 = 0, \quad \tan\beta = 10 \ , \tag{4.129}$$

which yields the right-handed stau ($\tilde{\tau}_R \equiv \tilde{\bar{\tau}}^\dagger$) as the NLSP. In both cases, the trilinear scalar coupling A_0 is put to zero for simplicity. Choosing $\tan\beta = 10$ as a representative value of Higgs vacuum expectation values, only the gaugino mass parameter $m_{1/2}$ remains as an independent variable. For both boundary conditions (4.128) and (4.129), the gaugino masses at the electroweak scale satisfy the familiar relations

$$\frac{M_3}{M_1} \simeq 6.0 \ , \quad \frac{M_2}{M_1} \simeq 1.9 \ . \tag{4.130}$$

In case of hybrid gauge-gravity mediation we will consider a particular model (the (17,23,9) model [75]) giving rise to a Higgs mass close to the tentative LHC result.

Let us first discuss the bounds on gravitino and NLSP masses in the CMSSM models. Electroweak precision tests (EWPT) yield important lower bounds on the superparticle mass spectrum [120]. In case of scenario (A) and ignoring the latest LHC hints, the universal gaugino mass $m_{1/2}$ is required to be high enough in order for the Higgs mass to fulfill the recent LHC lower bound $m_h > 115.5$ GeV [10]. This implies the lower limit $m_{\chi_1^0} > 190$ GeV. This limit was obtained by means of `SOFTSUSY` [110]. However, allowing large negative A_0 or scalar masses much larger than $m_{1/2}$ at the GUT scale would weaken this limit, and we will take $m_{\chi_1^0} > 100$ GeV as a lower bound for the neutralino mass subsequently. In the stau NLSP case, the lower bound comes from the absence of pair production of heavy charged particles at LEP and reads $m_{\tilde{\tau}_1} > 100$ GeV [4].

Requiring successful thermal leptogenesis and assuming a typical effective neutrino mass $\widetilde{m}_1 = 10^{-3}$ eV[3], we obtain a minimal reheating temperature of $T_R \sim 10^9$ GeV [49]. Using eq. (2.110) together with a lower bound on the gluino mass $m_g > 1.2$ TeV from the LHC [42] and demanding the observed dark matter density, we obtain a lower bound for the gravitino mass $m_{3/2} > 60$ GeV. Nota bene that the LHC bound was obtained assuming R-parity conservation. This bound is weakened if one allows for R-parity violation, due to changes in the distribution of missing transverse energy.

In addition to the lower limits, NLSP mass upper limits follow from the requirement that the gravitino does not overclose the Universe. Indeed by rewriting eq. (2.110) one obtains the constraint

$$m_{\rm NLSP} \simeq 310 \text{ GeV} \left(\frac{\xi}{0.2}\right) \left(\frac{m_{3/2}}{100 \text{ GeV}}\right)^{\frac{1}{2}} \left(\frac{10^9 \text{ GeV}}{T_R}\right)^{\frac{1}{2}} , \tag{4.131}$$

where $\xi = m_{\rm NLSP}/m_g$ is implicitly fixed by the supersymmetry breaking boundary conditions [120]. For each gravitino mass and reheating temperature, eq. (4.131) then gives the NLSP mass for which the observed dark matter density is obtained. The absolute bound on the NLSP mass can be obtained by requiring $m_{\rm NLSP} = m_{3/2}$. In case of scenario (A) eq. (4.131) implies $m_{\chi_1^0} < 690$ GeV for $\xi = 1/5.9$ and is essentially independent of m_0 and $\tan\beta$. For the stau NLSP, $\tan\beta = 10$ yields $\xi = 1/6.2$, which consequently leads to the more stringent bound $m_{\tilde{\tau}_1} < 615$ GeV. Note that there is a strong dependence on $\tan\beta$ in that case [120], and that ξ decreases with increasing $\tan\beta$.

In the case of a higgsino NLSP, the neutralino mass is given by $m_{\chi_1^0} = 205$ GeV, while the gluino mass is 3800 GeV [75]. Computing the gravitino mass with eq. (2.110) we obtain a value larger than the neutralino mass. Therefore, thermal leptogenesis is not viable in this case. Instead, we will assume that the hot phase of the universe was created in the decay of the false vacuum of unbroken $B - L$ [212, 213]. Since right-handed neutrinos are created from inflaton decays, this scenario allows for gravitino dark matter, leptogenesis and correct neutrino mass parameters while requiring lower reheating temperatures compared to the thermal leptogenesis case. The lower bound on the gravitino mass obtained in [213] for $m_g = 1$ TeV is 10 GeV. It is possible to scale this bound for other gluino masses using [212]

$$m_{3/2} = m_{3/2}^0 \left(\frac{m_g}{1000 \text{ GeV}}\right)^2 , \tag{4.132}$$

[3]Note that we assumed a neutrino mass scale of 0.01 eV for our model of spontaneous R-parity breaking; using $m_\nu = 10^{-3}$ one would slightly increase the scale of R-parity breaking without changes to the couplings due to the unknown mechanism of SUSY breaking.

where $m_{3/2}^0$ is the original mass, and we obtain $m_{3/2} > 144$ GeV for $m_g = 3800$ GeV. Therefore, we can have a higgsino-like neutralino NLSP and gravitino dark matter. Note that it is an interesting task to intertwine the breaking of R-parity with the begin of the hot phase, since both models are based on the breaking of $B - L$.

Summing up, we obtain following bounds on the NLSP and gravitino masses:

$$\text{CMSSM (A)} \quad 60 \text{ GeV} < m_{3/2} < 690 \text{ GeV} \ , \ 100 \text{ GeV} < m_{\chi_1^0} < 690 \text{ GeV} \ , \tag{4.133}$$

$$\text{CMSSM (B)} \quad 60 \text{ GeV} < m_{3/2} < 615 \text{ GeV} \ , \ 100 \text{ GeV} < m_{\tilde{\tau}_1} < 615 \text{ GeV} \ , \tag{4.134}$$

$$\text{Hybrid} \quad 144 \text{ GeV} < m_{3/2} < 205 \text{ GeV} \ , \ m_{\chi_1^0} = 205 \text{ GeV} \ . \tag{4.135}$$

Using these bounds as well as the constraints on the R-parity breaking parameters, we can make predictions for the NLSP decays at the LHC. In the case of the neutralino NLSP we have to distinguish the bino-like and the higgsino-like case.

4.4.1 Bino-like Neutralino

First, we have to translate the bound on the gravitino lifetime into the bound on R-parity violation. On the one hand, since according to the gravitino dark matter constraint the largest allowed bino mass scales like $M_1^{\max} \propto m_{3/2}^{1/2}$, the largest lifetime (4.110), and therefore the most conservative bound on ζ, is obtained for the smallest value of $m_{3/2}$. On the other hand, the limit on the gravitino lifetime becomes more severe for lighter gravitinos. Assuming a gravitino mass of 100 GeV, the bound on the lifetime from the Fermi-LAT data becomes $\tau_{3/2}(\gamma\nu) \gtrsim 1 \times 10^{27}$ s. Therefore, we obtain

$$\zeta \lesssim 9 \times 10^{-9} \ , \tag{4.136}$$

for a gravitino mass of 100 GeV. However, if one would ignore the LHC bound on gluinos or assume non-thermal leptogenesis [212, 213], and therefore allow for gravitino masses around 10 GeV, the bound on ζ would change to

$$\zeta \lesssim 1.4 \times 10^{-8} \ . \tag{4.137}$$

We will use the LHC bound on gluinos in the discussion of this section, but allow for larger values of ζ in the LHC study presented in the following chapter.

Furthermore, the observation of a photon line corresponding to a gravitino lifetime close to the present bound would determine the parameter ζ as

$$\zeta_{\text{obs}} = 10^{-9} \left(\frac{5 \times 10^{28}\text{s}}{\tau_{3/2}(\gamma\nu)} \right)^{1/2} \left(\frac{M_1}{200 \text{ GeV}} \right) \left(\frac{m_{3/2}}{100 \text{ GeV}} \right)^{-3/2} \ . \tag{4.138}$$

Note the strong dependence of ζ_{obs} on the gravitino mass. In (4.138) we have normalized these masses to the central values suggested by thermal leptogenesis, electroweak precision tests and gravitino dark matter [120].

Let us now examine the neutralino decays. The neutralino decay length is given by eq. (4.84). Figure 4.14 shows phase space suppression factors and neutralino branching ratios as a function of neutralino mass. We assumed a very light Higgs beyond the present LHC bound, in order to investigate the impact of this channel on the decay length. Furthermore,

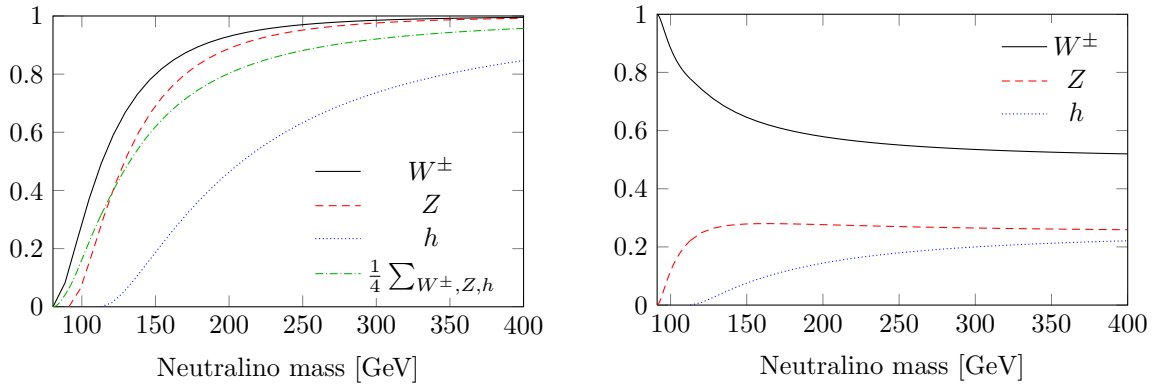

Figure 4.14: Phase space suppression factors (a) and branching ratios (b) of a bino-like neutralino as functions of the neutralino mass. The decays into W boson, Z boson, and Higgs are shown in black, red, and blue, respectively. A Higgs mass of 113 GeV and the validity of the Higgs decoupling limit are assumed. A total phase space suppression factor is shown in green.

we assumed the validity of the Higgs decoupling limit and set $\zeta_1 = \zeta_2 = \zeta_3$. For large NLSP masses, $m_{\chi_1^0} \gg m_h$, one has

$$BR\left(\chi_1^0 \to W^\pm e^\mp\right) \simeq 2\ BR\left(\chi_1^0 \to Z\nu\right) \simeq 2\ BR\left(\chi_1^0 \to h\nu\right)\ , \tag{4.139}$$

whereas in the region $m_{\chi_1^0} \simeq 100$ GeV

$$BR\left(\chi_1^0 \to W^\pm e^\mp\right) \simeq 5\ BR\left(\chi_1^0 \to Z\nu\right)\ , \tag{4.140}$$

and the decay into Higgs is not present. The Higgs channel becomes important only for heavy neutralinos and then contributes nearly with the same strength as the Z channel. We will return to this topic in the following discussion.

Note that both the gravitino and the neutralino NLSP lifetimes are functions just of ζ and the masses, without any further parameters. This direct connection between the gravitino and NLSP lifetimes is the basis of the LHC study in the next chapter. Thus, using the expressions for the neutralino decay width (4.84) and the gravitino decay length (4.53), we can express the neutralino lifetime directly in terms of the gravitino lifetime:

$$\tau_{\chi_1^0} = \frac{1}{8\sqrt{2}} \frac{c_w^2}{G_F} \frac{(M_2 - M_1)^2}{M_2^2} \frac{m_{3/2}^3}{M_P^2 m_{\chi_1^0}^2} \tau_{3/2}(\gamma\nu) \tag{4.141}$$

$$\left(\frac{1}{2} f_W(m_{\chi_1^0}) + \frac{1}{4} f_Z(m_{\chi_1^0}) + \frac{1}{4} f_h(m_{\chi_1^0})\right)^{-1} \left(1 + \mathcal{O}\left(s_{2\beta} \frac{m_Z^2}{\mu^2}\right)\right)\ . \tag{4.142}$$

Additionally, we are able to make a prediction for the minimal neutralino decay length at the

LHC:

$$c\tau_{\chi_1^0} \gtrsim 4 \text{ m } \left(\frac{m_{\chi_1^0}}{260 \text{ GeV}}\right)^{-3} \left(\frac{m_{3/2}}{100 \text{ GeV}}\right)^{3} \left(\frac{\tau_{3/2}(\gamma\nu)}{1\times 10^{27} \text{ s}}\right) \times \left(\frac{1}{2} f_W(m_{\chi_1^0}) + \frac{1}{4} f_Z(m_{\chi_1^0}) + \frac{1}{4} f_h(m_{\chi_1^0})\right)^{-1} \left(1 + \mathcal{O}\left(s_{2\beta}\frac{m_Z^2}{\mu^2}\right)\right) , \quad (4.143)$$

where we have used $m_{\chi_1^0} \simeq M_1$, $M_2 = 1.9 M_1$. In eqs. (4.141) and (4.143) the corrections to the leading order expressions are less than 10%. Evaluating the phase space factors, assuming a 115 GeV Higgs, we obtain $c\tau_{\chi_1^0} \gtrsim 4.6$ m.

The neutralino lifetime depends, in general, strongly on the neutralino and gravitino masses. However, the obtained bound is robust, since assuming a gravitino of 10 GeV, a neutralino of 100 GeV and taking the gravitino lifetime bound of 5×10^{28} from Fermi-LAT, we obtain a decay length of 21 m, due to phase space suppression factors.

In the last step, we evaluate the impact of the Higgs channel on the decay length. Since the minimal decay length is obtained for a neutralino mass of 260 GeV, it is not changed by taking the Higgs to have a mass of 125 GeV. Taking the Higgs channel not into account one would predict a minimal decay length of 5.6 meters. The maximal error on the decay length can be read off directly from the phase space suppression factors, cf. Fig. 4.14a. In the limit of a very heavy neutralino all functions $f_{W/Z/h}$ tend to 1. Thus, not taking the Higgs into account one overestimates the decay length by 33%.

In the next chapter we will be using the neutralino decays into the Z boson and neutrino for a phenomenological study and neglect the decay into the Higgs. Therefore, we will overestimate the neutralino branching ratio into Z and neutrino. In the heavy neutralino limit the error also amounts to 33%. However, the maximal neutralino mass considered by us will be around 300 GeV, in which case the error is only $\approx 25\%$.

We conclude that, given the current bounds on the gravitino lifetime, a bino-like neutralino NLSP may still decay into a gauge boson and a lepton inside the detector, yielding a spectacular signature. The sensitivity of the LHC experiments to the R-parity breaking parameter ζ is investigated in detail for various gluino and squark masses in the next chapter.

4.4.2 Higgsino-like Neutralino

In the case of a higgsino-like neutralino the bound on ζ is independent of the neutralino mass, which is given by μ but depends on the masses of the heavier bino wino-like neutralinos, which are 1800 GeV and 3800 GeV, respectively. The minimal gravitino mass is 144 GeV, and, therefore, the bound on the lifetime is given by 3×10^{26} s and we obtain

$$\zeta \lesssim 5.6 \times 10^{-8} . \quad (4.144)$$

Inserting this value of ζ in eq. (4.88) and taking into account $\tan\beta = 52$ yields the minimal neutralino decay length

$$c\tau_{\chi_1^0} \gtrsim 24 \text{ m}. \quad (4.145)$$

Note that this decay length is one order of magnitude larger than the minimal decay length of the bino-like neutralino.

Figure 4.15 shows the branching ratios of the higgsino-like neutralino as functions of the neutralino mass. Here, for illustration, we have varied the higgsino mass between 90 and 400

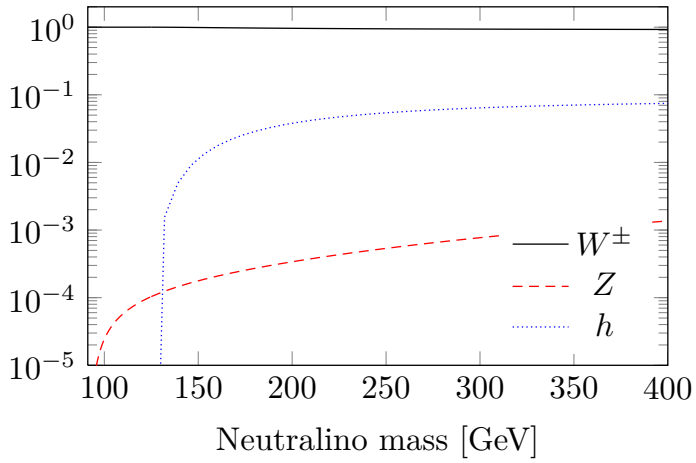

Figure 4.15: Higgsino-like neutralino branching ratios as functions of the neutralino mass.

GeV, while keeping the other parameters fixed. The neutralino decays to $\approx 100\%$ into the W boson and a charged lepton. The neutralino decays will take place everywhere in the detector, distorting, like in the bino-like neutralino case, the distribution of missing transverse energy.

The expression for the neutralino decay length can be simplified, using the fact that decays into the Z boson and Higgs are negligible. Expressing the neutralino lifetime in terms of the gravitino lifetime using $m_{\chi_1^0} \simeq \mu$, $\tan\beta \simeq 52$, and making an expansion in μ/M_1 we obtain

$$\tau_{\chi_1^0} \simeq \frac{1}{2\sqrt{2}} \frac{\tau_{3/2}}{G_F M_P^2} \frac{m_{3/2}^3}{m_{\chi_1^0}} \frac{c_w^2 s_w^2}{m_Z^2} f_W(m_{\chi_1^0})^{-1} \left(\frac{M_2 - M_1}{3M_1 c_w^2 + M_2 s_w^2} \right)^2 \left(1 + \mathcal{O}\left(\frac{\mu}{M_1} \right) \right) . \quad (4.146)$$

The approximate formula gives 26 m for the minimal decay length in excellent agreement with the exact result. Moreover, assuming that the ratio between M_2 and M_1 is fixed, the unknown high scale vanishes from the result. Taking, for example, $M_2 \simeq 2M_1$ the last bracket becomes close to 1/8. Using this approximation we obtain a decay length of 20 m, within 16% of the exact result.

Summing up, we expect the higgsino-like neutralino to decay within the range of the LHC detectors. Under the assumption of gauge coupling unification, the higgsino-like neutralino decay length can be deduced also directly from the gravitino lifetime. Additionally, since in this model all squarks and the gluino are very heavy and, therefore, most neutralinos will be produced directly via Drell-Yan processes, R-parity violation alleviates the detection at the LHC. We will see in the next chapter that otherwise the detection of higgsino-like neutralinos may become impossible.

4.4.3 Stau

As stated in Section 4.2.3 the R-parity violating decays of a $\tilde{\tau}_1$-NLSP strongly depend on the flavor structure and the supersymmetry breaking parameters. Since the decays are governed by a priori independent parameters ϵ, ϵ', ϵ'', we cannot connect them with gravitino decays. Therefore, we estimate the size of R-parity breaking parameters directly from our model of R-parity breaking, cf. Section 3.5. From Eqs. (3.47), (3.64) and $\eta \simeq 0.06$, one obtains for the

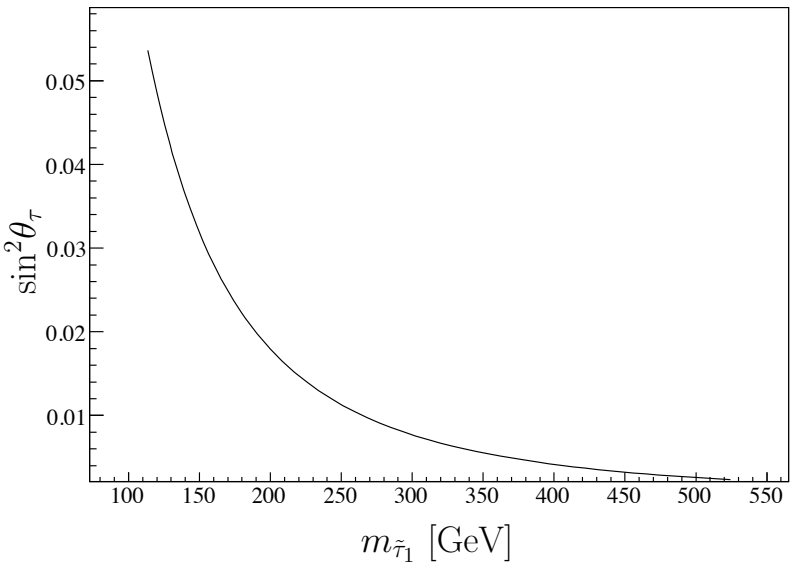

Figure 4.16: The $\tilde{\tau}$-mixing angle $\sin^2(\theta_\tau)$ as a function of the lightest $\tilde{\tau}$-mass $m_{\tilde{\tau}_1}$.

R-parity breaking parameter

$$\epsilon \simeq \zeta \simeq \eta\Theta \simeq 6 \times 10^{-8} \ , \tag{4.147}$$

which is consistent with the present upper bound (4.137).

The dependence of the mixing angle θ_τ on $m_{\tilde{\tau}_1}$ is shown in Fig. 4.16 for the boundary condition (4.129). For masses below the top-bottom threshold only leptonic $\tilde{\tau}_1$-decays are possible. When the decay into top-bottom pairs becomes kinematically allowed, $\sin^2\theta_\tau$ is small. However, the suppression by a small mixing angle is compensated by the larger Yukawa coupling compared to the leptonic decay mode. This is a direct consequence of the couplings $\hat{\lambda}'$ which were not taken into account in previous analyses.

Due to the competition between the mixing angle suppression and the hierarchical Yukawa couplings, the top-bottom threshold is clearly visible in the $\tilde{\tau}_1$-decay length as well as the branching ratios into leptons and heavy quarks. This is illustrated in Figs. 4.17 and 4.18, respectively, where these observables are plotted as functions of $m_{\tilde{\tau}_1}$. Representative values of the $\tilde{\tau}_1$-decay lengths below and above the top-bottom threshold are

$$m_{\tilde{\tau}_1} < m_t + m_b : \quad c\tau_{\tilde{\tau}_1}|_{150\ \mathrm{GeV}} = 1.4\ \mathrm{m} \left(\frac{\epsilon}{5\times 10^{-8}}\right)^{-2} \ , \tag{4.148}$$

$$m_{\tilde{\tau}_1} > m_t + m_b : \quad c\tau_{\tilde{\tau}_1}|_{250\ \mathrm{GeV}} = 0.6\ \mathrm{m} \left(\frac{\epsilon}{5\times 10^{-8}}\right)^{-2} \ . \tag{4.149}$$

Choosing for ϵ the representative value (4.138) from gravitino decay, $\epsilon = \zeta_{\mathrm{obs}} = 10^{-9}$, one obtains $c\tau_{\tilde{\tau}_1} = 4$ km(1 km) for $m_{\tilde{\tau}_1} = 150$ GeV(250 GeV). It is remarkable that such lifetimes can be measured at the LHC [71, 214, 215].

Is it possible to avoid the severe constraint from gravitino decays on the $\tilde{\tau}_1$-decay length? In principle, both observables are independent, and the unknown constants in the definition of

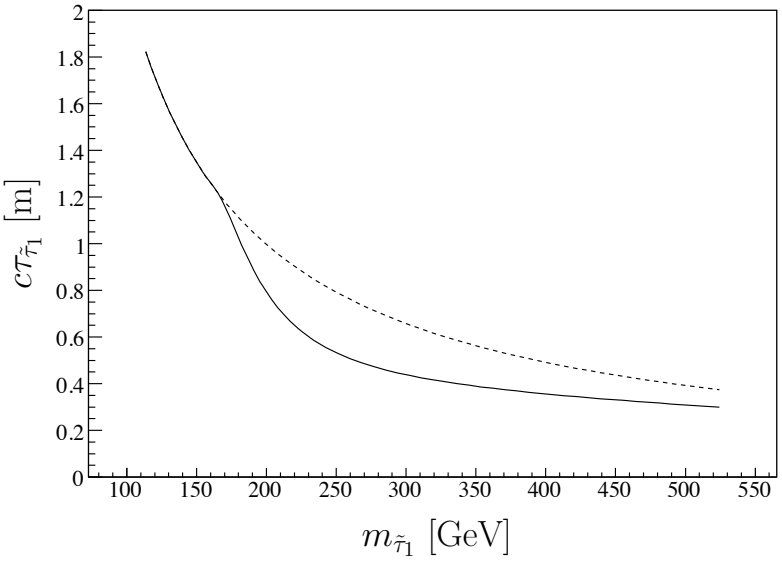

Figure 4.17: The $\tilde{\tau}_1$ decay length as a function of $m_{\tilde{\tau}_1}$. Above the top-bottom threshold hadronic decays decrease the $\tilde{\tau}_1$-lifetime.

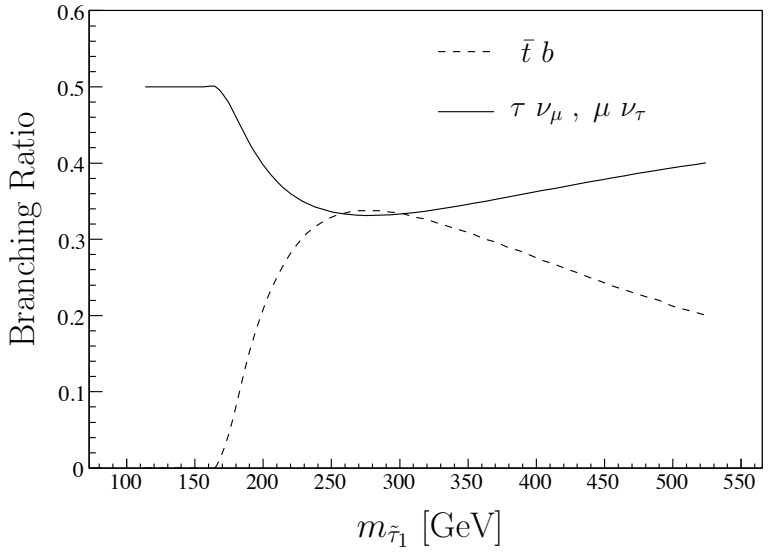

Figure 4.18: $\tilde{\tau}_1$-branching ratios as functions of $m_{\tilde{\tau}_1}$. The dependence on the $\tilde{\tau}_1$-mass is determined by the top-bottom threshold and the mass dependence of the $\tilde{\tau}_1$-mixing angle.

ϵ, ϵ' and ϵ'' can be adjusted such that $\zeta = 0$. However, this corresponds to a strong fine-tuning, unrelated to an underlying symmetry. To illustrate this, consider the case where the soft R-parity breaking parameters vanish at the GUT scale, $B_i = m_{id}^2 = 0$, which was discussed in Section 3. In bilinear R-parity breaking, also the R-parity violating Yukawa couplings vanish at the GUT scale. With the one-loop radiative corrections at the electroweak scale (cf. (3.78); $\epsilon_i = \mu_i/\mu$),

$$B_i(\Lambda_{\rm EW}) = \frac{\epsilon_i \mu}{16\pi^2}\left(\frac{6}{5}g'^2 M_1 + 6g^2 M_2\right)\ln\frac{\Lambda_{\rm GUT}}{\Lambda_{\rm EW}} \ , \quad m_{id}^2(\Lambda_{\rm EW}) = 0 \ ,$$

and $M_{1,2} \sim \mu$, one reads off from Eqs. (3.33), (3.40) and (3.41)

$$\epsilon_i', \epsilon_i'' = \mathcal{O}(\epsilon_i) \ . \tag{4.150}$$

Hence, all R-parity breaking parameters are naturally of the same order, unless the fine-tuning also includes radiative corrections between the GUT scale and the electroweak scale.

Even if one accepts the fine-tuning $\zeta = 0$, one still has to satisfy the cosmological bounds on R-parity violating couplings, which yield $\epsilon_i = \mu_i/\mu \lesssim 10^{-6}$ [192]. In the flavor model discussed in Section 3 this corresponds to the choice $a = 20$ in Eq. (3.71). For the smaller $\widetilde{\tau}_1$-mass, which is preferred by electroweak precision tests, one then obtains the lower bound on the decay length

$$c\tau_{\widetilde{\tau}_1}|_{150\ \rm GeV} \gtrsim 4\ \rm mm \ . \tag{4.151}$$

However, let us emphasize again that current constraints from Fermi-LAT on the diffuse gamma-ray spectrum indicate decay lengths several orders of magnitude larger.

4.4.4 Planck Mass Measurement

It has been pointed out in [57] that, in principle, one can determine the Planck mass from the decay properties of a $\tilde{\tau}$-NLSP together with the observation of a photon line in the diffuse gamma-ray flux, which is produced by gravitino decays. This is similar to the proposed microscopic determination of the Planck mass based on decays of very long lived $\tilde{\tau}$-NLSP's in the case of a stable gravitino [66].

From our analysis of NLSP decays in this section it is clear that bino-like neutralino NLSP decays are particularly well suited for a measurement of the Planck mass, which does not require any additional assumptions. Eq. (4.141) implies ($G_F = \sqrt{2}/(4v^2)$),

$$\begin{aligned} M_P =& c_w v \frac{M_2 - M_1}{M_2}\left(\frac{m_{3/2}}{m_{\chi_1^0}}\right)^{3/2}\left(\frac{\tau_{3/2}(\gamma\nu)}{\tau_{\chi_1^0}}\right)^{1/2} \\ & \times\left(2f_W(m_{\chi_1^0}) + f_Z(m_{\chi_1^0}) + f_h(m_{\chi_1^0})\right)^{-1/2}\left(1 + \mathcal{O}\left(s_{2\beta}\frac{m_Z}{\mu}\right)\right) \ . \end{aligned} \tag{4.152}$$

As expected, for gravitino and neutralino masses of the same order of magnitude, the ratio of the two-body lifetimes is determined by the ratio of the electroweak scale and the Planck mass,

$$\frac{\tau_{\chi_1^0}}{\tau_{3/2}(\gamma\nu)} \sim \frac{v^2}{M_P^2} \ . \tag{4.153}$$

Quantitatively, using the relation (4.130) for the gaugino masses, one finally obtains ($v = 174$ GeV),

$$M_P = 3.6 \times 10^{18}\ \text{GeV} \left(\frac{m_{3/2}}{m_{\chi_1^0}}\right)^{3/2} \left(\frac{\tau_{3/2}(\gamma\nu)}{10^{28}\ \text{s}}\right)^{1/2} \left(\frac{\tau_{\chi_1^0}}{10^{-7}\ \text{s}}\right)^{-1/2} \times \left(2f_W(m_{\chi_1^0}) + f_Z(m_{\chi_1^0}) + f_h(m_{\chi_1^0})\right)^{-1/2} \left(1 + \mathcal{O}\left(s_{2\beta}\frac{m_Z}{\mu}\right)\right) \ . \tag{4.154}$$

It is remarkable that the observation of a photon line in the diffuse gamma-ray flux, together with a measurement of the neutralino lifetime at the LHC, can provide a microscopic determination of the Planck mass.

Chapter 5

Hidden Supersymmetry at the LHC

We have seen in Chapter 2 that supersymmetry is the best motivated extension of the Standard Model. It provides a dark matter candidate, solves the hierarchy problem, and brings us closer to the goal of unification of forces. Already in the eighties, the common opinion was that SUSY is just around the corner [216], and yet it still has not been found so far. The search for supersymmetry is one of the main quests of the Large Hadron Collider, and the result of this search will have a profound impact on the field of particle physics. The idea of supersymmetry itself cannot be falsified at the LHC, but if all phenomena stay beyond the reach of any experiment, it not only loses some of its desired features, but also becomes merely a question of mathematics. The upcoming criticisms of the string theory (cf. [217,218]), which needs SUSY, and even of the whole field of cosmology and particle physics (cf. [219]) may be misguided, but will attain more weight in the light of the negative results. Therefore, it seems crucial to investigate all possible occurrences of SUSY models and to go beyond simplified models like CMSSM, since the mechanism of SUSY breaking is still poorly understood.

In the present chapter we will show that possible models motivated by the aim of consistent cosmology have features which impede a fast discovery at the LHC. Furthermore, we will present phenomenological studies how these models could nevertheless be discovered. Taking local supersymmetry seriously, we know that the gravitino must be present in the spectrum and could potentially cause problems, cf. Section 2.5.1. The problems are absent if the gravitino is very heavy, a situation arising in the AMSB models of SUSY breaking. cf. Section 2.4.3. In these models almost all SUSY particles are very heavy, such that the colored states cannot be produced at the LHC. The lightest states, which are produced via electroweak processes, could be higgsino-like making a discovery at the LHC almost impossible. Similar situation can arise in hybrid gauge-gravity mediation models with gravitino dark matter, cf. Section 2.4.2, which need additional moderate entropy production before nucleosynthesis for consistency with early universe cosmology.

Another solution to the NLSP decay problem present in models with gravitino dark matter, is the introduction of a small amount of R-parity violation created in, for example, the breaking of $B - L$, cf. Chapter 3. Even such tiny amount of R-parity violation distorts the usual LHC signatures, especially the distribution of missing transverse energy. We shall investigate the impact of R-parity breaking on the LHC phenomenology in Section 5.2. In this chapter we will use in the text and in tables the usual particle naming convention, where a bar over a particle name denotes the antiparticle, i.e. $\bar{l}$ standing for a generic antilepton etc. .

5.1 Higgsino World

The most characteristic feature of the higgsino world scenario is a large separation between the higgsino masses and the masses of the other superparticles. The particle content is that of the MSSM. Two higgsino-like neutralinos and a higgsino-like chargino are light: Their masses can be arbitrarily close to the direct chargino search bound from LEP, $m_{\chi_1^\pm} \gtrsim 105\,\text{GeV}$. There is also a light Standard Model-like Higgs around 120 GeV. The heavier Higgs bosons, as well as the gaugino-like neutralinos and chargino, gluino, squarks and sleptons, have masses of at least 500 GeV, and possibly ranging up to several TeV in case of hybrid gauge-gravity mediation, while their masses are around 10^4 GeV in the AMSB case, cf. Section 2.4.

This kind of spectrum is naturally compatible with both LHC and LEP search bounds. Concerning the LHC, the absence of any signals for supersymmetry in cascade decays of first-generation squarks and gluinos points to them being rather heavy. On the other hand, evading the new LHC bound on the lightest Higgs mass requires large loop corrections from third-generation soft terms, at least within the MSSM. This points to large third-generation squark masses (bringing with them the inevitable fine-tuning which is present in the remaining parameter regions of the MSSM). Charginos and neutralinos, by contrast, can comfortably have masses between around only 100 – 200 GeV.

The MSSM with light higgsinos and otherwise heavy superparticles has previously been studied e.g. in [220]. Additionally to the AMSB scenario [73] and the hybrid gauge-gravity mediation [74], other models have been constructed which predict precisely this pattern, such as the "lopsided gauge mediation" models of [221, 222].

In this section we are interested in the consequences of such scenario for SUSY searches at the LHC, in case of R-parity conservation. Irrespectively of the dark matter candidate, which is gravitino in the hybrid mediation case and higgsino in the AMSB case, the phenomenology at colliders will be very similar due to otherwise similar spectra and suppressed gravitino couplings. Therefore, we will closely examine the hybrid gauge-gravity mediation scenario while pointing out the possible differences in the AMSB case.

5.1.1 Model Parameters

The precise details of the superparticle spectrum depend on the messenger content of the model, on the exact choice of messenger scale and SUSY breaking scale, and on the assumptions about the gravity-mediated contributions to the soft terms. For our purposes of a first tentative study of collider phenomenology, it is convenient to adopt a simplified parametrization: We fix the gravitino mass to be $m_{3/2} = 100\,\text{GeV}$, and choose a common messenger mass just below the GUT scale, $M_\text{m} = 5 \times 10^{15}\,\text{GeV}$. Then the essential free parameters are the gaugino masses M_1, M_2 and M_3, the Higgs soft mass mixing B_μ, and the higgsino mass μ. At the GUT scale we expect $|B_\mu| \simeq |\mu|^2 \simeq m_{3/2}^2$ and $|M_{1,2,3}| \gg m_{3/2}$. Scalar soft masses are dominated by the gauge-mediated contribution, which is completely fixed after prescribing the gaugino masses. Explicitly, they are given by the standard minimal gauge mediation formula

$$m_\Phi^2 = 2 \left(\frac{g^2}{16\pi^2}\right)^2 \left(\sum_a C_a\, n_a\right) \left|\frac{F}{M_\text{m}}\right|^2 , \tag{5.1}$$

particle	model				
	Spectrum I	Spectrum II	HH50	HH50′	simplified
h_0	116	123	115	117	117
χ_1^0	124	205	206	207	125
$\chi_1^\pm$	129	207	389	395	
χ_2^0	134	206	389	395	
χ_3^0	559	1 788	635	771	
χ_4^0	1 059	3 775	649	778	
$\chi_2^\pm$	1 059	3 775	648	779	
H_0	641	1 115	861	958	
A_0	642	1 120	861	958	
$H^\pm$	648	1 123	865	962	
g	1 063	3 808	1 167	1 167	
$\tilde{t}_1$	665	2 311	860	660	659
$\tilde{b}_1$	797	2 490	1 034	943	
$\tilde{u}_1$	1 155	3 513	1 122	1 130	
$\tilde{d}_1$	1 065	3 370	1 119	1 127	
other squarks	1 070 – 1 500	3 300 – 4 500	1 120 – 1 160	990 – 1 270	
$\tilde{\tau}_1$	509	461	528	520	
other sleptons	790 – 1 160	1 700 – 3 200	530 – 600	530 – 600	

Table 5.1: A light and a heavy spectrum, with a CMSSM point HH50, a CMSSM-like point HH50′ and a simplified model for comparison. The parameters defining these models are listed in Table 5.2. Particle masses are in GeV.

where $a = 1, 2, 3$ labels the Standard Model gauge factors, C_a is the corresponding quadratic Casimir of Φ, the SUSY breaking scale F is

$$F = \sqrt{3}\, m_{3/2}\, M_{\text{Planck}} = (2 \times 10^{10}\,\text{GeV})^2 \ , \tag{5.2}$$

and the effective messenger numbers n_a are obtained by inverting the standard gaugino mass formula

$$M_a = \frac{g^2}{16\pi^2} n_a \frac{F}{M_\text{m}} \ . \tag{5.3}$$

We are neglecting the running of the gauge couplings between M_m and M_GUT, as well as the subdominant gravity-mediated contributions. Trilinear terms are again dominated by gravity mediation; for simplicity we choose them to be universal and set $A_0 = \mu$.

Having thus fixed the MSSM parameters at the messenger scale, we evolve them to the weak scale by means of their renormalization group equations using `SOFTSUSY` [110]. Reproducing the correct value of the Z mass further reduces the number of free parameters by one. In the end, within our simplified ansatz the mass spectrum is entirely determined by the five parameters M_1, M_2, M_3, μ and B_μ at the messenger scale. These are subject to the conditions that electroweak symmetry should be broken with $m_Z = 91\,\text{GeV}$, and that there

model	μ	$\sqrt{B_\mu}$	M_1	M_2	M_3	m_0	$m_0^{(3)}$	A_0	$A_0^{(3)}$	$\tan\beta$
Spectrum I	150	200	1 250	1 250	428					46
Spectrum II	250	250	4 080	4 600	1 800					52
HH50			500	500	500	500	500	0	0	10
HH50′			500	500	500	500	300	0	−1 000	10

Table 5.2: Defining parameters for a light and a heavy spectrum, with a CMSSM point and a CMSSM-like point for comparison. Particle masses are in GeV. In HH50′ third-generation squarks and sleptons were given a universal soft mass $m_0^{(3)}$ and a trilinear A-parameter $A_0^{(3)}$.

should be a separation of mass scales according to

$$\mu \sim \sqrt{B_\mu} \sim m_{3/2} \ll M_1 \sim M_2 \sim M_3 \ . \tag{5.4}$$

Table 5.1 shows two examples for low-energy spectra. Spectrum I has $\mu = 150\,\text{GeV}$, $\sqrt{B_\mu} = 200\,\text{GeV}$, $M_1 = M_2 = 1250\,\text{GeV}$ and $M_3 = 428\,\text{GeV}$; these parameters are chosen such that the model is close to the present LHC exclusion limits. Spectrum II has $\mu = 250\,\text{GeV}$, $\sqrt{B_\mu} = 250\,\text{GeV}$ $M_1 = 4080$ GeV, $M_2 = 4600$ GeV and $M_3 = 1800\,\text{GeV}$, for which the model would be invisible at the early LHC and almost impossible to find even at 14 TeV. Additionally, this spectrum has a Higgs mass close to the tentative LHC hint, and is furthermore very similar to the spectrum $(17, 23, 9)$ from [75], which was used in the previous chapter for the predictions of the higgsino decay length in case of R-parity violation. The numbers in the spectrum name refer to the effective messenger numbers connected to the gaugino mass parameters (eq. 5.3). Note that the spectrum in AMSB case would be even more extreme, neutralinos and charginos being the only particles which could be produced at present and future colliders. Our analysis in this section will be mostly concerned with the phenomenology of Spectrum I at $\sqrt{s} = 7\,\text{TeV}$.

For comparison, we have also included a similar CMSSM benchmark point HH50 and a CMSSM-like benchmark point HH50′. HH50 has $m_0 = m_{1/2} = 500\,\text{GeV}$, $\tan\beta = 10$, $\mu > 0$ and $A_0 = 0$. HH50′ is defined in the same way, but with the soft terms of the third generation chosen differently: Third-generation squarks and sleptons were given a universal soft mass $m_0^{(3)} = 300\,\text{GeV}$ and a trilinear A-parameter $A_0^{(3)} = -1\,\text{TeV}$. This choice was made in order to have a reference spectrum whose $\tilde{t}_1\tilde{t}_1^*$ production cross section is comparable to that of Spectrum I, while closely resembling the CMSSM. Finally, we also list a comparable simplified model, containing only the $\tilde{t}_1$ and a bino-like neutralino LSP. The model definitions are summarized in Table 5.2.

5.1.2 Signatures

The light higgsinos of the hybrid gauge-gravity mediation scenario (and also of the AMSB scenario) will be produced in copious numbers in electroweak processes at the LHC. The Drell-Yan process gives rise to $\chi_1^+\chi_1^-$, $\chi_1^\pm\chi_{1,2}^0$ and $\chi_1^0\chi_2^0$ final states, and W boson fusion can give like-sign $\chi_1^\pm\chi_1^\pm$ pairs. The subsequent decays of χ_2^0 and $\chi_1^\pm$ into χ_1^0 will lead to events with missing energy and soft jets or leptons.

Unfortunately, with the higgsino mass splittings in the range of only a few GeV, most of these jets and leptons are too soft to even trigger on, and those events with high enough p_T to

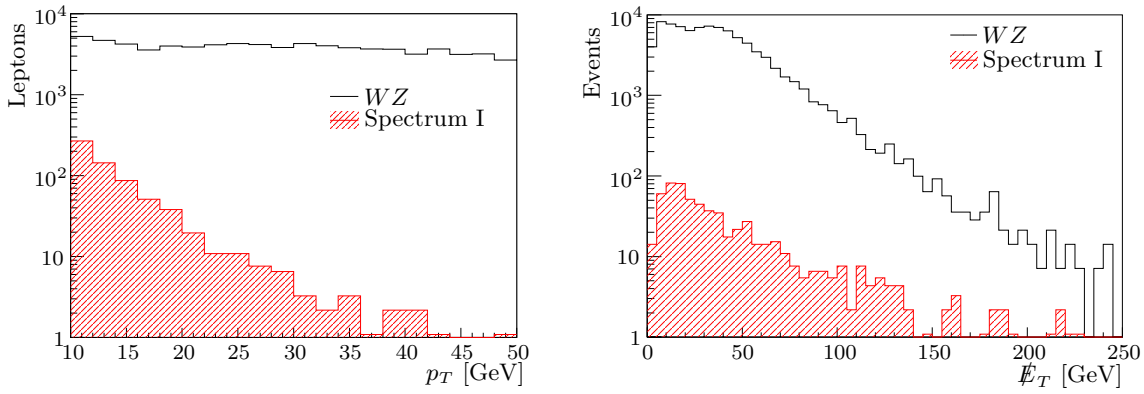

Figure 5.1: Lepton transverse momentum and missing transverse energy distributions of leptonic events from higgsino decays with Spectrum I. The higgsinos are produced in electroweak processes; the numbers are scaled to $20\,\text{fb}^{-1}$. For comparison, the SM background from WZ production (which is just one of the several contributing processes) is also shown. See Section 5.1.3 for details of the event simulation.

be detected are completely swamped by the Standard Model background. Demanding large missing transverse energy does not help much, since also the $\not{E}_T$ spectrum falls very rapidly. For illustration, the lepton p_T and $\not{E}_T$ distributions for Spectrum I are shown in Figure 5.1. We have also studied events with additional jets from initial-state gluon radiation, in order to increase the number of events with larger p_T and $\not{E}_T$. While this somewhat enhances the tails of the distributions, it also reduces the overall cross section, and the combined effect does very little to improve the overall situation. In conclusion we confirm the findings of [223] that, in order to find evidence for our scenario in electroweak processes, a linear collider would be far better suited. For the LHC, a monojet or a monophoton (from initial-state gluon or photon radiation) together with large missing E_T might be a useful signal, in combination with other searches. This is probably the only possibility to detect SUSY if the AMSB-like scenario is realized in nature. We will however not pursue this possibility in the present work because of the difficulties in accurately estimating the background without a full detector simulation. The experimental efforts in this direction [224–227] seem to be very promising. The results are however interpreted so far only in terms of contact interactions or for theories involving large extra dimensions. We will also not consider the possibility of searches for staus, since the mass predictions depend strongly on the parameters: The model $(17, 23, 9)$ from [75] being very similar to Spectrum II predicts a lightest stau with a mass of 550 GeV, contrary to 461 GeV in our case. Furthermore, such search is not a viable possibility in the AMSB scenario.

We are therefore led to consider those regions of parameter space where some colored superparticles are still light enough to be produced at the LHC. At this stage we ignore the LHC hint for a 125 GeV Higgs. The lightest colored superparticle in our class of models is always the lighter of the scalar top quarks $\tilde{t}_1$. At the LHC it may be produced in pairs, or it may appear in cascade decays of first-generation squarks and gluinos if these are kinematically accessible. It turns out that processes involving the $\tilde{t}_1$ are particularly well suited to find evidence for our scenario (or to constrain it), and also to distinguish it from more generic incarnations of the MSSM[1] .

[1]For some recent related studies of stops at the LHC, see for example [77, 228–231].

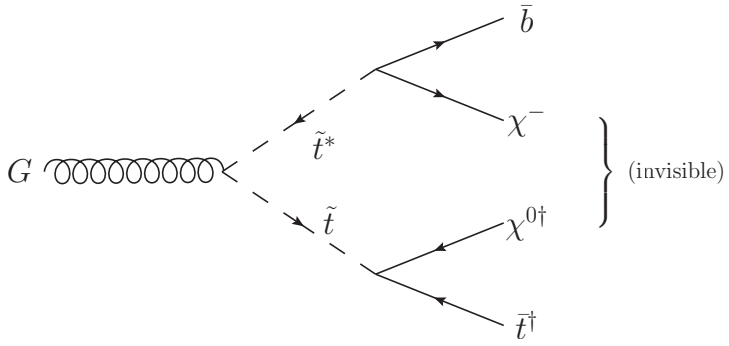

Figure 5.2: An example for a stop pair production event, showing up as to two high-energetic b-jets and missing energy.

For definiteness we will from now on focus on the Spectrum I benchmark point $M_1 = M_2 = 1250\,\text{GeV}$, $M_3 = 428\,\text{GeV}$, $\mu = 150\,\text{GeV}$, $\sqrt{B_\mu} = 200\,\text{GeV}$. In a sense this is a maximally optimistic set of parameters, chosen such that it is still marginally allowed by current search limits.

With superparticle masses as in Spectrum I, the clearest signatures at the early LHC will be jets with missing E_T. We will see that the cross sections for stop pair production on the one hand and the more familiar $\tilde{q}\tilde{q}$, $\tilde{q}\tilde{q}^*$, $\tilde{q}g$ and gg production (where $\tilde{q}$ stands for any first-generation squark) on the other hand are comparable; all these processes contribute to the signal.

More importantly, once there is evidence for supersymmetry in searches for jets plus missing E_T, our model can also be distinguished experimentally from generic variants of the MSSM which lack its characteristic features of light and near-degenerate higgsinos. This is achieved by focusing on the stop pair production channel. In Spectrum I, stop decays do not involve hard leptons, since possible leptons from χ_2^0 or $\chi_1^\pm$ decays are too soft to be detected. The signature of a $\tilde{t}_1$ is therefore always a hard b-jet plus missing E_T; a typical stop pair event is shown in Figure 5.2. By contrast, in generic supersymmetric models one usually expects also events with jets, missing E_T and isolated leptons, be it from cascade decays of squarks and gluinos or from $\tilde{t}$ decaying into charginos or non-LSP neutralinos. Once a signal is found in the jets + MET channel, we could use the absence of signals with leptons to severely constrain interpretations in terms of generic supersymmetry, thus providing further indirect evidence for our scenario.

We may even be able to discriminate between our model and a "simplified model" comprising only a $\tilde{t}_1$ and a bino-like χ_1^0. In such a framework, likewise, no events with hard isolated leptons are expected. However, because the only possible $\tilde{t}_1$ decay is then $\tilde{t}_1 \to t\chi_1^0$ with the t decaying further into bW, the b-jet spectrum turns out to be significantly different from that of our model, where about half of the stops decay directly into a b quark without an intermediate top.

In the following sections we present the results of three simulated searches. The first is for jets and large missing E_T, in order to show that early LHC will be able to find evidence for our model. The second also includes leptons, to show that early LHC will, furthermore, be able to distinguish our model from a comparable CMSSM-like model. More precisely, our model will be compared both with the CMSSM point HH50, which has similar $\tilde{g}$ and $\tilde{q}$ production cross sections, and with the CMSSM-like point HH50′, which in addition has

model	$\sigma(\tilde{q}\tilde{q}^*)$	$\sigma(\tilde{q}\tilde{q})$	$\sigma(\tilde{t}\tilde{t}^*)$	$\sigma(\tilde{b}\tilde{b}^*)$	$\sigma(gg)$	$\sigma(g\tilde{q})$	σ(tot)
Spectrum I	0.388	3.83	5.61	0.6	2.9	8.45	21.78
HH 50	1.79	12	0.682	0.044	1	9.3	24.8
HH 50'	1.65	11.5	5.96	0.136	0.979	8.9	29

Table 5.3: Production cross sections of different models in fb calculated with PROSPINO [232, 233]. The cross section for $\tilde{b}\tilde{b}^*$-production is given at the lowest order, all other cross sections are calculated at NLO.

sample	σ [pb]	events	
		expected	simulated
$t\bar{t}$	163	3.3×10^6	11.3×10^6
single top	85.1	1.7×10^6	1.7×10^6
W + jet	826	$1\,652 \times 10^4$	5×10^4
W^+W^-	44.974	899×10^3	$1\,000 \times 10^3$
W^+Z	11.580	358×10^3	400×10^3
W^-Z	6.342		
ZZ	6.195	124×10^3	150×10^3
$W^+W^-W^+$	4×10^{-2}	800	15 000
W^+W^-Z	3×10^{-2}	600	15 000
W^+ZZ	9×10^{-3}	180	15 000
ZZZ	3×10^{-3}	60	5 629

Table 5.4: Cross sections and numbers of generated events of SM background used in the present analysis. The single top production cross-section includes all LHC production channels. The cross sections for the tri-boson events are calculated at the Born level with MADGRAPH, all other cross sections are taken from [234–236]

also a comparable $\tilde{t}_1$ pair production cross section. Finally, we present a search with the cuts optimized to select events from $\tilde{t}_1$ pair production, and compare the result with the simplified model mentioned above.

5.1.3 Simulation of Signal and Background

All Monte Carlo samples were generated with MADGRAPH 4.4.44 [237] interfaced with PYTHIA 6.4.22 [238] using CTEQ6L1 parton distribution functions [239]. In order to generate signal events, decay widths of supersymmetric particles were computed with SDECAY [240] from spectra calculated with SOFTSUSY. The generic detector simulation DELPHES [241], tuned to the CMS detector, was used in order to account for effects of event reconstruction at the detector level.

The signal production cross sections are listed in Table 5.3. For Spectrum I 43 500 signal events were simulated, to be compared with 435 events expected at the early LHC with an assumed integrated luminosity yield of 20 fb^{-1}. The number of signal events passing the cuts should therefore eventually be divided by a normalization factor 100 for a realistic estimate. For HH50 and HH50′, we simulated 10 000 events each, with respectively 496 and 580 events

expected, so the normalization factors are 20 and 17 respectively.

The corresponding figures for Standard Model backgrounds are listed in Table 5.4. It turns out that $t\bar{t}$ is the most important background. Since, consequently, the best statistics is needed for this channel, we have simulated about three times more events than expected. For the remaining backgrounds, the number of simulated events roughly matches the number of expected events, or exceeds it in the case of tri-bosons (where the cross sections are small) in order to avoid large Monte Carlo errors. An exception are background events with vector bosons plus jets, where we have only simulated a small fraction of the expected events. However, as will become clear when we present the cut flows, this background is very efficiently removed by our cuts. Therefore, it can be safely neglected without having to simulate the full sample.

5.1.4 Event Selection and Analysis

Discovery with all-hadronic Search

The first analysis serves to show that LHC will be able to find evidence for our model, i.e. to distinguish its signatures from the Standard Model background.

In the first stage, candidate events with multiple high-energetic jets and missing transverse energy are selected with the following pre-selection cuts at the level of the detector simulation:

- $1 < N(j) < 5$, where $\quad p_T(j) > 100\,\text{GeV}$,
- $\not{E}_T > 50\,\text{GeV}$.

Furthermore, all events with an isolated lepton (electron or muon) with $p_T > 10\,\text{GeV}$ are rejected in order to suppress events with genuine missing energy from neutrinos:

- $N(l) = 0$.

After imposing these pre-selection cuts, we use a set of cuts optimized for discriminating between signal and background. Events are required to satisfy

- $HT' > 500\,\text{GeV}$,

where HT' is the sum of the transverse momenta of the two most energetic jets,

$$HT' = \sum_{i=1}^{2} p_T(j_i)\,. \tag{5.5}$$

Following the experimental analyses, we use the α_T variable [242–244] as the main discriminator against QCD multi-jet production, defined for di-jet events as:

$$\alpha_T = \frac{E_T(j_2)}{M_T} = \frac{E_T(j_2)}{\sqrt{\left(\sum_{i=1}^{2} E_T(j_i)\right)^2 - \left(\sum_{i=1}^{2} p_x(j_i)\right)^2 - \left(\sum_{i=1}^{2} p_y(j_i)\right)^2}}\,, \tag{5.6}$$

where j_2 denotes the next-to-leading jet. In our analysis we use p_T of the jets provided by `DELPHES` instead of E_T, and require the event to have

- $\alpha_T > 0.55$

		before	pre-cuts					
		cuts	$N(j)$	$\not{E}_T$	$N(l)$	HT'	α_T	$\not{E}_T$
Spectrum I	$\tilde{q}\tilde{q}^*$	720	569	555	420	401	86	78
	$\tilde{q}\tilde{q}$	7 660	6 416	6 329	4 788	4 581	919	761
	$\tilde{t}\tilde{t}^*$	11 220	8 909	8 729	7 690	5 123	1 074	864
	$\tilde{b}\tilde{b}^*$	1 200	993	983	866	691	162	138
	gg	5 800	4 678	4 622	3 573	3 250	809	631
	$\tilde{g}\tilde{q}$	16 900	13 425	13 257	10 237	9 655	2 080	1 685
weighted events								**42**
HH50		10 000	8 892	8 822	7 119	6 882	1 888	1 770
weighted events								**88**
HH50′		10 000	8 778	8 691	6 850	6 244	1 582	1 467
weighted events								**84**
SM	$t\bar{t}$	11.3×10^6	3.2×10^6	930 000	510 000	59 992	312	64
	t	1.7×10^6	160 197	23 773	15 089	2 062	6	3
	W + jet	50 000	120	5	2	0	0	0
	di-bosons	1.55×10^6	36 862	3 820	2 281	404	4	3
	tri-bosons	50 629	9 051	2 763	1 714	470	9	6
weighted events								**25**

Table 5.5: Cut flow of general all-hadronic analysis for different signals and backgrounds at $\sqrt{s} = 7\,\text{TeV}$. Figures are given for all events that were simulated. The bold numbers are the events surviving all cuts, properly normalized to an integrated luminosity of $20\,\text{fb}^{-1}$. The cut flow for the Spectrum I is shown separately for each different production channel.

in order to pass the cut. In events with jet multiplicity $N(j) > 2$, two pseudo jets are formed following the CMS strategy [244] and the α_T variable is constructed from the pseudojets. Finally, in order to further suppress the $t\bar{t}$ background, we demand a very high value of missing transverse energy:

- $\not{E}_T > 400\,\text{GeV}$.

Because of the high $\not{E}_T$ cut in combination with the selection based on α_T, we can safely neglect QCD di- and multi-jet background contributions. The resulting cut flow is shown in Table 5.5.

Evidently, with this analysis it will be possible to discriminate between our model and the Standard Model background. The same is true for the HH50 and HH50′ models. This result is of course unsurprising, since all these benchmark points were chosen to lie near the $1\,\text{fb}^{-1}$ exclusion bounds, and here we are assuming a data sample of $20\,\text{fb}^{-1}$.

Model Discrimination: CMSSM-like Models

The more interesting question is that of model discrimination. For this a fully hadronic search such as the one we just presented is not suitable, even though the number of events

		After pre-cuts	b-tag	HT'	α_T	$\not{E}_T$
Spectrum I	$\tilde{q}\tilde{q}^*$	420	78	77	0	0
	$\tilde{q}\tilde{q}$	4 788	1 153	1 126	226	183
	$\tilde{t}\tilde{t}^*$	7 690	3 851	3 268	834	562
	$\tilde{b}\tilde{b}^*$	866	445	405	112	87
	gg	3 573	1 843	1 793	465	351
	$g\tilde{q}$	10 237	3 940	3 862	845	652
weighted events						**18**
HH50		7119	631	619	124	108
weighted events						**5**
HH50′		6 850	930	841	158	124
weighted events						**7**
SM	$t\bar{t}$	51×10^4	20×10^4	48 624	391	25
	t	15 089	4 798	656	3	2
weighted events						**9**

Table 5.6: Cut flow of the hadronic analysis with b-tagging for different signals and the relevant backgrounds at $\sqrt{s} = 7\,\text{TeV}$. The remaining signal and background events, scaled to an integrated luminosity of $20\,\text{fb}^{-1}$, are printed in bold. The cut flow for Spectrum I is shown separately for each different production channel.

passing the above cuts is significantly different between our model and HH50 / HH50′. This difference could, after all, be accounted for by slightly different squark and gluino production cross sections – for instance, the HH50 and HH50′ spectra would just need to be slightly heavier in order to reproduce the 42 events after cuts which we found for our model.

In fact, some information can be gained already by requesting, in addition to the cuts of Section 5.1.4, that at least one jet should be b-tagged. We assume a p_T-independent b-tagging efficiency of 40 %, and a mistagging probability of 10 % as implemented in `DELPHES`. The additional cut is then

- $N(b\text{-jets}) \geq 1$.

The cut flow is shown in Table 5.6. Note that the number of events from both HH50 and HH50′ is dramatically reduced. This is partly because, in our model, a sizable fraction of events was due to $\tilde{t}$ pair production, and the gluino can only decay into $\tilde{t}_1$ or $\tilde{b}_1$. By contrast, in HH50 and HH50′ most events involve $\tilde{q}$ decays which do not necessarily lead to b-jets. Moreover, by vetoing events with isolated leptons, fewer $\tilde{t}_1$ events in our model are cut away than in HH50 and HH50′ – these models tend to produce more leptonic events, which we will now put to use in a separate semi-leptonic analysis.

More precisely, as explained in Section 5.1.2, $\tilde{t}_1$ decays in our model can give hard isolated leptons at most from secondary top decays (which is, incidentally, also true for $\tilde{b}_1$ and even $\tilde{g}$ decays, since the gluino can only decay into $\tilde{t}_1$ or $\tilde{b}_1$). In HH50 and HH50′ many more leptons are expected, jets with missing E_T and isolated leptons being one of the hallmark

		before	pre-cuts							
		cuts	$N(l)$	$N(j)$	$\not{E}_T$	$N(j)$	m_T	Iso	HT'	$\not{E}_T$
Spectrum I	$\tilde{q}\tilde{q}^*$	720	238	233	229	26	17	6	6	1
	$\tilde{q}\tilde{q}$	7 660	2 690	2 650	2 622	380	271	129	123	74
	$\tilde{t}\tilde{t}^*$	11 220	4 063	3 202	3 135	2 191	1 701	230	90	40
	$\tilde{b}\tilde{b}^*$	1 200	449	367	367	244	180	25	16	8
	gg	5 800	2 224	2 202	2 173	258	207	53	46	29
	$g\tilde{q}$	16 900	6 397	6 346	6 261	690	536	170	142	76
	events									**2**
HH50		10 000	2 432	2 352	2 330	615	438	242	225	147
	events									**7**
HH50′		10 000	2 699	2 519	2 496	796	576	308	246	147
	events									**9**
SM	$t\bar{t}$	11×10^6	4×10^6	1×10^6	440 000	350 000	45 584	29 942	1 266	3
	events									**1**

Table 5.7: Cut flow of semi-leptonic analysis for different signals and relevant background at $\sqrt{s} = 7\,\text{TeV}$. The remaining signal and background events, scaled to an integrated luminosity of $20\,\text{fb}^{-1}$, are printed in bold. The cut flow for Spectrum I is shown separately for each different production channel.

signatures for generic supersymmetry. This motivates a semi-leptonic search for better model discrimination.

An event is selected for further analysis if it contains exactly one lepton (muon or electron) candidate

- $N(l) = 1\ , \quad p_T(l) > 15\,\text{GeV}.$

Other than that, our pre-selection cuts are as before,

- $N(j) > 1\ , \quad p_T(j) > 100\,\text{GeV},$
- $\not{E}_T > 50\,\text{GeV}.$

The actual cuts are now as follows. We select events with exactly two high-energetic jets,

- $N(j) = 2.$

This criterion selects preferably the $\tilde{t}\tilde{t}^*$ production channel, since usually more than two jets are expected to appear in channels involving $\tilde{q}$ or $\tilde{g}$. Furthermore, we employ the transverse mass variable

$$m_T = \sqrt{2 p_T(l) \not{E}_T \left(1 - \cos\Delta\phi(l, \not{E}_T)\right)}\ , \tag{5.7}$$

where $\Delta\phi(l, \not{E}_T)$ is the angle between missing transverse energy and the momentum of the lepton in the transverse plane. This variable is bounded by the W boson mass if the lepton and $\not{E}_T$ originate in W boson decay. We select events with

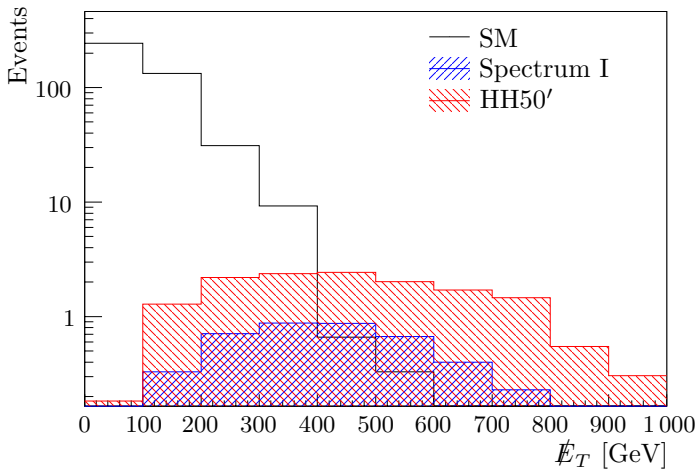

Figure 5.3: $\not{E}_T$ distribution in the semi-leptonic analysis before the final $\not{E}_T$ cut. SM events are black, events in Spectrum I are blue and events in HH50′ are red.

- $m_T > 100\,\text{GeV}$,

and ensure that the leptons in these events are isolated. Furthermore, as in the previous analysis we demand that the two jets have high transverse momentum and high missing transverse energy,

- $HT' > 500\,\text{GeV}$,
- $\not{E}_T > 400\,\text{GeV}$.

The resulting cut flow is displayed in Table 5.7. As advertised, the number of leptonic events to survive the cuts is not significantly above the SM background, whereas a significant number of events survive in HH50 and HH50′ (cf. Figure 5.3). This set of cuts therefore serves to discriminate between our model and CMSSM-like models.

Model Discrimination: A Simplified Model

The analysis of Section 5.1.4 relies on the presence of intermediate states (in the case of HH50 and HH50′, the wino-like $\chi_1^\pm$ and χ_2^0) whose decay into the LSP produces isolated leptons. In models with non-unified gaugino masses, the LSP could still be bino-like while all remaining charginos and neutralinos are much heavier. Can we still distinguish our model from a generic model with a comparably heavy $\tilde{t}_1$ and only a light bino LSP below it? It turns out that this is rather more difficult, but still possible.

The simplified model in Table 5.1 has been designed to reproduce the relevant collider signals. We use the production cross section of stop pairs taken from Spectrum I. The only active states are a moderately heavy $\tilde{t}_1$ and a light bino-like χ_1^0. Stops that are produced in pairs will decay as $\tilde{t}_1 \to t\chi_1^0$, with the t further decaying into bW. The signature is therefore b-jets and missing energy. A similar decay chain is also open in our model (as in the lower branch in Figure 5.2). However, in our model about 50 % of the stops will decay directly into b quarks and missing energy (as in the upper branch). These latter events will produce slightly harder b-jets than those involving an intermediate top.

		before	pre-cuts								
		cuts	$N(j)$	$\not{E}_T$	$N(j)$	b-tag	m_{jj}^T	HT'	$\Delta\phi$	$\not{E}_T$	$N(l)$
Spectrum I	$\tilde{q}\tilde{q}^*$	720	569	555	71	12	3	3	2	2	2
	$\tilde{q}\tilde{q}$	7 660	6 416	6 329	978	179	55	53	48	33	24
	$\tilde{t}\tilde{t}^*$	11 220	8 909	8 729	6 093	3 158	1 928	1 378	1 238	637	575
	$\tilde{b}\tilde{b}^*$	1 200	993	983	651	332	152	125	116	72	63
	gg	5 800	6 478	4 622	658	348	144	115	104	78	58
	$g\tilde{q}$	16 900	13 425	13 257	1 803	684	243	201	178	121	77
	events										**8**
simplified		11 220	8 179	7 986	5 328	2 107	1 339	782	666	316	243
	events										**2**
SM	$t\bar{t}$	1×10^7	3×10^6	1×10^6	739 752	290 416	268 254	34 062	8 669	34	16
	t	1.7×10^6	160 197	23 773	21 234	6 858	6 330	907	176	6	3
	events										**8**

Table 5.8: Cut flow of the analysis in which we examine the possibility to distinguish $\tilde{t}$ decays via bino-like neutralinos from decays via higgsino-like neutralinos at $\sqrt{s} = 7\,\text{TeV}$. The remaining signal and background events, scaled to an integrated luminosity of $20\,\text{fb}^{-1}$, are printed in bold.

To select the stop pair production channel in our model, we impose a series of simple cuts. At the pre-selection cut level, we select event with at least two and at most four high-energetic jets with p_T larger than 100 GeV, similar to the all-hadronic analysis:

- $1 < N(j) < 5$, where $\quad p_T(j) > 100\,\text{GeV}$,
- $\not{E}_T > 50\,\text{GeV}$.

Heavy squarks and gluinos will decay via long decay chains, typically giving rise to a large number of high-energetic jets. Therefore, we select events with exactly two high-energetic jets in order to single out stop pair production. Furthermore, we demand that at least one of these jets is a b-jet:

- $N(j) = 2$, where $\quad p_T(j) > 100\,\text{GeV}$,
- $N(b\text{-jets}) \geq 1$.

The invariant mass of the 2-jet system originating in such decays is sensitive to the masses of the parent particles. We select events with relatively small 2-jet transverse mass:

- $m_{jj}^T \equiv \sqrt{2p_T(j_1)p_T(j_2)\,(1 - \cos\Delta\phi(j_1, j_2))} < 500\,\text{GeV}$

In order to suppress the Standard Model background we employ following cuts:

- $HT' > 400\,\text{GeV}$,
- $\Delta\phi\left(\not{E}_T\,, j_2\right) > 1$,

- $\not{E}_T > 400\,\text{GeV}$,
- $N(l) = 0$.

Missing transverse energy in QCD di- and multi-jet events can only appear due to the mismeasurement of one of the jets. We assume that, in events with very large missing transverse energy and exactly two high-energetic jets, the mismeasured jet is the next-to-leading one. We therefore expect that no QCD event will survive the cuts on $\Delta\phi\left(\not{E}_T, j_2\right)$ and $\not{E}_T$. The resulting cut flow is displayed in Table 5.8.

Evidently, these cuts can discriminate between Spectrum I and the simplified model. Of course the latter is not a realistic scenario, and in a fully-fledged model cascade decays of heavier states may also be relevant. However, since the cuts single out the stop pair production channel in our model quite efficiently, it seems reasonable to expect that this remains true for a generic full model which the simplified model is taken to represent here. The cuts are even tight enough to remove almost all of the stop decay events in the simplified model, while leaving a substantial excess above the Standard Model background in our model (presumably coming from direct $\tilde{t}_1 \to b\chi_1^\pm$ decays). Note, however, that this analysis will be rather challenging with real data: Only few events survive, and the discrimination is not mainly due to a single cut, but rather to the combined effects of all of them.

Having investigated the Higgsino World scenario, we now turn our attention to the case of R-parity violation, leading also to veiled signatures.

5.2 R-parity Violation

The hybrid gauge-gravity mediation model can become cosmologically consistent not only with the help of additional entropy production before the BBN, which leads to the LHC signatures presented in the previous section, but also with the introduction of small R-parity violation. This is also the case for mSUGRA models with gravitino dark matter, cf. Section 2.4.1. Usually, the bulk of these models is viewed to be excluded by recent LHC data. However, not taking into account the LHC hint for a Higgs boson with a mass of 125 GeV, which is difficult to accommodate, a large region of mSUGRA parameter space becomes untested in case of small R-parity violation.

While the hybrid mediation scenario leads to higgsino-like neutralino NLSP, the mSUGRA scenario can have a bino-like neutralino or a stau as NLSP. In all cases, the decay lengths of the particles are macroscopic, cf. Section 4.4. Large macroscopic decay lengths are of great help in the search for decaying NLSPs. This remains true if the decay length is larger than the size of the detector since a sizable fraction of NLSPs may still decay inside the detector. This has been studied for neutral [214] as well as charged [215] NLSPs. Neutralino decay lengths varying from 0.1 mm to 100 m also arise in models with generalized gauge mediated supersymmetry breaking [245]. Alternatively, charged [246] and neutral [247] NLSP decays have been studied for models where the decay lengths are so small that no displaced vertices are observed and R-parity breaking Yukawa couplings determine the hierarchy of decay channels. In this case multi-lepton events, and their flavor structure, are of crucial importance.

The subject of this section is a quantitative analysis of bino-like neutralino NLSP decays at the LHC in the case of very small R-parity breaking. The goal is the determination of the sensitivity in the R-parity breaking parameter ζ for varying gluino and squark masses. We

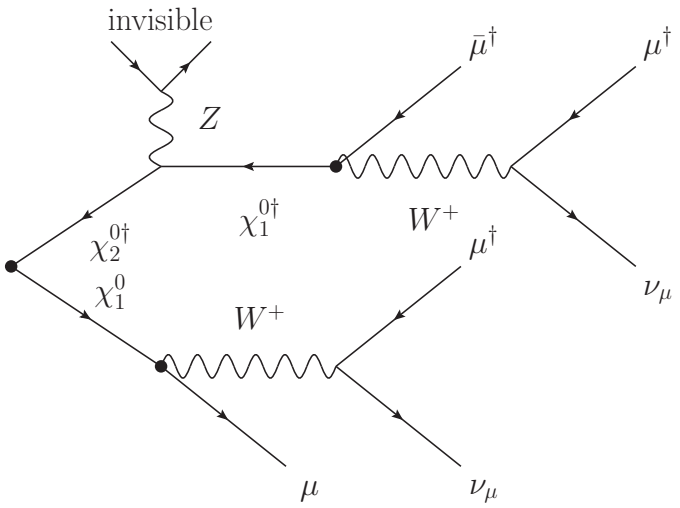

Figure 5.4: Typical R-parity violating decay chain involving higgsino-like neutralino at the LHC. The primary vertex and the secondary vertices are highlighted.

shall focus on events with a clean signature: cascade processes with jets where one of the produced neutralino NLSPs decays into Z boson and neutrino, with the subsequent decay of the Z boson into a muon pair, cf. Section 4.4.1. This allows us to determine a conservative 5σ discovery range. Finally, we estimate the discovery reach of the LHC if all NLSP decays are taken into account. Note that we will neglect the neutralino decay channel into the Higgs boson and neutrino, which is either absent for low neutralino masses or is suppressed. We shall point out the differences to the higgsino-like neutralino NLSP case, which has a branching ratio of order 1 into the W boson and charged lepton, cf. Section 4.4.2. A full quantitative analysis of this case is work in progress.

5.2.1 Decay Signatures of the higgsino-like Neutralino

Taking into account the LHC hint for the mass of the Higgs boson, we can assume that even the third generation squarks are fairly heavy and may be not accessible at the LHC, cf. Spectrum II in Tab. 5.1. Thus, the neutralinos will be produced in electroweak processes. While in the case of R-parity conservation, cf. Section 5.1, the only signal at the LHC would be a monojet (monophoton) signature, R-parity violation opens up new possibilities for detection. Nota bene that the final states will always look similar to the case of pure neutralino production even if charginos have been produced, due to small mass separation between the charged and neutral higgsino states.

The final state neutralinos decay in a secondary vertex into W bosons and leptons almost in 100% of decays. Fig. 5.4 shows an example of a decay cascade with muons in the final state. The distance between the collision point and the secondary vertex depends on the decay width of the neutralino (4.88), and hence on the R-parity breaking parameter ζ.

Table 5.9 summarizes all possible LHC signatures if the NLSP is higgsino-like neutralino for sufficiently large values of ζ such that it is probable that both neutralinos decay inside of the tracker volume. The signatures are classified according to the final states in the neutralino decays; amazingly there are only two type of signatures: leptonic signatures involving only leptons in the final state, and semi-leptonic signatures involving at least two charged

category	χ_1^0 decays	LHC signature
leptonic	$W^+W^-l\bar{l} \to \bar{l}l\bar{l}\bar{\nu}\nu$ $W^+W^+ll \to \bar{l}\bar{l}ll\nu\nu$ $W^-W^-\bar{l}\bar{l} \to ll\bar{l}\bar{l}\nu\nu$	$2l + 2\bar{l} + \not{E}_T$
semi-leptonic	$W^+W^-l\bar{l} \to jjll\bar{l}\bar{\nu}$ $W^+W^+ll \to jj\bar{l}ll\nu$	$2j + 2l + 1\bar{l} + \not{E}_T$
	$W^+W^-l\bar{l} \to jj\bar{l}l\bar{l}\bar{\nu}$ $W^-W^-\bar{l}\bar{l} \to jjll\bar{l}\bar{l}\nu$	$2j + 1l + 2\bar{l} + \not{E}_T$
	$W^+W^-l\bar{l} \to jjjjl\bar{l}$	$4j + 1l + 1\bar{l}$
(same sign, no $\not{E}_T$)	$W^+W^+ll \to jjjjll$ $W^-W^-\bar{l}\bar{l} \to jjjj\bar{l}\bar{l}$	$4j + 2l$ $4j + 2\bar{l}$

Table 5.9: All possible final states in higgsino-like neutralino case if both neutralinos decay inside the tracking volume.

category	χ_1^0 decays	LHC signature
leptonic *(opposite sign)*	$W^+l \to \bar{l}l\nu$ $W^-\bar{l} \to l\bar{l}\nu$	$1l + 1\bar{l} + \not{E}_T$
single lepton	$W^+l \to jjl$ $W^-\bar{l} \to jj\bar{l}$	$2j + 1l + \not{E}_T$ $2j + 1\bar{l} + \not{E}_T$

Table 5.10: All possible final states in higgsino-like neutralino case if one of the neutralinos decays outside the tracking volume.

leptons and jets. Note that all channels have only small amount of missing transverse energy $\not{E}_T$, and therefore they are not considered in the usual searches (cf. [248, 249]). Neutralino decays lead also to signatures containing same-sign lepton pairs but since no $\not{E}_T$ is present in these channels they are usually discarded in order to suppress various backgrounds [250]. Additionally, the leptonic signatures involve no jets in the final state from the hard process. Therefore, a possible search strategy would be a search for events without jets.

If the value of ζ is rather small one of the neutralinos will decay outside of the detector leading to signatures with larger amount of $\not{E}_T$ as shown in Table 5.10. The leptonic decays of one of the neutralinos inside the detector lead to a perfect opposite-sign signature. Furthermore, one could also search for single lepton events with large amount of missing transverse energy.

Let us now look at the decays of the bino-like neutralino and compare the results with the ones obtained in this section.

5.2.2 Decay Signatures of the bino-like Neutralino

Consider for simplicity, the following cascade process:

$$Gq \to g\tilde{q} \to jjj\chi_1^0\chi_1^0 \,, \tag{5.8}$$

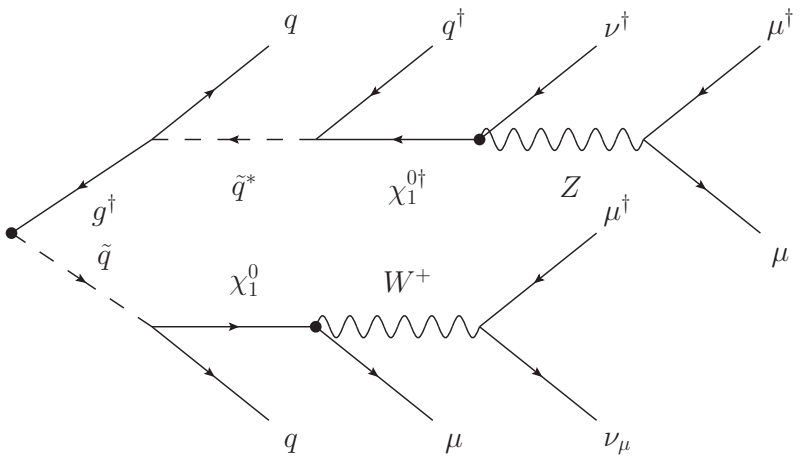

Figure 5.5: Typical R-parity violating decay chain involving bino-like neutralino at the LHC. The primary vertex and the secondary vertices are highlighted.

possible in mSUGRA scenarios with bino-like neutralino, where j denotes a jet. The final state neutralinos decay in a secondary vertex into W bosons and leptons as well as into Z bosons and neutrinos. Fig. 5.5 shows an example of a decay cascade with muons in final state. The distance between the collision point and the secondary vertex depends on the decay width of the neutralino (4.84), and hence on the R-parity breaking parameter ζ.

Table 5.11 summarizes the LHC signatures of the process (5.8) for sufficiently large values of ζ such that it is probable that both neutralinos decay inside of the tracker volume. All signatures contain at least three jets from the antecedent supersymmetric decays, contrary to the higgsino-like case. In general more complicated signatures can arise. Intermediate chargino decays can lead to additional gauge bosons in the final state, which then produce more jets or leptons. These decay chains as well as all production processes were taken into account in the simulation of the signal.

The signatures are classified similar to the higgsino-like case according to the final states in the neutralino decays: leptonic signatures involving only leptons in the final state, semi-leptonic signatures involving at least two charged leptons and jets, single lepton signatures containing only one lepton, all-hadronic signatures where only jets accompanied by neutrinos are present, and finally invisible channels where both neutralinos decay solely to neutrinos. Additionally, we single out channels having a considerable amount of missing transverse energy $\not{E}_T$ from Z boson decays, since $\not{E}_T$ is one of the main features searched for in usual searches for new physics. Such channels are not present in higgsino-like neutralino decays. The channels labeled as *opposite sign* could be found in usual supersymmetry (SUSY) searches as they include a considerable amount of $\not{E}_T$, many jets and one isolated lepton pair with different signs. However, some searches remove events with muon pairs having invariant mass around the Z pole in order to dispose of Drell-Yan $Z/\gamma^* \to l\bar{l}$ processes. Note that in the model presented in this section this cut would lead to a suppression of the signal. Other channels presented above are similar to the higgsino-like neutralino case, up to the number of jets in the final state.

If the value of ζ is rather small one of the neutralinos will decay outside of the detector leading to signatures with larger amount of $\not{E}_T$ as shown in Table 5.12. The leptonic decays of one of the neutralinos inside the detector lead to a perfect opposite-sign signature. As

category	χ_1^0 decays	LHC signature
leptonic	$W^+W^-l\bar{l} \to \bar{l}l\bar{l}\bar{\nu}\nu$	$3j + 2l + 2\bar{l} + \not{E}_T$
	$W^+W^+ll \to \bar{l}\bar{l}ll\nu\nu$	
	$W^-W^-\bar{l}\bar{l} \to ll\bar{l}\bar{l}\nu\nu$	
	$ZW^-\bar{l}\nu \to l\bar{l}l\bar{l}\nu\nu$	
	$ZW^+l\nu \to l\bar{l}\bar{l}l\nu\nu$	
	$ZZ\nu\nu \to l\bar{l}l\bar{l}\nu\nu$	
(opposite sign, $\not{E}_T$ from Z)	$ZW^+l\nu \to \nu\nu\bar{l}l\nu\nu$	$3j + 1l + 1\bar{l} + \not{E}_T$
	$ZW^-\bar{l}\nu \to \nu\nu l\bar{l}\nu\nu$	
	$ZZ\nu\nu \to \nu\nu l\bar{l}\nu\nu$	
semi-leptonic	$W^+W^-l\bar{l} \to jjll\bar{l}\nu$	$5j + 2l + 1\bar{l} + \not{E}_T$
	$W^+W^+ll \to jj\bar{l}ll\nu$	
	$ZW^+l\nu \to l\bar{l}jjl\nu$	
	$W^+W^-l\bar{l} \to jj\bar{l}l\bar{l}\nu$	$5j + 1l + 2\bar{l} + \not{E}_T$
	$W^-W^-\bar{l}\bar{l} \to jjll\bar{l}\nu$	
	$ZW^-\bar{l}\nu \to l\bar{l}jj\bar{l}\nu$	
	$ZW^+l\nu \to jj\bar{l}l\nu\nu$	$5j + 1l + 1\bar{l} + \not{E}_T$
	$ZW^-\bar{l}\nu \to jjl\bar{l}\nu\nu$	
	$ZZ\nu\nu \to jjl\bar{l}\nu\nu$	
	$W^+W^-l\bar{l} \to jjjjl\bar{l}$	$7j + 1l + 1\bar{l}$
(same sign, no $\not{E}_T$)	$W^+W^+ll \to jjjjll$	$7j + 2l$
	$W^-W^-\bar{l}\bar{l} \to jjjj\bar{l}\bar{l}$	$7j + 2\bar{l}$
single lepton *($\not{E}_T$ from Z)*	$ZW^+l\nu \to jjjjl\nu$	$7j + 1l + \not{E}_T$
	$ZW^-\bar{l}\nu \to jjjj\bar{l}\nu$	$7j + 1\bar{l} + \not{E}_T$
	$ZW^+l\nu \to \nu\nu jjl\nu$	$5j + 1l + \not{E}_T$
	$ZW^-\bar{l}\nu \to \nu\nu jj\bar{l}\nu$	$5j + 1\bar{l} + \not{E}_T$
all-hadronic *($\not{E}_T$ from Z)*	$ZZ\nu\nu \to jjjj\nu\nu$	$7j + \not{E}_T$
	$ZZ\nu\nu \to \nu\nu jj\nu\nu$	$5j + \not{E}_T$
invisible *($\not{E}_T$ from 2 Z)*	$ZZ\nu\nu \to \nu\nu\nu\nu\nu\nu$	$3j + \not{E}_T$

Table 5.11: Possible final states assuming process (5.8) if both neutralinos decay inside the tracking volume. In general more complicated signatures can arise.

mentioned above this signature can be hidden if one rejects events where the invariant mass distribution of the lepton pair is in the range of the Z boson mass. A universally working strategy is the search for single lepton events with large amount of missing transverse energy.

In general, the applicability and the reach of the usual SUSY searches applied to the models presented in this work depends crucially on the size of R-parity breaking. In order to further evaluate this statement, we investigated a number of characteristic variables in supersymmetric events for the case of bino-like neutralino. The situation in higgsino-like

category	χ_1^0 decays	LHC signature
leptonic	$W^+l \to \bar{l}l\nu$	
(opposite sign)	$W^-\bar{l} \to l\bar{l}\nu$	$3j + 1l + 1\bar{l} + \not{E}_T$
	$Z\nu \to l\bar{l}\nu$	
single lepton	$W^+l \to jjl$	$5j + 1l + \not{E}_T$
	$W^-\bar{l} \to jj\bar{l}$	$5j + 1\bar{l} + \not{E}_T$
all-hadronic	$Z\nu \to jj\nu$	$5j + \not{E}_T$
invisible	$Z\nu \to \nu\nu\nu$	$3j + \not{E}_T$

Table 5.12: Possible final states assuming process (5.8) if one of the neutralinos decays outside the tracking volume. In general more complicated signatures can arise.

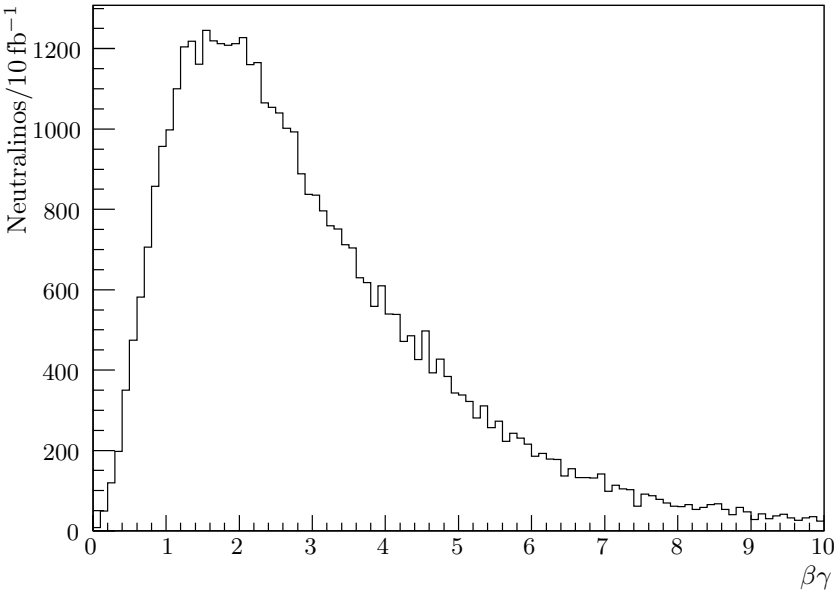

Figure 5.6: $\beta\gamma$ distribution of neutralinos at generator level for benchmark point HH27 (see Table 5.14). The number of neutralinos corresponds to twice the number of the events scaled to $10\,\mathrm{fb}^{-1}$ at $\sqrt{s} = 7\,\mathrm{TeV}$.

case should be comparable or even worse, since there is no $\not{E}_T$ from Z decays. The events were generated with `PYTHIA` as described in the next section, with the mSUGRA boundary conditions $m_{1/2} = m_0 = 270$, $\tan\beta = 10$, $A_0 = 0$, and $\mu > 0$. R-parity violating neutralino decays were taken into account.

Fig. 5.6 shows the distribution of the $\beta\gamma$ factors of the neutralinos. This factor enters the formula for the neutralino decay length and one sees from the plot that analytic results in the literature, which have been computed with $\beta\gamma = 1$, are correct within one order of magnitude. The most important kinematic property connected with the neutralino decay length is the amount of missing transverse momentum $\not{p}_T$ which is shown in Fig. 5.7 for different values of the R-parity violation parameter ζ. The missing transverse momentum was computed as the sum of the transverse momenta of all neutrinos produced in the detector before the hadronic

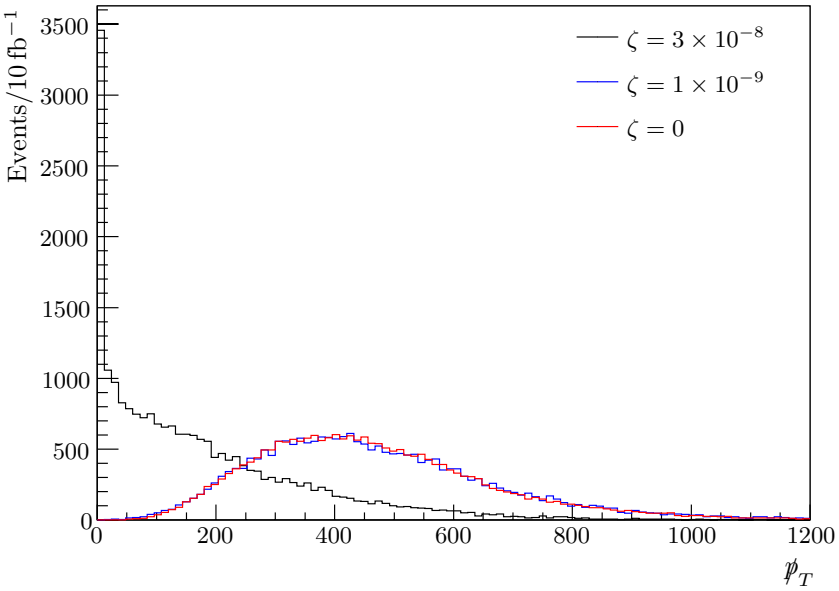

Figure 5.7: $\not{p}_T$ distribution at generator level for benchmark point HH27 (see Table 5.14) and different values of the R-parity breaking parameter ζ. Generator level $\not{p}_T$ is defined as sum over the p_T of i) neutralinos decaying outside of the detector (see Section 5.2.4) and ii) all neutrinos produced inside of the detector. The number of events is scaled to $10\,\text{fb}^{-1}$ at $\sqrt{s} = 7\,\text{TeV}$.

particle	transverse momentum	pseudorapidity	vertex position	
electron	$p_T > 7\,\text{GeV}$	$\lvert\eta\rvert < 2.5$	$r < 400\,\text{mm}$	$\lvert z\rvert < 1300\,\text{mm}$
muon	$p_T > 6\,\text{GeV}$	$\lvert\eta\rvert < 2.5$	$r < 4000\,\text{mm}$	$\lvert z\rvert < 6000\,\text{mm}$

Table 5.13: Cuts for the generator level particle selection for the study of particle multiplicity.

calorimeter ($r < 1800\,\text{mm}$, $|z| < 3700\,\text{mm}$) and the transverse momenta of the neutralinos decaying outside the hadronic calorimeter. The $\not{p}_T$ distribution of the R-parity conserving model $\zeta = 0$ cannot be distinguished from the model with $\zeta = 1 \times 10^{-9}$. However, the distribution is significantly different for $\zeta = 3 \times 10^{-8}$ since in this case most events have only very little missing transverse momentum due to early neutralino decays. This suggests that our model could only hardly be discovered in usual searches relying on $\not{E}_T$, in both bino and higgsino-like neutralino cases. Thus, it is crucial to reinterpret the usual SUSY searches at the LHC assuming now small R-parity violation as advocated in the present work, cf. Section 4.3.3.

Another general feature of models with relatively large ζ is the large possible number of leptons in the final state, illustrated in Fig. 5.8. The generator level particles selected for this plot had to fulfill the criteria shown in Table 5.13 imposed in order to select leptons from hard processes which could be reconstructed in a realistic detector. The cuts on the vertex position represent a pessimistic estimate of the reconstruction efficiency (see Section 5.2.4).

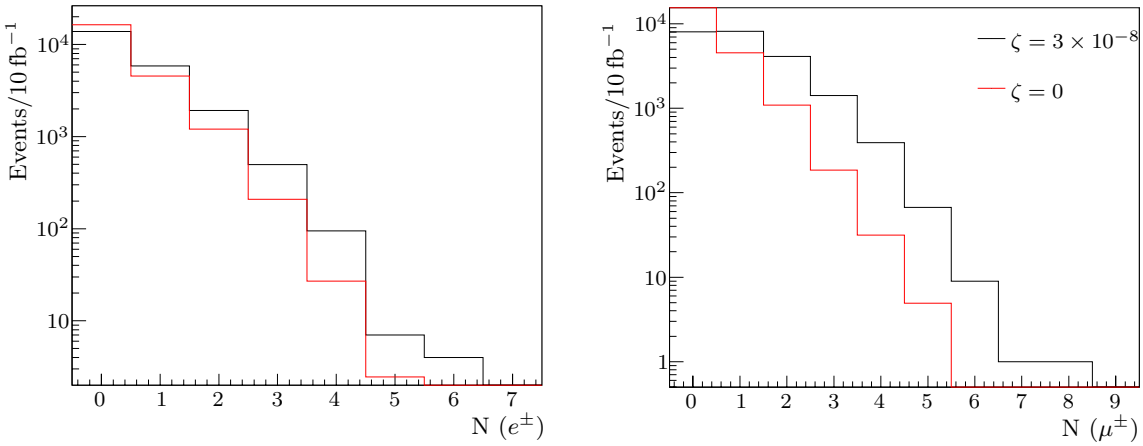

(a) Number of electrons.

(b) Number of muons.

Figure 5.8: The number of generated particles per event for the benchmark point HH27 after selection cuts described in Table 5.13. The color code for the curves in both plots is given in Fig. 5.8b. The number of events is scaled to 10 fb^{-1} at $\sqrt{s} = 7$ TeV.

5.2.3 Search Strategies

As mentioned in the previous section, one of the striking features of the presented model are events with secondary vertices and possibly many leptons in the final state. The search for a secondary vertex is crucial in order to ensure the R-parity violating nature of the decays. Possible search strategies can be optimized in order to find some of the channels described in Tables 5.9, 5.10, 5.11, and 5.12. It is remarkable that many channels allow for the full reconstruction of the neutralino mass: all decay chains including Z bosons in case of bino-like neutralino or decay chains with hadronically decaying W bosons in both bino and higgsino-like neutralino case. The reconstruction of the neutralino mass from the particles produced in the Z boson decay depends crucially on the full reconstruction of the secondary vertex, which is beyond the scope of this work[2]. This method of neutralino mass reconstruction works also in R-parity conserving models where the neutralino decays into Z boson and gravitino [245].

For example, one promising strategy in case of higgsino-like neutralino is based on events with zero jets and four leptons in the final state. Another strategy working for all ζ values considered in this work and for both higgsino and bino-like neutralino is based on *single lepton* events with some number of hard jets and missing transverse energy larger than 90 GeV. After the preselection one could look for events where the lepton is coming from a secondary vertex and try to reconstruct the W boson mass from a jet pair. In the final step one could try to reconstruct the neutralino mass from the jets selected in the previous step and the lepton. This search can be easily accommodated within the existing ATLAS search for secondary vertices [211], cf. Section 4.3.3. However, such study depends crucially on the knowledge of the detector response in the case of late decaying particles. A neutralino can decay in various detector components and lead to unusual signals. Furthermore, for such values of ζ where most decays take place not in the tracker this search would be successful only after the

[2]The four-vector pointing to the secondary vertex and the three-momenta of the leptons or jets from the Z boson provide sufficient information for the reconstruction of the neutralino mass.

experiments have gathered a very large number of inverse femtobarns of data. Additionally, the mass resolution is limited by the uncertainty in the jet energy scale and by the uncertainty in the determination of the jet momentum direction.

We will focus our study on leptonic final states from bino-like neutralino decays, which have a particularly clean signature, and reconstruct the Z boson coming from a secondary vertex. We will use only muon and track objects for which we assume to have modeled a realistic detector response (see Section 5.2.4). A possible background for this search are cosmic muons leaving no track in the detector. It is important to note that one would miss the signal in this channel entirely if one imposes a cosmic muon veto which rejects all events with muon pairs having no associated tracks (cf. [248]). While the search for secondary vertices in singe lepton events can be used for the discovery of decaying neutralinos, our study presented in the following section can be used for the determination of the neutralino wave function, since it is expected to fail in the case of the higgsino-like neutralino. Additionally, this search can be performed without the use of the tracker for the detection of secondary vertices, and hence it can lead faster to a discovery in case of the bino-like neutralino.

5.2.4 Simulation of Signal and Background

Benchmark Points

A typical set of boundary conditions for the supersymmetry breaking parameters of the MSSM at the grand unification scale is given by equal scalar and gaugino masses, $m_0 = m_{1/2}$. These boundary conditions lead to a bino-like neutralino χ_1^0 as NLSP. We choose a representative value of $\tan\beta$ and set the scalar trilinear couplings to zero,

$$A_0 = 0 \,, \quad \tan\beta = 10 \,. \tag{5.9}$$

Thus, the universal gaugino mass remains the only independent supersymmetry breaking parameter which will be varied in the present study. These boundary conditions correspond to the CMSSM choice (A) in Section 4.4.

We will ignore at this stage the recent LHC exclusion limits for the Higgs boson mass, since they can be accommodated by changing the values of m_0 and A_0, cf. Section 4.4. Furthermore, we will neglect the LHC hint for a Higgs boson with a mass of 125 GeV. On the other hand, we chose the parameter points to be still allowed after the ATLAS search for secondary vertices (cf. [211], Section 4.3.3 and Tab. 5.15), and to be consistent with our analysis in Section 4.4 . In the present study the lightest superparticle spectrum corresponds to the choice $m_0 = m_{1/2} = 270\,\text{GeV}$ (HH27). At this benchmark point the NLSP is a neutralino with mass $m_{\chi_1^0} = 105.8\,\text{GeV}$ and the lightest Higgs boson has a mass $m_h = 110.4\,\text{GeV}$.

In order to probe the region of gluino and squark masses accessible at the LHC [251], we increase the gaugino mass parameter in four steps: $m_{1/2} = 350,\ 500,\ 650,\ 800\,\text{GeV}$. Some particle masses at these points are shown in Table 5.14. For the different benchmark points the production cross sections, calculated with `PROSPINO` at $\sqrt{s} = 7\,\text{TeV}$, are given in Table 5.15.

For the R-parity breaking parameter ζ we choose the following values: $\zeta = 3 \times 10^{-8}$, $\zeta = 2 \times 10^{-8}$, 1×10^{-8}, 5×10^{-9}, 1×10^{-9}, 5×10^{-10} and 1×10^{-10}. Thus, we are probing the wide range of the R-parity breaking coupling starting right above the lower bound of $\zeta \lesssim 1.4 \times 10^{-8}$, cf. Section 4.4.1.

	GUT masses		particle masses			
	m_0	$m_{1/2}$	$m_{\chi_0^1}$	m_h	$m_{\widetilde{g}}$	$m_{\widetilde{u}}$
HH27	270	270	105.8	110.5	662.4	653.4
HH35	350	350	140.5	112.5	841.7	831.8
HH50	500	500	205.7	115.1	1170	1160
HH65	650	650	271.5	116.7	1492	1481
HH80	800	800	337.8	117.9	1809	1798

Table 5.14: Definition of the benchmark points together with some particle masses; all masses are in GeV.

	partial crosssections [fb]				
	$\sigma(\tilde{q}g)$	$\sigma(\tilde{q}\tilde{q})$	$\sigma(\tilde{q}\bar{\tilde{q}})$	$\sigma(gg)$	σ(tot) [fb]
HH27	1090 (739)	682 (570)	256 (174)	208 (83)	2236 (1566)
HH35	172 (105)	149 (126)	38 (25.2)	26 (8.47)	385 (265)
HH50	8.91 (4.36)	11.8 (10.1)	1.7 (1.02)	0.95 (0.206)	23.36 (15.7)
HH65	0.579 (0.216)	1.01 (0.877)	0.0943 (0.0458)	0.0466 (6.37×10^{-3})	1.73 (1.145)
HH80	0.0379 (0.0109)	0.0805 (0.0723)	5.37×10^{-3} (1.98×10^{-3})	2.44×10^{-3} (0.203×10^{-3})	0.126 (0.0854)

Table 5.15: Production cross sections at NLO (LO) at the benchmark points calculated with `PROSPINO`.

Major Backgrounds

Bino-like neutralino decays always have W and Z bosons in the final state (cf. Fig. 4.3) if one neglects the decays into the Higgs boson, as it is done in the present analysis. We focus on the reconstruction of Z boson decays to muon pairs. Therefore, we only consider SM backgrounds which lead to at least two muons in the final state originating from W or Z bosons:

- $t\bar{t}$ production: W bosons from top quark decays.
- Z production
- Di-boson production (WW, WZ, ZZ)
- Tri-boson production (WWW, WWZ, ZZW, ZZZ)

Table 5.16a gives an overview of the background samples used in our analysis. We have simulated 10 times more signal events for small values of ζ than for large values of ζ in order to improve the statistics. The numbers then correspond to 100, 10 fb^{-1}, respectively.

sample	σ [pb]	events	
		expected	simulated
$t\bar{t}$	163	1.6×10^5	11.3×10^6
Z	977	9.7×10^5	7×10^5
W^+W^-	44.974	4.5×10^4	$1\,000 \times 10^3$
W^+Z	11.580	17775	400×10^3
W^-Z	6.342		
ZZ	6.195	6195	150×10^3
$W^+W^-W^+$	4×10^{-2}	40	15 000
W^+W^-Z	3×10^{-2}	30	15 000
W^+ZZ	9×10^{-3}	9	15 000
ZZZ	3×10^{-3}	3	5 629

(a) Samples of SM background. The cross sections for the triboson events are calculated at the Born level with MADGRAPH, all other cross sections are taken from [234, 235, 253]. The number of expected events corresponds to an integrated luminosity of 1 fb^{-1}.

	ζ	events
HH27	$\geq 5 \times 10^{-9}$	22280
	$\leq 1 \times 10^{-9}$	222800
HH35	$\geq 5 \times 10^{-9}$	10000
	$\leq 1 \times 10^{-9}$	100000
HH50	$\geq 5 \times 10^{-9}$	10000
	$\leq 1 \times 10^{-9}$	100000
HH65	$\geq 5 \times 10^{-10}$	10000
	1×10^{-10}	100000
HH80	all ζ	10000

(b) Samples of signal events for different benchmark points (see Table 5.14) and $\zeta = \alpha \times 10^{-9}$ ($\alpha = 0.1, 0.5, 1, 5, 10, 20, 30$).

Table 5.16: Monte Carlo samples of SM background and signal events used for our analysis.

We assume that pure QCD background can be efficiently suppressed in multi-lepton final states with high transverse momentum (cf. [249, 252]). It turns out that $t\bar{t}$ is the most important background. Since, consequently, the best statistics is needed for this channel, we have simulated about hundred times more events than expected at 1 fb^{-1}. This is also roughly true for all other backgrounds, except for the Z boson production where the number of simulated events corresponds to the number of expected events at 1 fb^{-1}.

Event Simulation

All Monte Carlo samples were generated using CTEQ6L1 parton distribution functions. For the simulation of the background we used MADGRAPH 4.4.44 interfaced with PYTHIA 6.4.22.

Our simulation of the signal events relied on the following procedure. First, supersymmetric mass spectra were calculated with a modified version of SOFTSUSY assuming mSUGRA boundary conditions and R-parity conservation. The latter assumption is justified due to the tiny amount of R-parity breaking in our model. The SOFTSUSY version was modified in order to produce additionally to the spectrum, the R-parity violating neutralino decay width and branching ratios according to eq. (4.84), except for the decay channel into the Higgs boson and neutrino. The SOFTSUSY mass spectra were fed into SDECAY via the MADGRAPH homepage [254] in order to calculate the decay widths of the SUSY particles (besides the neutralino LSP). In the next step neutralino decay information was included into the SDECAY output. The signal process (production of gg, $g\widetilde{q}$, $\widetilde{q}\widetilde{q}$ and $\widetilde{q}\overline{\widetilde{q}}$) was simulated with MADGRAPH and then given to PYTHIA for computation of all subsequent decays according to the SDECAY output as well as for parton showering and hadronization. Table 5.16b shows the signal samples used in our analysis.

The generic detector simulation DELPHES, tuned to the CMS detector, was used in order to

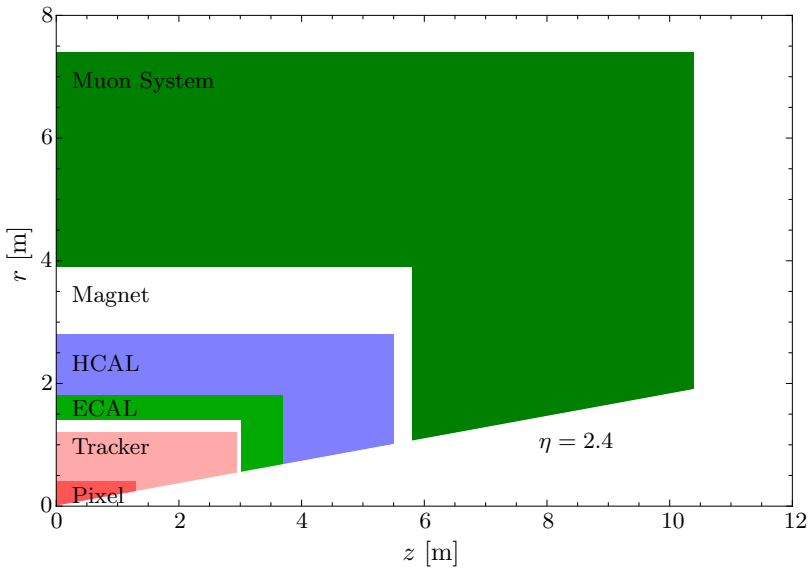

Figure 5.9: Layout of one quarter of the generic detector used for particle identification.

account for effects of event reconstruction at the detector level. However, DELPHES describes the detector geometry solely in terms of angular variables, i.e. the detector is stretched infinitely in the radial direction. This approximation is sufficient for most studies involving prompt decays but is untenable in the case of late decaying particles. We overcome this obstacle by adding vertex information from particles at the generator level to objects at the detector level. Usually, this information is provided by the detector simulation. Our procedure is described in detail in the following section. We emphasize that a full detector simulation, which includes vertex reconstruction, needs to be done to improve our analysis.

Muon Reconstruction Process

Particles produced in the late decay of the neutralino will not be properly reconstructed in a real detector if the position of their vertex is beyond or even within the crucial detector component responsible for the respective identification. For example, an electron produced inside of the electromagnetic calorimeter will leave no track in the tracker and will therefore be identified as a photon or jet. In order to simulate the detector response to such events, we use a detector geometry in the (r, z) coordinates, which is inspired by the CMS detector at the LHC (see Fig. 5.9). The angular position of the detector components is given by the CMS tune of DELPHES.

In order to be as conservative as possible, we only use muon and track objects for the present analysis, since these objects allow a simple simulation of detection efficiency losses due to the finite size of the detector. Namely, we assume that a muon can be reconstructed as long as its vertex is in front of the muon chambers, and analogously a track can be reconstructed if it originates approximately in the first third of the tracker (This region is called pixel detector in Fig. 5.9). For the matching between generator level particles and objects reconstructed by DELPHES we use the distance in pseudorapidity η and azimuthal angle ϕ, defined as $\Delta R = \sqrt{(\Delta\phi)^2 + (\Delta\eta)^2}$.

In the following we will call generator level muons, produced by PYTHIA, *GenMuons*,

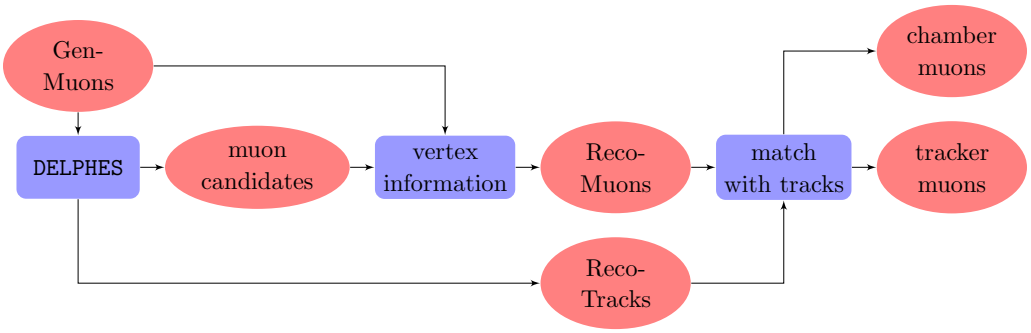

Figure 5.10: Muon reconstruction process.

muons reconstructed initially by DELPHES *muon candidates*, and track objects reconstructed by DELPHES *RecoTracks*. Only GenMuons and RecoTracks have the coordinates of their vertex.

First, we perform the following p_T cuts on muon candidates and RecoTracks:

- $p_T(\mu) > 20\,\text{GeV}$,
- $p_T(\text{Track}) > 15\,\text{GeV}$.

These cuts are guided by our SUSY search strategy (cf. Section 5.2.5), since we expect that muons coming from Z boson decay have high p_T, and a sufficiently high p_T cut can effectively suppress QCD fake leptons. Furthermore, DELPHES itself reconstructs only muons with p_T above 10 GeV. Additionally, these cuts were optimized in order to get a realistic muon reconstruction efficiency, see next section.

In the second step vertex information is added to the muon candidates by matching with GenMuons:

- A GenMuon is selected for matching with muon candidates if its vertex lies in front of the muon system : $r_\mu = \sqrt{x^2 + y^2} < 4000\,\text{mm}$, $|z_\mu| < 6000\,\text{mm}$ (see Fig. 5.9).
- The ΔR distance between each selected GenMuon and all muon candidates is computed.
- A GenMuon vertex is added to the muon candidate closest in ΔR, if $\Delta R < 0.1$ and GenMuon and muon candidate have the same charge.
- Muon candidates with added vertex information are called *RecoMuons*.

In the final step, muons with or without signal in the tracker are distinguished:

- A RecoTrack is selected for matching with RecoMuons if the track vertex lies in the following range: $r_T < 400\,\text{mm}$, $|z_T| < 1300\,\text{mm}$.
- Each selected RecoTrack is matched with the RecoMuon closest in ΔR, if $\Delta R < 0.1$.
- Matched RecoTracks and RecoMuons are called *tracker muons*. RecoMuons which cannot be matched with RecoTracks are called *chamber muons*. Each RecoMuon is therefore either a tracker muon or a chamber muon.

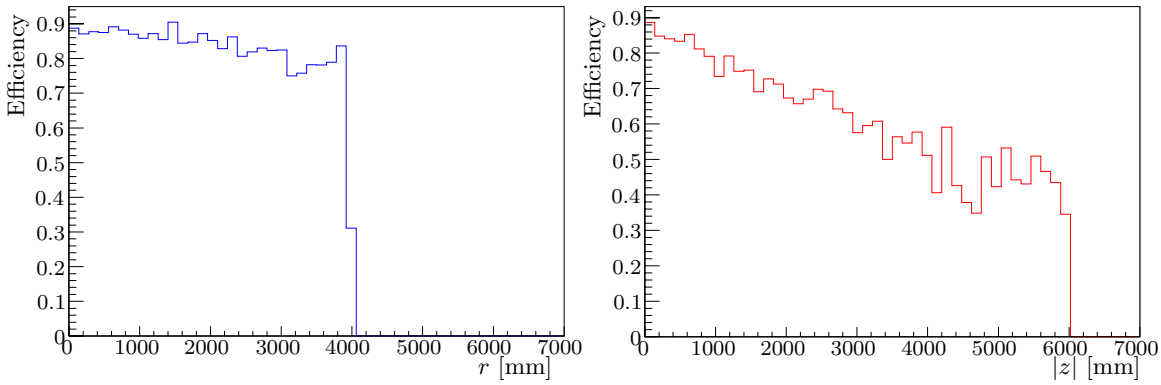

Figure 5.11: Muon reconstruction efficiency for the benchmark point HH27.

After the reconstruction procedure one is left with two kinds of muon objects: (i) chamber muons which have no track in the tracker and are therefore reconstructed solely by the muon chambers, and (ii) tracker muons which have a track. The muon reconstruction process is depicted in Fig. 5.10. The ΔR matching condition has been optimized in order to get a realistic muon reconstruction efficiency (see next section).

Muon Reconstruction Efficiency

In order to test our method of obtaining physically sensible objects, we compute the muon reconstruction efficiency in the following way:

- Muons are created as described above.
- GenMuons are matched with RecoMuons without any constraints on the position of the GenMuon vertex.
- The number of successfully matched objects is compared binwise (in bins of r and $|z|$) with the number of all GenMuons.

The second condition is necessary in order to see whether the assignment between RecoMuons and GenMuons is correct. Since the matching procedure only relies on angular variables, it is possible that a RecoMuon originally matched with a GenMuon created in front of the muon chamber belongs in fact (i.e. has smaller angular distance) to a GenMuon coming from a decay inside the muon chamber or even outside of the detector. Such wrong matchings would be seen in the efficiency plot as efficiencies not equal to zero in regions where muons could not be detected by the detector defined above ($r_\mu > 4000\,\text{mm}$, $|z_\mu| > 6000\,\text{mm}$).

Fig. 5.11 shows the computed muon efficiency in bins of r and $|z|$. As expected one sees a sharp decline in efficiency in the r plot at $r_\mu = 4000\,\text{mm}$, where the hard cut applies. The decline in the z plot is gradually, since physical particles have to fulfill both r and $|z|$ criteria. The particles originating at small values of r and large values of $|z|$ are not reconstructed due to the limited pseudorapidity coverage of the muon detector. The efficiency stays at zero beyond $r = 4000\,\text{mm}$ and $|z| = 6000\,\text{mm}$ as expected, confirming our method of muon reconstruction. We expect that the computed muon efficiency agrees within 15 % with efficiencies of present LHC detectors including losses due to muon-jet separation requirements.

5.2.5 Search for the Neutralino Decay $\chi_1^0 \to Z\nu$

As described in Section 5.2.3, our study is focused on the channel $\chi_1^0 \to Z\nu \to \mu^+\mu^-\nu$. This channel possesses certain physical and technical advantages. On the physical side reliable muon identification is possible already in the early stage of the LHC data taking and one can assume that QCD background can hardly fake two muons at the same time. Furthermore, this signal leads to spectacular events and has no easily identifiable SM background at all, as shown in this section. Additionally, the muon chamber is the detector component which is farthermost away from the primary vertex and hence one can expect that it will be possible to detect a significant number of clean late time decays even for very small R-parity breaking. On the technical side, muons seem to be the simplest objects for which a realistic detector response can be modeled within `DELPHES` (see Section 5.2.4), due to the limitations of this simulation in the presence of secondary vertices.

The spectacular feature of this signal are opposite sign muon pairs with invariant mass close to the Z boson mass, which have either associated tracks in the tracker with clearly visible secondary vertices or no associated tracks at all. Such muon pairs can only be hardly generated by usual SM background as it will be shown in the following. However, a similar signal can arise from cosmic muons traversing the detector. We could not create a Monte Carlo background sample for cosmic muons, and we simply assume that such background can be suppressed by use of the full timing information of the event: cosmic muons will first cause a signal in the muon chamber which is closest to the ceiling of the experimental hall followed by a signal in the opposite direction.

An intrinsic background for the presented search are muon pairs from R-parity violating decays, where one muon is coming from the W boson decay while the other muon is coming either from the neutralino decay into the W boson in either of the two branches or from the W or Z boson decay in the second branch, cf. Fig. 5.5. This background can be suppressed if one has access to the corresponding tracks by demanding that both of them originate from the same vertex. In the case of muons without tracks this background is irreducible. However it belongs itself to the signal one is looking for.

Event Selection

In order to find the signal we now employ a series of simple cuts on the reconstructed objects (muons, tracker muons, and chamber muons). As we will see, already with an integrated luminosity of only 1 fb^{-1} at $\sqrt{s} = 7\,\text{TeV}$ a discovery of the benchmark scenario HH27 with $\zeta = 3 \times 10^{-8}$ is possible.

First, we perform a selection cut on the number of muons in the event:

- $N(\text{muons}) \geq 2$.

We define two event classes depending on the number of tracker muons:

- Class 1: event contains at least two tracker muons $N(\text{tracker muons}) \geq 2$.
- Class 2: otherwise.

From the description of the signal presented above, we implement additionally two sets of cuts depending on the class of the event. The cuts for Class 1 events are:

	background				signal	
	$t\bar{t}$	Z	di-	tri-	ζ	
			boson		3×10^{-8}	10^{-9}
before cuts	11300000	700000	1550000	50629	22280	220000
$N(\text{muons}) \geq 2$	89951	9458	16586	1506	2912	4404
Is Class 1	89951	9458	16586	1506	1049	4342
$80\,\text{GeV} < M_{\mu^+\mu^-} < 100\,\text{GeV}$	12654	9118	11294	1051	195	980
$d(\text{Vertex}) > 5\,\text{mm}$	39	0	0	0	49	13
$\Delta d(\text{Vertex})_{ij} < 5\,\text{mm}$	1	0	0	0	36	0
Is Class 2	89950	9458	16586	1506	2876	4404
$N(\text{chamber muons}) \geq 2$	0	0	0	0	1049	18
$80\,\text{GeV} < M_{\mu^+\mu^-} < 100\,\text{GeV}$	0	0	0	0	138	2
Total	1	0	0	0	174	2

Table 5.17: Cut flow for HH27 at $\sqrt{s} = 7\,\text{TeV}$. The number of signal events for $\zeta = 3 \times 10^{-8}$ ($\zeta = 1 \times 10^{-9}$) corresponds to an integrated luminosity of $10\,\text{fb}^{-1}$ ($\approx 100\,\text{fb}^{-1}$).

- All possible invariant masses of opposite sign tracker muons are computed. An event passes the cut if at least one invariant mass is in the range of the Z boson mass: $80\,\text{GeV} < M_{\mu^+\mu^-} < 100\,\text{GeV}$. If the event contains more than one appropriate combination of the tracker muons, the muons from the combination with invariant mass closest to the Z boson mass are selected for further analysis.
- $d(\text{Vertex}) > 5\,\text{mm}$: Each of the tracks associated with the two selected tracker muons should have a vertex which is further than 5 mm away from the primary vertex. This value is approximately one order of magnitude larger than the current resolution of the inner tracker (cf. [252, 255]).
- $\Delta d(\text{Vertex})_{ij} < 5\,\text{mm}$: The distance between the two track vertices should be less than 5 mm.
- If the event fails one of the cuts it is classified as a Class 2 event.

The cuts for Class 2 events are:

- $N(\text{chamber muons}) \geq 2$: If an event has less than two tracker muons, it should have at least two chamber muons.
- All possible invariant masses of opposite sign chamber muons are computed. An event passes the cut if at least one invariant mass is in the range of the Z boson mass: $80\,\text{GeV} < M_{\mu^+\mu^-} < 100\,\text{GeV}$.

Since each Class 1 event is classified as a Class 2 event if it fails one of the cuts, no signal event is discarded because of the presence of muons with tracks not coming from neutralino decay.

Most events will fall into the second class. The analysis is then very simple and amounts to the search for events with muons without associated track in which the invariant mass of a

muon pair lies in the Z boson mass range. The cut flow is given in Table 5.17. As expected, no background events survived the cuts (assuming integrated luminosity of 1 fb^{-1}), since no standard model process should produce secondary vertices so far away from the primary interaction point. One background event from $t\bar{t}$ production survives the cut, assuming evaluation of 100 fb^{-1} of data. This event could originate from highly boosted B meson decay into a final state containing two muons. We conclude that SM contributions to the selected events would be vary rare. However, the major uncertainty in this study, the number of the background events from cosmic muons, cannot be estimated with the present software. Therefore, a full fledged analysis with full detector simulation taking into account the cosmic muon background is needed. In the following, we assume that this background can be efficiently suppressed with the full timing information of the event as described in the introduction to Section 5.2.5. Furthermore, we only estimate the systematic uncertainty due to the background and neglect statistical errors and the uncertainty of the muon reconstruction efficiency.

The significance of the signal is computed with the profile likelihood method [256] incorporated in the `SIGCALC` code [257]. We assume an integrated luminosity of $1\,\text{fb}^{-1}$ at $\sqrt{s} = 7\,\text{TeV}$ LHC and a ten times higher Monte Carlo luminosity $\mathcal{L}_{MC} = N_b/\sigma_b = 10\,\text{fb}^{-1}$ for all the background events. At this integrated luminosity 17 signal events and no background events survive the cuts, which corresponds to a significance $Z_{PL} = 9.03$. Instead, if one makes the pessimistic estimate that 1 background event from the cosmic muons passes the cuts one finds a significance $Z_{PL} = 6.39$. Therefore, we conclude that at the benchmark point HH27 with $\zeta = 3 \times 10^{-8}$, R-parity breaking neutralino decays can be discovered with the first inverse femtobarn of LHC data. Note that since the actual amount of data collected by the LHC experiments exceeds 1 fb^{-1} , it is crucial that they perform new searches for secondary vertices.

Discovery Reach at the LHC

In the previous section we have studied in detail the benchmark point HH27: $m_{1/2} = m_0 = 270\,\text{GeV}$, which yields the rather small superparticle masses $m_{\chi_1^0} = 106\,\text{GeV}$, $m_g \simeq 660\,\text{GeV}$ and $m_{\tilde{q}} \simeq 650\,\text{GeV}$ for the light quark flavors (cf. Table 5.14). From the decay rates given in Section 4.2.2 and the phase space factors shown in Fig. 4.14a one obtains for decay length and branching ratio into Z boson/neutrino final states:

$$c\tau_{\chi_1^0} \simeq 31\,\text{m}\left(\frac{\zeta}{10^{-8}}\right)^{-2}, \quad BR(\chi_1^0 \to Z\nu) \simeq 0.17\,. \tag{5.10}$$

Based on the production cross sections listed in Table 5.15 an integrated luminosity $\mathcal{L} = 10\,\text{fb}^{-1}$ yields about 22000 events and therefore 44000 NLSPs.

We have studied this benchmark point for two different values of the R-parity breaking parameter: $\zeta = 3 \times 10^{-8}$ and $\zeta = 1 \times 10^{-9}$. For the larger value of ζ one has $c\tau_{\chi_1^0} \simeq 3.4\,\text{m}$. Hence, essentially all neutralinos decay inside the detector, most of them close to the origin. The spacial distribution of secondary vertices is displayed in the contour plot Fig. 5.12. Using $BR(Z \to \mu^+\mu^-) \simeq 0.034$ and the branching ratio given in Eq. (5.10), one concludes that there are 251 events with a secondary χ_1^0-decay vertex, which contain a $\mu^+\mu^-$ pair with $M_{\mu^+\mu^-} \simeq M_Z$. This is consistent with the simulation which yields 282 events in the detector volume (cf. Fig. 5.13) and 174 events passing all cuts (cf. Table 5.17). The locations of the secondary vertices of these events are shown in Fig. 5.13.

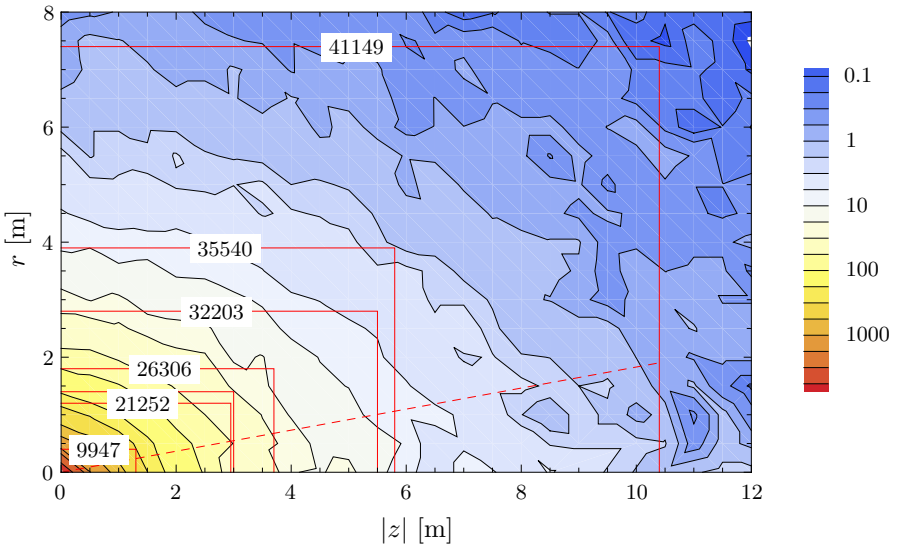

Figure 5.12: Contour plot for the density of neutralino decays inside the detector per m^{-3}; the numbers on the horizontal boundaries of the detector components correspond to the total number of decays in the enclosed volume; $m_{1/2} = m_0 = 270\,\mathrm{GeV}$, $\zeta = 3 \times 10^{-8}$ and $\mathcal{L} = 10\,\mathrm{fb}^{-1}$.

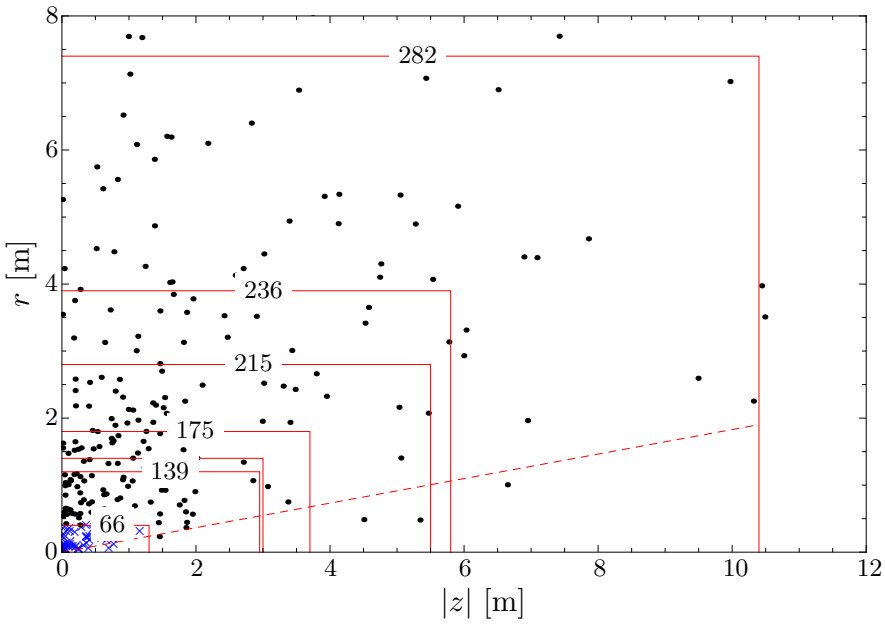

Figure 5.13: Location of secondary vertices for the decays $\chi_1^0 \to Z\nu$ with $Z \to \mu^+\mu^-$ (blue crosses: inside pixel detector, black dots: outside pixel detector); the numbers on the horizontal boundaries of the detector components give the number of decays in the enclosed volume; $m_{1/2} = m_0 = 270\,\mathrm{GeV}$, $\zeta = 3 \times 10^{-8}$ and $\mathcal{L} = 10\,\mathrm{fb}^{-1}$.

For the smaller value of the R-parity breaking parameter, $\zeta = 1 \times 10^{-9}$, the decay length increases to $c\tau_{\chi_1^0} \simeq 3.1\,\mathrm{km}$. Now most neutralino NLSPs decay outside the detector. This is apparent from Fig. 5.14 where the total number of decays in the different subvolumina of the detector are given. Compared to $\zeta = 3 \times 10^{-8}$, the number of decays inside the detector is smaller by a factor ~ 200, which roughly corresponds to the ratio of the decay lengths, as suggested in [214].

According to the simulation described in the previous section, for $\zeta = 1 \times 10^{-9}$ an integrated luminosity of $100\,\mathrm{fb}^{-1}$ is needed to obtain 2 signal events $\chi_1^0 \to Z\nu \to \mu^+\mu^-\nu$, which is consistent with the naive estimate within the statistical uncertainty and the detector efficiency. The number is very small compared to the total number of about 1000 decays in the detector volume used in the present analysis (cf. Section 5.2.4), which is a consequence of the tiny branching ratio into the chosen specific final state. It is likely that a substantially larger fraction of the events can be used in the search for a decaying neutralino. In [214] it has been argued that already 10 χ_1^0 decays inside the detector may be sufficient for the discovery of a decaying NLSP, which would require an integrated luminosity of only $1\,\mathrm{fb}^{-1}$. It remains to be seen whether for events with a secondary vertex and jets, signal and background can be sufficiently well separated.

Let us now consider the benchmark point HH50: $m_{1/2} = m_0 = 500\,\mathrm{GeV}$, which implies the heavier superparticle masses $m_{\chi_1^0} = 206\,\mathrm{GeV}$ and $m_g \simeq m_{\tilde{q}} \simeq 1200\,\mathrm{GeV}$ for the light quark flavors (cf. Table 5.14). The phase space suppression for gauge boson channels is now negligible, $f_W \simeq f_Z \simeq 1$, while the Higgs channel is still suppressed. Thus, one obtains for decay length and branching ratio into Z boson/neutrino final states:

$$c\tau_{\chi_1^0} \simeq 5.4\,\mathrm{m}\left(\frac{\zeta}{10^{-8}}\right)^{-2}, \quad BR(\chi_1^0 \to Z\nu) \simeq 0.32\ . \tag{5.11}$$

The BR into the Z boson is 14% too large, since the Higgs channel was excluded. However, the error is acceptable. The total production cross section for these heavier gluino/squark pairs is about two orders of magnitude smaller (cf. Table 5.15), and therefore an integrated luminosity $\mathcal{L} = 10\,\mathrm{fb}^{-1}$ only yields 460 NLSPs.

We have studied this benchmark point again for the two different values of the R-parity breaking parameter $\zeta = 3 \times 10^{-8}$ and $\zeta = 1 \times 10^{-9}$. For the larger value of ζ one has $c\tau_{\chi_1^0} \simeq 60\,\mathrm{cm}$, and essentially all neutralinos decay inside the detector. The branching ratio into the considered final state is now somewhat larger, $BR(\chi_1^0 \to Z\nu \to \mu^+\mu^-\nu) \simeq 0.01$, so that one expects about 5 events with this final state, which is consistent with our simulation. Hence, for this larger value of the R-parity breaking parameter and this benchmark point, the discovery of a decaying NLSP appears feasible already in the early phase of the LHC.

For $\zeta = 1 \times 10^{-9}$, the decay length is $c\tau_{\chi_1^0} \simeq 540\,\mathrm{m}$ and most neutralino NLSPs decay outside the detector. The spacial distribution of secondary vertices inside the detector, in total 12 for $10\,\mathrm{fb}^{-1}$, is shown in Fig. 5.15. Due to the 1 % branching ratio into the $Z\nu \to \mu^+\mu^-\nu$ final state one then estimates that $1000\,\mathrm{fb}^{-1}$ will be needed for a discovery, which is consistent with our simulation.

In Fig. 5.16 we have summarized the results of our simulations for the decay chain $\chi_1^0 \to Z\nu$ with $Z \to \mu^+\mu^-$. The benchmark points HH27–HH80 correspond to gluino and squark masses ranging from 650 GeV to 1800 GeV (cf. Table 5.14). The bands reflect the different number of events required for a 5σ discovery depending on the simulated background. The central value corresponds to 6 signal events (with luminosity $\mathcal{L}$) with no background events for a

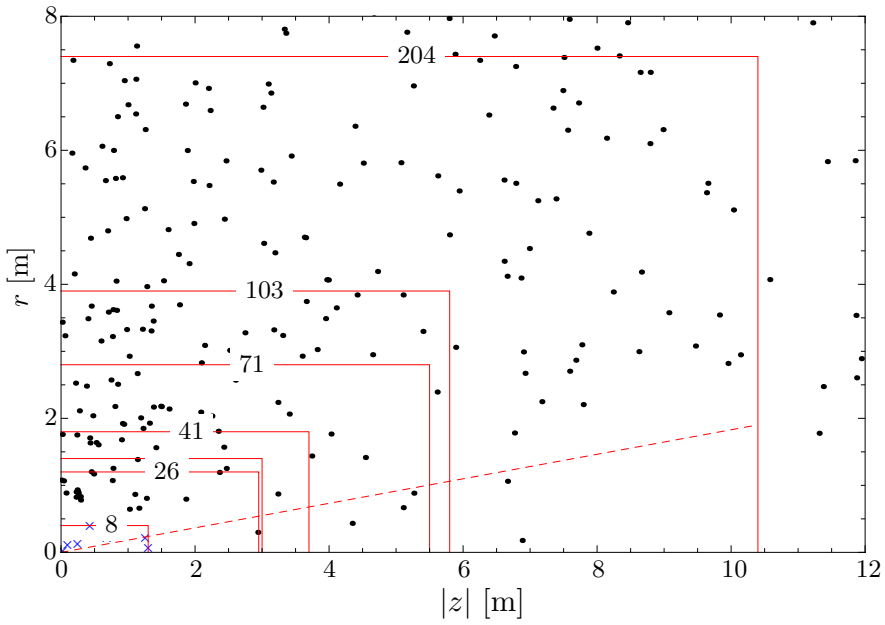

Figure 5.14: Location of all neutralino decays inside of the detector (blue crosses: decays inside pixel detector; black dots: decays outside pixel detector); the numbers on the horizontal boundaries of the detector components correspond to the total number of decays in the enclosed volume; $m_{1/2} = m_0 = 270\,\text{GeV}$, $\zeta = 1 \times 10^{-9}$ and $\mathcal{L} = 10\,\text{fb}^{-1}$.

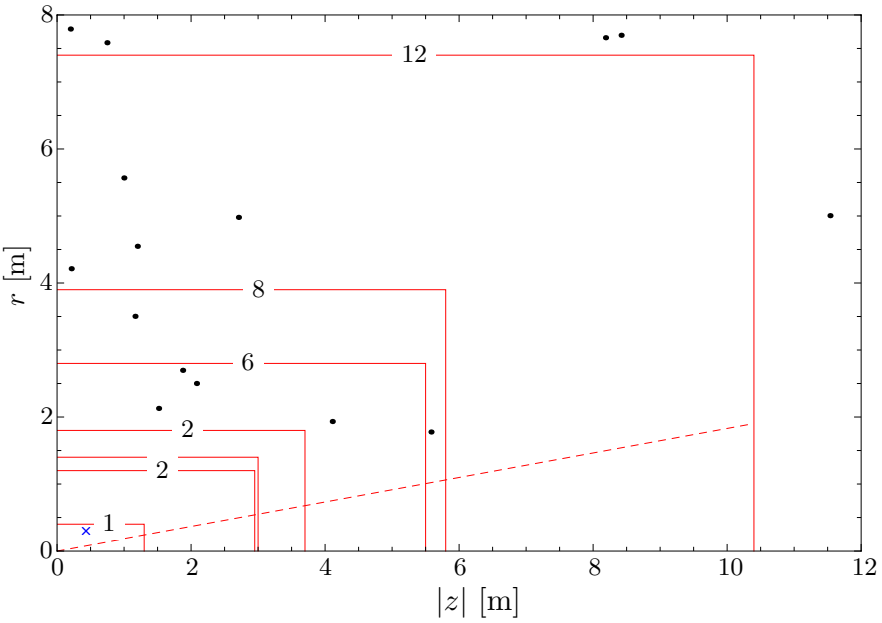

Figure 5.15: Location of all neutralino decays inside of the detector (blue cross: decay inside pixel detector; black dots: decays outside pixel detector); the numbers on the horizontal boundaries of the detector components correspond to the total number of decays in the enclosed volume; $m_{1/2} = m_0 = 500\,\text{GeV}$, $\zeta = 1 \times 10^{-9}$ and $\mathcal{L} = 10\,\text{fb}^{-1}$.

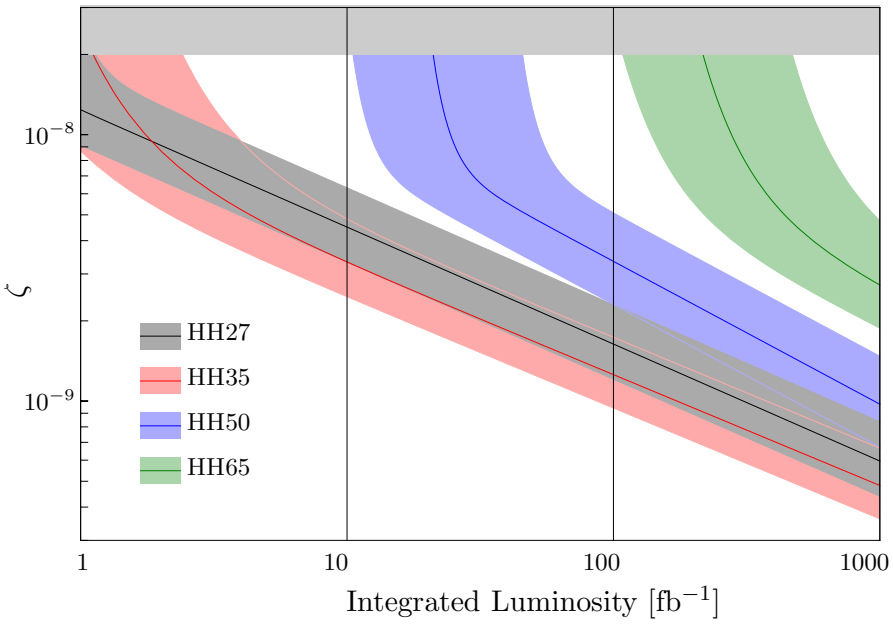

Figure 5.16: 5σ discovery reach in ζ for quasi-stable neutralino NLSPs via the decays $\chi_1^0 \to Z\nu$ with $Z \to \mu^+\mu^-$. The different bench mark points correspond to gluino and squark masses between 650 GeV and 1800 GeV; the bands represent different assumptions about the background (see text).

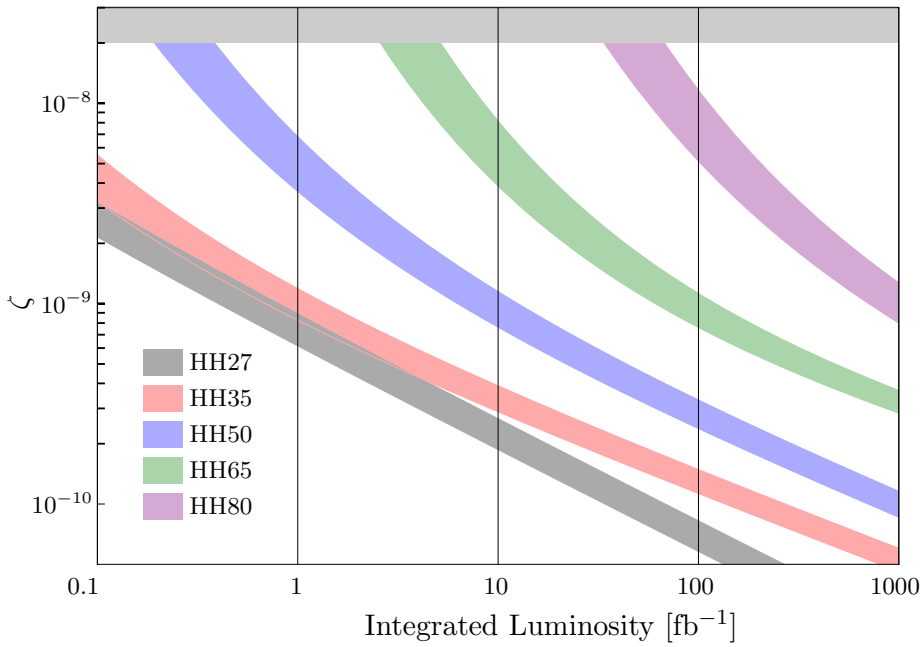

Figure 5.17: Estimate of the 5σ discovery reach in ζ for quasi-stable neutralino NLSPs at the LHC; the lower (upper) boundary of the bands corresponds to 10 (20) decays inside the detector. The different bench mark points correspond to gluino and squark masses between 650 GeV and 1800 GeV.

simulated luminosity of $10 \times \mathcal{L}$; the lower (upper) boundary represents 3 (13) signal events (with luminosity $\mathcal{L}$) with no (1) background event for a simulated luminosity of $100 \times \mathcal{L}$ ($10 \times \mathcal{L}$). Since we expect at least 1 background event from $t\bar{t}$ at 100 fb^{-1}, the upper bounds represent a realistic estimate of the discovery reach for such large luminosities. We conclude that with 10 fb^{-1} a 5σ discovery of a quasi-stable neutralino is possible for squark and gluino masses of 830 GeV (cf. HH35) and an R-parity breaking parameter $\zeta = 3 \times 10^{-9}$, which is one order of magnitude smaller than the present astrophysical bound, cf. Section 4.3.

We expect that the sensitivity in the parameter ζ can be significantly improved if also neutralino decays with jets are taken into account. Fig. 5.17 represents an estimate of the discovery reach for quasi-stable neutralino NLSPs at the LHC, assuming 10–20 decays inside the detector (cf. [214]). The parameter space, which can be probed, is now significantly extended. As an example, with 10 fb^{-1} and squark and gluino masses of 830 GeV (cf. HH35), one is now sensitive to $\zeta = 3 \times 10^{-10}$, which lies two orders of magnitude below the present astrophysical bound. Correspondingly, for heavier gluinos and squarks, $m_g \simeq m_{\tilde{q}} \simeq 1480$ GeV (cf. HH65), one can probe values of the R-parity breaking parameter down to $\zeta = 3 \times 10^{-9}$.

5.3 Summary

Supersymmetry could still be just around the corner, even though the corner has now moved a bit. Should LHC do not observe candidate SUSY signatures within the next year, it will become clear that SUSY models studied in the last decades are not realized in nature. It is therefore important to study the collider characteristics of physically well motivated scenarios beyond the border of simplified models, designed for their simple collider phenomenology, or simple ad-hoc parametrizations such as the CMSSM. The models considered in the present work are supersymmetric extensions of the Standard Model consistent with primordial nucleosynthesis, thermal leptogenesis and either neutralino or gravitino dark matter. In both cases supersymmetry can be easily hidden from the usual SUSY searches relying on missing transverse energy signature and long decay chains involving many jets.

In the *Higgsino World* scenario the R-parity is conserved, and the gravitino is either very heavy or the lightest supersymmetric particle. In both cases the phenomenology at colliders is governed by the higgsino-like neutralino (N)LSP. Taking the LHC hint for the Higgs boson mass seriously, the AMSB and hybrid gauge-gravity mediation model predict that all colored particles are too heavy to be produced at the LHC. The directly produced higgsino pairs have no p_T and decay invisibly, since the mass differences between charged and neutral states are to small to produce detectable leptons. The only possibility for the discovery is then the monojet (monophoton) signature, where the missing transverse momentum arises from the initial state radiation.

Allowing for lower Higgs boson masses, the stops may be accessible at the LHC in the hybrid gauge-gravity mediation model. Then, with early LHC data, evidence for this model could be found in jets plus missing transverse energy searches. Moreover, with dedicated cuts and using also the leptonic search channels, it will be possible to distinguish this model from more commonly studied standard SUSY frameworks, such as the CMSSM or a bino-LSP simplified model.

If *R-parity is violated* in nature and gravitino is the LSP, the LHC phenomenology is governed by the NLSP decays. Even in the case of a very long lived NLSP, enough particles decay inside of the detector to change the missing transverse energy signature, such that usual

searches become ineffective. If the NLSP is higgsino-like neutralino, some of the decay chains have additionally no jets in the final state.

Nevertheless, the LHC experiments could discover these models by analyzing events involving secondary vertices far away from the primary interaction point. Irrespectively of the wave function of the neutralino, a search for secondary vertices in single muon events seems promising. On the other hand, one can focus on events with a clean signature: cascade processes with jets where one of the produced neutralino NLSPs decays into Z boson and neutrino, with a subsequent decay of the Z boson into a muon pair. Such events are expected if the neutralino is bino-like, and therefore this search can be used to reject the higgsino-like neutralino hypothesis. The results for the discovery reach for quasi-stable neutralino NLSPs in this case roughly agree with the simple estimates which one obtains from the branching ratios into the $Z(\mu^+\mu^-)\nu$ final state together with the assumption that these events are nearly background free. It is remarkable that already with $10\,\mathrm{fb}^{-1}$ a 5σ discovery is possible for squark and gluino masses of 830 GeV and an R-parity breaking parameter $\zeta = 3 \times 10^{-9}$, which is one order of magnitude smaller than the present astrophysical bound.

Chapter 6

Conclusions and Outlook

The start of operation of the Large Hadron Collider marks a new milestone in the exploration of the microcosm which began more than one hundred years ago with the discovery of the atomic nucleus by Ernest Rutherford. The LHC enters new territory in terms of energy and therefore length scale, and it is expected that it not only reconfirms the current paradigm by finding the Higgs boson, but also finds new phenomena expected to be there from theoretical considerations such as the hierarchy problem. The most studied extension of the Standard Model stabilizing the Fermi scale is supersymmetry. Besides having rich collider phenomenology, SUSY also solves one of the astrophysical puzzles providing a number of possible dark matter candidates.

However, in spite of numerous predictions for an early discovery, the LHC experiments see no hints for popular SUSY models so far. The main result of the present work is the conclusion that supersymmetry is naturally hidden from the usual search strategies in models aiming for consistency between leptogenesis, primordial nucleosynthesis and dark matter constraints, especially in the light of the recent LHC hint for the value of the Higgs mass.

Locally supersymmetric extensions of the Standard Model predict the existence of the spin-3/2 superpartner of the graviton - the gravitino. Assuming that the baryon asymmetry of the universe is created via the leptogenesis process, which needs high temperature in the plasma, gravitinos are produced in thermal scatterings in the early universe. If the mass of the gravitino is very large, it decays before the onset of big bang nucleosynthesis. If the lightest supersymmetric particle is then the neutralino, it serves as a perfect WIMP dark matter candidate. On the other hand, the gravitino itself can be the lightest supersymmetric particle and hence a dark matter candidate. In this case, the next-to-lightest supersymmetric particle has either to decay before the BBN, or its density should be diluted, for example via late-time entropy production. The first condition can be satisfied if the R-parity is slightly violated. Although, the gravitino is no longer stable in this case, its lifetime exceeds the age of the universe, since its decays are doubly suppressed by the Planck mass and the small R-parity breaking parameter. Therefore, the gravitino remains a viable dark matter candidate.

The present thesis investigates in detail the phenomenological consequences of locally supersymmetric models satisfying the conditions sketched above. After a short review of the main arguments in favor of supersymmetry, we have presented the formalism needed for the construction of locally supersymmetric extensions of the Standard Model. Since the exact SUSY breaking mechanism is unknown, we have reviewed a number of models leading to supersymmetric spectra consistent with cosmology.

In the AMSB case, the gravitino is very heavy and the only particles accessible at the LHC are the various higgsino states, the higgsino-like neutralino being the dark matter candidate. In the hybrid gauge-gravity mediation model of SUSY breaking, the gravitino is the dark matter candidate, but otherwise the spectrum is similar to the AMSB case, especially if one demands the Higgs mass to be 125 GeV. Relaxing this requirement, the model can accommodate a stop which could be produced at the LHC. The decays of the higgsino-like neutralino NLSP pose no problems for big bang nucleosynthesis either because they are sufficiently fast if R-parity is violated, or because the density of neutralinos is diluted by the additional entropy production. If one allows for R-parity violation and neglects the latest LHC hints for the Higgs boson mass, some parts of the parameter space of mSUGRA models, which are otherwise excluded, become also viable.

The realization that R-parity violation can make a number of models with gravitino dark matter cosmologically consistent is the reason for a detailed study of R-parity breaking in this work. Having presented R-symmetry and argued why R-parity was introduced, we then have shown that there are no a priori reasons for it to be conserved. Afterwards, we have introduced various patterns of R-parity breaking. Our focus has lied on the bilinear breaking scenario, which has been analyzed in a basis of scalar $SU(2)$ doublets, where all bilinear terms vanish. In this basis one has R-parity violating Yukawa, gaugino and gravitino couplings. They are given in terms of ordinary Yukawa couplings and 9 R-parity breaking parameters ϵ_i, ϵ_i' and ϵ_i'', $i = 1, ..., 3$, which are constrained by the flavor symmetry of our model. The R-parity violating couplings include terms proportional to the up-quark Yukawa couplings, which were not taken into account in previous analyses. Using this approach, we have been able to identify a number of gravitino decay channels including all channels found in the literature. Hereafter, we have presented an explicit model giving rise to small R-parity breaking couplings from spontaneous breaking of $B - L$.

The cosmologically consistent SUSY breaking models studied in the present work lead either to a (bino or higgsino-like) neutralino or a scalar tau NLSP, assuming the scenario with gravitino dark matter. If R-parity is broken, the collider phenomenology of these models is governed by the decays of the NLSPs into the particles of the Standard Model. On the other hand, the decays of the gravitino can lead to a signature in cosmic rays. Using our description of bilinear R-parity breaking, we have obtained to good approximation analytical expressions for the R-parity breaking matrix elements of the neutral current, the charged current and the supercurrent. Using these matrix elements, as well as the trilinear R-parity breaking couplings, we have explicitly computed R-parity violating gravitino, neutralino and stau decay widths. In case of the gravitino, we were interested only in the decay into photon and neutrino. In case of the neutralino, we have given the results for the bino and higgsino-like neutralino case. All computations, including the gravitino decay, were made using the two-component formalism for fermions, which is summarized in the appendices. This summary includes also the new developed tools needed for the computations of gravitino decays.

Having calculated the decay widths of the relevant particles, we have recapitulated the cosmological bounds on the size of R-parity violation ($10^{-13} \lesssim \epsilon \lesssim 10^{-6}$) and have compared these bounds with the results obtained indirectly from various processes and with the direct searches at colliders. The most promising study, which is able to reach the parameter region favored by cosmology, is the search for muon tracks coming from secondary vertices performed by the ATLAS experiment at the LHC. However, the most stringent limits on R-parity violating couplings, so far, can be derived from the bounds on the gravitino lifetime obtained from the gamma ray searches for decaying dark matter.

One of the main results of this work is the connection between gravitino and neutralino decays. We have shown that the lower bound on the neutralino decay length ($c\tau_{\chi_1^0} \gtrsim 4.6$ m bino-like, $c\tau_{\chi_1^0} \gtrsim 24$ m higgsino-like) is a direct consequence of the Fermi-LAT constraints on decaying dark matter. On the other hand, the lower bound on the stau decay length ($c\tau_{\tilde{\tau}_1} \gtrsim 4$ mm) is determined by the cosmological bounds on R-parity breaking couplings, which follow from the requirement that the baryon asymmetry is not washed out.

In the final chapter we have gone beyond the predictions for the NLSP decay lengths and have performed a series of studies evaluating the LHC discovery potential for the models presented throughout the present work using generic detector simulation `DELPHES`. The main result of these studies, and of the present work, is the conclusion that all models presented so far have features which impede a fast discovery at the LHC.

First, we have studied the LHC predictions for AMSB and hybrid gauge-gravity mediation models which are cosmologically consistent in case of conserved R-parity. The assumption that the mass of the lightest Higgs boson is 125 GeV, restricts the hybrid scenario to the heavy spectra, such that the phenomenology of both models is very similar, and is governed by the higgsino-like neutralino (N)LSP. This is the *Higgsino World* scenario. Since all colored superparticles are not accessible at the LHC, only charged and neutral higgsinos are produced in various electroweak processes. The particles are produced without transverse momentum and leave thus no missing transverse energy signature. Furthermore, the mass difference between the charged and neutral higgsino states is very small and therefore no visible leptons are produced in the decays of the charged higgsinos. We have verified these statements and showed that the discovery of neutralinos with missing transverse energy signature is impossible by comparing missing transverse energy and lepton transverse momentum spectra of the higgsinos and the WZ boson background after detector simulation. Thus, the only possibility to discover such scenario at the LHC is a monojet of a monophoton signature arising if the higgsino receives transverse momentum from initial state radiation seen in the detector as a jet or a photon.

If the Higgs boson mass is below 125 GeV, the hybrid gauge-gravity mediation models allowing for light stop become viable. In this case, usual SUSY searches could find these models with more data. We have shown that using leptonic decay channels and dedicated cuts a discrimination between the hybrid gauge-gravity mediated scenario and the CMSSM is possible.

R-parity can also be violated in hybrid gauge-gravity SUSY breaking scenario. In this case, the higgsino LSP will decay into the particles of the Standard Model as described above. We have investigated which type of signatures would appear at the LHC, and have proposed search strategies based on the appearance of secondary vertices. Note that SUSY is hidden from usual searches in this case as well, since the decays of the neutralinos inside of various detector components distort missing transverse energy signature.

We have investigated the impact of neutralino decays on missing transverse energy in more detail for the case of bino-like neutralino, which is the NLSP in mSUGRA scenarios. As stated above, they become allowed if one neglects the LHC hint for the mass of the lightest Higgs boson. We have presented the distribution of the missing transverse momentum for different values of the R-parity violating coupling at the generator level. If the value of the coupling is around 10^{-9} the distribution becomes similar to the R-parity conserving case and a large portion of models is excluded by usual SUSY searches. However, the situation is different for smaller couplings, in which case the missing transverse energy distribution peaks

at zero.

Finally, we have determined the range of the R-parity breaking couplings which can be probed at the $\sqrt{s} = 7$ TeV LHC using bino-like neutralino decays into Z boson and neutrino followed by the decay of the Z boson into a muon pair. This analysis required the implementation of the finite NLSP decay length into the `DELPHES` detector simulation. The LHC experiments should be able to make a 5σ discovery with 10 fb^{-1} of data for squark and gluino masses of 830 GeV and an R-parity breaking couplings of order 3×10^{-9}, which is one order of magnitude smaller than the present astrophysical bound. Note that this region of the mSUGRA parameter space is already excluded in case of R-parity conservation.

We conclude that irrespective of the Higgs boson mass, the LHC experiments should look for unusual signatures like monojets (monophotons) or secondary vertices far away from the primary interaction point in order not to miss SUSY. If the hint for the Higgs boson mass becomes confirmed, then some version of the Higgsino World scenario seems probable and the colored particles are not accessible at the LHC. In this case a linear collider like ILC or CLIC can become invaluable. Furthermore, it is important to understand the response of the LHC detectors to neutral particles decaying throughout the whole detector volume. The impact of such decays on usual searches cannot be understood without the full detector simulation. It is important to see how the already obtained results which exclude parts of the MSSM parameter space would change if interpreted in models with R-parity violation. It is unclear at which value of the R-parity breaking parameter the models become excluded again, because of the essentially same signature as in the R-parity conserving case. In a future work we will investigate the LHC discovery prospects for a decaying higgsino-like neutralino.

The best discovery strategy for the future is a combination of LHC searches for new physics with further direct and indirect dark matter detection experiments. If dark matter is made of gravitinos all direct detection experiments should not be able to see a signal, even in the case of R-parity violation [72]. On the other hand, recent astrophysical result [258] suggests that the structure of the dark matter halo is such that the local dark matter density is negligible. This would also lead to a negative result for direct detection experiments even in the case of WIMP dark matter - an interesting conspiracy in nature.

Nevertheless, signals from particle dark matter decays or annihilations should be seen in various cosmic ray channels. Thus, a combination of a positive or a negative direct detection result with a signal from cosmic rays and a signature at the LHC should allow for identifying the nature of dark matter. If only negative results come from above (indirect detection experiments) and below (direct detection experiments and LHC), we will be forced to reevaluate our understanding of galaxy dynamics, gravitation and quantum field theory. In any case, mankind will never stop to seek the first principles of things.

Acknowledgments

First of all, I would like to thank my supervisor Wilfried Buchmüller for many helpful discussions, valuable advice and, especially, for the support during the hard times I've gone through while preparing this thesis. Many thanks also go to Peter Schleper for proposing to me this interesting collaboration and acting as second examiner. Both of them share a genuine enthusiasm for physics and are interested in every small detail, which was a great motivation for me throughout these years.

I am grateful to Felix Brümmer and Jonas Schmidt for a stimulating and fruitful collaboration on parts of the topics discussed in this thesis. I learned a lot from them. I am very thankful to Jan Hajer who worked together with me all these years on many projects and was able to stand my slightly panic phone calls from home with questions concerning the results. Furthermore, I am indebted to Felix Brümmer for putting the articles in the right place from the initial random distribution which he found in the manuscript. In general, I want to thank him for reading this thesis and providing me with helpful suggestions. Of course, he is not to blame for all the errors and omissions that remain, the solely responsibility for that lying with me. In addition, I would like to thank Jasper Hasenkamp and Kai Schmitz for many helpful discussions about the early universe cosmology and the life as a scientist.

Many thanks go to the entire DESY theory group for an enjoyable time. I would like to thank especially my friends Falk Lindner, Markus Rummel, Martin Schasny and Kai Schmitz for all the time we spent together which made these years happy in spite of everything.

I am thankful to Dominik, Jan, Philipp and Stella for being there when I needed them, for laughter and tears, for so many things I cannot say in words. I am always with you. I am grateful to my mother for the continuous support and all the sacrifices she has made for me. Finally, I would like to thank Norina, my love - she has made it all possible.

Appendix A

Two Component Spinor Techniques

This appendix summarizes the two-component spinor technique extensively introduced in [111] and used throughout the present work. Additionally, we provide rules needed for the computation of the gravitino decays and the derivation of the gravitino polarization tensor in the two-component formalism. Parts of the presentation follow [111], [259], and [260].

The use of two-component spinors may be motivated from different perspectives. First of all, in 3+1 dimensions they are the defining elements out of which the more familiar four-component spinors and world tensors can be readily build. As Penrose and Rindler note: "Spinor calculus may be regarded as applying at a deeper level of structure of space-time than that described by the standard world-tensor calculus." [261]. The reason for this is the structure of the rotation group $SO(3)$, which is not *simply-connected*. Rotation of an object through 2π corresponds to a closed curve in the group manifold which cannot be continuously deformed to a point. Therefore, rotation through 2π cannot correspond to no rotation at all, whereas rotation through 4π can. *Spinorial objects* are geometrical objects which are congruent with the structure of space-time, such that a rotation through 2π about any axis will send them into something distinct, and a further rotation through 2π is needed to send them to the original state. A geometrical description of two-spinors as well as their application in general relativity can be found in [261].

The use of four-component spinors in particle physics can be motivated in theories which conserve parity, such as QED and QCD, since Dirac-spinors are four-dimensional irreducible spinor representations of the orthochronous Lorentz group, which includes space-reversal [259]. However, the electroweak interactions have a *chiral* nature, i.e. they maximally violate parity. Therefore, the defining degrees of freedom for matter particles are two-component spinors, which transform as irreducible representations under the standard model gauge group. Furthermore, two-component spinors arise naturally in the context of supersymmetric theories, due to the spinorial nature of the supersymmetry generators, and the holomorphic structure of the superpotential. Even in the case of the parity-conserving QCD, the use of two-component spinors can be justified, since they tremendously simplify calculations via the helicity amplitude method. A historical overview as well as citations of the original works on this topic can be found in [111].

First, we recapitulate the structure of the Lorentz group.

A.1 Structure of the Lorentz Group

The space-time background of QFT is flat Minkowski space $\mathcal{M}$. The Lorentz-invariant inner product of two vectors x and y in $\mathcal{M}$, with components x^μ and y^μ, is given by

$$xy = x^\mu y^\mu g_{\mu\nu}, \tag{A.1}$$

where

$$(g_{\mu\nu}) = \mathrm{diag}(+1, -1, -1, -1) \tag{A.2}$$

is the metric tensor. A Lorentz transformation $\Lambda : \mathcal{M} \to \mathcal{M}$ is a linear transformation satisfying $(\Lambda x)(\Lambda y) = xy$. The set of all Lorentz transformations forms the Lorentz group L. From Eq. (A.1) follows that every $\Lambda \in L$ satisfies following equation (treating g and Λ as matrices):

$$\Lambda^T g \Lambda = g. \tag{A.3}$$

From this equation follows that $\det\Lambda^2 = 1$ and thus $\det\Lambda = \pm 1$. The 00-component of the equation A.3 reads:

$$\left(\Lambda_0^0\right)^2 - \sum_{i=1}^{3} \left(\Lambda_0^i\right)^2 = 1. \tag{A.4}$$

what leads to $\left|\Lambda_0^0\right| \geq 1$. Thus the group L consists of four topological components:

$$\begin{array}{lll}
L_+^\uparrow & : \det\Lambda = +1 \quad \Lambda_0^0 \geq 1 & \text{contains the identity} \\
L_-^\uparrow & : \det\Lambda = -1 \quad \Lambda_0^0 \geq 1 & \text{contains space inversion} \\
L_+^\downarrow & : \det\Lambda = +1 \quad \Lambda_0^0 \leq -1 & \text{contains space-time inversion} \\
L_-^\downarrow & : \det\Lambda = -1 \quad \Lambda_0^0 \leq -1 & \text{contains time inversion}
\end{array}$$

Only the $L_+^\uparrow$ component is a group itself - it contains the identity element. This subgroup is called the *restricted* Lorentz group. This group is not simply connected, since it entails the non-simply connected rotation group, whose fundamental group is a cyclic group of order 2. The universal cover of the Lorentz group is the group of 2×2 complex matrices with determinant 1 - the group $SL(2, \mathbb{C})$. The covering homomorphism

$$\Lambda : \begin{cases} SL(2,\mathbb{C}) & \to L_+^\uparrow \\ A & \mapsto \Lambda(A) \end{cases}$$

is declared in the following way. First a bijective map from the Minkowski space into the space of 2×2 matrices is defined via:

$$x \mapsto \underset{\sim}{x} = x^0 \mathbf{1}_{2\times 2} + \vec{x} \cdot \vec{\sigma} = \begin{pmatrix} x^0 + x^3 & x^1 - ix^2 \\ x^1 + ix^2 & x^0 - x^3 \end{pmatrix}. \tag{A.5}$$

This map leads to the following equation:

$$\det \underset{\sim}{\mathrm{x}} = \mathrm{x}^2, \tag{A.6}$$

and finally a Lorentz transformation $\Lambda(A)$ can be defined as:

$$\underset{\sim}{\Lambda(A)} x = A \underset{\sim}{x} A^*. \tag{A.7}$$

In the next step we explore the irreducible representations of the Lorentz group.

A.2 Spinor Representations of $SL(2, C)$

A field $\psi(x)$ is a function with some components which transform in a definite way under the Lorentz transformations:

$$\psi'(x') = D(A)\psi(x), \qquad x' = \Lambda(A)x, \qquad A \in SL(2, \mathbb{C}). \tag{A.8}$$

The group $SL(2, \mathbb{C})$ supersedes the Lorentz group and $D(A)$ is a matrix representation of $SL(2, \mathbb{C})$. The fields can be classified according to irreducible representations of $SL(2, \mathbb{C})$. The group $SL(2, \mathbb{C})$ has exactly two defining representations, all other matrix representations are direct sums of these two.

The defining representation is described by:

$$D^{\frac{1}{2}0}(A) = A \tag{A.9}$$

The group acts naturally upon the two dimensional complex vector space $\mathbb{C}^2$ whose elements are called *spinors*. Such spinor ψ has two complex components:

$$\psi = \begin{pmatrix} \psi_1 \\ \psi_2 \end{pmatrix}. \tag{A.10}$$

The spinor transformation law reads:

$$\psi'_\alpha = A_\alpha^{\ \beta}\psi_\beta, \qquad A \in SL(2, \mathbb{C}). \tag{A.11}$$

Only undotted indices are used for spinors in the defining representation.

The conjugate representation is described by:

$$D^{0\frac{1}{2}}(A) = A^*, \tag{A.12}$$

where A^* is the complex conjugate of A. This representation acts on complex conjugated spinors $\psi^\dagger = (\psi^\dagger_{\dot\alpha})$ which transform analogue to the ψ's:

$$\psi^{\dagger\prime}_{\dot\alpha} = A^*_{\dot\alpha}{}^{\dot\beta}\psi^\dagger_{\dot\beta}, \qquad A \in SL(2, \mathbb{C}). \tag{A.13}$$

Both representations are inequivalent and dotted indices are reserved for the spinors of the conjugate representation.

If one performs spinor multiplication or construction of Lorentz tensors, the height of the spinor indices must be consistent, i.e. lowered indices must only be contracted with raised indices. As a convention, *descending* contracted undotted indices and *ascending* contracted dotted indices can be suppressed. A spinor index can be lowered or raised with the use of the spinor metric tensors. The rules for spinor algebra are summarized in section A.5.

A general spinor s of type (j, k) is a tensor with complex components $s_{\alpha_1\cdots\alpha_{2j},\dot\alpha_1\cdots\dot\alpha_{2k}}$ whose transformation properties are implied by this notation. The tensor should be symmetric under permutations of the first 2j undotted and the last 2k dotted indices. It can be shown that the representation D^{jk} of the $SL(2, \mathbb{C})$ which acts on the space of all spinors of type (j, k) is irreducible. The dimension of this representation space is $(2j + 1)(2k + 1)$ and this dimension is also assigned per definition to the representation D^{jk}.

If the representation D^{jk} is limited to the subgroup $SU(2)$, the defining and conjugate representations become equivalent and the representation D^{jk} becomes the reducible representation $D^j \otimes D^k$ of the $SU(2)$. It can be decomposed into irreducible parts, as it is done in the theory of angular momentum. The decomposition reads in terms of dimensions:

$$(2j+1)(2k+1) = \sum_{s=|j-k|}^{j+k} s. \tag{A.14}$$

Now a connection between fields and corresponding spin can be established: If a field $\psi(x)$ transforms under Lorentz-transformations according to the irreducible representation D^{jk} of $SL(2,\mathbb{C})$ it is called an irreducible field. It can possess following spin quantum numbers:

$$s = |j-k|, |j-k|+1, \ldots, j+k. \tag{A.15}$$

However, this connection only shows which particle species can be potentially described by the field under consideration, it is imaginable that some possible spin values do not occur. The vector field $A_\mu(x)$, for example, is a $(\frac{1}{2},\frac{1}{2})$ spinor and can describe spin-1 and spin-0 particles. Nevertheless, it is possible to isolate the spin-1 part and to suppress the spin-0 contribution[1], as done in electrodynamics. In the next section we classify the fermion fields.

A.3 Properties of Fermion Fields

First we examine a *massless* field transforming as the $D^{\frac{1}{2}0}$ representation of the $SL(2,\mathbb{C})$. The particle it describes obviously has spin-1/2, and its dynamics is governed by the *Weyl equation*. Analyzing the plane wave solutions of this equations one finds that the spin direction is constrained to be antiparallel to the momentum. Therefore, the particle described by this field is said to be *left-handed*. This particle and in general all massless spin-1/2 particles are called *Weyl fermions*.

In the next step, we examine the properties of the same field, but now assuming that it is massive. In this case, the particle described by the field is called a *Majorana fermion*. We denote the field by ζ_α; its free-field Lagrangian density is:

$$\mathcal{L} = i\xi^\dagger \bar{\sigma}^\mu \partial_\mu \xi - \frac{1}{2} m(\xi\xi + \xi^\dagger\xi^\dagger). \tag{A.16}$$

On-shell, ξ satisfies the free-field Dirac equation:

$$i\bar{\sigma}^{\mu\dot{\alpha}\beta}\partial_\mu \xi_\beta = m\xi^{\dot{\alpha}}. \tag{A.17}$$

After quantization it can be expanded in a Fourier series:

$$\xi_\alpha(x) = \sum_s \int \frac{d^3\vec{p}}{(2\pi)^{3/2}(2E_p)^{1/2}} \left[x_\alpha(\vec{p},s)a(\vec{p},s)e^{-ip\cdot x} + y_\alpha a^\dagger(\vec{p},s)e^{ip\cdot x} \right], \tag{A.18}$$

$$\xi^\dagger_{\dot{\alpha}}(x) \equiv (\xi_\alpha(x))^\dagger = \sum_s \int \frac{d^3\vec{p}}{(2\pi)^{3/2}(2E_p)^{1/2}} \left[x^\dagger_{\dot{\alpha}}(\vec{p},s)a^\dagger(\vec{p},s)e^{ip\cdot x} + y^\dagger_{\dot{\alpha}} a(\vec{p},s)e^{-ip\cdot x} \right], \tag{A.19}$$

[1] Lorenz gauge condition of electrodynamics excludes spin-0 photons

where $E_p = \sqrt{|\vec{p}|^2 + m^2}$, and the creation and annihilation operators $a^\dagger$ and a satisfy the usual anticommutation relations. The anticommuting properties of the fields are encoded in the creation and annihilation operators. Therefore the spinor wave-functions x_α and y_α are commuting.

Finally, we analyze a *collection* of massive spin-1/2 fermions in the mass-eigenstate basis. If the original Lagrangian was not in the mass-eigenstate basis, the mass matrix can be diagonalized using the Takagi diagonalization technique leading to real non-negative masses. This technique is introduced later in Appendix B. The Lagrangian reads:

$$\mathcal{L} = i\xi^{\dagger i}\overline{\sigma}^\mu \partial_\mu \xi_i - \frac{1}{2} m_i (\xi_i \xi_i + \xi^{\dagger i}\xi^{\dagger i}), \tag{A.20}$$

where i denotes each fermion in the collection and the sum over i is implicit. If the non-zero masses are non-degenerate, then the corresponding field describes a neutral *Majorana fermion* as in the singe-field case. If one of the masses is zero, then the corresponding field is a massless Weyl fermion as in the first example.

In case of two mass-degenerate fermion fields eq. (A.20) possesses a global internal $O(2)$ flavor symmetry, $\xi_i \to \mathcal{O}_i^j \xi_j$, where $\mathcal{O}^T\mathcal{O} = \mathbf{1}_{2\times 2}$. Corresponding to this symmetry, there is a conserved Noether current and a corresponding conserved charge:

$$J^\mu = i(\xi^{\dagger 1}\overline{\sigma}^\mu \xi_2 - \xi^{\dagger 2}\overline{\sigma}^\mu \xi_1). \tag{A.21}$$

It is possible to diagonalize the current by means of field redefinitions:

$$\chi \equiv \frac{1}{\sqrt{2}}(\xi_1 + i\xi_2), \qquad \eta \equiv \frac{1}{\sqrt{2}}(\xi_1 - i\xi_2). \tag{A.22}$$

$$J^\mu = \chi^\dagger \overline{\sigma}^\mu \chi - \eta^\dagger \overline{\sigma}^\mu \eta. \tag{A.23}$$

Therefore, the fermions χ and η are eigenstates of the charge operator Q with eigenvalues ± 1. Rewriting the Lagrangian A.20 for two fermions with equal mass in the new basis, one finds:

$$\mathcal{L} = i\chi^\dagger \overline{\sigma}^\mu \partial_\mu \chi + i\eta^\dagger \overline{\sigma}^\mu \partial_\mu \eta - m(\chi\eta + \chi^\dagger \eta^\dagger). \tag{A.24}$$

On-shell, the new fields satisfy the Dirac equations:

$$i\overline{\sigma}^\mu \partial_\mu \chi = m\eta^\dagger, \qquad i\overline{\sigma}^\mu \partial_\mu \eta = m\chi^\dagger. \tag{A.25}$$

In the $\chi - \eta$ basis the global $SO(2)$ symmetry is realized as the $U(1)$ symmetry $\chi \to e^{i\theta}\chi$ and $\eta \to e^{-i\theta}\eta$, where θ is the rotation angle from the corresponding $SO(2)$ rotation matrix. Hence, a single *Dirac fermion* is build from two spinor fields: χ and $\eta^\dagger$. The decomposition in Fourier-modes reads:

$$\chi_\alpha(x) = \sum_s \int \frac{d^3\vec{p}}{(2\pi)^{3/2}(2E_p)^{1/2}} \left[x_\alpha(\vec{p},s) a(\vec{p},s) e^{-ip\cdot x} + y_\alpha b^\dagger(\vec{p},s) e^{ip\cdot x} \right], \tag{A.26}$$

$$\eta_\alpha(x) = \sum_s \int \frac{d^3\vec{p}}{(2\pi)^{3/2}(2E_p)^{1/2}} \left[x_\alpha(\vec{p},s) b(\vec{p},s) e^{-ip\cdot x} + y_\alpha a^\dagger(\vec{p},s) e^{ip\cdot x} \right], \tag{A.27}$$

where the creation and annihilation operators satisfy the usual anticommutator relations.

Summing up, we note that massive spin-1/2 particles are Dirac or Majorana fermions depending on the nature of the global symmetry that is present in the fermion Lagrangian, in particular in the mass terms. An arbitrary collection of two-component fermion fields transforming in the $D^{\frac{1}{2}0}$ representation will consist of Majorana fermions if no such symmetry exist. If the Lagrangian is invariant under a symmetry group G, then the collection of fermions will split into a sum of multiplets transforming irreducibly under G. If a multiplet transforms under a real representation of G, then the corresponding fermion mass eigenstates are *Majorana fermions*. If the multiplet transforms under a complex representation of G, then the corresponding fermion mass eigenstates are *Dirac fermions*. Due to similarities in the description of massless Weyl fermions and the massive particles, the massive fields are also called *left-handed* or *right-handed* depending on whether they transform in the defining or the conjugate representation of $SL(2,\mathbb{C})$. Having established the notions of different fermion fields we present the basic Feynman rules in the next section.

A.4 Feynman Rules

We exclude propagators from the discussion of the Feynman rules, since they are not needed in the present work. Furthermore, we omit the discussion of mass-matrix diagonalization because it is treated explicitly in Appendix B and can be found in [111].

A.4.1 External Particles

The rules for the external particles follow from the Lorentz group transformation properties of the fields. The rules are extracted from the terms in the Lagrangian by identifying the incoming and outgoing particles and the transformation properties of the corresponding operators under $SL(2,\mathbb{C})$ (daggered or undaggered index). The two-component external state spinors are assigned in the following way:

- For an initial-state fermion if the corresponding operator transforms as $(\frac{1}{2},0)$: x
- For an initial-state fermion if the corresponding operator transforms as $(0,\frac{1}{2})$: $y^\dagger$
- For a final-state fermion if the corresponding operator transforms as $(\frac{1}{2},0)$: y
- For a final-state fermion if the corresponding operator transforms as $(0,\frac{1}{2})$: $x^\dagger$

where the momentum and spin arguments of the spinor wave functions are suppressed. Note that our rules differ slightly from the one in reference [111], since we want to identify the correct scattering amplitude directly from the interaction Lagrangian. The arrows on the lines indicate the spinor index structure of the external state spinors. Fields associated with a spinor wave function with undotted index flow into the vertices, and fields associated with a spinor wave function with dotted index flow out of the vertices. The rules for external fermions are summarized in Fig. A.1. The rules for external boson lines are independent from the treatment of fermions:

- For an initial state (incoming) or final-state (outgoing) spin-0 boson: 1
- For an initial state (incoming) spin-1 boson: ε^μ
- For an final state (outgoing) spin-1 boson: $\varepsilon^{\mu *}$

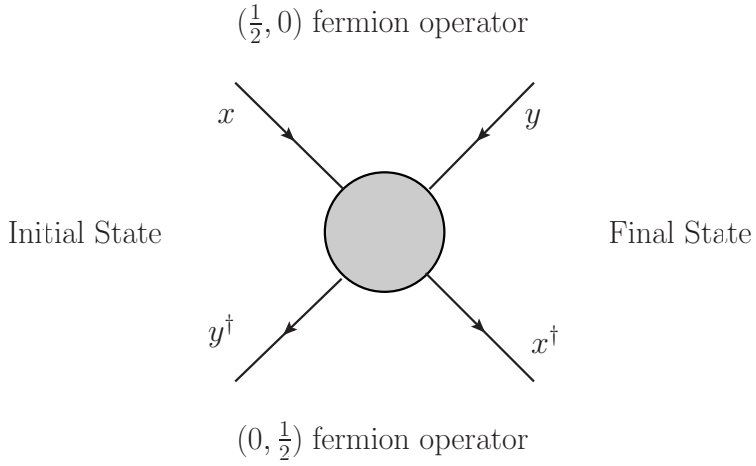

Figure A.1: Assignment rules for the external spinor wave-functions. The rules are governed by the transformation properties of the fermion operators in the Lagrangian i.e. $(\frac{1}{2},0)$ or $(0,\frac{1}{2})$. Note that the figure is changed compared to reference [111].

In these rules we have suppressed momentum and helicity arguments of the spin-1 polarization vectors.

The rules for the gravitino follow closely the rules for the fermions. The two-component external state wave function x has to be changed to the positive frequency wave function ψ_μ^+ and y to the negative frequency wave function ψ_μ^- in all the rules presented above.

A.4.2 Interaction Vertices

In this section we consider only renormalizable Lorentz-invariant interactions which involve fermions. The aforementioned conditions constrain the interactions to consist of bilinears in the fermionic fields transforming as a Lorentz scalar or vector, coupled to the appropriate bosonic scalar or vector field. The scalar fields interact with the fermionic bilinears via the Yukawa interaction:

$$\mathcal{L}_{\text{int}} = -\frac{1}{2}Y^{Ijk}\phi_I\psi_j\psi_k - \frac{1}{2}Y_{Ijk}\phi^I\psi^{\dagger j}\psi^{\dagger k}, \tag{A.28}$$

where the indices run over the gauge-group representation and flavor degrees of freedom. The fermionic multiplet will in general consist of Majorana and Dirac fermions. The scalar multiplet can involve complex scalars Φ_I in which case $\Phi^I \equiv (\Phi_I)^*$. The Lagrangian is written in terms of mass-eigenstates and the form of the Yukawa-matrices is constrained by selection rules imposed by conserved symmetries. The Feynman rules arising from the Yukawa-interaction Lagrangian are shown in Fig. A.2. In the case of a complex scalar the arrow on the scalar line shows the flow of analycity, i.e. it keeps track of the position of the scalar flavor index entering or leaving the vertex. The arrows on the fermion fields were explained in the previous section. Figure A.2 shows two version for each Feynman rule. The versions differ in the position of the fermion indices. One always employ the version of the rule which allows for the correct spinor index contraction defined in Section A.2 and summarized in Section A.5. The renormalizable interactions of vector bosons with fermions and scalars are constructed by demanding that the Lagrangian of the theory should be invariant under gauge transformations for some gauge group G. The vector fields arise as Lie-algebra valued

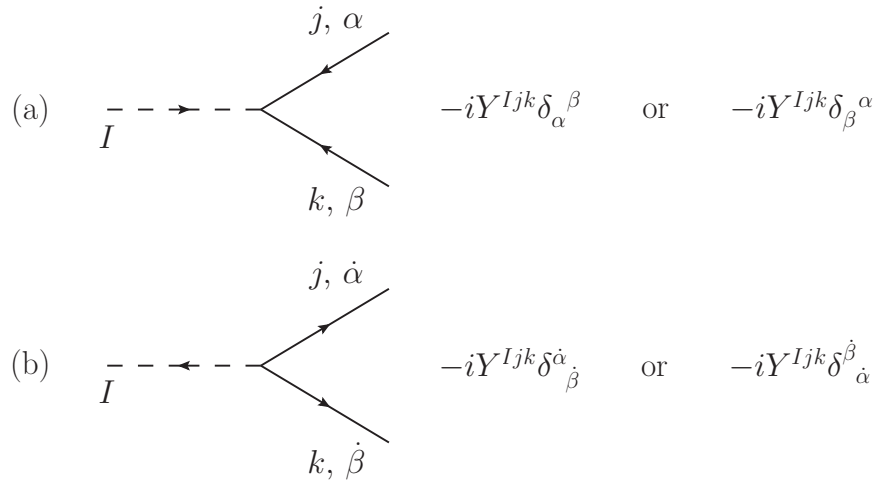

Figure A.2: Feynman rules for Yukawa couplings of scalars to fermions. The choice of which rule to use depends on the index structure of the amplitude. When indices are suppressed, the spinor index part is proportional to the identity matrix.

gauge-fields corresponding to the connection in the fiber bundle. The interactions arise from replacing ordinary derivatives by covariant derivatives in order to compare different fibers. The covariant derivative has the following form:

$$(D_\mu)_i{}^j = \partial_\mu \delta_i{}^j + i g_a A^a_\mu (\mathbf{T}^a)_i{}^j \ . \tag{A.29}$$

The index a runs over the adjoint representation of the gauge group, and the $(\mathbf{T^a})_i^j$ are hermitean representation matrices of the generators of the Lie algebra of the gauge group acting on the fermions in the defining representation of the $SL(2,\mathbb{C})$. For a $U(1)$ gauge group the representation matrices of the generators are replaced by real numbers corresponding to the $U(1)$ charges of the left-handed fermions. There is a separate coupling g_a for each simple group or $U(1)$ factor of the gauge group G[2]. In the gauge interaction basis for the left-handed fermions, the interaction Lagrangian following from the covariant derivative is given by:

$$\mathcal{L}_{int} = -\lambda^{\dagger i} \overline{\sigma}^\mu g_a A^a_\mu (\mathbf{T}^a)_i{}^j \lambda_j . \tag{A.30}$$

If the gauge bosons become massive due to the Higgs mechanism, the vector boson squared mass matrix has to be diagonalized. If there is an unbroken $U(1)$ symmetry, then the physical gauge bosons will carry a conserved $U(1)$ charge. The Feynman rules arising from the covariant derivative are shown in Fig. A.3. For simplicity, we wrote the interaction in the gauge-eigenstate basis but they can always be re-expressed in terms of physical mass-eigenstate gauge boson fields.

A.4.3 General Structure of Amplitudes

Having collected the rules for the external particles and the vertices, it is possible to compute the amplitudes for a given processes not involving propagators. First one draws all possible diagrams compatible with the rules given in the previous sections. The amplitude is a sum

[2]For details see [111].

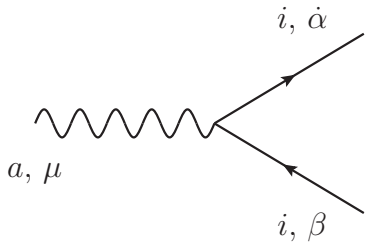

$$-i(T^a)_i{}^j\bar{\sigma}_\mu^{\dot{\alpha}\beta} \qquad \text{or} \qquad i(T^a)_i{}^j\sigma_{\mu\beta\dot{\alpha}}$$

Figure A.3: Feynman rules for interactions of fermions with gauge bosons. The choice of the rule to use depends on the index structure of the amplitude. Here we assume, for simplicity, that gauge bosons are massless. In massive case the couplings times the generators of the gauge group are replaced by the appropriate linear combinations. The coupling is absorbed into the definition of the generator of the gauge group.

of contributions from each diagram. Every contribution is obtained by combining the factors corresponding to the external wave functions and vertices. The factors are combined according to following rule:

- Starting from any external wave function spinor factors corresponding to vertices (and in general propagators) are written from left to right following the line until it ends at another external state wave function. A x or y [$x^\dagger$, $y^\dagger$] external state spinor at the beginning of the amplitude should have a raised undotted [lowered dotted] spinor index. If the amplitude ends with an x or y [$x^\dagger$, $y^\dagger$] external state spinor, it should have a lowered undotted [raised dotted index]. This rule determines whether one uses the σ or $\bar{\sigma}$ version of rules for interaction vertices.

The Fermi-Dirac statistics is implemented by the following rule:

- A relative minus sign is imposed between terms contributing to a given amplitude whenever the ordering of external state spinors (written from left to right) differs by an odd permutation.

A.4.4 Conventions for Fermion and Antifermion Names and Fields

Following [111] we establish conventions for labelling Feynman diagrams which involve two-component fermion fields. In the case of Majorana fermions there is a one-to-one correspondence between the particle names and the undaggered field transforming as $(\frac{1}{2}, 0)$. In the case of Dirac fermions there are always two fields corresponding to each particle name which we choose to be in the representation $D^{\frac{1}{2},0}$ and denote with f and $\bar{f}$. Nota bene that the bar is part of the field name and does not refer to complex conjugation.

We label fermions by the two-component fields and *not by the particle name*. The names of the SM and MSSM fermions and corresponding two-component fields are shown in Table A.1. For each particle we list fields which have the same quantum numbers, i.e. the fields which contain the annihilation operator for that one-particle state. Fermion lines in Feynman diagrams are labelled according to the following conventions:

- An initial-state external fermion line is labelled by the corresponding undaggered field if the arrow points into the vertex, and by the daggered field if the arrow points outside of the vertex.

- A final-state external fermion line is labelled by the corresponding daggered field if the arrow points into the vertex, and by undaggered field if the arrow points away from the vertex.
- In the definition of the Feynman rules for interaction vertices, the external lines are always labelled by the undaggered fields regardless of the arrow direction.

These conventions are summarized for the case of Dirac fermions in Fig. A.4, and for the case of Majorana fermions in Fig. A.5. Having established the rules and conventions necessary

Fermion Name	Two-component fields
Lepton	l, $\bar{l}^\dagger$
Anti-Lepton	$\bar{l}$, $l^\dagger$
Neutrino	ν, $-$
Anti-Neutrino	$-$, $\nu^\dagger$
Quark	q, $\bar{q}^\dagger$
Anti-Quark	$\bar{q}$, $q^\dagger$
Neutralino	χ_i^0, $\chi_i^{0\dagger}$
Chargino	χ_i^-, $\chi_i^{+\dagger}$
Anti-Chargino	χ_i^+, $\chi_i^{-\dagger}$
Gluino	g, $g^\dagger$
Gravitino	ψ_μ, $\psi_\mu^\dagger$

Table A.1: Fermion and antifermion names and two-component fields in the SM and the MSSM. In the listing of two-component fields, the first is an undaggered field and the second is a daggered field. The bars on the fermion fields are part of their names. In this table we consider neutrinos to be massless Weyl fermions.

for computations with two-component spinors, we summarize our conventions and list some key results from the spinor algebra in the next section.

A.5 Summary of Spinor Algebra and Conventions

Metric Signature Convention The metric tensor is taken to be:

$$g_{\mu\nu} = g^{\mu\nu} = \mathrm{diag}(+1, -1, -1, -1), \tag{A.31}$$

where $\mu, \nu = 0, 1, 2, 3$ are spacetime vector indices. Contravariant four-vectors are defined with raised indices, and covariant four-vectors are defined with lowered indices:

$$x^\mu = (t; \vec{x}), \tag{A.32}$$
$$p^\mu = (E; \vec{p}), \tag{A.33}$$
$$A^\mu(x) = \left(\Phi(t; \vec{x}); \vec{A}(t; \vec{x})\right), \tag{A.34}$$
$$J^\mu(x) = \left(\rho(t; \vec{x}); \vec{J}(t; \vec{x})\right), \tag{A.35}$$

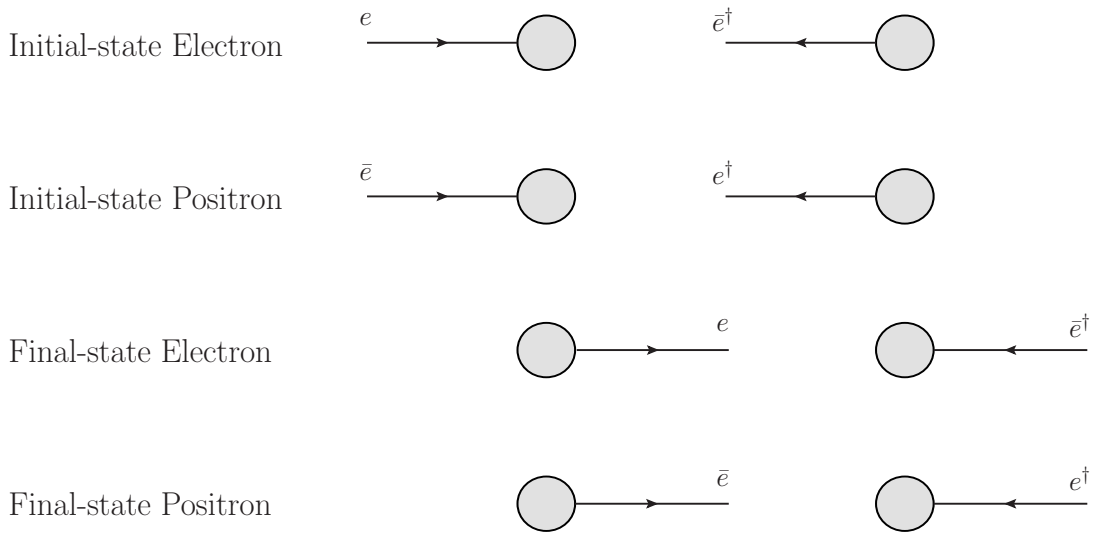

Figure A.4: The two-component field labelling conventions for external Dirac fermions in a Feynman diagram for a physical process. The top row corresponds to an initial-state electron, the second row to an initial-state positron, the third row to a final-state electron, and the fourth row to a final-state positron. Fermion lines are labelled by the two-component field names.

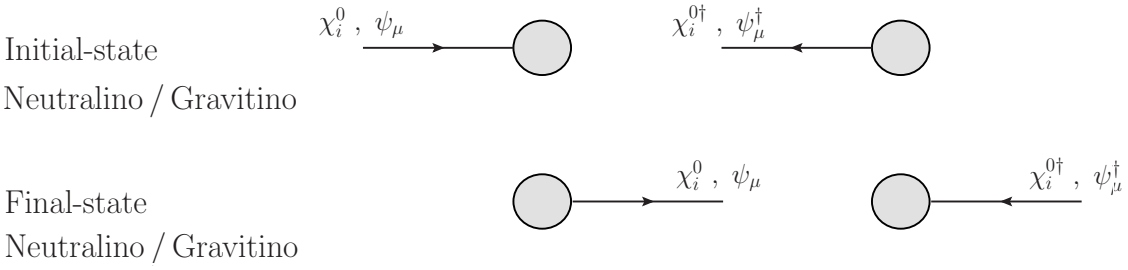

Figure A.5: The two-component field labelling conventions for external Majorana fermions in a Feynman diagram for a physical process. The top row corresponds to an initial-state neutralino/gravitino, and the second row to a final-state neutralino/gravitino. Fermion lines are labelled by the two-component field names.

$$\partial_\mu \equiv \frac{\partial}{\partial x^\mu} = (\partial/\partial t, \vec{\nabla}), \tag{A.36}$$

$$D_\mu \equiv I_{d_R}\partial_\mu + igA_\mu, \tag{A.37}$$

where $A_\mu = A_\mu^a \mathbf{T}^a$ is the matrix gauge field for a representation R of dimension d_R, and I_{d_R} is the $d_R \times d_R$ identity matrix.

Antisymmetric Symbols The totally antisymmetric pseudo-tensor $\epsilon^{\mu\nu\rho\sigma}$ is defined such that

$$\epsilon^{0123} = -\epsilon_{0123} = +1. \tag{A.38}$$

As stated in section A.2 the defining $D^{\frac{1}{2}0}$ and conjugate $D^{0\frac{1}{2}}$ representations of $SL(2,\mathbb{C})$ are related by hermitean conjugation. Therefore, one can describe all degrees of freedom

using only spinors transforming in the defining representation. In combining spinors to make Lorentz tensors, it is useful to regard $\psi^\dagger_{\dot\alpha}$ as a row vector, and ψ_α as a column vector, with:

$$\psi^\dagger_{\dot\alpha} \equiv (\psi_\alpha)^\dagger \,. \tag{A.39}$$

This notation is publicized in [111] and differs from the notation of Wess and Bagger [78] which uses a bar for hermitean conjugation $\bar\psi_{\dot\alpha} \equiv (\psi_\alpha)^\dagger$. The spinor indices are raised and lowered with the two-index antisymmetric epsilon symbol or *spinor metric tensor* with non-zero components:

$$\epsilon^{12} = -\epsilon^{21} = \epsilon_{21} = -\epsilon_{12} = 1, \tag{A.40}$$

and the same set of sign conventions for the corresponding dotted spinor indices. The formal definitions are: $\epsilon^{\dot\alpha\dot\beta} \equiv (\epsilon^{\alpha\beta})^*$ and $\epsilon_{\dot\alpha\dot\beta} \equiv (\epsilon_{\alpha\beta})^*$. In addition we define the two-index symmetric Kronecker delta symbol,

$$\delta^1_1 = \delta^2_2 = 1, \qquad \delta^1_2 = \delta^1_2 = 0, \tag{A.41}$$

and $\delta^{\dot\beta}_{\dot\alpha} \equiv (\delta^\alpha_\beta)^*$. Per definition the numerical values of undotted and dotted Kronecker delta symbols coincide.

Spinor products In order to construct Lorentz invariant Lagrangians and observables, one has to use spinor products to create objects transforming as Lorentz tensors. Combining spinors one has to take care of spinor indices, i.e. lowered indices must only be contracted with raised indices. As a convention one suppresses descending contracted undotted indices and ascending contracted dotted indices:

$$\overset{\alpha}{}_{\alpha}, \qquad \overset{}{}_{\dot\alpha}{}^{\dot\alpha}. \tag{A.42}$$

Sigma Matrix Conventions Lorentz vectors are obtained by introducing the sigma matrices $\sigma^\mu_{\alpha\dot\beta}$ and $\bar\sigma^{\mu\dot\alpha\beta}$ defined by:

$$\begin{aligned} \sigma^0 = \bar\sigma^0 &= \begin{pmatrix} 1 & 0 \\ 0 & 1 \end{pmatrix}, & \sigma^1 = -\bar\sigma^1 &= \begin{pmatrix} 0 & 1 \\ 1 & 0 \end{pmatrix}, \\ \sigma^2 = -\bar\sigma^2 &= \begin{pmatrix} 0 & -i \\ i & 0 \end{pmatrix}, & \sigma^3 = -\bar\sigma^3 &= \begin{pmatrix} 1 & 0 \\ 0 & -1 \end{pmatrix}. \end{aligned} \tag{A.43}$$

The sigma matrices are hermitean, and have been defined with an upper (contravariant) index to be independent of metric signature convention. If one denotes the 2×2 identity matrix by $\mathbf{1}_{2\times2}$ and the three-vector of Pauli matrices by $\vec\sigma \equiv (\sigma^1, \sigma^2, \sigma^3)$, the definition above is equivalent to

$$\sigma^\mu = (\mathbf{1}_{2\times2}; \vec\sigma)\,, \qquad \bar\sigma^\mu = (\mathbf{1}_{2\times2}; -\vec\sigma)\,. \tag{A.44}$$

The corresponding quantities with lower indices are obtained by contraction with the metric tensor:

$$\sigma_\mu = g_{\mu\nu}\sigma^\nu = (\mathbf{1}_{2\times2}; -\vec\sigma)\,, \qquad \bar\sigma_\mu = g_{\mu\nu}\bar\sigma^\nu = (\mathbf{1}_{2\times2}; \vec\sigma)\,. \tag{A.45}$$

The generators of the defining and conjugate representation of the Lorentz group are, respectively, given by:

$$\sigma^{\mu\nu} \equiv \frac{i}{4}\left(\sigma^\mu\bar\sigma^\nu - \sigma^\nu\bar\sigma^\mu\right), \qquad \bar\sigma^{\mu\nu} \equiv \frac{i}{4}\left(\bar\sigma^\mu\sigma^\nu - \bar\sigma^\nu\sigma^\mu\right). \tag{A.46}$$

Nota bene that these definitions differ from the conventions of Wess and Bagger [78]. In their notation and with their metric signature $(-,+,+,+)$ the sigma matrices read:

$$\left(\sigma^{\mu}_{\alpha\dot{\beta}}\right)^{WB} = (-\mathbf{1}_{2\times 2}, \vec{\sigma}) \qquad \left(\bar{\sigma}^{\mu\dot{\alpha}\beta}\right)^{WB} = (-\mathbf{1}_{2\times 2}, -\vec{\sigma}) \tag{A.47}$$

$$\left(\sigma_{\mu\alpha\dot{\beta}}\right)^{WB} = (\mathbf{1}_{2\times 2}, \vec{\sigma}) \qquad \left(\bar{\sigma}_{\mu}^{\dot{\alpha}\beta}\right)^{WB} = (\mathbf{1}_{2\times 2}, -\vec{\sigma}) \tag{A.48}$$

One consequence of this definition of the sigma matrices is the inverse sign of γ_5 in the chiral representation which associates a lowered undotted [raised dotted] two-component spinor with a right-handed [left-handed] four-component spinor. In order to convert various identities involving a number of sigma matrices to the conventions of Wess and Bagger, one first has to take care of the metric signature, and then usually interchange $\sigma \leftrightarrow \bar{\sigma}$. The conversion for the case involving sigma matrices and fermions is more subtle.

We will use following identities to simplify expressions involving products of of σ and $\bar{\sigma}$ matrices:

$$\sigma^{\mu}_{\alpha\dot{\alpha}}\bar{\sigma}_{\mu}^{\dot{\beta}\beta} = 2\delta_{\alpha}{}^{\beta}\delta^{\dot{\beta}}_{\dot{\alpha}}, \tag{A.49}$$

$$\sigma^{\mu}_{\alpha\dot{\alpha}}\sigma_{\mu\beta\dot{\beta}} = 2\epsilon_{\alpha\beta}\epsilon_{\dot{\alpha}\dot{\beta}}, \tag{A.50}$$

$$\sigma^{\mu\dot{\alpha}\alpha}\sigma_{\mu}^{\dot{\beta}\beta} = 2\epsilon^{\alpha\beta}\epsilon^{\dot{\alpha}\dot{\beta}}, \tag{A.51}$$

$$\left[\sigma^{\mu}\bar{\sigma}^{\nu} + \sigma^{\nu}\bar{\sigma}^{\mu}\right]_{\alpha}{}^{\beta} = 2g^{\mu\nu}\delta_{\alpha}{}^{\beta}, \tag{A.52}$$

$$\left[\bar{\sigma}^{\mu}\sigma^{\nu} + \bar{\sigma}^{\nu}\sigma^{\mu}\right]^{\dot{\alpha}}_{\dot{\beta}} = 2g^{\mu\nu}\delta^{\dot{\alpha}}_{\dot{\beta}}, \tag{A.53}$$

$$\sigma^{\mu}\bar{\sigma}^{\nu}\sigma^{\rho} = g^{\mu\nu}\sigma^{\rho} - g^{\mu\rho}\sigma^{\nu} + g^{\nu\rho}\sigma^{\mu} + i\epsilon^{\mu\nu\rho\kappa}\sigma_{\kappa}, \tag{A.54}$$

$$\bar{\sigma}^{\mu}\sigma^{\nu}\bar{\sigma}^{\rho} = g^{\mu\nu}\bar{\sigma}^{\rho} - g^{\mu\rho}\bar{\sigma}^{\nu} + g^{\nu\rho}\bar{\sigma}^{\mu} - i\epsilon^{\mu\nu\rho\kappa}\bar{\sigma}_{\kappa}. \tag{A.55}$$

Computations of cross sections and decay rates require traces of alternating products of σ and $\bar{\sigma}$ matrices:

$$\mathrm{Tr}\left[\sigma^{\mu}\bar{\sigma}^{\nu}\right] = \mathrm{Tr}\left[\bar{\sigma}^{\mu}\sigma^{\nu}\right] = 2g^{\mu\nu}, \tag{A.56}$$

$$\mathrm{Tr}\left[\sigma^{\mu}\bar{\sigma}^{\nu}\sigma^{\rho}\bar{\sigma}^{\kappa}\right] = 2\left(g^{\mu\nu}g^{\rho\kappa} - g^{\mu\rho}g^{\nu\kappa} + g^{\mu\kappa}g^{\nu\rho} + i\epsilon^{\mu\nu\rho\kappa}\right), \tag{A.57}$$

$$\mathrm{Tr}\left[\bar{\sigma}^{\mu}\sigma^{\nu}\bar{\sigma}^{\rho}\sigma^{\kappa}\right] = 2\left(g^{\mu\nu}g^{\rho\kappa} - g^{\mu\rho}g^{\nu\kappa} + g^{\mu\kappa}g^{\nu\rho} - i\epsilon^{\mu\nu\rho\kappa}\right). \tag{A.58}$$

Traces involving a larger even number of sigma matrices can be systematically obtained from the equations above by repeated use of eqs. (A.52) and (A.53) and the cyclic property of the trace. Traces involving an odd number of sigma matrices cannot arise, since the spinor indices cannot be connected consistently in this case.

Sometimes it is needed to reverse the order of anticommuting spinors or of the commuting spinor wave functions. Therefore, it is convenient to introduce the following notation:

$$(-1)^{A} \equiv \begin{cases} +1\,, & \text{commuting spinors,} \\ -1\,, & \text{anticommuting spinors,} \end{cases} \tag{A.59}$$

in order to cover both cases simultaneously. The following identities hold for the general

spinors z_i:

$$z_1 z_2 = -(-1)^A z_2 z_1, \tag{A.60}$$
$$z_1^\dagger z_2^\dagger = -(-1)^A z_2^\dagger z_1^\dagger, \tag{A.61}$$
$$z_1 \sigma^\mu z_2^\dagger = (-1)^A z_2^\dagger \overline{\sigma}^\mu z_1, \tag{A.62}$$
$$z_1 \sigma_\mu \bar{\sigma}^\nu z_2 = -(-1)^A z_2 \sigma^\nu \overline{\sigma}^\mu z_1, \tag{A.63}$$
$$z_1^\dagger \overline{\sigma}^\mu \sigma^\nu z_2^\dagger = -(-1)^A z_2^\dagger \bar{\sigma}^\nu \sigma^\mu z_1^\dagger. \tag{A.64}$$

Spin-sum Identities Having obtained the identities involving sigma matrices, we have to state the spin-sum identities arising in computations of unpolarized squared matrix elements. The results are:

$$\sum_s x_\alpha(\vec{p},s) x^\dagger_{\dot\beta}(\vec{p},s) = p\cdot\sigma_{\alpha\dot\beta}, \qquad \sum_s x^{\dagger\dot\alpha}(\vec{p},s) x^\beta(\vec{p},s) = p\cdot\bar\sigma^{\dot\alpha\beta}, \tag{A.65}$$
$$\sum_s y^{\dagger\dot\alpha}(\vec{p},s) y^\beta(\vec{p},s) = p\cdot\bar\sigma^{\dot\alpha\beta}, \qquad \sum_s y_\alpha(\vec{p},s) y^\dagger_{\dot\beta}(\vec{p},s) = p\cdot\sigma_{\alpha\dot\beta}, \tag{A.66}$$
$$\sum_s x_\alpha(\vec{p},s) y^\beta(\vec{p},s) = m\delta_\alpha{}^\beta, \qquad \sum_s y_\alpha(\vec{p},s) x^\beta(\vec{p},s) = -m\delta_\alpha{}^\beta, \tag{A.67}$$
$$\sum_s y^{\dagger\dot\alpha}(\vec{p},s) x^\dagger_{\dot\beta}(\vec{p},s) = m\delta^{\dot\alpha}{}_{\dot\beta}, \qquad \sum_s x^{\dagger\dot\alpha}(\vec{p},s) y^\dagger_{\dot\beta}(\vec{p},s) = -m\delta^{\dot\alpha}{}_{\dot\beta}. \tag{A.68}$$

They are applicable to spin sums and helicity sums, and hold for both massive and massless spin-1/2 fermions.

Polarization-sum Identities First we list the polarization-sum identities for the massless and massive spin-1 particles. In the massless case we obtain:

$$\sum_\lambda \varepsilon^*_\mu(p)\varepsilon_\nu(p) = -g_{\mu\nu}, \tag{A.69}$$

while in the massive case the sum is changed to:

$$\sum_\lambda \varepsilon^*_\mu(p)\varepsilon_\nu(p) = -g_{\mu\nu} + \frac{p_\mu p_\nu}{m_A^2}, \tag{A.70}$$

where m_A is the mass of the boson.

Finally, we derive the polarization sums $P^\pm_{\mu\nu}$, $\overline{P}^\pm_{\mu\nu}$ of the gravitino in the two-component notation following the approach from the four-component formalism [113, 114, 262]. The polarization sums are given by:

$$P^\pm_{\mu\nu}(p) = \sum_s \psi^\pm_\mu(p,s)\psi^{\dagger\pm}_\nu(p,s), \tag{A.71}$$
$$\overline{P}^\pm_{\mu\nu}(p) = \sum_s \psi^{\pm\dagger}_\mu(p,s)\psi^\pm_\nu(p,s). \tag{A.72}$$

First, we note the spinor index structure of $P^\pm_{\mu\nu}$ which can be read from its explicit expression:

$$\left[P^\pm_{\mu\nu}\right]_{\alpha\dot\beta} = \sum_s \psi^\pm_{\mu\alpha}(p,s)\psi^{\dagger\pm}_{\nu\dot\beta}(p,s). \tag{A.73}$$

In the next step we use the Rarita-Schwinger equations in momentum space to obtain the following relations:

$$p^\mu P^\pm_{\mu\nu} = 0, \qquad \overline{\sigma}^\mu P^\pm_{\mu\nu} = 0, \qquad (\bar{\sigma}p)P^\pm_{\mu\nu}(\bar{\sigma}p) = m^2_{3/2}\overline{P}^\pm_{\mu\nu}. \tag{A.74}$$

The momentum of the gravitino in its rest frame is given by $p^\mu = (m_{3/2}, 0, 0, 0)^T$, and the first relation implies that the only non-vanishing components of $P^\pm_{\mu\nu}$ in the rest frame are $P^\pm_{ij}$, where i, j are spatial indices.

The most general polarization tensor compatible with the transformation properties under the Lorentz group and the spinor index structure is then given in the gravitino rest frame by:

$$P^\pm_{ij} = a(\sigma^0 m_{3/2})g_{ij} + b(\sigma^0 m_{3/2})\bar{\sigma}_i\sigma_j, \tag{A.75}$$

where a, b are some arbitrary constants. The second relation in eq. (A.74) implies

$$\bar{\sigma}^i P^\pm_{ij} = a\bar{\sigma}_j(\sigma^0 m_{3/2}) + \bar{\sigma}^i(\sigma^0 m_{3/2})\bar{\sigma}_i\sigma_j = (a+3b)\bar{\sigma}_j(\sigma^0 m_{3/2}) = 0, \tag{A.76}$$

where we have used eqs. (A.49). Thus, we obtain $b = -1/3a$. The last relation in eq. (A.74) determines the form of $\overline{P}^\pm_{\mu\nu}$. The factor a can be guessed from the results of the four-component formalism to be -1. In the last step we have to generalize the expression to an arbitrary frame. Using the following substitution rules:

$$(\sigma^0 m_{3/2}) \to (\sigma p), \quad g_{ij} \to \left(g_{\mu\nu} - \frac{p_\mu p_\nu}{m^2_{3/2}}\right), \quad \bar{\sigma}_i \to \left(g_{\mu\sigma} - \frac{p_\mu p_\sigma}{m^2_{3/2}}\right)\bar{\sigma}^\sigma, \tag{A.77}$$

we obtain the result:

$$P^\pm_{\mu\nu} = -(\sigma p)\left(\left(g_{\mu\nu} - \frac{p_\mu p_\nu}{m^2_{3/2}}\right) - \frac{1}{3}\left(g_{\mu\sigma} - \frac{p_\mu p_\sigma}{m^2_{3/2}}\right)\left(g_{\nu\lambda} - \frac{p_\nu p_\lambda}{m^2_{3/2}}\right)\bar{\sigma}^\sigma\sigma^\lambda\right). \tag{A.78}$$

Appendix B

Gauge and Mass Eigenstates

In this appendix we introduce techniques for the diagonalization of mass matrices and derive neutral and charged currents used in the present work.

B.1 Mass Matrix Diagonalization

Complex symmetric matrices, for example mass matrices of neutral fermions, are diagonalized by the Takagi diagonalization, see [111] for details and a historical introduction. The technique is based upon the existence of the unitary matrix $U^{(n)}$ with the property:

$$U^{(n)T} M U^{(n)} = \mathrm{diag}(m_1, m_2, \ldots, m_n) \ , \tag{B.1}$$

for every complex symmetric $n \times n$ matrix M. The m_k are the singular values of M, defined as non-negative square roots of the eigenvalues of $M^\dagger M$. Since all matrices encountered explicitly in the present work are real, the Takagi diagonalization matrix $U^{(n)}$ is obtained from a real orthogonal matrix Z, which diagonalizes M:

$$Z^T M Z = \mathrm{diag}(\epsilon_1 m_1, \epsilon_2 m_2, \ldots, \epsilon_n m_n) \ , \tag{B.2}$$

via

$$U^{(n)}_{ij} = \sqrt{\epsilon_i} Z_{ij}. \tag{B.3}$$

Here the m_k are real and non-negative, and the $\epsilon_k m_k$ are the real eigenvalues of M with corresponding signs $\epsilon_k = \pm 1$.

Arbitrary complex matrices, for example mass matrices of charged fermions, are diagonalized via the singular value decomposition, which is often called bi-unitary transformation in physical literature . In this case, a complex $n \times n$ matrix M is diagonalized via two unitary matrices $U^{(c)}$ and $\widetilde{U}^{(c)}$:

$$U^{(c)\dagger} M \widetilde{U}^{(c)} = \mathrm{diag}(m_1, m_2, \ldots, m_n) \ , \tag{B.4}$$

where m_k are the singular values of M.

B.1.1 Perturbative Matrix Diagonalization

Instead of using exact numerical matrix diagonalization methods, we perturbatively diagonalize the matrices in order to obtain approximate analytical results. This method is justified,

since i) in all cases considered in the present work, the electroweak symmetry breaking effects are only small perturbations on the mass matrices of neutral and charged fermions, ii) there is a hierarchy between the gaugino and higgsino mass terms:

$$m_Z < |\mu \pm M_1| \, , \, |\mu \pm M_2| \ , \tag{B.5}$$

and iii) in case of R-parity violation, the R-parity violating coupling is very small. Therefore, we have two expansion parameters: $\epsilon = m_Z/M$, where M denotes the largest entry in the matrix, and ζ.

In order to diagonalize a mass matrix M to the given order in ϵ and ζ, we perform the following set of steps, here, for example, for charged fermions:

- Assuming real M, we set ϵ and ζ to zero and diagonalize the simple mass matrix with usual methods.
- Using the results from the previous step, we construct the most general matrices $\widetilde{U}^{(c)}$ and $U^{(c)}$ from the generators of the orthogonal group as expansions in ϵ and ζ up to the given maximal order.
- The matrix M is then also written as expansion in ϵ and ζ.
- For a given order, there are several possibilities how the parameters ϵ and ζ are distributed among the matrices M, $\widetilde{U}^{(c)}$, and $U^{(c)}$. We take into account all possibilities and write the result as a sum.
- In the final step, we solve the equation

$$\left[U^{(c)\dagger} M \widetilde{U}^{(c)}\right]_{ij} = \quad 0\Big|_{i \neq j} \, , \tag{B.6}$$

  in each order of the expansion. In the end we combine the results.

This procedure can be performed in a consistent way and leads to correct transformation matrices and also mass eigenstates. In case of the symmetric matrices, we use the same method and ensure that the mass values are positive by multiplying the result by -1, if needed, according to eq. (B.3). Having established our technique for mass matrix diagonalization, we can proceed with the transformation of neutral current and charged current into the mass-eigenstate basis.

B.2 Neutral and Charged Currents

For the computation of the neutralino decays we need the couplings of the gauge fields, i.e. photon, Z and W boson to charged and neutral matter. The couplings of the gauge bosons to fermions arise from the covariant derivatives in the fermionic kinetic terms. In the two-component notation the kinetic terms have the form:

$$\mathcal{L} = i \lambda^{i\dagger} \overline{\sigma}^{\mu} (D_\mu)_i{}^j \lambda_j \ , \tag{B.7}$$

where i and j are gauge group indices. The covariant derivative has the form:

$$(D_\mu)_i{}^j = \partial_\mu \delta_i{}^j + i g_{(a)} A^a_\mu (\mathbf{T}^a)_i{}^j \ , \tag{B.8}$$

where the index a runs over the adjoint representation of the gauge group, and the $(\mathbf{T^a})_i^{\ j}$ are hermitian representation matrices of the generators of the Lie-algebra $\mathfrak{g}$ corresponding to the gauge group G acting on the left-handed fermions. For a $U(1)$ gauge group the representation matrices of the generators are replaced by real numbers corresponding to the $U(1)$ charges of the fermions. There is a separate coupling g_a for each simple group or $U(1)$ factor of the gauge group G[1]. In the gauge interaction basis for the left-handed fermions the interaction Lagrangian following from the covariant derivative is given by:

$$\mathcal{L} = -\lambda^{i\dagger}\overline{\sigma}^{\mu} g_{(a)} A^a_\mu (\mathbf{T}^a)_i^{\ j} \lambda_j \ . \tag{B.9}$$

In the case of the electroweak theory, we have to re-express the hermitian matrix gauge field in terms of physical mass-eigenstate gauge boson fields.

The covariant derivative of the electroweak sector of the standard model is given by:

$$(D_\mu)_i^{\ j} = \partial_\mu \delta_i^{\ j} + igW^a_\mu (\mathbf{T}^a)_i^{\ j} + ig' Y B_\mu \delta_i^{\ j} \ , \tag{B.10}$$

where Y is the hypercharge of the matter field. The physical mass-eigenstate gauge boson fields are linear combinations of the original W^a_μ and B_μ fields:

$$\begin{aligned} W^\pm_\mu &= \frac{1}{\sqrt{2}} \left(W^1_\mu \mp i W^2_\mu\right) \ , \\ Z_\mu &= \cos\theta_w W^3_\mu - \sin\theta_w B_\mu \ , \qquad\qquad A_\mu = \sin\theta_w W^3_\mu + \cos\theta_w B_\mu \ , \end{aligned} \tag{B.11}$$

where

$$\sin\theta_w = \frac{g'}{\sqrt{g^2+g'^2}} \ , \qquad\qquad \cos\theta_w = \frac{g}{\sqrt{g^2+g'^2}} \ . \tag{B.12}$$

In the following we use the abbreviations c_w for $\cos\theta_w$ and s_w for $\sin\theta_w$.

First, we rewrite the covariant derivative for the fermion fields transforming in the fundamental representation of $SU(2)_\mathrm{L}$:

$$\begin{aligned} (D_\mu)_i^{\ j} &= \partial_\mu \delta_i^{\ j} + \frac{i}{2} g \left(W^1_\mu \sigma^1 + W^2_\mu \sigma^2\right) + igW^3_\mu \sigma^3 + ig' Y B_\mu \delta_i^{\ j} \\ &= \partial_\mu \delta_i^{\ j} + \frac{i}{2} g \left(\begin{pmatrix} 0 & 1 \\ 0 & 0 \end{pmatrix} \sqrt{2} W^+_\mu + \begin{pmatrix} 0 & 0 \\ 1 & 0 \end{pmatrix} \sqrt{2} W^-_\mu \right) + \frac{i}{2} g W^3_\mu \sigma^3 + ig' Y B_\mu \delta_i^{\ j} \\ &= \partial_\mu \delta_i^{\ j} + \frac{i}{\sqrt{2}} g \left(W^+_\mu T^+ + W^-_\mu T^-\right) + \frac{i}{2} g W^3_\mu \sigma^3 + ig' Y B_\mu \delta_i^{\ j} \ , \end{aligned} \tag{B.13}$$

where σ are the Pauli matrices, and

$$T^\pm = \frac{1}{2}\left(\sigma^1 \pm i\sigma^2\right) \ . \tag{B.14}$$

Then, using the inverse relations between the original gauge fields and mass eigenstates:

$$B_\mu = c_w A_\mu - s_w Z_\mu \ , \qquad\qquad W^3_\mu = s_w A_\mu + c_w Z_\mu \ , \tag{B.15}$$

[1] For details see [111].

we rewrite the neutral part of the interaction omitting the representation indices:

$$\begin{aligned}\frac{i}{2}gW_\mu^3\sigma^3 + ig'YB_\mu &= igT^3\left(s_wA_\mu + c_wZ_\mu\right) + ig'Y\left(c_wA_\mu - s_wZ_\mu\right)\\ &= i\left(gc_wT^3 - g's_wY\right)Z_\mu + i\left(gs_wT^3 + g'c_wY\right)A_\mu\\ &= i\frac{g}{c_w}\left(T^3 - s_w^2Q\right)Z_\mu + ieQA_\mu\ ,\end{aligned} \tag{B.16}$$

where we have identified the coupling of the massless photon as the elementary charge e, and the combination of the unbroken generator of the gauge group and the hypercharge as the electromagnetic charge operator Q:

$$gs_w = g'c_w = e\ , \qquad\qquad Q = T^3 + Y\ . \tag{B.17}$$

Therefore, we find for the covariant derivative in terms of the mass-eigenstate field (omitting the representation indices):

$$D_\mu = \partial_\mu + \frac{i}{\sqrt{2}}g\left(W_\mu^+T^+ + W_\mu^-T^-\right) + i\frac{g}{c_w}\left(T^3 - s_w^2Q\right)Z_\mu + ieQA_\mu\ . \tag{B.18}$$

Using this form of the covariant derivative we can derive the couplings of the fermions transforming in the fundamental representation of $SU(2)$ to the gauge fields.

$$\mathcal{L}_{\text{int}} = -\lambda_i^\dagger\overline{\sigma}^\mu\left(\frac{g}{\sqrt{2}}\left(W_\mu^+T^+ + W_\mu^-T^-\right) + \frac{g}{c_w}\left(T^3 - s_w^2Q\right)Z_\mu + eQA_\mu\right)\lambda_i\ , \tag{B.19}$$

where now the index i runs over all fermions in the fundamental representation. For the up-type Higgs doublet we obtain the following interaction Lagrangian:

$$\begin{aligned}\mathcal{L}_{\text{int}}^{H_u} =& -\frac{g}{\sqrt{2}}h_u^{+\dagger}\overline{\sigma}^\mu W_\mu^+h_u^0 + \frac{g}{\sqrt{2}}h_u^{0\dagger}\overline{\sigma}^\mu W_\mu^-h_u^+ - \frac{g}{c_w}\frac{1}{2}h_u^{+\dagger}\overline{\sigma}^\mu h_u^+Z_\mu + s_w^2\frac{g}{c_w}h_u^{+\dagger}\overline{\sigma}^\mu h_u^+Z_\mu\\ &+ \frac{g}{c_w}\frac{1}{2}h_u^{0\dagger}\overline{\sigma}^\mu h_u^0Z_\mu - eh_u^{+\dagger}\overline{\sigma}^\mu h_u^+A_\mu\ .\end{aligned} \tag{B.20}$$

For the down-type Higgs doubling we similarly obtain:

$$\begin{aligned}\mathcal{L}_{\text{int}}^{H_d} =& -\frac{g}{\sqrt{2}}h_d^{0\dagger}\overline{\sigma}^\mu W_\mu^+h_d^- + \frac{g}{\sqrt{2}}h_d^{-\dagger}\overline{\sigma}^\mu W_\mu^-h_d^0 - \frac{g}{c_w}\frac{1}{2}h_d^{0\dagger}\overline{\sigma}^\mu h_d^0Z_\mu + \frac{g}{c_w}\frac{1}{2}h_d^{-\dagger}\overline{\sigma}^\mu h_d^-Z_\mu\\ &- s_w^2\frac{g}{c_w}h_d^{-\dagger}\overline{\sigma}^\mu h_d^-Z_\mu + eh_d^{-\dagger}\overline{\sigma}^\mu h_d^-A_\mu\ .\end{aligned} \tag{B.21}$$

The interaction Lagrangian for the lepton doublet has the form:

$$\begin{aligned}\mathcal{L}_{\text{int}}^{e} =& -\frac{g}{\sqrt{2}}\nu_i^\dagger\overline{\sigma}^\mu W_\mu^+e_i + \frac{g}{\sqrt{2}}e_i^\dagger\overline{\sigma}^\mu W_\mu^-\nu_i - \frac{g}{c_w}\frac{1}{2}\nu_i^\dagger\overline{\sigma}^\mu\nu_iZ_\mu + \frac{g}{c_w}\frac{1}{2}e_i^\dagger\overline{\sigma}^\mu e_iZ_\mu\\ &- s_w^2\frac{g}{c_w}e_i^\dagger\overline{\sigma}^\mu e_iZ_\mu + ee_i^\dagger\overline{\sigma}^\mu e_iA_\mu\ .\end{aligned} \tag{B.22}$$

The interaction Lagrangian for the lepton singlet is then:

$$\mathcal{L}_{\text{int}}^{e^c} = s_w^2\frac{g}{c_w}\bar{e}_i^\dagger\overline{\sigma}^\mu\bar{e}_iZ_\mu - e\bar{e}_i^\dagger\overline{\sigma}^\mu\bar{e}_iA_\mu\ . \tag{B.23}$$

In the next step we have to obtain the interaction terms for the gaugino fields transforming in the adjoint representation of $SU(2)$, these are the winos. The generators of the adjoint representation are:

$$T^1 = \begin{pmatrix} 0 & 0 & 0 \\ 0 & 0 & -i \\ 0 & i & 0 \end{pmatrix} , \qquad T^2 = \begin{pmatrix} 0 & 0 & i \\ 0 & 0 & 0 \\ -i & 0 & 0 \end{pmatrix} , \qquad T^3 = \begin{pmatrix} 0 & -i & 0 \\ i & 0 & 0 \\ 0 & 0 & 0 \end{pmatrix} . \tag{B.24}$$

We denote the wino triplet by (w^1, w^2, w^3). The winos will mix and form charged combinations similarly to the gauge bosons. Since they have no hypercharge, the interaction Lagrangian has the following form:

$$\mathcal{L}^w_{\text{int}} = -g \left(w^{1\dagger}, w^{2\dagger}, w^{3\dagger} \right) \overline{\sigma}^\mu \begin{pmatrix} -iW^3 w^2 + iW^2 w^3 \\ iW^3 w^1 - iW^1 w_3 \\ -iW^2 w^1 + iW^1 w^2 \end{pmatrix} . \tag{B.25}$$

After the multiplication we obtain:

$$\begin{aligned} \mathcal{L}^w_{\text{int}} = &- \Big(g(-iw^{1\dagger}\overline{\sigma}^\mu w^2 + iw^{2\dagger}\overline{\sigma}^\mu w^1) W^3 & \text{(B.26)} \\ &+ g(iw^{3\dagger}\overline{\sigma}^\mu (W^1 w^2 - W^2 w^1) + i(w^{1\dagger}\overline{\sigma}^\mu W^2 - w^{2\dagger}\overline{\sigma}^\mu W^1) w^3) \Big) . & \text{(B.27)} \end{aligned}$$

Next, we define the following fields:

$$w^\pm = \frac{1}{\sqrt{2}} (w^1 \mp i w^2) , \qquad w^{\pm\dagger} = \frac{1}{\sqrt{2}} (w^{1\dagger} \pm i w^{2\dagger}) , \tag{B.28}$$

and observe:

$$\begin{aligned} w^{+\dagger} + w^{+\dagger} - w^{-\dagger} w^{-\dagger} &= -iw^{1\dagger} w^2 + iw^{2\dagger} w^1 , \\ w^- W^+ - w^+ W^- &= i(W^1 w^2 - W^2 w^1) , \\ w^{-\dagger} W^- - w^{+\dagger} W^+ &= i(w^{1\dagger} W^2 - w^{2\dagger} W^1) . \end{aligned} \tag{B.29}$$

Using these relations and the relations between W^3 and mass-eigenstate fields, we obtain:

$$\begin{aligned} \mathcal{L}^w_{\text{int}} = &- \Big(g(w^{+\dagger}\overline{\sigma}^\mu w^{+\dagger} - w^{-\dagger}\overline{\sigma}^\mu w^{-\dagger})(c_w A_\mu - s_w Z_\mu) & \text{(B.30)} \\ &+ g(w^{3\dagger}\overline{\sigma}^\mu w^- - w^{+\dagger}\overline{\sigma}^\mu w^3) W^+ + (w^{-\dagger}\overline{\sigma}^\mu w^3 - w^{3\dagger}\overline{\sigma}^\mu w^+) W^- \Big) \\ = &\left(-eA_\mu - \frac{g}{c_w} Z_\mu \right) (w^{+\dagger}\overline{\sigma}^\mu w^+ - w^{-\dagger}\overline{\sigma}^\mu w^-) \\ &- g \left(w^{3\dagger}\overline{\sigma}^\mu w^- - w^{+\dagger}\overline{\sigma}^\mu w^3 \right) W^+ - g \left(w^{-\dagger}\overline{\sigma}^\mu w^3 - w^{3\dagger}\overline{\sigma}^\mu w^+ \right) W^- . \end{aligned}$$

Combining all these results, we arrive at the couplings of the gauge fields to charged and neutral matter:

$$\mathcal{L} = -eJ_{e\mu} A^\mu - \frac{g}{c_w} J_{Z\mu} Z^\mu - \frac{g}{\sqrt{2}} J^-_\mu W^{+\mu} - \frac{g}{\sqrt{2}} J^+_\mu W^{-\mu} . \tag{B.31}$$

The currents in the gauge eigenstate basis are

$$\begin{aligned}
J_{e\mu} =& J^3_{e\mu} + J^{2,1}_{e\mu} \\
=& \, w^{+\dagger}\bar{\sigma}_\mu w^+ - w^{-\dagger}\bar{\sigma}_\mu w^- - e_i^\dagger \bar{\sigma}_\mu e_i + \bar{e}_i^\dagger \bar{\sigma}_\mu \bar{e}_i - h_d^{-\dagger}\bar{\sigma}_\mu h_d^- + h_u^{+\dagger}\bar{\sigma}_\mu h_u^+ \, , \\
J_{Z\mu} =& -\frac{1}{2} h_u^{0\dagger}\bar{\sigma}_\mu h_u^0 + \frac{1}{2} h_d^{0\dagger}\bar{\sigma}_\mu h_d^0 + \frac{1}{2}\nu_i^\dagger \bar{\sigma}_\mu \nu_i \\
& + w^{+\dagger}\bar{\sigma}_\mu w^+ - w^{-\dagger}\bar{\sigma}_\mu w^- - \frac{1}{2} e_i^\dagger \bar{\sigma}_\mu e_i - \frac{1}{2} h_d^{-\dagger}\bar{\sigma}_\mu h_d^- + \frac{1}{2} h_u^{+\dagger}\bar{\sigma}_\mu h_u^+ - s_w^2 J^{2,1}_{e\mu} \, , \\
J^-_\mu =& \sqrt{2}\left(w^{3\dagger}\bar{\sigma}_\mu w^- - w^{+\dagger}\bar{\sigma}_\mu w^3 \right) + \nu_i^\dagger \bar{\sigma}_\mu e_i + h_d^{0\dagger}\bar{\sigma}_\mu h_d^- + h_u^{+\dagger}\bar{\sigma}_\mu h_u^0 \, , \\
J^+_\mu =& \sqrt{2}\left(w^{-\dagger}\bar{\sigma}_\mu w^3 - w^{3\dagger}\bar{\sigma}_\mu w^+ \right) - e_i^\dagger \bar{\sigma}_\mu \nu_i - h_d^{-\dagger}\bar{\sigma}_\mu h_d^0 - h_u^{0\dagger}\bar{\sigma}_\mu h_u^+ \, .
\end{aligned} \tag{B.32}$$

The upper indices of the electromagnetic currents indicate the transformation properties of the fields in the current under the $SU(2)_\mathrm{L}$. Having derived the currents, we have to transform them into the mass-eigenstate basis of fermions. Therefore, we have to diagonalize the mass matrices $\mathcal{M}^N$ and $\mathcal{M}^C$.

B.2.1 Currents in the mass-eigenstate Basis

The mass matrices $\mathcal{M}^N$ and $\mathcal{M}^C$ read

$$\mathcal{M}^N = \begin{pmatrix}
M_1 & 0 & m_Z s_\beta s_w & -m_Z c_\beta s_w & -\zeta_i m_Z s_w \\
0 & M_2 & -m_Z s_\beta c_w & m_Z c_\beta c_w & \zeta_i m_Z c_w \\
m_Z s_\beta s_w & -m_Z s_\beta c_w & 0 & -\mu & 0 \\
-m_Z c_\beta s_w & m_Z c_\beta c_w & -\mu & 0 & 0 \\
-\zeta_i m_Z s_w & \zeta_i m_Z c_w & 0 & 0 & 0
\end{pmatrix} ,$$

$$\mathcal{M}^C = \begin{pmatrix}
M_2 & \sqrt{2}\, m_Z s_\beta c_w & 0 & 0 & 0 \\
\sqrt{2}\, m_Z c_\beta c_w & \mu & \zeta_1 h^e_{11}\mu & \zeta_2 h^e_{22}\mu & \zeta_3 h^e_{33}\mu \\
\sqrt{2}\,\zeta_1 m_Z c_w & 0 & h^e_{11} v c_\beta & 0 & 0 \\
\sqrt{2}\,\zeta_2 m_Z c_w & 0 & 0 & h^e_{22} v c_\beta & 0 \\
\sqrt{2}\,\zeta_3 m_Z c_w & 0 & 0 & 0 & h^e_{33} v c_\beta
\end{pmatrix} . \tag{B.33}$$

They are diagonalized by Takagi diagonalization and singular value decomposition, respectively,

$$U^{(n)T}\mathcal{M}^N U^{(n)} = \mathcal{M}^N_\mathrm{diag} \, , \qquad\qquad U^{(c)\dagger}\mathcal{M}^C \widetilde{U}^{(c)} = \mathcal{M}^C_\mathrm{diag} \, , \tag{B.34}$$

where $U^{(n)\dagger}U^{(n)} = U^{(c)\dagger}U^{(c)} = \widetilde{U}^{(c)\dagger}\widetilde{U}^{(c)} = \mathbf{1}$. These unitary transformations relate the neutral and charged gauge-eigenstates to the mass-eigenstates (χ^0_a, ν'_i) $(a = 1, \ldots, 4)$ and (χ^-_α, e'_i), (χ^+_α, e'^c_i) $(\alpha = 1, 2)$, respectively

$$\begin{pmatrix} b \\ w^3 \\ h_u^0 \\ h_d^0 \\ \nu_i \end{pmatrix} = U^{(n)} \begin{pmatrix} \chi_1^0 \\ \chi_2^0 \\ \chi_3^0 \\ \chi_4^0 \\ \nu'_i \end{pmatrix} , \qquad \begin{pmatrix} w^- \\ h_d^- \\ e_i \end{pmatrix} = U^{(c)} \begin{pmatrix} \chi_1^- \\ \chi_2^- \\ e'_i \end{pmatrix} , \qquad \begin{pmatrix} w^+ \\ h_u^+ \\ e_i^c \end{pmatrix} = \widetilde{U}^{(c)} \begin{pmatrix} \chi_1^+ \\ \chi_2^+ \\ e'^c_i \end{pmatrix} . \tag{B.35}$$

The transformation matrices are given by:

$$U^{(n)} = \left(\begin{array}{c|c} U_{ab}^{(\chi^0)} & U_{ai}^{(\chi^0,\nu)} \\ \hline U_{ia}^{(\nu,\chi^0)} & U_{ij}^{(\nu)} \end{array} \right) , \tag{B.36}$$

$$U^{(c)} = \left(\begin{array}{c|c} U_{\alpha\beta}^{(\chi^-)} & U_{\alpha i}^{(\chi^-,e)} \\ \hline U_{i\alpha}^{(e,\chi^-)} & U_{ij}^{(e)} \end{array} \right) , \qquad \widetilde{U}^{(c)} = \left(\begin{array}{c|c} \widetilde{U}_{\alpha\beta}^{(\chi^+)} & \widetilde{U}_{\alpha i}^{(\chi^+,\bar{e})} \\ \hline \widetilde{U}_{i\alpha}^{(\bar{e},\chi^+)} & \widetilde{U}_{ij}^{(\bar{e})} \end{array} \right) . \tag{B.37}$$

Note that we perform a perturbative diagonalization of the mass matrices as described in the previous section. Therefore, the transformation matrices are given by an expansion in ζ and ϵ, where $\epsilon = \frac{m_Z}{M}$, and M is the largest mass parameter of either M_1, M_2 or μ. The parameter choice neither effects the expansion of the transformation matrices, nor the mass eigenstates.

Explicit Results for bino-like Neutralino

Let us now give some explicit results for the unitary transformation matrices for the case of bino-like neutralino. The unitary matrix $U^{(n)}$ is given by

$$\begin{aligned} U_{ab}^{(\chi^0)} = & \begin{pmatrix} 1 & 0 & 0 & 0 \\ 0 & 1 & 0 & 0 \\ 0 & 0 & -\frac{1}{\sqrt{2}} & \frac{1}{\sqrt{2}} \\ 0 & 0 & \frac{1}{\sqrt{2}} & \frac{1}{\sqrt{2}} \end{pmatrix} \\ & + \begin{pmatrix} -\frac{{m_Z}^2\left({M_1}^2+2\mu s_{2\beta}M_1+\mu^2\right)s_w^2}{2\left({M_1}^2-\mu^2\right)^2} & \frac{{m_Z}^2(M_2+\mu s_{2\beta})s_{2w}}{2(M_1-M_2)\left({M_2}^2-\mu^2\right)} & \frac{m_Z(c_\beta+s_\beta)s_w}{\sqrt{2}(M_1-\mu)} & \frac{m_Z(c_\beta-s_\beta)s_w}{\sqrt{2}(M_1+\mu)} \\ -\frac{{m_Z}^2(M_1+\mu s_{2\beta})s_{2w}}{2(M_1-M_2)\left({M_1}^2-\mu^2\right)} & -\frac{{m_Z}^2c_w^2\left({M_2}^2+2\mu s_{2\beta}M_2+\mu^2\right)}{2\left({M_2}^2-\mu^2\right)^2} & -\frac{m_Zc_w(c_\beta+s_\beta)}{\sqrt{2}(M_2-\mu)} & \frac{m_Zc_w(s_\beta-c_\beta)}{\sqrt{2}(M_2+\mu)} \\ \frac{m_Z(\mu c_\beta+M_1s_\beta)s_w}{{M_1}^2-\mu^2} & -\frac{m_Zc_w(\mu c_\beta+M_2s_\beta)}{{M_2}^2-\mu^2} & \frac{{m_Z}^2(c_\beta+s_\beta)}{\mu^2}x_1 & \frac{(c_\beta-s_\beta){m_Z}^2}{\mu^2}x_2 \\ -\frac{m_Z(M_1c_\beta+\mu s_\beta)s_w}{{M_1}^2-\mu^2} & \frac{m_Zc_w(M_2c_\beta+\mu s_\beta)}{{M_2}^2-\mu^2} & \frac{(c_\beta+s_\beta){m_Z}^2}{\mu^2}x_3 & \frac{(c_\beta-s_\beta){m_Z}^2}{\mu^2}x_4 \end{pmatrix} \\ & \times \left(1+\mathcal{O}\left(\frac{m_Z^2}{\mu^2}\right)\right) , \end{aligned} \tag{B.38}$$

where we used the abbreviations

$$x_1 = \frac{\mu}{4\sqrt{2}}\left(\frac{(M_2s_\beta-(M_2-2\mu)c_\beta)c_w^2}{(M_2-\mu)^2}+\frac{(M_1s_\beta-(M_1-2\mu)c_\beta)s_w^2}{(M_1-\mu)^2}\right) , \tag{B.39}$$

$$x_2 = \frac{\mu}{4\sqrt{2}}\left(-\frac{((M_2+2\mu)c_\beta+M_2s_\beta)c_w^2}{(M_2+\mu)^2}-\frac{((M_1+2\mu)c_\beta+M_1s_\beta)s_w^2}{(M_1+\mu)^2}\right) , \tag{B.40}$$

$$x_3 = \frac{\mu}{4\sqrt{2}}\left(\frac{((M_2-2\mu)s_\beta-M_2c_\beta)c_w^2}{(M_2-\mu)^2}+\frac{((M_1-2\mu)s_\beta-M_1c_\beta)s_w^2}{(M_1-\mu)^2}\right) , \tag{B.41}$$

$$x_4 = \frac{\mu}{4\sqrt{2}}\left(\frac{(M_2c_\beta+(M_2+2\mu)s_\beta)c_w^2}{(M_2+\mu)^2}+\frac{(M_1c_\beta+(M_1+2\mu)s_\beta)s_w^2}{(M_1+\mu)^2}\right) . \tag{B.42}$$

The numerical error of the matrix (B.38) in our parameter range of interest is smaller than 40% of the given NLO term. We do not discuss the slow convergence for this R-parity conserving sub-matrix further, since this is beyond the scope of our analysis.

Furthermore,

$$U_{ai}^{(\chi^0,\nu)} = \zeta_i \begin{pmatrix} s_w \frac{m_Z}{M_1} \\ -c_w \frac{m_Z}{M_2} \\ -\frac{{m_Z}^2 c_\beta \left(M_1 c_w^2 + M_2 s_w^2\right)}{M_1 M_2 \mu} \\ \frac{{m_Z}^2 s_\beta \left(M_1 c_w^2 + M_2 s_w^2\right)}{M_1 M_2 \mu} \end{pmatrix} \left(1 + \mathcal{O}\left(s_{2\beta} \frac{m_Z^2}{\mu^2}\right)\right) , \tag{B.43}$$

$$U_{ia}^{(\nu,\chi^0)} = \zeta_i \begin{pmatrix} -s_w \frac{m_Z}{M_1} \\ c_w \frac{m_Z}{M_2} \\ \frac{{m_Z}^2 \left(M_1 c_w^2 + M_2 s_w^2 - \mu\right)(c_\beta + s_\beta)}{\sqrt{2}(M_1 - \mu)\mu(\mu - M_2)} \\ \frac{{m_Z}^2 \left(M_1 c_w^2 + M_2 s_w^2 + \mu\right)(c_\beta - s_\beta)}{\sqrt{2}\mu(M_1 + \mu)(M_2 + \mu)} \end{pmatrix} \left(1 + \mathcal{O}\left(\frac{m_Z^2}{\mu^2}\right)\right) , \tag{B.44}$$

$$U_{ij}^{(\nu)} = \delta_{ij} + \mathcal{O}\left(\zeta^2 \frac{m_Z^2}{\mu^2}\right) . \tag{B.45}$$

The uncertainties in Eq. (B.43) evaluate numerically to less than 5%. For $U_{ia}^{(\nu,\chi^0)}$ they are less than $0.15, 0.10, 0.25, 0.25$, for $a = 1, \ldots, 4$, respectively.

The chargino matrix is diagonalized by the following transformation:

$$\widetilde{U}_{\alpha\beta}^{(\chi^+)} = \begin{pmatrix} 1 & 0 \\ 0 & 1 \end{pmatrix} + \begin{pmatrix} -\frac{{m_Z}^2 c_w^2 (\mu c_\beta + M_2 s_\beta)^2}{\left({M_2}^2 - \mu^2\right)^2} & \frac{\sqrt{2} m_Z c_w (\mu c_\beta + M_2 s_\beta)}{\mu^2 - {M_2}^2} \\ -\frac{\sqrt{2} m_Z c_w (\mu c_\beta + M_2 s_\beta)}{\mu^2 - {M_2}^2} & -\frac{{m_Z}^2 c_w^2 (\mu c_\beta + M_2 s_\beta)^2}{\left({M_2}^2 - \mu^2\right)^2} \end{pmatrix} \left(1 + \mathcal{O}\left(\frac{m_Z^2}{\mu^2}\right)\right) , \tag{B.46}$$

$$\widetilde{U}_{ij}^{(\bar{e})} = \delta_{ij} + \mathcal{O}\left(\zeta^2\right) . \tag{B.47}$$

Numerically, the relative correction to the NLO contribution to $\widetilde{U}_{\alpha\beta}^{(\chi^+)}$ is less than 25%. The off-diagonal elements of the matrix $\widetilde{U}^{(c)}$ to leading order in h_{ii}^e are

$$\begin{aligned} \widetilde{U}_{\alpha i}^{(\chi^+,\bar{e})} =& -\zeta_i h_{ii}^e \begin{pmatrix} 0 \\ 1 \end{pmatrix} \\ &+ \zeta_i h_{ii}^e \begin{pmatrix} \frac{\sqrt{2} m_Z c_w (M_2 s_\beta - v c_\beta)}{{M_2}^2} \\ \frac{2 {m_Z}^2 c_\beta c_w^2 (v\mu c_\beta + M_2 (v - \mu) s_\beta)}{{M_2}^2 \mu^2} \end{pmatrix} \left(1 + \mathcal{O}\begin{pmatrix} \frac{s_{2\beta} m_Z^2}{\mu^2} \\ \frac{m_Z^2}{\mu^2} \end{pmatrix}\right) , \end{aligned} \tag{B.48}$$

$$\begin{aligned} \widetilde{U}_{i\alpha}^{(\bar{e},\chi^+)} =& \zeta_i h_{ii}^e \begin{pmatrix} 0 \\ 1 \end{pmatrix} \\ &+ \zeta_i h_{ii}^e \begin{pmatrix} \frac{\sqrt{2} m_Z c_w \left(M_2 s_\beta \mu^2 + \left({M_2}^2 (v + \mu) - v\mu^2\right) c_\beta\right)}{{M_2}^2 \left(M_2^2 - \mu^2\right)} \\ -\frac{{m_Z}^2 \mu^2 c_w^2 y}{\left(\mu^2 - {M_2}^2\right)^2} \end{pmatrix} \left(1 + \mathcal{O}\left(\frac{m_Z^2}{\mu^2}\right)\right) , \end{aligned} \tag{B.49}$$

where

$$y = \frac{1}{\mu^4} \left(s_{2\beta} M_2 \left(M_2^2 \mu - 2\mu^3 + v(\mu^2 - M_2^2)\right) + c_\beta^2 \mu (2v(\mu^2 - M_2^2) - \mu^3) + s_\beta^2 \mu^2 (M_2^2 - 2\mu^2)\right) . \tag{B.50}$$

The numerical relative correction to the NLO term in $\widetilde{U}^{(\bar{e},\chi^+)}_{i\alpha}$ is smaller than $0.10, 0.15$ for $\alpha = 1, 2$, respectively. For $\widetilde{U}^{(\chi^+,\bar{e})}_{1i}$ it is smaller[2] than 1%, and smaller than 10% for $\widetilde{U}^{(\chi^+,e^c)}_{2i}$.

The block diagonal elements of the matrix $U^{(c)}$ are

$$U^{(\chi^-)}_{\alpha\beta} = \begin{pmatrix} 1 & 0 \\ 0 & 1 \end{pmatrix} + \begin{pmatrix} -\frac{{m_Z}^2 c_w^2 (M_2 c_\beta + \mu s_\beta)^2}{\left({M_2}^2 - \mu^2\right)^2} & -\frac{\sqrt{2} m_Z c_w (M_2 c_\beta + \mu s_\beta)}{\mu^2 - {M_2}^2} \\ \frac{\sqrt{2} m_Z c_w (M_2 c_\beta + \mu s_\beta)}{\mu^2 - {M_2}^2} & -\frac{{m_Z}^2 c_w^2 (M_2 c_\beta + \mu s_\beta)^2}{\left({M_2}^2 - \mu^2\right)^2} \end{pmatrix} \left(1 + \mathcal{O}\left(\frac{m_Z^2}{\mu^2}\right)\right) , \tag{B.51}$$

$$U^{(e)}_{ij} = \delta_{ij} + \mathcal{O}\left(\zeta^2\right) . \tag{B.52}$$

Numerically, the relative correction to the NLO contribution to $U^{(\chi^-)}_{\alpha\beta}$ is smaller than 20%. The off-diagonal elements of $U^{(c)}$ are

$$U^{(\chi^-,e)}_{\alpha i} = \zeta_i \begin{pmatrix} -\frac{\sqrt{2} m_Z c_w}{M_2} \\ \frac{{m_Z}^2 c_w^2 s_\beta}{M_2 \mu} \end{pmatrix} \left(1 + \mathcal{O}\left(\frac{s_{2\beta} m_Z^2}{\mu^2}\right)\right) , \tag{B.53}$$

$$U^{(e,\chi^-)}_{i\alpha} = \zeta_i \begin{pmatrix} \frac{\sqrt{2} m_Z c_w}{M_2} \\ \frac{{m_Z}^2 c_w^2 (\mu c_\beta + M_2 s_\beta)}{\mu^3 - {M_2}^2 \mu} \end{pmatrix} \left(1 + \mathcal{O}\left(\frac{s_{2\beta} m_Z^2}{\mu^2}\right)\right) . \tag{B.54}$$

Here we ignored corrections that are proportional to the Yukawa couplings h^e_{ii} or higher powers thereof. The numerical value of the higher order correction relative to the NLO term is smaller than 1% for $U^{(\chi^-,e)}_{\alpha i}$, smaller than 5% for $U^{(e,\chi^-)}_{i1}$, and smaller than 15% for $U^{(e,\chi^-)}_{i2}$.

Current Transformations

The higgsino and neutrino gauge-eigenstates read in terms of the mass eigenstates:

$$\begin{aligned}
b &= U^{(\chi^0)}_{1b} \chi^0_b + U^{(\chi^0,\nu)}_{1j} \nu'_j , && && && \\
w^3 &= U^{(\chi^0)}_{2b} \chi^0_b + U^{(\chi^0,\nu)}_{2j} \nu'_j , & w^- &= U^{(\chi^-)}_{1\beta} \chi^-_\beta + U^{(\chi^-,e)}_{1j} e'_j , & w^+ &= \widetilde{U}^{(\chi^+)}_{1\beta} \chi^+_\beta + \widetilde{U}^{(\chi^+,\bar{e})}_{1j} \bar{e}'_j , \\
h^0_u &= U^{(\chi^0)}_{3b} \chi^0_b + U^{(\chi^0,\nu)}_{3j} \nu'_j , & && h^+_u &= \widetilde{U}^{(\chi^+)}_{2\beta} \chi^+_\beta + \widetilde{U}^{(\chi^+,\bar{e})}_{2j} \bar{e}'_j , \\
h^0_d &= U^{(\chi^0)}_{4b} \chi^0_b + U^{(\chi^0,\nu)}_{4j} \nu'_j , & h^-_d &= U^{(\chi^-)}_{2\beta} \chi^-_\beta + U^{(\chi^-,e)}_{2j} e'_j , & && \\
\nu_i &= U^{(\nu,\chi^0)}_{ib} \chi^0_b + U^{(\nu)}_{ij} \nu'_j , & e_i &= U^{(e,\chi^-)}_{i\beta} \chi^-_\beta + U^{(e)}_{ij} e'_j , & e^c_i &= \widetilde{U}^{(\bar{e},\chi^+)}_{i\beta} \chi^+_\beta + \widetilde{U}^{(\bar{e})}_{ij} \bar{e}'_j .
\end{aligned} \tag{B.55}$$

Therefore, the photon current in the mass eigenstate basis is given by:

$$\begin{aligned}
J_{e\mu} = &(\chi^{+\dagger}_\beta \widetilde{U}^{(\chi^+)}_{1\beta} + \bar{e}'^\dagger_j \widetilde{U}^{(\chi^+,\bar{e})}_{1j}) \bar{\sigma}_\mu (\widetilde{U}^{(\chi^+)}_{1\beta} \chi^+_\beta + \widetilde{U}^{(\chi^+,\bar{e})}_{1j} \bar{e}'_j) \\
&- (\chi^{-\dagger}_\beta U^{(\chi^-)}_{1\beta} + e'^\dagger_j U^{(\chi^-,e)}_{1j}) \bar{\sigma}_\mu (U^{(\chi^-)}_{1\beta} \chi^-_\beta + U^{(\chi^-,e)}_{1j} e'_j) \\
&- (\chi^{-\dagger}_\beta U^{(e,\chi^-)}_{i\beta} + e'^\dagger_j U^{(e)}_{ij}) \bar{\sigma}_\mu (U^{(e,\chi^-)}_{i\beta} \chi^-_\beta + U^{(e)}_{ij} e'_j) \\
&+ (\chi^{+\dagger}_\beta \widetilde{U}^{(\bar{e},\chi^+)}_{i\beta} + \bar{e}'^\dagger_j \widetilde{U}^{(e^c)}_{ij}) \bar{\sigma}_\mu (\widetilde{U}^{(\bar{e},\chi^+)}_{i\beta} \chi^+_\beta + \widetilde{U}^{(\bar{e})}_{ij} \bar{e}'_j) \\
&- (\chi^{-\dagger}_\beta U^{(\chi^-)}_{2\beta} + e'^\dagger_j U^{(\chi^-,e)}_{2j}) \bar{\sigma}_\mu (U^{(\chi^-)}_{2\beta} \chi^-_\beta + U^{(\chi^-,e)}_{2j} e'_j) \\
&+ (\chi^{+\dagger}_\beta \widetilde{U}^{(\chi^+)}_{2\beta} + \bar{e}'^\dagger_j \widetilde{U}^{(\chi^+,\bar{e})}_{2j}) \bar{\sigma}_\mu (\widetilde{U}^{(\chi^+)}_{2\beta} \chi^+_\beta + \widetilde{U}^{(\chi^+,\bar{e})}_{2j} \bar{e}'_j) ,
\end{aligned} \tag{B.56}$$

[2]The numerical calculation of the error reaches our numerical precision. The given value is calculated from the comparison with the analytical NNLO expression.

which can be expanded to

$$\begin{aligned}
J_{e\mu} = &\chi_\alpha^{+\dagger}\widetilde{U}_{1\alpha}^{(\chi^+)}\bar{\sigma}_\mu\widetilde{U}_{1\beta}^{(\chi^+)}\chi_\beta^+ + \chi_\alpha^{+\dagger}\widetilde{U}_{1\alpha}^{(\chi^+)}\bar{\sigma}_\mu\widetilde{U}_{1j}^{(\chi^+,\bar{e})}\bar{e}' \\
&+ \bar{e}_i'^{\dagger}\widetilde{U}_{1i}^{(\chi^+,\bar{e})}\bar{\sigma}_\mu\widetilde{U}_{1\beta}^{(\chi^+)}\chi_\beta^+ + \bar{e}_i'^{\dagger}\widetilde{U}_{1i}^{(\chi^+,\bar{e})}\bar{\sigma}_\mu\widetilde{U}_{1j}^{(\chi^+,\bar{e})}\bar{e}' \\
&- \chi_\alpha^{-\dagger}U_{1\alpha}^{(\chi^-)}\bar{\sigma}_\mu U_{1\beta}^{(\chi^-)}\chi_\beta^- - \chi_\alpha^{-\dagger}U_{1\alpha}^{(\chi^-)}\bar{\sigma}_\mu U_{1j}^{(\chi^-,e)}e_j' \\
&- e_i'^{\dagger}U_{1i}^{(\chi^-,e)}\bar{\sigma}_\mu U_{1\beta}^{(\chi^-)}\chi_\beta^- - e_i'^{\dagger}U_{1i}^{(\chi^-,e)}\bar{\sigma}_\mu U_{1j}^{(\chi^-,e)}e_j' \\
&- \chi_\alpha^{-\dagger}U_{i\alpha}^{(e,\chi^-)}\bar{\sigma}_\mu U_{i\beta}^{(e,\chi^-)}\chi_\beta^- - \chi_\alpha^{-\dagger}U_{i\alpha}^{(e,\chi^-)}\bar{\sigma}_\mu U_{ij}^{(e)}e_j' \\
&- e_i'^{\dagger}U_{ki}^{(e)}\bar{\sigma}_\mu U_{k\beta}^{(e,\chi^-)}\chi_\beta^- - e_i'^{\dagger}U_{ki}^{(e)}\bar{\sigma}_\mu U_{kj}^{(e)}e_j' \\
&+ \chi_\alpha^{+\dagger}\widetilde{U}_{i\alpha}^{(\bar{e},\chi^+)}\bar{\sigma}_\mu\widetilde{U}_{i\beta}^{(\bar{e},\chi^+)}\chi_\beta^+ + \chi_\alpha^{+\dagger}\widetilde{U}_{i\alpha}^{(\bar{e},\chi^+)}\bar{\sigma}_\mu\widetilde{U}_{ij}^{(\bar{e})}\bar{e}' \\
&+ \bar{e}_i'^{\dagger}\widetilde{U}_{ki}^{(\bar{e})}\bar{\sigma}_\mu\widetilde{U}_{k\beta}^{(\bar{e},\chi^+)}\chi_\beta^+ + \bar{e}_i'^{\dagger}\widetilde{U}_{ki}^{(\bar{e})}\bar{\sigma}_\mu\widetilde{U}_{kj}^{(\bar{e})}\bar{e}' \\
&- \chi_\alpha^{-\dagger}U_{2\alpha}^{(\chi^-)}\bar{\sigma}_\mu U_{2\beta}^{(\chi^-)}\chi_\beta^- - \chi_\alpha^{-\dagger}U_{2\alpha}^{(\chi^-)}\bar{\sigma}_\mu U_{2j}^{(\chi^-,e)}e_j' \\
&- e_i'^{\dagger}U_{2i}^{(\chi^-,e)}\bar{\sigma}_\mu U_{2\beta}^{(\chi^-)}\chi_\beta^- - e_i'^{\dagger}U_{2i}^{(\chi^-,e)}\bar{\sigma}_\mu U_{2j}^{(\chi^-,e)}e_j' \\
&+ \chi_\alpha^{+\dagger}\widetilde{U}_{2\alpha}^{(\chi^+)}\bar{\sigma}_\mu\widetilde{U}_{2\beta}^{(\chi^+)}\chi_\beta^+ + \chi_\alpha^{+\dagger}\widetilde{U}_{2\alpha}^{(\chi^+)}\bar{\sigma}_\mu\widetilde{U}_{2j}^{(\chi^+,\bar{e})}\bar{e}' \\
&+ \bar{e}_i'^{\dagger}\widetilde{U}_{2i}^{(\chi^+,\bar{e})}\bar{\sigma}_\mu\widetilde{U}_{2\beta}^{(\chi^+)}\chi_\beta^+ + \bar{e}_i'^{\dagger}\widetilde{U}_{2i}^{(\chi^+,\bar{e})}\bar{\sigma}_\mu\widetilde{U}_{2j}^{(\chi^+,\bar{e})}\bar{e}' \ . \qquad \text{(B.57)}
\end{aligned}$$

Finally, the simplified expression reads

$$\begin{aligned}
J_{e\mu} = &\chi_\alpha^{-\dagger}\bar{\sigma}_\mu V_{\alpha\beta}^{(\chi^-)}\chi_\beta^- + \chi_\alpha^{+\dagger}\bar{\sigma}_\mu V_{\alpha\beta}^{(\chi^+)}\chi_\beta^+ + e_i^\dagger\bar{\sigma}_\mu V_{ij}^{(e)}e_j + \bar{e}_i^\dagger\bar{\sigma}_\mu V_{ij}^{(\bar{e})}\bar{e}_j \\
&+ \left(\chi_\alpha^{-\dagger}\bar{\sigma}_\mu V_{\alpha j}^{(\chi^-,e)}e_j + \chi_\alpha^{+\dagger}\bar{\sigma}_\mu V_{\alpha j}^{(\chi^+,\bar{e})}\bar{e}_j + h.c.\right) \ , \qquad \text{(B.58)}
\end{aligned}$$

where we have defined:

$$\begin{aligned}
V_{\alpha\beta}^{(\chi^-)} &= -U_{1\alpha}^{(\chi^-)}U_{1\beta}^{(\chi^-)} - U_{2\alpha}^{(\chi^-)}U_{2\beta}^{(\chi^-)} - \sum_i U_{i\alpha}^{(e,\chi^-)}U_{i\beta}^{(e,\chi^-)} \ , \\
V_{\alpha\beta}^{(\chi^+)} &= \widetilde{U}_{1\alpha}^{(\chi^+)}\widetilde{U}_{1\beta}^{(\chi^+)} + \widetilde{U}_{2\alpha}^{(\chi^+)}\widetilde{U}_{2\beta}^{(\chi^+)} + \sum_i \widetilde{U}_{i\alpha}^{(\bar{e},\chi^+)}\widetilde{U}_{i\beta}^{(\bar{e},\chi^+)} \ , \\
V_{ij}^{(e)} &= -U_{1i}^{(\chi^-,e)}U_{1j}^{(\chi^-,e)} - U_{2i}^{(\chi^-,e)}U_{2j}^{(\chi^-,e)} - \sum_k U_{ki}^{(e)}U_{kj}^{(e)} \ , \\
V_{ij}^{(\bar{e})} &= \widetilde{U}_{1i}^{(\chi^+,\bar{e})}\widetilde{U}_{1j}^{(\chi^+,\bar{e})} + \widetilde{U}_{2i}^{(\chi^+,\bar{e})}\widetilde{U}_{2j}^{(\chi^+,\bar{e})} + \sum_k \widetilde{U}_{ki}^{(\bar{e})}\widetilde{U}_{kj}^{(\bar{e})} \ , \\
V_{\alpha j}^{(\chi^-,e)} &= -U_{1\alpha}^{(\chi^-)}U_{1j}^{(\chi^-,e)} - U_{2\alpha}^{(\chi^-)}U_{2j}^{(\chi^-,e)} - \sum_i U_{i\alpha}^{(e,\chi^-)}U_{ij}^{(e)} \ , \\
V_{\alpha j}^{(\chi^+,\bar{e})} &= \widetilde{U}_{1\alpha}^{(\chi^+)}\widetilde{U}_{1j}^{(\chi^+,\bar{e})} + \widetilde{U}_{2\alpha}^{(\chi^+)}\widetilde{U}_{2j}^{(\chi^+,\bar{e})} + \sum_i \widetilde{U}_{i\alpha}^{(\bar{e},\chi^+)}\widetilde{U}_{ij}^{(\bar{e})} \ . \qquad \text{(B.59)}
\end{aligned}$$

The neutral current in the mass eigenstate basis is given by

$$\begin{aligned}
J_{Z\mu} = &-\frac{1}{2}(\chi_b^{0\dagger}U_{3b}^{(\chi^0)} + \nu_j'^{\dagger}U_{3j}^{(\chi^0,\nu)})\bar{\sigma}_\mu(U_{3b}^{(\chi^0)}\chi_b^0 + U_{3j}^{(\chi^0,\nu)}\nu_j') \\
&+ \frac{1}{2}(\chi_b^{0\dagger}U_{4b}^{(\chi^0)} + \nu_j'^{\dagger}U_{4j}^{(\chi^0,\nu)})\bar{\sigma}_\mu(U_{4b}^{(\chi^0)}\chi_b^0 + U_{4j}^{(\chi^0,\nu)}\nu_j')
\end{aligned}$$

$$
\begin{aligned}
&+\frac{1}{2}(\chi_b^{0\dagger}U_{ib}^{(\nu,\chi^0)}+\nu_j'^{\dagger}U_{ij}^{(\nu)})\bar{\sigma}_\mu(U_{ib}^{(\nu,\chi^0)}\chi_b^0+U_{ij}^{(\nu)}\nu_j')\\
&+(\chi_\beta^{+\dagger}\widetilde{U}_{1\beta}^{(\chi^+)}+\bar{e}_j'^{\dagger}\widetilde{U}_{1j}^{(\chi^+,\bar{e})})\bar{\sigma}_\mu(\widetilde{U}_{1\beta}^{(\chi^+)}\chi_\beta^+\widetilde{U}_{1j}^{(\chi^+,\bar{e})}\bar{e}_j')\\
&-(\chi_\beta^{-\dagger}U_{1\beta}^{(\chi^-)}+e_j'^{\dagger}U_{1j}^{(\chi^-,e)})\bar{\sigma}_\mu(U_{1\beta}^{(\chi^-)}\chi_\beta^-+U_{1j}^{(\chi^-,e)}e_j')\\
&-\frac{1}{2}(\chi_\beta^{-\dagger}U_{i\beta}^{(e,\chi^-)}+e_j'^{\dagger}U_{ij}^{(e)})\bar{\sigma}_\mu(U_{i\beta}^{(e,\chi^-)}\chi_\beta^-+U_{ij}^{(e)}e_j')\\
&-\frac{1}{2}(\chi_\beta^{-\dagger}U_{2\beta}^{(\chi^-)}+e_j'^{\dagger}U_{2j}^{(\chi^-,e)})\bar{\sigma}_\mu(U_{2\beta}^{(\chi^-)}\chi_\beta^-+U_{2j}^{(\chi^-,e)}e_j')\\
&+\frac{1}{2}(\chi_\beta^{+\dagger}\widetilde{U}_{2\beta}^{(\chi^+)}+\bar{e}_j'^{\dagger}\widetilde{U}_{2j}^{(\chi^+,\bar{e})})\bar{\sigma}_\mu(\widetilde{U}_{2\beta}^{(\chi^+)}\chi_\beta^+\widetilde{U}_{2j}^{(\chi^+,\bar{e})}\bar{e}_j')-s_w^2J_{e\mu}\ ,
\end{aligned}
\tag{B.60}
$$

which expands to

$$
\begin{aligned}
J_{Z\mu}=&-\frac{1}{2}\chi_a^{0\dagger}U_{3a}^{(\chi^0)}\bar{\sigma}_\mu U_{3b}^{(\chi^0)}\chi_b^0-\frac{1}{2}\chi_a^{0\dagger}U_{3a}^{(\chi^0)}\bar{\sigma}_\mu U_{3j}^{(\chi^0,\nu)}\nu_j'\\
&-\frac{1}{2}\nu_j'^{\dagger}U_{3j}^{(\chi^0,\nu)}\bar{\sigma}_\mu U_{3b}^{(\chi^0)}\chi_b^0-\frac{1}{2}\nu_i'^{\dagger}U_{3i}^{(\chi^0,\nu)}\bar{\sigma}_\mu U_{3j}^{(\chi^0,\nu)}\nu_j'\\
&+\frac{1}{2}\chi_a^{0\dagger}U_{4a}^{(\chi^0)}\bar{\sigma}_\mu U_{4b}^{(\chi^0)}\chi_b^0+\frac{1}{2}\chi_a^{0\dagger}U_{4a}^{(\chi^0)}\bar{\sigma}_\mu U_{4j}^{(\chi^0,\nu)}\nu_j'\\
&+\frac{1}{2}\nu_j'^{\dagger}U_{4j}^{(\chi^0,\nu)}\bar{\sigma}_\mu U_{4b}^{(\chi^0)}\chi_b^0+\frac{1}{2}\nu_i'^{\dagger}U_{4i}^{(\chi^0,\nu)}\bar{\sigma}_\mu U_{4j}^{(\chi^0,\nu)}\nu_j'\\
&+\frac{1}{2}\chi_a^{0\dagger}U_{ia}^{(\nu,\chi^0)}\bar{\sigma}_\mu U_{ib}^{(\nu,\chi^0)}\chi_b^0+\frac{1}{2}\chi_a^{0\dagger}U_{ia}^{(\nu,\chi^0)}\bar{\sigma}_\mu U_{ij}^{(\nu)}\nu_j'\\
&+\frac{1}{2}\nu_j'^{\dagger}U_{ij}^{(\nu)}\bar{\sigma}_\mu U_{ib}^{(\nu,\chi^0)}\chi_b^0+\frac{1}{2}\nu_i'^{\dagger}U_{ki}^{(\nu)}\bar{\sigma}_\mu U_{kj}^{(\nu)}\nu_j'\\
&+\chi_\alpha^{+\dagger}\widetilde{U}_{1\alpha}^{(\chi^+)}\bar{\sigma}_\mu\widetilde{U}_{1\beta}^{(\chi^+)}\chi_\beta^++\chi_\alpha^{+\dagger}\widetilde{U}_{1\alpha}^{(\chi^+)}\bar{\sigma}_\mu\widetilde{U}_{1j}^{(\chi^+,\bar{e})}\bar{e}_j'\\
&+\bar{e}_i'^{\dagger}\widetilde{U}_{1i}^{(\chi^+,\bar{e})}\bar{\sigma}_\mu\widetilde{U}_{1\beta}^{(\chi^+)}\chi_\beta^++\bar{e}_i'^{\dagger}\widetilde{U}_{1i}^{(\chi^+,\bar{e})}\bar{\sigma}_\mu\widetilde{U}_{1j}^{(\chi^+,\bar{e})}\bar{e}_j'\\
&-\chi_\alpha^{-\dagger}U_{1\alpha}^{(\chi^-)}\bar{\sigma}_\mu U_{1\beta}^{(\chi^-)}\chi_\beta^--\chi_\alpha^{-\dagger}U_{1\alpha}^{(\chi^-)}\bar{\sigma}_\mu U_{1j}^{(\chi^-,e)}e_j'\\
&-e'^{\dagger}U_{1i}^{(\chi^-,e)}\bar{\sigma}_\mu U_{1\beta}^{(\chi^-)}\chi_\beta^--e_i'^{\dagger}U_{1i}^{(\chi^-,e)}\bar{\sigma}_\mu U_{1j}^{(\chi^-,e)}e_j'\\
&-\frac{1}{2}\chi_\alpha^{-\dagger}U_{i\alpha}^{(e,\chi^-)}\bar{\sigma}_\mu U_{i\beta}^{(e,\chi^-)}\chi_\beta^--\frac{1}{2}\chi_\alpha^{-\dagger}U_{i\alpha}^{(e,\chi^-)}\bar{\sigma}_\mu U_{ij}^{(e)}e_j'\\
&-\frac{1}{2}e_i'^{\dagger}U_{ki}^{(e)}\bar{\sigma}_\mu U_{k\beta}^{(e,\chi^-)}\chi_\beta^--\frac{1}{2}e_i'^{\dagger}U_{ki}^{(e)}\bar{\sigma}_\mu U_{kj}^{(e)}e_j'\\
&-\frac{1}{2}\chi_\alpha^{-\dagger}U_{2\alpha}^{(\chi^-)}\bar{\sigma}_\mu U_{2\beta}^{(\chi^-)}\chi_\beta^--\frac{1}{2}\chi_\alpha^{-\dagger}U_{2\alpha}^{(\chi^-)}\bar{\sigma}_\mu U_{2j}^{(\chi^-,e)}e_j'\\
&-\frac{1}{2}e_i'^{\dagger}U_{2i}^{(\chi^-,e)}\bar{\sigma}_\mu U_{2\beta}^{(\chi^-)}\chi_\beta^--\frac{1}{2}e_i'^{\dagger}U_{2i}^{(\chi^-,e)}\bar{\sigma}_\mu U_{2j}^{(\chi^-,e)}e_j'\\
&+\frac{1}{2}\chi_\alpha^{+\dagger}\widetilde{U}_{2\alpha}^{(\chi^+)}\bar{\sigma}_\mu\widetilde{U}_{2\beta}^{(\chi^+)}\chi_\beta^++\frac{1}{2}\chi_\alpha^{+\dagger}\widetilde{U}_{2\alpha}^{(\chi^+)}\bar{\sigma}_\mu\widetilde{U}_{2j}^{(\chi^+,\bar{e})}\bar{e}_j'\\
&+\frac{1}{2}\bar{e}_i'^{\dagger}\widetilde{U}_{2i}^{(\chi^+,\bar{e})}\bar{\sigma}_\mu\widetilde{U}_{2\beta}^{(\chi^+)}\chi_\beta^++\frac{1}{2}\bar{e}_i'^{\dagger}\widetilde{U}_{2i}^{(\chi^+,\bar{e})}\bar{\sigma}_\mu\widetilde{U}_{2j}^{(\chi^+,\bar{e})}\bar{e}_j'-s_w^2J_{e\mu}\ .
\end{aligned}
\tag{B.61}
$$

This expression can be combined to

$$
\begin{aligned}
J_{Z\mu}=&\chi_a^{0\dagger}\bar{\sigma}_\mu V_{ab}^{(\chi^0)}\chi_b^0+\chi_\alpha^{-\dagger}\bar{\sigma}_\mu V_{\alpha\beta}^{(\chi^-)}\chi_\beta^-+\chi_\alpha^{+\dagger}\bar{\sigma}_\mu V_{\alpha\beta}^{(\chi^+)}\chi_\beta^++\nu_i^{\dagger}\bar{\sigma}_\mu V_{ij}^{(\nu)}\nu_j+e_i^{\dagger}\bar{\sigma}_\mu V_{ij}^{(e)}e_j\\
&+\bar{e}_i^{\dagger}\bar{\sigma}_\mu V_{ij}^{(\bar{e})}\bar{e}_j+\Big(\chi_a^{0\dagger}\bar{\sigma}_\mu V_{aj}^{(\chi,\nu)}\nu_j+\chi_\alpha^{-\dagger}\bar{\sigma}_\mu V_{\alpha j}^{(\chi^-,e)}e_j+\chi_\alpha^{+\dagger}\bar{\sigma}_\mu V_{\alpha j}^{(\chi^+,\bar{e})}\bar{e}_j+\text{h.c.}\Big)-s_w^2J_{e\mu}\ ,
\end{aligned}
\tag{B.62}
$$

where

$$
\begin{aligned}
V_{ab}^{(\chi^0)} &= -\frac{1}{2}U_{3a}^{(\chi^0)}U_{3b}^{(\chi^0)} + \frac{1}{2}U_{4a}^{(\chi^0)}U_{4b}^{(\chi^0)} + \frac{1}{2}\sum_i U_{ia}^{(\nu,\chi^0)}U_{ib}^{(\nu,\chi^0)} \ , \\
V_{\alpha\beta}^{(\chi^-)} &= -U_{1\alpha}^{(\chi^-)}U_{1\beta}^{(\chi^-)} - \frac{1}{2}U_{2\alpha}^{(\chi^-)}U_{2\beta}^{(\chi^-)} - \frac{1}{2}\sum_i U_{i\alpha}^{(e,\chi^-)}U_{i\beta}^{(e,\chi^-)} \ , \\
V_{\alpha\beta}^{(\chi^+)} &= \widetilde{U}_{1\alpha}^{(\chi^+)}\widetilde{U}_{1\beta}^{(\chi^+)} + \frac{1}{2}\widetilde{U}_{2\alpha}^{(\chi^+)}\widetilde{U}_{2\beta}^{(\chi^+)} \ , \\
V_{ij}^{(\nu)} &= -\frac{1}{2}U_{3i}^{(\chi^0,\nu)}U_{3j}^{(\chi^0,\nu)} + \frac{1}{2}U_{4i}^{(\chi^0,\nu)}U_{4j}^{(\chi^0,\nu)} + \frac{1}{2}\sum_k U_{ki}^{(\nu)}U_{kj}^{(\nu)} \ , \\
V_{ij}^{(e)} &= -U_{1i}^{(\chi^-,e)}U_{1j}^{(\chi^-,e)} - \frac{1}{2}U_{2i}^{(\chi^-,e)}U_{2j}^{(\chi^-,e)} - \frac{1}{2}\sum_k U_{ki}^{(e)}U_{kj}^{(e)} \ , \\
V_{ij}^{(\bar{e})} &= \widetilde{U}_{1i}^{(\chi^+,\bar{e})}\widetilde{U}_{1j}^{(\chi^+,\bar{e})} + \frac{1}{2}\widetilde{U}_{2i}^{(\chi^+,\bar{e})}\widetilde{U}_{2j}^{(\chi^+,\bar{e})} \ , \\
V_{aj}^{(\chi,\nu)} &= -\frac{1}{2}U_{3a}^{(\chi^0)}U_{3j}^{(\chi^0,\nu)} + \frac{1}{2}U_{4a}^{(\chi^0)}U_{4j}^{(\chi^0,\nu)} + \frac{1}{2}\sum_k U_{ka}^{(\nu,\chi^0)}U_{kj}^{(\nu)} \ , \\
V_{\alpha j}^{(\chi^-,e)} &= -U_{1\alpha}^{(\chi^-)}U_{1j}^{(\chi^-,e)} - \frac{1}{2}U_{2\alpha}^{(\chi^-)}U_{2j}^{(\chi^-,e)} - \frac{1}{2}\sum_i U_{i\alpha}^{(e,\chi^-)}U_{ij}^{(e)} \ , \\
V_{\alpha j}^{(\chi^+,\bar{e})} &= \widetilde{U}_{1\alpha}^{(\chi^+)}\widetilde{U}_{1j}^{(\chi^+,\bar{e})} + \frac{1}{2}\widetilde{U}_{2\alpha}^{(\chi^+)}\widetilde{U}_{2j}^{(\chi^+,\bar{e})} \ .
\end{aligned}
\tag{B.63}
$$

The charged current is given by

$$
\begin{aligned}
J_\mu^- = \sqrt{2}\Big(& (\chi_b^{0\dagger}U_{2b}^{(\chi^0)} + \nu_j'^{\dagger}U_{2j}^{(\chi^0,\nu)})\bar{\sigma}_\mu(U_{1\beta}^{(\chi^-)}\chi_\beta^- + U_{1j}^{(\chi^-,e)}e_j') \\
& - (\chi_\beta^{+\dagger}\widetilde{U}_{1\beta}^{(\chi^+)} + \bar{e}_j'^{\dagger}\widetilde{U}_{1j}^{(\chi^+,\bar{e})})\bar{\sigma}_\mu(U_{2b}^{(\chi^0)}\chi_b^0 + U_{2j}^{(\chi^0,\nu)}\nu_j')\Big) \\
& + (\chi_b^{0\dagger}U_{ib}^{(\nu,\chi^0)} + \nu_j'^{\dagger}U_{ij}^{(\nu)})\bar{\sigma}_\mu(U_{i\beta}^{(e,\chi^-)}\chi_\beta^- + U_{ij}^{(e)}e_j') \\
& + (\chi_b^{0\dagger}U_{3b}^{(\chi^0)} + \nu_j'^{\dagger}U_{3j}^{(\chi^0,\nu)})\bar{\sigma}_\mu(U_{2\beta}^{(\chi^-)}\chi_\beta^- + U_{2j}^{(\chi^-,e)}e_j') \\
& + (\chi_\beta^{+\dagger}\widetilde{U}_{2\beta}^{(\chi^+)} + \bar{e}_j'^{\dagger}\widetilde{U}_{2j}^{(\chi^+,\bar{e})})\bar{\sigma}_\mu(U_{3b}^{(\chi^0)}\chi_b^0 + U_{3j}^{(\chi^0,\nu)}\nu_j') \ .
\end{aligned}
\tag{B.64}
$$

After the insertion of the mass eigenstate fields, we obtain

$$
\begin{aligned}
J_\mu^- = & \sqrt{2}\ \chi_b^{0\dagger}U_{2b}^{(\chi^0)}\bar{\sigma}_\mu U_{1\beta}^{(\chi^-)}\chi_\beta^- + \sqrt{2}\ \chi_b^{0\dagger}U_{2b}^{(\chi^0)}\bar{\sigma}_\mu U_{1j}^{(\chi^-,e)}e_j' \\
& + \sqrt{2}\ \nu_j'^{\dagger}U_{2j}^{(\chi^0,\nu)}\bar{\sigma}_\mu U_{1\beta}^{(\chi^-)}\chi_\beta^- + \sqrt{2}\ \nu_k'^{\dagger}U_{2k}^{(\chi^0,\nu)}\bar{\sigma}_\mu U_{1j}^{(\chi^-,e)}e_j' \\
& - \sqrt{2}\ \chi_\beta^{+\dagger}\widetilde{U}_{1\beta}^{(\chi^+)}\bar{\sigma}_\mu U_{2b}^{(\chi^0)}\chi_b^0 - \sqrt{2}\ \chi_\beta^{+\dagger}\widetilde{U}_{1\beta}^{(\chi^+)}\bar{\sigma}_\mu U_{2k}^{(\chi^0,\nu)}\nu_k' \\
& - \sqrt{2}\ \bar{e}_j'^{\dagger}\widetilde{U}_{1j}^{(\chi^+,\bar{e})}\bar{\sigma}_\mu U_{2b}^{(\chi^0)}\chi_b^0 - \sqrt{2}\ \bar{e}_j'^{\dagger}\widetilde{U}_{1j}^{(\chi^+,\bar{e})}\bar{\sigma}_\mu U_{2k}^{(\chi^0,\nu)}\nu_k' \\
& + \chi_b^{0\dagger}U_{ib}^{(\nu,\chi^0)}\bar{\sigma}_\mu U_{i\beta}^{(e,\chi^-)}\chi_\beta^- + \chi_b^{0\dagger}U_{ib}^{(\nu,\chi^0)}\bar{\sigma}_\mu U_{ij}^{(e)}e_j' \\
& + \nu_j'^{\dagger}U_{ij}^{(\nu)}\bar{\sigma}_\mu U_{i\beta}^{(e,\chi^-)}\chi_\beta^- + \nu_k'^{\dagger}U_{ik}^{(\nu)}\bar{\sigma}_\mu U_{ij}^{(e)}e_j' \\
& + \chi_b^{0\dagger}U_{3b}^{(\chi^0)}\bar{\sigma}_\mu U_{2\beta}^{(\chi^-)}\chi_\beta^- + \chi_b^{0\dagger}U_{3b}^{(\chi^0)}\bar{\sigma}_\mu U_{2j}^{(\chi^-,e)}e_j' \\
& + \nu_j'^{\dagger}U_{3j}^{(\chi^0,\nu)}\bar{\sigma}_\mu U_{2\beta}^{(\chi^-)}\chi_\beta^- + \nu_k'^{\dagger}U_{3k}^{(\chi^0,\nu)}\bar{\sigma}_\mu U_{2j}^{(\chi^-,e)}e_j'
\end{aligned}
$$

$$+ \chi_\beta^{+\dagger} \widetilde{U}_{2\beta}^{(\chi^+)} \bar{\sigma}_\mu U_{3b}^{(\chi^0)} \chi_b^0 + \chi_\beta^{+\dagger} \widetilde{U}_{2\beta}^{(\chi^+)} \bar{\sigma}_\mu U_{3j}^{(\chi^0,\nu)} \nu_j'$$
$$+ \bar{e}_j'^{\dagger} \widetilde{U}_{2j}^{(\chi^+,\bar{e})} \bar{\sigma}_\mu U_{3b}^{(\chi^0)} \chi_b^0 + \bar{e}_j'^{\dagger} \widetilde{U}_{2j}^{(\chi^+,\bar{e})} \bar{\sigma}_\mu U_{3k}^{(\chi^0,\nu)} \nu_k' \ . \tag{B.65}$$

The final expression for the charged current is given by

$$J_\mu^- = \chi_a^{0\dagger} \bar{\sigma}_\mu V_{a\beta}^{(\chi)} \chi_\beta^- + \chi_\alpha^{+\dagger} \bar{\sigma}_\mu V_{\alpha b}^{(\chi)} \chi_b^0 + \chi_a^{0\dagger} \bar{\sigma}_\mu V_{aj}^{(\chi,e)} e_j + \bar{e}_i^\dagger \bar{\sigma}_\mu V_{ib}^{(\chi,e)} \chi_b^0$$
$$+ \nu_i^\dagger \bar{\sigma}_\mu V_{i\beta}^{(\nu,\chi)} \chi_\beta^- + \chi_\alpha^{+\dagger} \bar{\sigma}_\mu V_{\alpha j}^{(\nu,\chi)} \nu_j + \nu_i^\dagger \bar{\sigma}_\mu V_{ij}^{(\nu,e)} e_j + \bar{e}_i^\dagger \bar{\sigma}_\mu V_{ij}^{(\nu,e)} \nu_j \ , \tag{B.66}$$

where we have defined

$$V_{a\beta}^{(\chi)} = \sqrt{2}\ U_{2a}^{(\chi^0)} U_{1\beta}^{(\chi^-)} + U_{3a}^{(\chi^0)} U_{2\beta}^{(\chi^-)} + \sum_k U_{ka}^{(\nu,\chi^0)} U_{k\beta}^{(e,\chi^-)} \ ,$$
$$V_{\alpha b}^{(\chi)} = -\sqrt{2}\ \widetilde{U}_{1\alpha}^{(\chi^+)} U_{2b}^{(\chi^0)} + \widetilde{U}_{2\alpha}^{(\chi^+)} U_{3b}^{(\chi^0)} \ ,$$
$$V_{aj}^{(\chi,e)} = \sqrt{2}\ U_{2a}^{(\chi^0)} U_{1j}^{(\chi^-,e)} + U_{3a}^{(\chi^0)} U_{2j}^{(\chi^-,e)} + \sum_k U_{ka}^{(\nu,\chi^0)} U_{kj}^{(e)} \ ,$$
$$V_{ib}^{(\chi,e)} = -\sqrt{2}\ \widetilde{U}_{1i}^{(\chi^+,\bar{e})} U_{2b}^{(\chi^0)} + \widetilde{U}_{2i}^{(\chi^+,\bar{e})} U_{3b}^{(\chi^0)} \ ,$$
$$V_{i\beta}^{(\nu,\chi)} = \sqrt{2}\ U_{2i}^{(\chi^0,\nu)} U_{1\beta}^{(\chi^-)} + U_{3i}^{(\chi^0,\nu)} U_{2\beta}^{(\chi^-)} + \sum_k U_{ki}^{(\nu)} U_{k\beta}^{(e,\chi^-)} \ ,$$
$$V_{\alpha j}^{(\nu,\chi)} = -\sqrt{2}\ \widetilde{U}_{1\alpha}^{(\chi^+)} U_{2j}^{(\chi^0,\nu)} + \widetilde{U}_{2\alpha}^{(\chi^+)} U_{3j}^{(\chi^0,\nu)} \ ,$$
$$V_{ij}^{(\nu,e)} = \sqrt{2}\ U_{2i}^{(\chi^0.\nu)} U_{1j}^{(\chi^-,e)} + U_{3i}^{(\chi^0,\nu)} U_{2j}^{(\chi^-,e)} + \sum_k U_{ki}^{(\nu)} U_{kj}^{(e)} \ ,$$
$$V_{ij}^{(\nu,e)} = -\sqrt{2}\ \widetilde{U}_{1i}^{(\chi^+,\bar{e})} U_{2j}^{(\chi^0.\nu)} + \widetilde{U}_{2i}^{(\chi^+,\bar{e})} U_{3j}^{(\chi^0,\nu)} \ . \tag{B.67}$$

After the diagonalization of the mass matrices we obtain analytical expressions for the various matrix elements. Assuming bino-like neutralino, i.e. expanding in $\epsilon = m_Z/\mu$, we obtain following expression for the R-parity violating part of the neutral CKM-like matrix element:

$$V_{aj}^{(\chi,\nu)} = \ -\zeta_j \frac{m_Z}{2} \begin{pmatrix} \frac{s_w}{M_1} \\ -\frac{c_w}{M_2} \\ \frac{m_Z}{\sqrt{2}\mu} v_1 \\ \frac{m_Z}{\sqrt{2}\mu} v_2 \end{pmatrix} \left(1 + \mathcal{O} \begin{pmatrix} \frac{s_{2\beta} m_Z^2}{\mu^2} \\ \frac{m_Z^2}{\mu^2} \\ \frac{m_Z^2}{\mu^2} \\ \frac{s_{2\beta} m_Z^2}{\mu^2} \end{pmatrix} \right) \ , \tag{B.68}$$

with abbreviations

$$v_1 = (s_\beta + c_\beta) \frac{M_1 c_w^2 + M_2 s_w^2 - \mu}{(M_1 - \mu)(M_2 - \mu)} - (s_\beta - c_\beta) \left(\frac{s_w^2}{M_1} + \frac{c_w^2}{M_2} \right) \ , \tag{B.69}$$

$$v_2 = (s_\beta - c_\beta) \frac{M_1 c_w^2 + M_2 s_w^2 + \mu}{(M_1 + \mu)(M_2 + \mu)} - (s_\beta + c_\beta) \left(\frac{s_w^2}{M_1} + \frac{c_w^2}{M_2} \right) \ . \tag{B.70}$$

Numerically, the relative errors are smaller than 0.10, 0.20, 0.15, 0.05 for $a = 1, \ldots, 4$. For the R-parity violating part of the charged CKM-like matrix we find

$$V_{aj}^{(\chi,e)} = \ -\zeta_j mZ \begin{pmatrix} \frac{s_w}{M_1} \\ \frac{c_w}{M_2} \\ \frac{m_Z}{\sqrt{2}\mu} \widetilde{v}_1 \\ \frac{m_Z}{\sqrt{2}\mu} \widetilde{v}_2 \end{pmatrix} \left(1 + \mathcal{O} \begin{pmatrix} \frac{s_{2\beta} m_Z^2}{\mu^2} \\ \frac{m_Z^2}{\mu^2} \\ \frac{m_Z^2}{\mu^2} \\ \frac{s_{2\beta} m_Z^2}{\mu^2} \end{pmatrix} \right) \ , \tag{B.71}$$

with abbreviations

$$\widetilde{v}_1 = (s_\beta + c_\beta)\frac{M_1 c_w^2 + M_2 s_w^2 - \mu}{(M_1 - \mu)(M_2 - \mu)} - 2(s_\beta + c_\beta)\frac{\mu c_w^2}{M_2(M_2 - \mu)} + 2s_\beta \frac{c_w^2}{M_2} \ , \tag{B.72}$$

$$\widetilde{v}_2 = (s_\beta - c_\beta)\frac{M_1 c_w^2 + M_2 s_w^2 + \mu}{(M_1 + \mu)(M_2 + \mu)} - 2(s_\beta + \frac{\mu}{M_2} c_\beta)\frac{M_1 + \mu}{(M_1 + \mu)(M_2 + \mu)} c_w^2 \ . \tag{B.73}$$

Note that we would obtain same results for the higgsino-like neutralino, however, in different order.

Bibliography

[1] S. Weinberg, *The making of the standard model*, *Eur.Phys.J.* **C34** (2004) 5–13, [hep-ph/0401010].

[2] ALEPH Collaboration, DELPHI Collaboration, L3 Collaboration, OPAL Collaboration, SLD Collaboration, LEP Electroweak Working Group, SLD Electroweak Group, SLD Heavy Flavour Group, *Precision electroweak measurements on the Z resonance*, *Phys.Rept.* **427** (2006) 257–454, [hep-ex/0509008].

[3] LEP Working Group for Higgs boson searches, ALEPH Collaboration, DELPHI Collaboration, L3 Collaboration, OPAL Collaboration, *Search for the Standard Model Higgs boson at LEP*, *Phys.Lett.* **B565** (2003) 61–75, [hep-ex/0306033].

[4] Particle Data Group, *Review of particle physics*, *J.Phys.G* **G37** (2010) 075021.

[5] J. M. Cornwall, D. N. Levin, and G. Tiktopoulos, *Uniqueness of spontaneously broken gauge theories*, *Phys.Rev.Lett.* **30** (1973) 1268–1270.

[6] J. M. Cornwall, D. N. Levin, and G. Tiktopoulos, *Derivation of gauge invariance from high-energy unitarity bounds on the S matrix*, *Phys.Rev.* **D10** (1974) 1145.

[7] C. Llewellyn Smith, *High-energy behavior and gauge symmetry*, *Phys.Lett.* **B46** (1973) 233–236.

[8] B. W. Lee, C. Quigg, and H. Thacker, *Weak interactions at very high-energies: The role of the Higgs boson mass*, *Phys.Rev.* **D16** (1977) 1519.

[9] M. Baak, M. Goebel, J. Haller, A. Hoecker, D. Ludwig, *et. al.*, *Updated status of the global electroweak fit and constraints on new physics*, arXiv:1107.0975.

[10] ATLAS Collaboration, *Combined search for the Standard Model Higgs boson using up to 4.9 fb-1 of pp collision data at sqrt(s) = 7 TeV with the ATLAS detector at the LHC*, arXiv:1202.1408.

[11] CMS Collaboration, *Search for the Standard Model Higgs boson in the decay channel H to ZZ to 4 leptons in pp collisions at sqrt(s) = 7 TeV*, arXiv:1202.1997.

[12] W. Murray, *LHC Higgs boson searches*, arXiv:1201.4576.

[13] Clay Mathematics Institute, *Yang-Mills theory*, 2000. http://www.claymath.org/millennium/Yang-Mills_Theory/.

[14] Super-Kamiokande Collaboration, *Evidence for oscillation of atmospheric neutrinos*, *Phys.Rev.Lett.* **81** (1998) 1562–1567, [hep-ex/9807003].

[15] KamLAND Collaboration, *First results from KamLAND: Evidence for reactor anti-neutrino disappearance*, *Phys.Rev.Lett.* **90** (2003) 021802, [hep-ex/0212021].

[16] SNO Collaboration, *Direct evidence for neutrino flavor transformation from neutral current interactions in the Sudbury Neutrino Observatory*, *Phys.Rev.Lett.* **89** (2002) 011301, [nucl-ex/0204008].

[17] P. Minkowski, *mu –> e gamma at a rate of one out of 1-billion muon decays?*, *Phys.Lett.* **B67** (1977) 421.

[18] R. N. Mohapatra and G. Senjanovic, *Neutrino mass and spontaneous parity violation*, *Phys.Rev.Lett.* **44** (1980) 912.

[19] T. Yanagida, *Horizontal symmetry and masses of neutrinos*, *Prog.Theor.Phys.* **64** (1980) 1103.

[20] E. W. Kolb and M. S. Turner, *The early universe*, vol. 69 of *Frontiers in Physics*. Addison-Wesley, 1990.

[21] V. Mukhanov, *Physical foundations of cosmology*. Cambridge University Press, 2005.

[22] F. Bezrukov and M. Shaposhnikov, *The Standard Model Higgs boson as the inflaton*, *Phys.Lett.* **B659** (2008) 703–706, [arXiv:0710.3755].

[23] R. N. Lerner and J. McDonald, *Higgs inflation and naturalness*, *JCAP* **1004** (2010) 015, [arXiv:0912.5463].

[24] M. P. Hertzberg, *On inflation with non-minimal coupling*, *JHEP* **1011** (2010) 023, [arXiv:1002.2995].

[25] C. Burgess, H. M. Lee, and M. Trott, *Comment on Higgs inflation and naturalness*, *JHEP* **1007** (2010) 007, [arXiv:1002.2730]. 5 pages, 1 figure V3: Journal Version.

[26] A. Sakharov, *Violation of CP invariance, C asymmetry, and baryon asymmetry of the universe*, *Pisma Zh.Eksp.Teor.Fiz.* **5** (1967) 32–35. Reprinted in *Kolb, E.W. (ed.), Turner, M.S. (ed.): The early universe* 371-373, and in *Lindley, D. (ed.) et al.: Cosmology and particle physics* 106-109, and in Sov. Phys. Usp. 34 (1991) 392-393 [Usp. Fiz. Nauk 161 (1991) No. 5 61-64].

[27] W. Buchmuller and O. Philipsen, *Phase structure and phase transition of the SU(2) Higgs model in three-dimensions*, *Nucl.Phys.* **B443** (1995) 47–69, [hep-ph/9411334].

[28] K. Kajantie, M. Laine, K. Rummukainen, and M. E. Shaposhnikov, *Is there a hot electroweak phase transition at m(H) larger or equal to m(W)?*, *Phys.Rev.Lett.* **77** (1996) 2887–2890, [hep-ph/9605288].

[29] M. Gurtler, E.-M. Ilgenfritz, and A. Schiller, *Where the electroweak phase transition ends*, *Phys.Rev.* **D56** (1997) 3888–3895, [hep-lat/9704013].

[30] C. Dappiaggi, T.-P. Hack, J. Moller, and N. Pinamonti, *Dark energy from quantum matter*, arXiv:1007.5009.

[31] S. Weinberg, *The cosmological constant problem*, *Rev.Mod.Phys.* **61** (1989) 1–23. Morris Loeb Lectures in Physics, Harvard University, May 2, 3, 5, and 10, 1988.

[32] F. Zwicky, *Spectral displacement of extra galactic nebulae*, *Helv.Phys.Acta* **6** (1933) 110–127.

[33] L. Bergstrom, *Nonbaryonic dark matter: Observational evidence and detection methods*, *Rept.Prog.Phys.* **63** (2000) 793, [hep-ph/0002126].

[34] J. Einasto, *Dark matter*, arXiv:0901.0632.

[35] M. Milgrom, *A modification of the Newtonian dynamics as a possible alternative to the hidden mass hypothesis*, *Astrophys.J.* **270** (1983) 365–370.

[36] B. Paczynski, *Gravitational microlensing by the galactic halo*, *Astrophys.J.* **304** (1986) 1–5.

[37] K. Griest, *Galactic microlensing as a method of detecting massive compact halo objects*, *Astrophys.J.* **366** (1991) 412–421.

[38] G. Bertone, D. Hooper, and J. Silk, *Particle dark matter: Evidence, candidates and constraints*, *Phys.Rept.* **405** (2005) 279–390, [hep-ph/0404175].

[39] J. L. Feng, *Dark matter candidates from particle physics and methods of detection*, *Ann.Rev.Astron.Astrophys.* **48** (2010) 495, [arXiv:1003.0904].

[40] G. Jungman, M. Kamionkowski, and K. Griest, *Supersymmetric dark matter*, *Phys.Rept.* **267** (1996) 195–373, [hep-ph/9506380].

[41] XENON100 Collaboration, *Dark matter results from 100 Live Days of XENON100 data*, *Phys.Rev.Lett.* **107** (2011) 131302, [arXiv:1104.2549]. 5 pages, 5 figures/ matches accepted version.

[42] S. Koay and C. Collaboration, *Supersymmetry searches at the Compact Muon Solenoid (CMS) experiment, 2011*, arXiv:1202.1000.

[43] ATLAS Collaboration, *Search for supersymmetry with jets, missing transverse momentum and at least one hadronically decaying tau lepton in proton-proton collisions at sqrt(s) = 7 TeV with the ATLAS detector*, arXiv:1204.3852. 7 pages plus author list (20 pages total), 3 figures, 3 tables, minor formatting change, submitted to Physics Letters B.

[44] D. Z. Freedman, P. van Nieuwenhuizen, and S. Ferrara, *Progress toward a theory of supergravity*, *Phys.Rev.* **D13** (1976) 3214–3218.

[45] S. Deser and B. Zumino, *Consistent supergravity*, *Phys.Lett.* **B62** (1976) 335.

[46] H. Pagels and J. R. Primack, *Supersymmetry, cosmology and new TeV physics*, *Phys.Rev.Lett.* **48** (1982) 223.

[47] W. Buchmuller, *Gravitino dark matter*, *AIP Conf.Proc.* **1200** (2010) 155–164, [arXiv:0910.1870].

[48] M. Fukugita and T. Yanagida, *Baryogenesis without grand unification*, *Phys.Lett.* **B174** (1986) 45.

[49] W. Buchmuller, P. Di Bari, and M. Plumacher, *Leptogenesis for pedestrians*, *Annals Phys.* **315** (2005) 305–351, [hep-ph/0401240].

[50] W. Buchmuller, R. Peccei, and T. Yanagida, *Leptogenesis as the origin of matter*, *Ann.Rev.Nucl.Part.Sci.* **55** (2005) 311–355, [hep-ph/0502169]. 53 pages, minor corrections, one figure and references added, matches published version.

[51] M. Bolz, A. Brandenburg, and W. Buchmuller, *Thermal production of gravitinos*, *Nucl.Phys.* **B606** (2001) 518–544, [hep-ph/0012052].

[52] M. Kawasaki and T. Moroi, *Gravitino production in the inflationary universe and the effects on big bang nucleosynthesis*, *Prog.Theor.Phys.* **93** (1995) 879–900, [hep-ph/9403364].

[53] S. Weinberg, *Cosmological constraints on the scale of supersymmetry breaking*, *Phys.Rev.Lett.* **48** (1982) 1303.

[54] T. Gherghetta, G. F. Giudice, and J. D. Wells, *Phenomenological consequences of supersymmetry with anomaly induced masses*, *Nucl.Phys.* **B559** (1999) 27–47, [hep-ph/9904378].

[55] M. Ibe, R. Kitano, H. Murayama, and T. Yanagida, *Viable supersymmetry and leptogenesis with anomaly mediation*, *Phys.Rev.* **D70** (2004) 075012, [hep-ph/0403198].

[56] W. Buchmuller, V. Domcke, and K. Schmitz, *WIMP dark matter from gravitino decays and leptogenesis*, arXiv:1203.0285.

[57] W. Buchmuller, L. Covi, K. Hamaguchi, A. Ibarra, and T. Yanagida, *Gravitino dark matter in R-parity breaking vacua*, *JHEP* **0703** (2007) 037, [hep-ph/0702184].

[58] F. Takayama and M. Yamaguchi, *Gravitino dark matter without R-parity*, *Phys.Lett.* **B485** (2000) 388–392, [hep-ph/0005214].

[59] G. Bertone, W. Buchmuller, L. Covi, and A. Ibarra, *Gamma-rays from decaying dark matter*, *JCAP* **0711** (2007) 003, [arXiv:0709.2299].

[60] A. Ibarra and D. Tran, *Gamma ray spectrum from gravitino dark matter decay*, *Phys.Rev.Lett.* **100** (2008) 061301, [arXiv:0709.4593].

[61] K. Ishiwata, S. Matsumoto, and T. Moroi, *High energy cosmic rays from the decay of gravitino dark matter*, *Phys.Rev.* **D78** (2008) 063505, [arXiv:0805.1133].

[62] W. Buchmuller, A. Ibarra, T. Shindou, F. Takayama, and D. Tran, *Probing gravitino dark matter with PAMELA and Fermi*, *JCAP* **0909** (2009) 021, [arXiv:0906.1187].

[63] N.-E. Bomark, S. Lola, P. Osland, and A. Raklev, *Photon, neutrino and charged particle spectra from R-violating gravitino decays*, *Phys.Lett.* **B686** (2010) 152–161, [arXiv:0911.3376].

[64] A. Ibarra and D. Tran, *Antimatter signatures of gravitino dark matter decay*, *JCAP* **0807** (2008) 002, [arXiv:0804.4596].

[65] L. Covi, M. Grefe, A. Ibarra, and D. Tran, *Unstable gravitino dark matter and neutrino flux*, *JCAP* **0901** (2009) 029, [arXiv:0809.5030]. 24 pages, 8 figures/ references added and typos corrected, agrees with published version.

[66] W. Buchmuller, K. Hamaguchi, M. Ratz, and T. Yanagida, *Supergravity at colliders*, *Phys.Lett.* **B588** (2004) 90–98, [hep-ph/0402179].

[67] J. R. Ellis, A. R. Raklev, and O. K. Oye, *Gravitino dark matter scenarios with massive metastable charged sparticles at the LHC*, *JHEP* **0610** (2006) 061, [hep-ph/0607261].

[68] N.-E. Bomark, S. Lola, P. Osland, and A. Raklev, *Gravitino dark matter and the flavour structure of R-violating operators*, *Phys.Lett.* **B677** (2009) 62–70, [arXiv:0811.2969].

[69] S. Bobrovskyi, W. Buchmuller, J. Hajer, and J. Schmidt, *Broken R-parity in the sky and at the LHC*, *JHEP* **1010** (2010) 061, [arXiv:1007.5007].

[70] S. Bobrovskyi, W. Buchmuller, J. Hajer, and J. Schmidt, *Quasi-stable neutralinos at the LHC*, *JHEP* **1109** (2011) 119, [arXiv:1107.0926].

[71] S. Asai, Y. Azuma, M. Endo, K. Hamaguchi, and S. Iwamoto, *Stau kinks at the LHC*, *JHEP* **1112** (2011) 041, [arXiv:1103.1881].

[72] M. Grefe, *Unstable gravitino dark matter - Prospects for indirect and direct detection*, arXiv:1111.6779. Presented 6 Jul 2011.

[73] K. S. Jeong, M. Shimosuka, and M. Yamaguchi, *Light higgsino in heavy gravitino scenario: (Un)natural solution to the $\mu/B\mu$ problem*, arXiv:1112.5293.

[74] F. Brummer and W. Buchmuller, *Light higgsinos as heralds of higher-dimensional unification*, *JHEP* **1107** (2011) 010, [arXiv:1105.0802].

[75] F. Brummer and W. Buchmuller, *The Fermi scale as a focus point of high-scale gauge mediation*, arXiv:1201.4338.

[76] J. Hasenkamp and J. Kersten, *Leptogenesis, gravitino dark matter and entropy production*, *Phys.Rev.* **D82** (2010) 115029, [arXiv:1008.1740].

[77] M. Papucci, J. T. Ruderman, and A. Weiler, *Natural SUSY endures*, arXiv:1110.6926. 55 pages, 21 figures.

[78] J. Wess and J. Bagger, *Supersymmetry and supergravity*. Princeton Series in Physics. Princeton University Press, 1992.

[79] S. Bobrovskyi, F. Brummer, W. Buchmuller, and J. Hajer, *Searching for light higgsinos with b-jets and missing leptons*, *JHEP* **1201** (2012) 122, [arXiv:1111.6005].

[80] Y. A. Golfand and E. P. Likhtman, *Extension of the algebra of poincare group generators and violation of P invariance*, *JETP Lett.* **13** (1971) 323–326.

[81] A. Neveu and J. H. Schwarz, *Factorizable dual model of pions*, *Nucl. Phys.* **B31** (1971) 86–112.

[82] P. Ramond, *Dual theory for free fermions*, *Phys. Rev.* **D3** (1971) 2415–2418.

[83] D. V. Volkov and V. P. Akulov, *Possible universal neutrino interaction*, *JETP Lett.* **16** (1972) 438–440.

[84] J. Wess and B. Zumino, *Supergauge transformations in four-dimensions*, *Nucl. Phys.* **B70** (1974) 39–50.

[85] R. Haag, *Local quantum physics: Fields, particles, algebras.* Springer, 1992.

[86] S. R. Coleman and J. Mandula, *All possible symmetries of the S matrix*, *Phys. Rev.* **159** (1967) 1251–1256.

[87] R. Haag, J. T. Lopuszanski, and M. Sohnius, *All possible generators of supersymmetries of the S matrix*, *Nucl. Phys.* **B88** (1975) 257.

[88] J. Wess, *From symmetry to supersymmetry*, *Eur.Phys.J.* **C59** (2009) 177–183.

[89] P. Binétruy, *Supersymmetry: Theory, experiment, and cosmology.* Oxford University Press, 2006.

[90] J. R. Ellis and D. Ross, *A Light Higgs boson would invite supersymmetry*, *Phys.Lett.* **B506** (2001) 331–336, [hep-ph/0012067].

[91] O. Buchmueller, R. Cavanaugh, A. De Roeck, M. Dolan, J. Ellis, *et. al.*, *Higgs and supersymmetry*, arXiv:1112.3564.

[92] J. Ellis, *Prospects for discovering supersymmetry at the LHC*, *Eur.Phys.J.* **C59** (2009) 335–343, [arXiv:0810.1178].

[93] R. Haag, *Some people and some problems met in half a century of commitment to mathematical physics*, *Eur.Phys.J.* **H35** (2010) 263–307.

[94] P. Fayet, *R-parity, the Supersymmetric Standard Model and the phenomenology of supersymmetry*, in *History of original Ideas and basic discoveries in Particle Physics* (H. Newman and T. Ypsilantis, eds.), vol. 352 of *NATO Series B*, p. 639. Plenum, 1996.

[95] G. W. Hou, *Search for TeV scale physics in heavy flavour decays*, *Eur.Phys.J.* **C59** (2009) 521–541, [arXiv:0808.1932].

[96] G. Scharf, *Finite quantum electrodynamics: The causal approach.* Texts and monographs in physics. Springer, 1996.

[97] G. Scharf, *Quantum gauge theories: A true ghost story.* Wiley, 2001.

[98] M. Quiros, *Constraints on the Higgs boson properties from the effective potential*, hep-ph/9703412. To appear in 'Perspectives on Higgs Physics II', G. L. Kane, ed., World Scientific, Singapore.

[99] J. Ellis, J. Espinosa, G. Giudice, A. Hoecker, and A. Riotto, *The probable fate of the Standard Model*, *Phys.Lett.* **B679** (2009) 369–375, [arXiv:0906.0954].

[100] M. Shaposhnikov and C. Wetterich, *Asymptotic safety of gravity and the Higgs boson mass*, *Phys.Lett.* **B683** (2010) 196–200, [arXiv:0912.0208].

[101] CMS collaboration, *Combination of CMS searches for a Standard Model Higgs boson*, 2011. CMS PAS HIG-11-032.

[102] H. Baer and X. Tata, *Weak scale supersymmetry: From superfields to scattering events*. Cambridge University Press, 2006.

[103] S. P. Martin, *A supersymmetry primer*, hep-ph/9709356.

[104] G. Giudice and A. Masiero, *A natural solution to the mu problem in supergravity theories*, *Phys.Lett.* **B206** (1988) 480–484.

[105] P. Van Nieuwenhuizen, *Supergravity*, *Phys.Rept.* **68** (1981) 189–398.

[106] E. Cremmer, S. Ferrara, L. Girardello, and A. Van Proeyen, *Yang-Mills theories with local supersymmetry: Lagrangian, transformation laws and super-Higgs effect*, *Nucl.Phys.* **B212** (1983) 413.

[107] T. Moroi, *Effects of the gravitino on the inflationary universe*, hep-ph/9503210. Ph.D. Thesis.

[108] L. Randall and R. Sundrum, *Out of this world supersymmetry breaking*, *Nucl.Phys.* **B557** (1999) 79–118, [hep-th/9810155].

[109] G. F. Giudice, M. A. Luty, H. Murayama, and R. Rattazzi, *Gaugino mass without singlets*, *JHEP* **9812** (1998) 027, [hep-ph/9810442].

[110] B. Allanach, *SOFTSUSY: a program for calculating supersymmetric spectra*, *Comput.Phys.Commun.* **143** (2002) 305–331, [hep-ph/0104145]. Updated for SOFTSUSY3.3. Can be downloaded from http://projects.hepforge.org/softsusy/ Further updated versions of the manual will be available by replacements to the electronic arXiv.

[111] H. K. Dreiner, H. E. Haber, and S. P. Martin, *Two-component spinor techniques and feynman rules for quantum field theory and supersymmetry*, *Phys.Rept.* **494** (2010) 1–196, [arXiv:0812.1594].

[112] W. Rarita and J. Schwinger, *On a theory of particles with half integral spin*, *Phys.Rev.* **60** (1941) 61.

[113] M. Bolz, *Thermal production of gravitinos*, . Ph.D. Thesis (Advisor: W. Buchmuller).

[114] M. Grefe, *Neutrino signals from gravitino dark matter with broken R-parity*, arXiv:1111.6041. Presented Sep 2008.

[115] J. R. Ellis, A. D. Linde, and D. V. Nanopoulos, *Inflation can save the gravitino*, *Phys.Lett.* **B118** (1982) 59.

[116] J. R. Ellis, J. E. Kim, and D. V. Nanopoulos, *Cosmological gravitino regeneration and decay*, *Phys.Lett.* **B145** (1984) 181.

[117] T. Moroi, H. Murayama, and M. Yamaguchi, *Cosmological constraints on the light stable gravitino*, *Phys.Lett.* **B303** (1993) 289–294.

[118] J. Pradler and F. D. Steffen, *Thermal gravitino production and collider tests of leptogenesis*, *Phys.Rev.* **D75** (2007) 023509, [hep-ph/0608344].

[119] V. S. Rychkov and A. Strumia, *Thermal production of gravitinos*, *Phys.Rev.* **D75** (2007) 075011, [hep-ph/0701104].

[120] W. Buchmuller, M. Endo, and T. Shindou, *Superparticle mass window from leptogenesis and decaying gravitino dark matter*, *JHEP* **0811** (2008) 079, [arXiv:0809.4667]. 14 pages, 3 figures.

[121] M. Kawasaki, K. Kohri, T. Moroi, and A. Yotsuyanagi, *Big-bang nucleosynthesis and gravitino*, *Phys.Rev.* **D78** (2008) 065011, [arXiv:0804.3745].

[122] K. Kohri, T. Moroi, and A. Yotsuyanagi, *Big-bang nucleosynthesis with unstable gravitino and upper bound on the reheating temperature*, *Phys.Rev.* **D73** (2006) 123511, [hep-ph/0507245].

[123] J. R. Ellis, D. V. Nanopoulos, and S. Sarkar, *The cosmology of decaying gravitinos*, *Nucl.Phys.* **B259** (1985) 175.

[124] M. Reno and D. Seckel, *Primordial nucleosynthesis: The effects of injecting hadrons*, *Phys.Rev.* **D37** (1988) 3441.

[125] S. Dimopoulos, R. Esmailzadeh, L. J. Hall, and G. Starkman, *Limits on late decaying particles from nucleosynthesis*, *Nucl.Phys.* **B311** (1989) 699.

[126] R. H. Cyburt, J. R. Ellis, B. D. Fields, and K. A. Olive, *Updated nucleosynthesis constraints on unstable relic particles*, *Phys.Rev.* **D67** (2003) 103521, [astro-ph/0211258].

[127] J. Hasenkamp, *Dark radiation from the axino solution of the gravitino problem*, *Phys.Lett.* **B707** (2012) 121–128, [arXiv:1107.4319]. 11 pages + refs.

[128] M. Viel, J. Lesgourgues, M. G. Haehnelt, S. Matarrese, and A. Riotto, *Constraining warm dark matter candidates including sterile neutrinos and light gravitinos with WMAP and the Lyman-alpha forest*, *Phys.Rev.* **D71** (2005) 063534, [astro-ph/0501562].

[129] K. Jedamzik, *Big bang nucleosynthesis constraints on hadronically and electromagnetically decaying relic neutral particles*, *Phys.Rev.* **D74** (2006) 103509, [hep-ph/0604251].

[130] J. L. Feng, S.-f. Su, and F. Takayama, *SuperWIMP gravitino dark matter from slepton and sneutrino decays*, *Phys.Rev.* **D70** (2004) 063514, [hep-ph/0404198].

[131] W. Buchmuller, L. Covi, J. Kersten, and K. Schmidt-Hoberg, *Dark matter from gaugino mediation*, *JCAP* **0611** (2006) 007, [hep-ph/0609142]. 18 pages, updated to published version (minor modifications, reference added) Report-no: DESY 06-158 Journal-ref: JCAP 11 (2006) 007.

[132] L. Covi, J. Hasenkamp, S. Pokorski, and J. Roberts, *Gravitino dark matter and general neutralino NLSP*, *JHEP* **0911** (2009) 003, [arXiv:0908.3399].

[133] C. F. Berger, L. Covi, S. Kraml, and F. Palorini, *The number density of a charged relic*, *JCAP* **0810** (2008) 005, [arXiv:0807.0211].

[134] M. Kusakabe, T. Kajino, T. Yoshida, and G. J. Mathews, *Effect of long-lived strongly interacting relic particles on big bang nucleosynthesis*, *Phys.Rev.* **D80** (2009) 103501, [arXiv:0906.3516].

[135] M. Pospelov, *Particle physics catalysis of thermal big bang nucleosynthesis*, *Phys.Rev.Lett.* **98** (2007) 231301, [hep-ph/0605215].

[136] R. H. Cyburt, J. R. Ellis, B. D. Fields, K. A. Olive, and V. C. Spanos, *Bound-state effects on light-element abundances in gravitino dark matter scenarios*, *JCAP* **0611** (2006) 014, [astro-ph/0608562]. 22 pages 6 figures Report-no: CERN-PH-TH/2006-168, UMN-TH-2516/06, FTPI-MINN-06/29.

[137] K. Hamaguchi, T. Hatsuda, M. Kamimura, Y. Kino, and T. Yanagida, *Stau-catalyzed Li-6 production in big-bang nucleosynthesis*, *Phys.Lett.* **B650** (2007) 268–274, [hep-ph/0702274].

[138] M. Kawasaki, K. Kohri, and T. Moroi, *Big-bang nucleosynthesis with long-lived charged slepton*, *Phys.Lett.* **B649** (2007) 436–439, [hep-ph/0703122]. 9 pages, 3 figures.

[139] M. Ratz, K. Schmidt-Hoberg, and M. W. Winkler, *A Note on the primordial abundance of stau NLSPs*, *JCAP* **0810** (2008) 026, [arXiv:0808.0829].

[140] J. Pradler and F. D. Steffen, *Thermal relic abundances of long-lived staus*, *Nucl.Phys.* **B809** (2009) 318–346, [arXiv:0808.2462].

[141] L. Boubekeur, K. Y. Choi, R. Ruiz de Austri, and O. Vives, *The degenerate gravitino scenario*, *JCAP* **1004** (2010) 005, [arXiv:1002.0340].

[142] T. Kanzaki, M. Kawasaki, K. Kohri, and T. Moroi, *Cosmological constraints on gravitino LSP scenario with sneutrino NLSP*, *Phys.Rev.* **D75** (2007) 025011, [hep-ph/0609246]. 20 pages, 6 figures.

[143] L. Covi and S. Kraml, *Collider signatures of gravitino dark matter with a sneutrino NLSP*, *JHEP* **0708** (2007) 015, [hep-ph/0703130].

[144] J. R. Ellis, K. A. Olive, and Y. Santoso, *Sneutrino NLSP scenarios in the NUHM with gravitino dark matter*, *JHEP* **0810** (2008) 005, [arXiv:0807.3736].

[145] A. De Simone, M. Garny, A. Ibarra, and C. Weniger, *Supersymmetric leptogenesis with a light hidden sector*, *JCAP* **1007** (2010) 017, [arXiv:1004.4890].

[146] C. Cheung, J. Mardon, Y. Nomura, and J. Thaler, *A definitive signal of multiple supersymmetry breaking*, *JHEP* **1007** (2010) 035, [arXiv:1004.4637].

[147] H. K. Dreiner, M. Hanussek, J.-S. Kim, and S. Sarkar, *Gravitino cosmology with a very light neutralino*, arXiv:1111.5715.

[148] W. Buchmuller, K. Hamaguchi, M. Ibe, and T. Yanagida, *Eluding the BBN constraints on the stable gravitino*, *Phys.Lett.* **B643** (2006) 124–126, [hep-ph/0605164].

[149] J. Hasenkamp, *Towards a consistent cosmology with supersymmetry and leptogenesis*. PhD thesis, University of Hamburg, 2012.

[150] J. Hasenkamp and J. Kersten, *Dark and visible matter with broken R-parity and the axion multiplet*, *Phys.Lett.* **B701** (2011) 660–666, [arXiv:1103.6193]. 13 pages + refs, 1 table, v2: refs added, minor changes in presentation, v3: refs added, added discussion of decays into Higgs and Higgsino, matches published version.

[151] P. Fayet, *Supergauge invariant extension of the Higgs mechanism and a model for the electron and its neutrino*, *Nucl.Phys.* **B90** (1975) 104–124.

[152] P. Fayet, *Supersymmetry and weak, electromagnetic and strong interactions*, *Phys.Lett.* **B64** (1976) 159.

[153] P. Fayet, *Spontaneously broken supersymmetric theories of weak, electromagnetic and strong interactions*, *Phys.Lett.* **B69** (1977) 489.

[154] P. Fayet, *Mixing between gravitational and weak interactions through the massive gravitino*, *Phys.Lett.* **B70** (1977) 461.

[155] P. Fayet, *Supersymmetric theories of particles.*, in *New Frontiers in High Energy Physics* (A. Perlmutter and L. F. Scott, eds.), Proc. Orbis Scientiae, p. 413. Plenum, 1978.

[156] G. R. Farrar and P. Fayet, *Phenomenology of the production, decay, and detection of new hadronic states associated with supersymmetry*, *Phys.Lett.* **B76** (1978) 575–579.

[157] R. Barbier, C. Berat, M. Besancon, M. Chemtob, A. Deandrea, *et. al.*, *R-parity violating supersymmetry*, *Phys.Rept.* **420** (2005) 1–202, [hep-ph/0406039].

[158] A. E. Nelson and N. Seiberg, *R symmetry breaking versus supersymmetry breaking*, *Nucl.Phys.* **B416** (1994) 46–62, [hep-ph/9309299].

[159] S. Dimopoulos and H. Georgi, *Softly broken supersymmetry and SU(5)*, *Nucl.Phys.* **B193** (1981) 150.

[160] S. Weinberg, *Supersymmetry at ordinary energies. 1. Masses and conservation laws*, *Phys.Rev.* **D26** (1982) 287.

[161] N. Sakai and T. Yanagida, *Proton decay in a class of supersymmetric grand unified models*, *Nucl.Phys.* **B197** (1982) 533.

[162] V. Kuzmin, V. Rubakov, and M. Shaposhnikov, *On the anomalous electroweak baryon number nonconservation in the early universe*, *Phys.Lett.* **B155** (1985) 36.

[163] B. de Carlos and P. White, *R-parity violation effects through soft supersymmetry breaking terms and the renormalization group*, *Phys.Rev.* **D54** (1996) 3427–3446, [hep-ph/9602381].

[164] E. Nardi, *Renormalization group induced neutrino masses in supersymmetry without R-parity*, *Phys.Rev.* **D55** (1997) 5772–5779, [hep-ph/9610540].

[165] H. K. Dreiner and H. Pois, *Two Loop supersymmetric renormalization group equations including R-parity violation and aspects of unification*, hep-ph/9511444.

[166] L. J. Hall and M. Suzuki, *Explicit R-parity breaking in supersymmetric models*, *Nucl.Phys.* **B231** (1984) 419.

[167] J. Hajer, *Gravitino and scalar tau-lepton decays in supersymmetric models with broken R-parity*, Master's thesis, University of Hamburg, 2010. DESY-THESIS-2010-021.

[168] R. Tatar and T. Watari, *Proton decay, Yukawa couplings and underlying gauge symmetry in string theory*, *Nucl.Phys.* **B747** (2006) 212–265, [hep-th/0602238].

[169] W. Buchmuller, K. Hamaguchi, O. Lebedev, and M. Ratz, *Supersymmetric Standard Model from the heterotic string (II)*, *Nucl.Phys.* **B785** (2007) 149–209, [hep-th/0606187].

[170] W. Buchmuller and T. Yanagida, *Quark lepton mass hierarchies and the baryon asymmetry*, *Phys.Lett.* **B445** (1999) 399–402, [hep-ph/9810308]. 7 pages Report-no: DESY-98-155.

[171] W. Buchmuller, D. Delepine, and L. T. Handoko, *Neutrino mixing and flavor changing processes*, *Nucl.Phys.* **B576** (2000) 445–465, [hep-ph/9912317].

[172] C. Froggatt and H. B. Nielsen, *Hierarchy of quark masses, Cabibbo angles and CP violation*, *Nucl.Phys.* **B147** (1979) 277.

[173] K. Babu, *TASI Lectures on Flavor Physics*, arXiv:0910.2948.

[174] B. Allanach, A. Dedes, and H. Dreiner, *R parity violating minimal supergravity model*, *Phys.Rev.* **D69** (2004) 115002, [hep-ph/0309196].

[175] F. de Campos, O. Eboli, M. Magro, W. Porod, D. Restrepo, *et. al.*, *Probing bilinear R-parity violating supergravity at the LHC*, *JHEP* **0805** (2008) 048, [arXiv:0712.2156].

[176] G. G. Ross and J. W. F. Valle, *Supersymmetric models without R-parity*, *Phys. Lett.* **B151** (1985) 375.

[177] J. R. Ellis, G. Gelmini, C. Jarlskog, G. G. Ross, and J. W. F. Valle, *Phenomenology of supersymmetry with broken R-parity*, *Phys. Lett.* **B150** (1985) 142.

[178] M. Hirsch, W. Porod, and D. Restrepo, *Collider signals of gravitino dark matter in bilinearly broken R-parity*, *JHEP* **03** (2005) 062, [hep-ph/0503059].

[179] R. Hempfling, *Neutrino masses and mixing angles in SUSY GUT theories with explicit R-parity breaking*, *Nucl.Phys.* **B478** (1996) 3–30, [hep-ph/9511288].

[180] V. D. Barger and R. Phillips, *Collider Physics*. Frontiers in Physics. Addison-Wesley, 1987. Now updated 1996 edition.

[181] M. Kawasaki, K. Kohri, and T. Moroi, *Big-bang nucleosynthesis and hadronic decay of long-lived massive particles*, *Phys.Rev.* **D71** (2005) 083502, [astro-ph/0408426].

[182] F. D. Steffen, *Gravitino dark matter and cosmological constraints*, *JCAP* **0609** (2006) 001, [hep-ph/0605306].

[183] F. R. Klinkhamer and N. Manton, *A saddle point solution in the Weinberg-Salam theory*, *Phys.Rev.* **D30** (1984) 2212.

[184] J. Callan, Curtis G., R. Dashen, and D. J. Gross, *The structure of the gauge theory vacuum*, *Phys.Lett.* **B63** (1976) 334–340.

[185] R. Jackiw and C. Rebbi, *Vacuum periodicity in a Yang-Mills quantum theory*, *Phys.Rev.Lett.* **37** (1976) 172–175.

[186] A. Bouquet and P. Salati, *R parity breaking and cosmological consequences*, *Nucl.Phys.* **B284** (1987) 557.

[187] B. A. Campbell, S. Davidson, J. R. Ellis, and K. A. Olive, *Cosmological baryon asymmetry constraints on extensions of the standard model*, *Phys.Lett.* **B256** (1991) 457.

[188] W. Fischler, G. Giudice, R. Leigh, and S. Paban, *Constraints on the baryogenesis scale from neutrino masses*, *Phys.Lett.* **B258** (1991) 45–48.

[189] B. A. Campbell, S. Davidson, J. R. Ellis, and K. A. Olive, *On the baryon, lepton flavor and right-handed electron asymmetries of the universe*, *Phys.Lett.* **B297** (1992) 118–124, [hep-ph/9302221].

[190] H. K. Dreiner and G. G. Ross, *Sphaleron erasure of primordial baryogenesis*, *Nucl.Phys.* **B410** (1993) 188–216, [hep-ph/9207221].

[191] B. A. Campbell, S. Davidson, J. R. Ellis, and K. A. Olive, *On B+L violation in the laboratory in the light of cosmological and astrophysical constraints*, *Astropart.Phys.* **1** (1992) 77–98.

[192] M. Endo, K. Hamaguchi, and S. Iwamoto, *Lepton flavor violation and cosmological constraints on R-parity violation*, *JCAP* **1002** (2010) 032, [arXiv:0912.0585].

[193] L. Baudis, M. Gunther, J. Hellmig, G. Heusser, M. Hirsch, *et. al.*, *The Heidelberg - Moscow experiment: Improved sensitivity for Ge-76 neutrinoless double beta decay*, *Phys.Lett.* **B407** (1997) 219–224.

[194] M. C. Herbst, *A search for R-parity violating squark production with the H1 experiment at HERA*, . presented 23 Nov 2011.

[195] P. Jackson, *Search for R-parity violating supersymmetry with the ATLAS detector*, arXiv:1112.0369.

[196] ATLAS Collaboration, *Search for supersymmetry in final states with jets, missing transverse momentum and one isolated lepton in sqrts = 7 TeV pp collisions using 1 fb^{-1} of ATLAS data*, *Phys.Rev.* **D85** (2012) 012006, [arXiv:1109.6606]. 18 pages plus author list (30 pages total), 9 figures, 4 tables, final version to appear in Physical Review D.

[197] D. Carvalho, M. Gomez, and J. Romao, *Charged lepton flavor violation in supersymmetry with bilinear R-parity violation*, *Phys.Rev.* **D65** (2002) 093013, [hep-ph/0202054]. 29 pages, 8 figures. Constraint from solar neutrino data included, conclusions changed respect v1.

[198] Y. Grossman and S. Rakshit, *Neutrino masses in R-parity violating supersymmetric models*, *Phys.Rev.* **D69** (2004) 093002, [hep-ph/0311310].

[199] H. Dreiner and T. Stefaniak, *Bounds on R-parity violation from resonant slepton production at the LHC*, arXiv:1201.5014.

[200] PAMELA Collaboration, *An anomalous positron abundance in cosmic rays with energies 1.5-100 GeV*, *Nature* **458** (2009) 607–609, [arXiv:0810.4995].

[201] Fermi LAT Collaboration, *Fermi LAT observations of cosmic-ray electrons from 7 GeV to 1 TeV*, *Phys.Rev.* **D82** (2010) 092004, [arXiv:1008.3999].

[202] H.E.S.S. Collaboration, *The energy spectrum of cosmic-ray electrons at TeV energies*, *Phys.Rev.Lett.* **101** (2008) 261104, [arXiv:0811.3894].

[203] H.E.S.S. Collaboration, *Probing the ATIC peak in the cosmic-ray electron spectrum with H.E.S.S*, *Astron.Astrophys.* **508** (2009) 561, [arXiv:0905.0105].

[204] PAMELA Collaboration, *PAMELA results on the cosmic-ray antiproton flux from 60 MeV to 180 GeV in kinetic energy*, *Phys.Rev.Lett.* **105** (2010) 121101, [arXiv:1007.0821].

[205] H. Fuke, J. Koglin, T. Yoshida, T. Aramaki, W. Craig, *et. al.*, *Current status and future plans for the general antiparticle spectrometer (GAPS)*, *Adv.Space Res.* **41** (2008) 2056–2060.

[206] V. Choutko and F. Giovacchini, *Cosmic rays antideuteron sensitivity for AMS-02 experiment*, in *Proceedings of the 30th International Cosmic Ray Conference* (R. Caballero, J. D'Olivo, G. Medina-Tanco, L. Nellen, F. A. Sanchez, and V.-G. J.F., eds.), vol. 4, pp. 765–768, 2008.

[207] C. Weniger, *A tentative gamma-ray line from dark matter annihilation at the Fermi Large Area Telescope*, arXiv:1204.2797.

[208] The Fermi-LAT collaboration, *The spectrum of the isotropic diffuse gamma-ray emission derived from first-year Fermi Large Area Telescope data*, *Phys.Rev.Lett.* **104** (2010) 101101, [arXiv:1002.3603].

[209] A. Abdo, M. Ackermann, M. Ajello, W. Atwood, L. Baldini, *et. al.*, *Fermi LAT Search for photon lines from 30 to 200 GeV and dark matter implications*, *Phys.Rev.Lett.* **104** (2010) 091302, [arXiv:1001.4836].

[210] G. Vertongen and C. Weniger, *Hunting dark matter gamma-ray lines with the Fermi LAT*, *JCAP* **1105** (2011) 027, [arXiv:1101.2610].

[211] ATLAS Collaboration, *Search for displaced vertices arising from decays of new heavy particles in 7 TeV pp collisions at ATLAS*, *Phys.Lett.* **B707** (2012) 478–496, [arXiv:1109.2242].

[212] W. Buchmuller, K. Schmitz, and G. Vertongen, *Entropy, baryon asymmetry and dark matter from heavy neutrino decays*, *Nucl.Phys.* **B851** (2011) 481–532, [arXiv:1104.2750].

[213] W. Buchmuller, V. Domcke, and K. Schmitz, *Spontaneous B-L breaking as the origin of the hot early universe*, arXiv:1202.6679. 64 pages, 8 figures, 1 table. v2: minor numerical corrections, slightly different parameter point chosen in section 4, final results unchanged.

[214] K. Ishiwata, T. Ito, and T. Moroi, *Long-lived unstable superparticles at the LHC*, *Phys.Lett.* **B669** (2008) 28–33, [arXiv:0807.0975].

[215] S. Asai, K. Hamaguchi, and S. Shirai, *Measuring lifetimes of long-lived charged massive particles stopped in LHC detectors*, *Phys.Rev.Lett.* **103** (2009) 141803, [arXiv:0902.3754].

[216] G. Taubes, *Nobel dreams: Power, deceit, and the ultimative experiment.* Random House, 1986.

[217] L. Smolin, *The trouble with physics.* Houghton Mifflin Company, 2006.

[218] P. Woit, *Not even wrong.* Basic Books, 2006.

[219] R. Laughlin, *A different universe.* Basic Books, 2005.

[220] G. L. Kane, *A Higgsino-LSP world*, . in "Perspectives on supersymmetry" (1998), 352-354.

[221] C. Csáki, A. Falkowski, Y. Nomura, and T. Volansky, *New approach to the mu-Bmu problem of gauge-mediated supersymmetry breaking*, *Phys.Rev.Lett.* **102** (2009) 111801, [arXiv:0809.4492].

[222] A. De Simone, R. Franceschini, G. F. Giudice, D. Pappadopulo, and R. Rattazzi, *Lopsided gauge mediation*, *JHEP* **1105** (2011) 112, [arXiv:1103.6033].

[223] H. Baer, V. Barger, and P. Huang, *Hidden SUSY at the LHC: the light higgsino-world scenario and the role of a lepton collider*, *JHEP* **1111** (2011) 031, [arXiv:1107.5581].

[224] CDF Collaboration, *A Search for dark matter in events with one jet and missing transverse energy in $p\bar{p}$ collisions at $\sqrt{s} = 1.96$ TeV*, arXiv:1203.0742. Long author list - awaiting processing.

[225] ATLAS Collaboration, *Search for new phenomena in events with a monojet and large missing transverse momentum at the LHC using the ATLAS detector*, arXiv:1202.0158. Presented at the 2011 Hadron Collider Physics symposium (HCP-2011), Paris, France, November 14-18 2011, 3 pages, 3 figures.

[226] S. A. Malik, *Search for new physics with monojet plus missing transverse energy at CMS*, arXiv:1110.1609.

[227] S. Worm, "Searches for dark matter in monojets and monophoton events at CMS." Talk given at the Recontres de Moriond: EW interactions and unified theories., 2012.

[228] S. Bornhauser, M. Drees, S. Grab, and J. Kim, *Light stop searches at the LHC in events with two b-jets and missing energy*, *Phys.Rev.* **D83** (2011) 035008, [arXiv:1011.5508].

[229] X.-J. Bi, Q.-S. Yan, and P.-F. Yin, *Probing light stop pairs at the LHC*, *Phys.Rev.* **D85** (2012) 035005, [arXiv:1111.2250]. 35pages, 13figures.

[230] N. Desai and B. Mukhopadhyaya, *Constraints on supersymmetry with light third family from LHC data*, arXiv:1111.2830.

[231] C. Brust, A. Katz, S. Lawrence, and R. Sundrum, *SUSY, the third generation and the LHC*, *JHEP* **1203** (2012) 103, [arXiv:1110.6670]. 42 pages, 8 figures, 1 table. V2: minor corrections, references added.

[232] W. Beenakker, R. Hopker, M. Spira, and P. M. Zerwas, *Squark and gluino production at hadron colliders*, *Nucl. Phys.* **B492** (1997) 51–103, [hep-ph/9610490].

[233] W. Beenakker, M. Kramer, T. Plehn, M. Spira, and P. M. Zerwas, *Stop production at hadron colliders*, *Nucl. Phys.* **B515** (1998) 3–14, [hep-ph/9710451].

[234] N. Kidonakis, *Top quark pair and single top production at Tevatron and LHC energies*, *PoS* **ICHEP2010** (2010) 059, [arXiv:1008.2460].

[235] J. M. Campbell, R. Ellis, and C. Williams, *Vector boson pair production at the LHC*, *JHEP* **1107** (2011) 018, [arXiv:1105.0020].

[236] P. Torrielli and S. Frixione, *Matching NLO QCD computations with PYTHIA using MC@NLO*, *JHEP* **1004** (2010) 110, [arXiv:1002.4293].

[237] J. Alwall, P. Demin, S. de Visscher, R. Frederix, M. Herquet, *et. al.*, *MadGraph/MadEvent v4: The new web generation*, *JHEP* **0709** (2007) 028, [arXiv:0706.2334].

[238] T. Sjöstrand, S. Mrenna, and P. Z. Skands, *PYTHIA 6.4 Physics and manual*, *JHEP* **0605** (2006) 026, [hep-ph/0603175].

[239] J. Pumplin, D. Stump, J. Huston, H. Lai, P. M. Nadolsky, *et. al.*, *New generation of parton distributions with uncertainties from global QCD analysis*, *JHEP* **0207** (2002) 012, [hep-ph/0201195].

[240] M. Mühlleitner, *SDECAY: A Fortran code for SUSY particle decays in the MSSM*, *Acta Phys.Polon.* **B35** (2004) 2753–2766, [hep-ph/0409200].

[241] S. Ovyn, X. Rouby, and V. Lemaitre, *DELPHES, a framework for fast simulation of a generic collider experiment*, arXiv:0903.2225.

[242] L. Randall and D. Tucker-Smith, *Dijet searches for supersymmetry at the LHC*, *Phys.Rev.Lett.* **101** (2008) 221803, [arXiv:0806.1049].

[243] CMS Collaboration, *Susy searches with dijet events*, *CMS Physics Analysis Summary SUS-08-005* (Oct, 2008).

[244] CMS Collaboration, *Search strategy for exclusive multi-jet events from supersymmetry at CMS*, *CMS Physics Analysis Summary SUS-09-001* (Jul, 2009).

[245] P. Meade, M. Reece, and D. Shih, *Long-Lived neutralino NLSPs*, *JHEP* **10** (2010) 067, [arXiv:1006.4575].

[246] K. Desch, S. Fleischmann, P. Wienemann, H. K. Dreiner, and S. Grab, *Stau as the lightest supersymmetric particle in R-parity violating SUSY models: Discovery potential with early LHC data*, *Phys. Rev.* **D83** (2011) 015013, [arXiv:1008.1580].

[247] N.-E. Bomark, D. Choudhury, S. Lola, and P. Osland, *Flavour structure of R-violating neutralino decays at the LHC*, arXiv:1105.4022.

[248] ATLAS Collaboration, *Search for supersymmetric particles in events with lepton pairs and large missing transverse momentum in $\sqrt{s} = 7$ TeV proton-proton collisions with the ATLAS experiment*, arXiv:1103.6214.

[249] CMS Collaboration, *Search for physics beyond the Standard Model in opposite-sign dilepton events at $\sqrt{s} = 7$ TeV*, arXiv:1103.1348.

[250] CMS Collaboration, *Search for new physics with same-sign isolated dilepton events with jets and missing transverse energy at the LHC*, arXiv:1104.3168.

[251] CMS Collaboration, *CMS technical design report, volume II: Physics performance*, *J.Phys.G* **G34** (2007) 995–1579.

[252] ATLAS Collaboration, *Expected performance of the ATLAS experiment - detector, trigger and physics*, arXiv:0901.0512.

[253] R. Gavin, Y. Li, F. Petriello, and S. Quackenbush, *FEWZ 2.0: A code for hadronic Z production at next-to-next-to-leading order*, *Comput.Phys.Commun.* **182** (2011) 2388–2403, [arXiv:1011.3540].

[254] J. Alwall *et. al.*, "Madgraph." http://madgraph.hep.uiuc.edu/.

[255] CMS Collaboration, *CMS physics: Technical design report*, .

[256] G. Cowan, K. Cranmer, E. Gross, and O. Vitells, *Asymptotic formulae for likelihood-based tests of new physics*, *Eur.Phys.J.* **C71** (2011) 1554, [arXiv:1007.1727].

[257] G. Cowan, "Sigcalc." http://www.pp.rhul.ac.uk/~cowan/stat/SigCalc/.

[258] C. M. Bidin, G. Carraro, R. Mendez, and R. Smith, *Kinematical and chemical vertical structure of the Galactic thick disk II. A lack of dark matter in the solar neighborhood*, *Astrophys.J.* **751** (2012) 30, [arXiv:1204.3924].

[259] G. Roepstorff, *Einführung in die Quantenfeldtheorie*, 2000.
http://www.physik.rwth-aachen.de/fileadmin/user_upload/www_physik/Bibliothek/Skripte/Roepstorff/qft-2000.pdf.

[260] K. Fredenhagen, *Quantenfeldtheorie I*, 2006.
http://unith.desy.de/research/aqft/lecture_notes/.

[261] R. Penrose and W. Rindler, *Spinors and space-time, Vol. 1: Two spinor calculus and relativistic fields*. Cambridge Monographs On Mathematical Physics. Cambridge University Press, 1984.

[262] D. Lurie, *Particles and fields*. Interscience Publishers, 1968. (ISBN-10: 0-470-55642-0).